DISSERTATION

APPLICATION OF ALCOHOLS IN SPARK IGNITION ENGINES

Submitted by

Saeid Aghahossein Shirazi

Department of Chemical and Biological Engineering

In partial fulfillment of the requirements

For the Degree of Doctor of Philosophy

Colorado State University

Fort Collins, Colorado

Summer 2018

Doctoral Committee:

Advisor: Kenneth Reardon

Thomas Foust
David Dandy
Anthony Marchese
Bret Windom

ABSTRACT

APPLICATION OF ALCOHOLS IN SPARK IGNITION ENGINES

Replacing petroleum fuels with sustainable biofuels is a viable option for mitigation of climate change. Alcohols are the most common biofuels worldwide and can be produced biologically from sugary, starchy and lignocellulosic biomass feedstocks. Alcohols are particularly attractive options as fuels for spark ignition engines due to the high octane values of these molecules and their positive influence on performance and emissions.

In the context of the US Department of Energy's Co-Optimization of Fuels and Engines (Co-Optima) initiative, a systematic product design methodology was developed to identify alcohols that might be suitable for blending with gasoline for use in spark ignition engines. A detailed database of 943 molecules was established including all possible molecular structures of saturated linear, branched, and cyclic alcohols (C1-C10) with one hydroxyl group. An initial decision framework for removing problematic compounds was devised and applied. Next, the database and decision framework were used to evaluate alcohols suitable for blending in gasoline for spark ignition engines. Three scenarios were considered: (a) low-range (less than 15 vol%) blends with minimal constraints; (b) ideal low-range blends; and (c) high-range (greater than 40 vol%) blends. A dual-alcohol blending approach has been tested. In addition, the azeotropic volatility behavior and mixing/sooting potential of the single and dual-alcohol gasoline blends were studied by monitoring the distillation composition evolution and coupling this with results of a droplet evaporation model. Although nearly all of the work done on alcohol-gasoline blends has been on single-alcohol blends, the results of this study suggest that dual-alcohol blends can

overcome many of the limitations of single-alcohol blends to provide a broader spectrum of advantaged properties. A third study focused on the possibility of replacing anhydrous ethanol fuel with hydrous ethanol at the azeotrope composition, which can result in significant energy and cost savings during production. In this collaborative study, the thermophysical properties and evaporation dynamics of a range of hydrous and anhydrous ethanol blends with gasoline were characterized. The results showed that hydrous ethanol blends have the potential to be used in current internal combustion engines as a drop-in fuel with few or no modifications.

ACKNOWLEDGEMENTS

I extend my gratitude to my academic advisor Dr. Reardon for his inspiration, continuous support, and timely guidance throughout my studies at Colorado State University. I am fortunate to be a part of his research team. I owe my deepest gratefulness for his generous financial support for my studies.

I am thankful to my exam committee Dr. Thomas Foust, Dr. David Dandy, Dr. Anthony J. Marchese, and Dr. Bret Windom for their contribution in editing this report, words of encouragement and suggestion to make this report better. I would like to especially thank Dr. Foust for providing the necessary resources throughout my dissertation and Dr. Windom for his willingness to invest a lot of time discussing research.

I acknowledge funding for this work by Alliance for Sustainable Energy, LLC, the manager and operator of the National Renewable Energy Laboratory for the U.S. Department of Energy (DOE) under Contract No. DE-AC36-08GO28308. The views expressed in this document do not necessarily represent the views of the DOE or the U.S. Government. The U.S. Government retains and the publisher, by accepting the article for publication, acknowledges that the U.S. Government retains a nonexclusive, paid-up, irrevocable, worldwide license to publish or reproduce the published form of this work, or allow others to do so, for U.S. Government purposes. This research was conducted as part of the Co-Optimization of Fuels & Engines (Co-Optima) project sponsored by the U.S. Department of Energy (DOE) Office of Energy Efficiency and Renewable Energy (EERE), Bioenergy Technologies and Vehicle Technologies Offices. I also acknowledge funding from the US National Science Foundation (Grant No. DGE-0801707). I acknowledge the travel award from the Colorado Center for Biorefining and Bioproducts (C2B2).

I would like to thank undergraduate fellow Jake Martinson for helping me with the experiments and database completion.

I would like to thank my wife Bahar for her love, constant support, and above all for being my best friend. I owe you everything.

I would like to convey my deep gratitude to my dearest parents and brother for all their help, love, support, and unwavering belief in me during all these years away from home. Without you, I would not be the person I am today.

DEDICATION

To my beloved parents

Hossein Aghahossein Shirazi & *Zohreh Ohadi Esfehani*

TABLE OF CONTENTS

1 Introduction

1.1. Background

The most common transportation fuel for spark ignition (SI) engines is gasoline which is claimed to be the most cost-effective system at least for the near future [1]. However, it is essential to seek renewable and sustainable sources of energy due to the depleting petroleum reserves, energy crisis, and global warming [2]. To address this concern, a significant fraction of future energy supply for transportation sector must lie with biofuels obtained from crops and waste products. The Clean Air Act amendment of 1990 mandated the use of reformulated and oxygenated gasoline in order to decrease emissions [3]. The use of renewable oxygenates in gasolines has some benefits: reduction in fossil fuel consumption and greenhouse gas emissions; improvement in combustion characteristics; societal contributions such as employment in the agricultural sector [4]. Long-chain biodiesels and short-chain bio-alcohols are currently receiving attention as bio-based blendstocks for diesel and gasoline, respectively. In the United States, alcohols can be blended with gasoline up to an oxygen content of 3.7 mass % as stated in the Substantially Similar rule published by Environmental Protection Agency (EPA) [5].

To ensure reduction in greenhouse gas emissions and energy security, EPA created the Renewable Fuel Standard (RFS) program which requires the production of 36 billion gallons of biofuels annually by 2022 [6]. Up to now, ethanol and bio-based synthetic hydrocarbons have been the primary candidates to fulfill the RFS demand. However, other bio-derived molecules may also offer potential as alternative fuels. Higher alcohols (term used to describe any saturated mono-alcohol with higher molecular weight than ethanol) might be good options due to their higher energy densities than ethanol. Although the properties of C1 to C4 alcohol blends with gasoline

and their influences on SI engine performance have been widely investigated, there is a lack of comprehensive study on longer chain alcohols.

1.2. Co-Optimization of Fuels and Engines (Co-Optima)

The Co-Optimization of Fuels and Engines (Co-Optima) program is a research and development collaboration between the U.S. Department of Energy, nine national laboratories, and industry which intends to concurrently transform transportation fuels and vehicles [7]. The Co-Optima program takes an integrated approach toward developing engines, fuels, and marketplace strategies to increase performance and energy efficiency, decrease environmental impact, and accelerate widespread adoption of new combustion strategies.

This research was conducted as part of the Co-Optima project sponsored by the U.S. Department of Energy, Office of Energy Efficiency and Renewable Energy, Bioenergy Technologies, and Vehicle Technologies Offices.

1.3. Projects

There are many alcohols that could potentially be used as fuels, but it is not feasible to experimentally characterize all of them. Thus, detailed laboratory investigation must be done only on the most promising fuel candidates based on reported and estimated data, and models of blended fuel properties. To implement any new alternative fuel in the existing engines and infrastructures, the fuel needs to meet standard fuel properties for petroleum-based transportation fuels to avoid prohibitive capital investments for replacing the current infrastructures. Thus, it is necessary to evaluate the physiochemical properties of new alternative fuels, especially in blends. Although the performance of a fuel in the engine is too complex to be explained solely by physicochemical properties, these properties can contribute to limit the large number of candidates.

In the context of the Co-Optima program, the following projects were carried out:

- Project I (Chapter 3): Identification of potential fuel molecules via database preparation and screening (submitted as "Development and Application of a Fuel Property Database for Mono-Alcohols as Fuel Blend Components for Spark Ignition Engines" by Saeid Aghahossein Shirazi, Thomas D. Foust and Kenneth F. Reardon).
- Project II (Chapter 4): Identification of best blending approach, characterization of dual-alcohol blends, and study the evaporation dynamics of candidate blends via droplet evaporation model (to be submitted as "Dual-Alcohol Blending Effects on Gasoline Properties" by Saeid Aghahossein Shirazi, Bahareh Abdollahipoor, Jake Martinson, Bret Windom and Kenneth F. Reardon).
- Project III (Chapters 5 and 6): Characterization of physiochemical properties and volatility behavior of hydrous and anhydrous ethanol gasoline blends (Chapter 5 submitted as "Physiochemical Property Characterization of Hydrous and Anhydrous Ethanol Blended Gasoline" by Saeid Aghahossein Shirazi, Bahareh Abdollahipoor, Jake Martinson, Kenneth F. Reardon and Bret C. Windom ; Chapter 6 submitted as "Azeotropic Volatility Behavior of Hydrous and Anhydrous Ethanol Gasoline Mixtures" by Bahareh Abdollahipoor, Saeid Aghahossein Shirazi, Kenneth F. Reardon and Bret C. Windom).

1.4. Project Objectives

1.4.1. Project I: Database development and application (Chapter 3)

Although methanol, ethanol, and butanol have been widely studied, many other alcohols could be considered for use as fuels or in fuel blends. However, it is not possible to experimentally investigate the fuel potential of these molecules. To address this issue, in Project I of this study, a systematic product design methodology was developed to identify alcohols that might be suitable for blending with gasoline for use in SI engines. A detailed database was developed with 13 fuel

properties of all possible molecular structures of saturated linear, branched, and cyclic alcohols (C1-C10) with one hydroxyl group. Where available, fuel property data were obtained from literature reports. Property estimation methods were exploited for compounds without property data. An initial decision framework for removing problematic compounds was devised and applied. Next, the database and decision framework were used to evaluate alcohols suitable for blending in gasoline for spark ignition engines. Three scenarios were considered: (a) low-range (less than 15 vol%) blends with minimal constraints; (b) ideal low-range blends; and (c) high-range (greater than 40 vol%) blends.

1.4.2. Project II: Dual-alcohol blending effects on gasoline properties (Chapter 4)

While the use of a neat alcohol as a fuel for spark-ignition engines would displace large amounts of petroleum, neat alcohols cannot provide the distillation temperature range required for smooth driveability and often exhibit high enthalpies of vaporization and low vapor pressures, which create cold-start problems. Even gasoline blends containing high concentrations of single alcohols have shortfalls. Blends of lower alcohols (methanol and ethanol) exhibit azeotropic behavior, low calorific value, and low stability, while the low volatility of higher alcohols significantly limits the maximum fraction at which they can be blended. One way to circumvent these issues is to use a dual-alcohol approach, mixing a lower and a higher alcohol with gasoline to obtain a blend with a vapor pressure close to that of the neat gasoline. In project II of this study, the fuel potentials of ten dual-alcohol blends over a wide range of blending ratios (10 to 80 vol %) and corresponding single alcohol-gasoline blends were evaluated based on their vapor-liquid equilibrium and physiochemical properties as compared to the neat gasoline. Furthermore, this was the first investigation of the fuel potential of 3-methyl-3-pentanol in single- and dual-alcohol blends and iso-butanol in dual-alcohol blends. In addition, the azeotropic volatility behavior and

mixing/sooting potential of the single and dual-alcohol gasoline blends were examined by monitoring the distillate composition during the distillation and coupling this with results of droplet evaporation model.

1.4.3. Project III: Characterization of hydrous ethanol blends (Chapters 5 and 6)

After fermentation, the concentration of bioethanol is only 8-12 wt%. To produce anhydrous ethanol fuel, a significant amount of energy is required for separation and dehydration. Once the azeotrope composition is reached, distillation can no longer be exploited for purification and other expensive methods must be used. Replacing anhydrous ethanol fuel with hydrous ethanol (at the azeotropic composition) can result in significant energy and cost savings during production. Currently there is a lack of available thermophysical property data for hydrous ethanol gasoline fuel blends. These data are important to understand the effect of water on critical fuel properties and to evaluate the potential of using hydrous ethanol fuels in conventional and optimized spark ignition engines. In Project III of this study, the thermophysical properties, volatility behavior, evaporation dynamic, and mixing/sooting potential of various hydrous and anhydrous ethanol blends with gasoline were characterized to investigate the potential of replacing hydrous ethanol with anhydrous ethanol in the current system.

References

1- Bergthorson JM, Thomson MJ. A review of the combustion and emissions properties of advanced transportation biofuels and their impact on existing and future engines. Renew Sustain Energy Rev 2015;42:1393–417. doi:10.1016/j.rser.2014.10.034.

2- Reddy HK, Muppaneni T, Rastegary J, Shirazi SA, Ghassemi A, Deng S. ASI: Hydrothermal extraction and characterization of bio-crude oils from wet *Chlorella sorokiniana* and *Dunaliella tertiolecta*. Environ Prog Sustain Energy 2013;32:910–5. doi:10.1002/ep.11862.

3- Surisetty VR, Dalai AK, Kozinski J. Alcohols as alternative fuels: An overview. Appl Catal A Gen 2011;404:1–11. doi:10.1016/j.apcata.2011.07.021.

4- U.S. Environmental Protection Agency. Renewable Fuel Standard Program (RFS2) Regulatory Impact Analysis. 2010. doi:EPA-420-R-10-006., February 2010.

5- Yan Y, Liao JC. Engineering metabolic systems for production of advanced fuels. J Ind Microbiol Biotechnol 2009;36:471–9. doi:10.1007/s10295-009-0532-0.

6- Kirchstetter TW, Singer BC, Harley RA, Kendall GR, Ghan W. Impact of oxygenated gasoline use on California light-duty vehicle emissions. Environ Sci Technol 1996;30:661–70. doi:10.1021/es950406p.

7- Farrell JT. Co-Optimization of Fuels & Engines (Co-Optima) Initiative. National Renewable Energy Lab. (NREL), Golden, CO (United States); 2017 Oct 4.

2 Literature Review

2.1. Introduction

Due to price fluctuations and environmental problems of fossil fuels, scientists turned their attention to biofuels and most efforts have been devoted to alcohols aiming to ensure the energy security. Alcohols are particularly attractive options as fuel for spark ignition (SI) engines due to the high octane number and the positive influence on performance. In this chapter, properties of alcohol-gasoline blends for application in spark ignition engines are discussed. Special emphasis is placed on the effect of fuels on engine performance and emissions. Although overall positive influence of alcohols on performance and exhaust emissions of SI engines has been demonstrated, further research must be conducted to find the optimum alcohol blends along with the proper corresponding engine tuning to maximize the efficiency of SI engines. Furthermore, any advances in the production process such as finding low-cost feedstocks and developing high-yield production pathways can trigger the introduction of promising alcohols to the transportation section.

Lower alcohols (methanol and ethanol) are strong solvents and highly corrosive to some metallic and non-metallic parts of the engine. Lower alcohols can cause corrosion in three ways: general corrosion due to ionic impurities such as chloride ions and acetic acid in low quality commercial oxygenates; dry corrosion due to the high polarity of these alcohols; wet corrosion [1, 2]. In addition, lower alcohols have properties that make them different from gasoline in terms of handling, distribution, storage, combustion and emission characteristics. Given the dissimilarities and limitations, some modifications are required to best use of alcohol fuels in the market. One option to fully take advantage of alcohols is to redesign engines and distribution systems to become

compatible with alcohols as Brazilian did. In Brazil which has the most developed technology for the alcohol fueled cars, several changes had been made to gasoline engines to make alcohol engines more functional and economical. Some of these modifications are as follows: the intake manifold was redesigned to provide more heat for evaporation due to the high heat of vaporization (HoV) of alcohols; fuel tanks were coated with pure tin; cadmium brass was used for fuel lines instead of zinc steel alloy; compression ratio (CR) was increased to ~ 12:1 due to the alcohols' higher octane ratings; palladium and rhodium catalytic converters catalyst was replaced by palladium and molybdenum [3]. Although these modifications generally improve the combustion and emission efficiencies of alcohol engines [1,3], implementation of this approach in countries with infrastructures optimized for gasoline fuels is prohibitively expensive. To avoid enormous capital investments, a more economical approach is to find and use additives to improve characteristics of blends aiming to make drop-in bio-based blendstocks which match standard specifications for petroleum-based transportation fuels [1, 4].

Currently, only lower alcohols have been used as gasoline blendstocks in the market because of well-established and low-cost production [5]; however, they have limitations such as low energy density, high corrosivity [6], high hygroscopicity and water solubility [7], poor stability in gasoline [1], and azeotropic behavior when blended with gasoline [8,9]. In contrast, higher alcohols offer higher energy density [10], low water affinity, non-corrosive behavior, enhanced materials compatibility [10], better stability in gasoline [11], and less (or no) azeotropic behavior in gasoline blends [9]. Higher alcohols have more similarities to gasoline in terms of physicochemical properties which make them more compatible to existing infrastructures and engines compared to lower alcohols [6]. Therefore, higher alcohols can be used as co-solvents along with lower alcohols to offset their shortcomings [12].

2.2. An introduction to C1-C4 alcohols

2.2.1. Methanol

Methanol is the lowest molecular weight alcohol with chemical formula of CH_3OH. It is a tasteless and colorless liquid with mild odor. Beside fuel industries, it has applications in antifreeze, plastics and polymer industries [13]. Methanol is the cheapest liquid alternative fuel per calorific unit and which makes it attractive [14]. In comparison to gasoline, methanol has a lower carbon-hydrogen ratio, wider flammability limit, higher flame speed, higher octane value, and higher HoV (due to the charge cooling effect) [15]. Therefore, addition of methanol to gasoline has a general positive impact on combustion and emissions. For example, thermal efficiency is generally improved because of higher flame speed, octane value, and HoV while CO, UHC, and soot emissions are generally reduced due to the more complete combustion [16-18]. Methanol also has some limitations. Methanol flames hard to see and can cause potential safety hazards [3]. Methanol has a lower energy density due to the high oxygen content (almost one third of gasoline). If methanol is used in a pure state as a fuel, low vapor pressure and high HoV can cause cold-start problems [16]. In addition, materials in the engine and fuel delivery system must be replaced with more compatible metals and polymers because of methanol's high corrosivity [16]. If methanol is blended with gasoline, high vapor pressure, relatively low solubility in gasoline and easy phase separation at low temperatures are disadvantages [17].

Methanol is mostly produced from natural gas for economic reasons, but it also can be produced from coal and renewable resources such as wood, forest waste, peat, municipal solid wastes, sewage and CO_2 [13, 16, 17]. In general, methanol production consists of two steps: conversion of feedstock to a syngas followed by the catalytic synthesis of methanol from the synthesis gas [19- 23].

For methane, synthesis gas is produced by steam reforming which is an endothermic reaction [24]:

$CH_4 + H_2O \leftrightarrow CO + 3H_2$ (R2.1)

For coal, carbon monoxide and hydrogen are manufactured through gasification process using both oxygen and steam (including water-shift reaction) [25]:

$C + ½O_2 \leftrightarrow CO$ (R2.2)

$C + H_2O \leftrightarrow CO + H_2$ (R2.3)

$CO + H_2O \leftrightarrow CO_2 + H_2$ (R2.4)

$CO_2 + C \leftrightarrow 2\ CO$ (R2.5)

Syngas is obtained from biomass by a similar process, but the product contains tar and ash that must be removed prior to the catalytic reactor. After upgrading, syngas with low methane content and proper H_2-CO ratio will be obtained [26].

Once the syngas is manufactured, methanol is produced over a catalyst. For instance, in case of natural gas, the global reaction is as follow:

$CO + CO_2 + 7\ H_2 \rightarrow 2\ CH_3OH + 2\ H_2 + H_2O$ (R2.6)

The considerable excess hydrogen surplus can be consumed by external source of CO_2 (if available) and converted to additional methanol. The catalytic synthesis of methanol is highly exothermic and this extra energy can be used to generate electricity in the process. Several technoeconomical assessments have been conducted aiming to find optimum pathway to reduce manufacturing costs [21, 22]. There are also some processes for methanol production which are not based on syngas such as microbial formation [26- 31], direct oxidation with oxygen or via intermediates such as methyl chloride and methyl bisulphate [23], and CO_2 hydrogenation [32, 33].

2.2.2. Ethanol

Ethanol with molecular formula of C_2H_5OH is a colorless, transparent liquid hydrocarbon with a strong odor and a sharp burning taste. Historically, ethanol obtained from fermentation has been used in beverage industries, but it was just offered as a potential fuel in 1930s and was introduced to market only after 1970 in USA [34]. Ethanol contains a hydroxyl group in its structure which makes it more reactive than gasoline. It can cause structural weakening by accumulating in elastomers in fuel system. In addition, ethanol is corrosive to some metal components in conventional gasoline engines. Although these problems have been addressed using corrosion inhibitors, the compatibility of these additives with ethanol-gasoline blends needs to be addressed [35]. Ethanol is produced from renewable sources with relatively cheap price and able to improve national energy security, reduce the reliance on petroleum fuels, and boost incomes in agriculture sectors [36]. Given that the use of ethanol in its pure state mandates some modifications in the current systems and engines, Environmental Protection Agency granted a waiver for low concentration blends of ethanol (up to 15% ethanol volume) for use as an automotive spark-ignition engine fuel in the U.S. and for up to 85% by volume for flexible-fuel engines [37].

Ethanol has many advantages over gasoline as an SI engine fuel. Ethanol's oxygen content improves combustion efficiency and produces a high combustion temperature [34]. Ethanol has a higher octane rating compared to gasoline which allows higher compression ratio engines to be used leading to higher fuel efficiencies [34,38,39]. In addition, this feature of ethanol can decrease costs of petroleum refineries because they are no longer obliged to produce high-grade gasoline with high octane number. However, the heat of evaporation of ethanol is much higher than gasoline. Thus, more energy is required to vaporize the fuel which effectively cools the cylinder prior to combustion, increases volumetric efficiency, and improves engine's performance and

exhaust emissions [34, 41, 42]. Use of ethanol will reduce the concentration of aromatics and sulfur contents in the gasoline [43]. Higher laminar flame propagation speed of ethanol relative to gasoline makes combustion occur earlier, resulting in a higher thermal efficiency [34]. It has been shown that ethanol and ethanol blends with gasoline significantly reduce CO and UHC emissions. Also, lower C/H atom ratio of ethanol can potentially cause a reduction in CO_2 emissions [35, 41]. Neat ethanol has a higher flash point and lower vapor pressure compared to gasoline which makes it safe for transportation and storage in current systems [35].

Ethanol also exhibits some disadvantages. Ethanol contains only two-thirds of gasoline's heating value which can adversely impact the fuel economy. Low vapor pressure of neat ethanol can cause cold start problems while high vapor pressure of ethanol-gasoline blends (low to medium blending ratios) increases evaporative emissions [41]. High heat of vaporization of ethanol may cause poor cold startability and increases intake valve deposits [42]. Ethanol and ethanol blends have been proved to produce more unregulated pollutants like aldehydes compared to gasoline [44]. Polarity and hydrophilic nature of ethanol use can cause corrosion on ferrous components such as fuel tank [45]. Ethanol is manufactured through three main pathways [1]: 1. Biological: Fermentation of sugary, starchy, and lignocellulosic feedstocks; 2. Chemical: Direct hydration of ethylene; 3. Thermochemical: High temperature catalytic conversion of synthesis gas to a mixture of alcohols via Fischer–Tropsch process.

Today, fermentation is the primary method for ethanol production which uses sucrose-containing biomass such as sugar cane, sugar beet, sweet sorghum and fruits in addition to starchy biomass such as corn, milo, wheat, rice, potato, cassava, sweet potatoes, and barley. Ethanol from sugary and starchy biomass is called first generation bio-ethanol [1,34].

$C_{12}H_{22}O_{11} + H_2O \rightarrow 2C_6H_{12}O_6$ (R2.7)

$C_6H_{12}O_6 \rightarrow 2CH_3CH_2OH + 2CO_2$ (R2.8)

Since there is always controversy over the dilemma of food versus fuel regarding sugary and starchy feedstocks, ethanol production from lignocellulosic biomass fermentation has become a viable option. Ethanol from lignocellulosic biomass is called second generation bio-ethanol. This process includes pretreatment of substrates, hydrolysis of cellulose and hemicellulose, saccharification process to release the fermentable sugars from polysaccharides, fermentation of C5 and C6 sugars, separation of lignin residue, and eventually distillation step for recovery and concentration of ethanol. Currently, ethanol production from lignocellulosic feedstocks is prohibitively expensive and requires a cost reduction especially in pretreatment and hydrolysis steps [43, 46].

Ethanol also can be produced synthetically through the reversible reaction of ethylene with steam in the presence of the solid silicon dioxide coated with phosphoric acid catalyst.

$CH_2 = CH_2 + H_2O \leftrightarrow CH_3CH_2OH$ (R2.9)

Although this continuous flow process is more efficient than fermentation, fermentation is considered a more environmentally-friendly method because synthetic production of ethanol is highly energy intensive and uses petroleum products as feedstocks [1].

Furthermore, synthesis gas obtained from gasification can be converted catalytically to a mixture of alcohols through a continuous flow process with relatively high yield. It has been considered an advantageous method because synthesis gas can be obtained from a wide range of biomass and residues such as forest or agricultural surplus and household waste [1].

2.2.3. Propanol isomers

Propanol (C_3H_7OH) is a 3-carbon alcohol with higher energy density than ethanol which makes it a potential alternative as blending component with gasoline. Propanol has two isomers: n-propanol and isopropanol. 1-propanol (n-propanol) is a straight chain molecule that is currently used as a solvent in the paint and cosmetics industries [47] as well as a diluting agent to reduce viscosity of biodiesel [48]. Isopropanol is the simplest secondary alcohol which is a colorless and flammable liquid with a strong odor [49]. It is a very valuable chemical with many industrial applications whose worldwide production exceeds 10^6 tons per year [50]. Isopropanol can be used as the catalyst instead of methanol in transesterification process for biodiesel production and it can also be dehydrated to yield propylene which is currently derived from petroleum for making polypropylene [51]. In the automotive fuel segment, propanol isomers are forgotten fuels because currently their large scale production is more expensive than ethanol and their use is hard to justify. This is the reason that studies on combustion and emission characteristics of these alcohol fuels are too limited compared to methanol, ethanol and butanol.

Syngas obtained from gasification of biomass or municipal wastes can be converted to 1-propanol from certain species of *Clostridium* (*Clostridium ljungdahlii* and *Clostridium ragsdalei*) via threonine catabolism, but none of these pathways can yield more than 70 mg/L [52,47]. So far, no existing microorganism has been identified to produce 1-propanol naturally from glucose in substantial amount suitable for industrial scale production [48]. Hence, some researchers have switched to bio-synthetic pathways instead of using the pathways naturally evolved for alcohol production in microorganisms. They have devised a systematic approach to synthesize higher alcohols (1-propanol and 1-butanol) with the use of native amino acid available in all organisms as alcohol production precursors aiming to minimize metabolic perturbation caused by toxic

intermediates. In these studies, engineered *Escherichia coli* strain which can be manipulated more easily compared to *Clostridium* species have been shown to produce 1-propanol via 2-ketobutyrate with relatively high yield [47, 53]. Furthermore, recently some metabolic engineering strategies have been exploited to improve the amount of 1-propanol production from the engineered *Escherichia coli* [54].

Several species of *Clostridium,* including 52 strains of *Clostridium beijerinckii* and *Clostridium isopropylicum,* have been evaluated for isopropanol production. However, these species produce isopropanol together with butanol; therefore, they have not been considered feasible pathways to produce substantial quantity of isopropanol [51, 55]. Some studies produced isopropanol through a synthetic metabolic pathway by using engineered cyanobacteria (*Synechocystis elongates* PCC 7942) from cellular acetyl-CoA via a four-step process and reported 26.5 mg/L production of isopropanol after 9 days under the optimized conditions [55-57]. The highest level of isopropanol production was suggested by Inokuma et al. [51]. They improved isopropanol production by metabolically engineered *Escherichia coli* strain TA76, the optimization of fermentation conditions and isopropanol removal by gas stripping. They reported 143 g/L of isopropanol after 240 h with a yield of 67.4 mol %.

2.2.4. Butanol isomers

Butanol has the chemical formula of C_4H_9OH and occurs in four isomeric structures based on the location of the hydroxyl group. 1-Butanol or n-butanol ($CH_3CH_2CH_2CH_2OH$) has a straight-chain structure and hydroxyl group is located at the terminal carbon. 2-Butanol or sec-butanol ($CH_3CH\ (OH)\ CH_2CH_3$) also has a linear structure but the hydroxyl group is located at the internal carbon. However, iso-butanol ($(CH_3)_2CHCH_2OH$) and tert-butanol ($(CH_3)_3COH$) are branched with the hydroxyl group at the terminal carbon for iso-butanol and internal carbon for tert-butanol.

The difference in the chemical structures result in different thermodynamic properties. Main applications of butanol isomers are as follow [58]:

- n-butanol: solvents, plasticizers, chemical intermediate, cosmetics
- iso-butanol: solvents, paint additive, ink ingredient, industrial cleaners
- sec-butanol: solvents, chemical intermediate, industrial cleaners, Perfumes
- tert-butanol: solvents, denaturant for ethanol, industrial cleaners, chemical intermediate

Among the different isomers, sec-butanol and tert-butanol are not qualified as fuels for SI engines because sec-butanol has a motor octane rating of 32 which is too low and tert-butanol has a high melting point (about 25°C) [59]. However, n-butanol and iso-butanol (i-butanol) have been considered as potent alternatives for gasoline engines. Thus, from this point forward with butanol isomers, we mean n-butanol and i-butanol.

Typically, the lower heating value (LHV) of alcohols increases with increase in carbon atom number. Hence, the LHV of both n-Butanol and i-butanol are greater than ethanol and closer to that of gasoline. In addition, the closer the stoichiometric air-fuel ratio of butanol isomers to the gasoline, allow their introduction to the fuel system at higher blending ratios than ethanol without changes in the current vehicle systems [60]. In addition, the distribution of butanol isomers is much easier than ethanol because they have low tendency to separate from the gasoline if contaminated with water. High tolerance to water contamination makes the use of these fuels feasible in the existing distribution pipelines with no corrosivity to aluminum or polymer components in the fuel system and no need for transportation via rail, barge or truck which is the case for ethanol [61-63]. Lower HoV and autoignition temperature of butanol isomers relative to ethanol can improve the atomization and avoid cold start and ignition problems [60, 62]. Lower polarity of butanol eliminates the problem of increased RVP specific for ethanol and methanol when blended with

gasoline. This causes lower evaporative emissions during the fueling as well as lower tendency for cavitation and vapor lock problem [64]. Low volatility also makes them safer to use at high ambient temperatures especially by taking the high flash point into account [58].

The auto-ignition temperatures for i-butanol and n-butanol are 415 and 385 °C, respectively [65]. Studies on reaction pathways of iso-butanol and n-butanol also confirm that i-butanol is less reactive than n-butanol at low temperature combustion [66-68]. In these studies, it was shown that the combustion reaction of both isomers is initiated by H-atom abstraction. However, burning n-butanol generates mostly H radicals while i-butanol forms mostly methyl radicals which are less reactive than H radicals. Thus, n-butanol has a shorter ignition time compared to i-butanol. Furthermore, n-butanol has a faster flame propagation speed relative to i-butanol at all equivalence ratios and pressures [69]. Hence, it can be concluded that differences in emissions and performance of theses isomers have its roots mainly in the different flame propagations and combustion characteristics.

Isomers of butanol can be produced from fossil fuel sources via various methods. However, to meet the goal of reducing greenhouse gas emissions, production of butanol through biological pathways is of interest. One of the major obstacles of bio-butanol introduction into market is the cost of production which is currently less competitive with gasoline and ethanol mainly due to the low efficiency of industrial fermentation. In addition, the biological pathway generates some by-products such as hydrogen, acetic, lactic and propionic acids, acetone, isopropanol and ethanol which makes the purification even more costly [70, 71]. Currently, many biotechnology companies around the world are working on solutions to increase the efficiency of ABE (acetone, butanol, and ethanol) fermentation to commercialize bio-butanol [58].

Bio-butanol is naturally produced from several *Clostridia* via fermentation from feedstocks that are the same as other biofuels; i.e., sugar beets, wheat, corn, sugar cane, straw, sorghum, and cassava [72]. Microorganisms of the genus *Clostridium* are spore-forming anaerobes and the fermentation of these microorganisms consists of two phases: acidogenic phase and solventogenic. In the acidogenic phase, pathways for acid formation are activated which results in products such as acetate, butyrate, hydrogen, and CO_2. In the next phase (solventogenic), acids are re-integrated and produce mainly butanol, ethanol and acetone and in some cases iso-propanol [58].

ABE fermentation of *Clostridium* currently suffers from several drawbacks. *Clostridium* are not able to metabolize when more than 20 g/L of solvents are available which significantly limits the amount of carbon substrate in the fermentation and subsequently reduces the final solvent productivity [73]. In addition, since these microorganisms are anaerobes, air cannot be pumped into the bioreactor [74]. One of the major problems is solvent toxicity because Clostridium species produce butanol during the phase of sporification in which the functionality of these organisms becomes suspended temporarily because of butanol presence. This is because butanol damages the cell membrane initiating a rise in membrane fluidity [75]. Thus, to realize the idea of industrial production of bio-butanol, series of studies have been conducted to improve major aspects of butanol production process including substrate cost, production yield, solvent toxicity, and downstream processing cost [58, 76]. To meet these goals, several scientific efforts have focused on metabolic engineering of *Clostridium acetobutylicum* [77-80], improvements in fermentation and recovery process [81-84], finding economic and non-food biomass as a substrate for fermentation [85], and studying of *Escherichia coli* as alternative host for bio-butanol synthesis [47, 86, 87].

2.3. Spark ignition engines

In this section, two typical injection systems used in spark ignition engines are briefly described for better understanding of upcoming discussions in the following chapters. In conventional port fuel injection (PFI) engines, the fuel is injected to the intake manifold located upstream of the intake valve. The air also enters the intake manifold via a throttle valve. The fuel is pre-vaporized and well mixed with the air prior to the introduction into the cylinder. In the cylinder, the premixed air-fuel mixture is ignited by a spark plug at the desired point within the piston's cycle of motion. As a result, a high-temperature turbulent premixed flame is generated, which propagates through the well-mixed fuel–air engine charge [88-90]. Conventional PFI engines have some shortfalls: pressure drop across the throttling valve; limited CR and high NO_x emission [91]. To address PFI's limitations, the idea of direct injection spark ignition (DISI) engines was generated to enhance efficiency and fuel economy by eliminating the throttle valve and controlling the engine power via varying the total amount of fuel injected directly into the engine cylinder per cycle [92]. These modifications made engines more fuel flexible and allow higher compression ratios to be used [5]. Fuel economy in such systems is claimed to be 20–25% better than PFI engines [93]. Furthermore, a high pressure fueling system is used in DISI engines to provide a finer atomization [88]. However, a stratified fuel–air engine charge increases soot emissions [93].

2.4. General alcohol blending effect on gasoline properties

2.4.1. Alcohol effect on knock performance

Engine knock is a sharp rise in pressure that is not synchronized with the combustion event and can result in severe damage to the engine. Thus, an appropriate fuel for SI engines must be resistant to autoignition to avoid knock. The index usually used for ignition quality of a fuel is

referred to as octane rating. Research octane number (RON) is used to simulate city driving speed with frequent acceleration while motor octane number (MON) tends to simulate highway driving at higher speeds of the engine [1]. Generally, octane number increases when a fuel contains molecules with methyl branching, double bonds, aromatic rings [4], and oxygen content [94]. Combustion is a complex process in which hydrocarbon molecules produce intermediates which are subsequently transformed to stable products. The combustion process develops according to a radical chain mechanism. The evolution of combustion process and operating kinetic mechanism depend highly on temperature. In a combustion process, an end-gas undergoes a two-stage ignition process where a cool flame proceeds to hot ignition. Cool flames appear in a temperature range that transition from low temperature to high temperature mechanism occurs [95]. Mechanisms at low and high temperatures should be studied distinctly because different branching agents are effective at each condition.

High temperature chemistry accounts for combustion efficiency and pollutant emissions [5]. In contrast, low temperature chemistry accounts mainly for ignition properties of a fuel. At low temperature chemistry, there is a convoluted competition between multiple chemical reactions involving alkylperoxy radicals (ROO•) [96]. Westbrook et al. [97] developed a detailed chemical kinetic reaction mechanism including both high and low temperature reaction pathways to describe oxidation of n-alkanes larger than n-heptane. In this study, it was shown that at temperatures below 1200 K, for all hydrocarbons the reaction is initiated by H-abstraction from the alkane by oxygen molecules to generate alkyl (•R) and hydroperoxy (•OOH) radicals. At a temperature range between 500 to 600 K, alkyl radicals react quickly with oxygen molecules to produce peroxyalkyl radicals (ROO•). Peroxyalkyl radicals (ROO•) can form peroxide species and small radicals via several pathways. Peroxides play an important role because they have an O-OH bond which can

be simply cracked and form two radicals. Subsequently, these radicals attack alkane molecules to generate alkyl radicals. Increases in number of active radicals cause an exponential acceleration of reaction rates to a certain temperature. However, as temperature increases, the reversible reaction of alkyl radicals with oxygen molecules gets reversed and proceeds in the opposite direction in favor of alkenes formation led to overall reaction rate reduction. This behavior is called negative-temperature coefficient (NTC). In a NTC region ignition delay time increases as temperature increases; i.e., the fuel is less reactive in this region [98]. It typically occurs in a temperature range from 500 to 850 K [99]. The rate of these reactions inhibits cool flame reactions at higher temperatures which results in a slight temperature increase at low temperature chemistry.

If an air-fuel mixture undergoes a transition to high temperature chemistry prior to consumption by the propagating turbulent flame, knocking would occur. Hence, as stated earlier, differences in octane ratings arise from differences in low-temperature combustion chemistry of fuels; i.e., fuel knock performance is directly related to the fuel's ability to undergo cool flame reactions to allow autoignition at lower temperatures [5]. Therefore, fuels with lower octane numbers have more propensity to undergo an ignition process at low-temperature conditions.

The major attraction of ethanol is its high octane rating. Blending ethanol with gasoline increases the octane value without affecting the three-way catalytic converter [100]. Some measurements have shown a non-linear dependence of RONs on the ethanol content on a mole and a volume basis [101-103]. In some cases, the blending effect is synergistic, meaning that the octane number of the blend is greater than that obtained by linear interpolation from that of pure constituents [101]. However, in some other studies an antagonistic blending effect (octane number lower than that obtained by linear interpolation from that of its pure constituents) was observed [102]. These differences have their roots in ethanol content and composition of gasoline. Ethanol

content is an important factor because Cooperative Fuel Research (CFR) engines are sensitive to the charge cooling, and ethanol with its high HoV exhibits a significant charge cooling effect [103]. Gasoline composition is also important. For instance, antagonism of ethanol and aromatics (such as toluene) can act against synergism of ethanol and paraffins with respect to the octane number [102].

In terms of combustion chemistry, this is how ethanol increases octane number: neat ethanol shows no significant H- abstraction below 725 K; thus, subsequent reactions of CH_3CHO only occur at temperatures above conditions favoring negative temperature coefficient behavior; i.e., the presence of ethanol reduces alkylperoxy and hydro-peroxy-alkyl reactions (cool-flame reactions). As a conclusion, pure ethanol resists oxidation at low temperatures. However, when ethanol is present as a blend component along with hydrocarbons such as paraffins that are known to exhibit low temperature chemistry, the scenario is different. For instance, oxidation of E85-n-heptane15 blend at 628 K and 12.5 atm begins with oxidation of paraffins to produce HO_2 radicals that subsequently react with ethanol to form C_2H_5O radicals. Then these radicals rapidly react with O_2 to form acetaldehyde while regenerating HO_2. The HO_2 stimulates a near-straight chain HO_2 induction cycle (the two latter reactions) to produce CH_3CHO and H_2O_2 as intermediate products. However, low temperature reactions of CH_3CHO are not significant channels of carbon flux; Instead, low temperature reactivity is imparted by slower radical propagation and branching reactions associated with n-heptane which serves to slow the rate of radical pool growth [104]. It shows that blends of ethanol with hydrocarbons exhibit no global low temperature reactivity. Therefore, it can be stated that ethanol provides a sink of reactive species (OH radicals) that disturb the chain branching of the hydrocarbon fuels at low temperature conditions [5] and consequently increases octane number of the blend compared to the base-gasoline.

Propanol and butanol exhibit similar behavior as ethanol at low temperatures, but pentanol is the lowest molecular weight alcohol that exhibits high reactivity at low temperatures because the inhibiting effect of hydroxyl group decreases due to the longer hydrocarbon chain [104]. However, some of the highly branched higher alcohols have high octane rating values [14, 105]. As already mentioned, it is the high temperature chemistry that accounts for the combustion efficiency and emissions. In contrast to low temperature, alcohols have higher reactivity than their corresponding hydrocarbon at high temperatures [106] resulting in a higher turbulent premixed flame speed [107]. It is shown that high temperature reactivity of all linear normal alcohols longer than methanol (ethanol to n-octanol) is similar [108].

2.4.2. Alcohol effect on volatility

In general, hydrocarbons and polar compounds with similar volatility can form positive azeotropes. For instance, ethanol can form azeotropes with C5-C8 hydrocarbons (alkanes, olefins, aromatics) with boiling points in the range from 30 °C to 120 °C. The resulting azeotropes have vapor pressures higher than ideal solution vapor pressures obtained from Raoult's law. Formation of azeotropes is a function of pressure such that a higher pressure results in more azeotrope production and vice versa [109]. When a hydrocarbon is heavy with high boiling point, more ethanol is required to form an azeotrope and the resultant azeotrope would have higher boiling point compared to azeotropes derived from ethanol and light hydrocarbons. This explains why alkanes can lower the azeotrope boiling point more than aromatics of similar volatility while saturated cyclic hydrocarbons lie between the alkanic and aromatic azeotropes [109].

The key SI engine fuel characteristic for a good driveability is volatility, which is the tendency to vaporize. Vapor pressure, vapor lock index and distillation curve are parameters characterizing the volatility.

Vapor pressure is the most important property for cold-start and warm-up driveability. If vapor pressure is low, an engine may have to crank a long time before it starts or even may not start at all. Vapor pressure should be high enough to avoid cold-start problems while not too high to cause vapor lock and evaporative emissions [110]. Reid vapor pressure (RVP) is the vapor pressure over the liquid level at a temperature of 100°F (37.8 °C) while the volume ratio of the vapor and liquid phase of the sample is 4:1 (ASTM D 323). RVPs of alcohols are far less than gasoline. However, blending highly polar lower alcohols (up to certain ratios) with gasoline forms a near-azeotropic mixture with higher RVP than the base-gasoline. The highest RVPs are observed with relatively low concentrations of lower alcohols (5-10 vol %) [9]. Utilization of higher alcohols as co-solvents in blends is a viable option to control the RVP.

Vapor lock is a problem that occurs when the liquid fuel turns into gas phase in the fuel delivery system. It mostly happens in carbureted engines because this problem has been addressed in modern vehicles with utilization of high pressure injection systems. The ASTM standard for SI engine fuels (ASTM D4814) specifies minimum temperatures at which the vapor-to-liquid ratio equals 20 ($T_{V/L=20}$) to avoid vapor lock and carburetor icing [111].

The distillation curve is a plot of the boiling temperature of a fluid mixture versus the volume fraction distilled and can be related to many parameters such as engine starting ability especially in cold weather, vehicle drivability, fuel system icing and vapor lock, fuel injection schedule, fuel autoignition, and even exhaust emissions such as carbon monoxide, particulates, nitrogen oxides, and unburned hydrocarbons [112-114]. Front end volatility (T0 to T20) gives information about the cold start, engine warm-up, evaporative emissions, and vapor lock. Midrange volatility (T20 to T90) can be used to interpret warm up, acceleration, and cold weather performance ability of a fuel. Information regarding tail end volatility (T90 to end-point) is used

to estimate propensity for deposits formation and oil dilution [114]. Typical gasoline is composed of compounds with boiling points ranging from 20 to 225 °C. The ASTM D4814 sets maximum levels for T10, T90, and end-point distillation temperatures and a range for T50 to guarantee smooth driveability and avoid cold-start and oil dilution problems. Trespassing T10 and end-point limitations can cause cold start problems and oil dilution, respectively. The range for T50 is set to ensure the balance between low and high boiling point compounds [115].

Addition of lower alcohols causes a significant reduction, especially in the first 50% evaporated fraction, because of near-azeotropic behavior which is evident as a localized plateau region in the distillation curve. It is called near azeotropic mixture because it is not a true azeotrope with a totally flat distillation curve. For this behavior, in the United States, refiners vary butane concentrations in the fuel blends containing ethanol to meet summer and winter front end distillation specifications. In contrast, higher alcohols exert smaller changes to the distillation characteristics due to the less polarity compared to the lower alcohols. Higher alcohols increase the front-end distillation temperatures due to the higher boiling points and lower vapor pressures. The impact of alcohols on T10 is minor for low to medium blending ratios; however, changes in T10 become considerable when high concentrations of alcohols are used. T50 is always affected by the presence of alcohols but changes in T90 are negligible [116-118].

2.4.3. Alcohol effect on lower heating value

Due to the relatively high oxygen content of lower alcohols, the energy per unit mass is significantly lower than gasoline [119]. Significant lower LHV combined with higher stoichiometric air-fuel ratio of lower alcohols compared to gasoline adversely impacts fuel economy. However, it should be considered that combustion of lower alcohols is more complete than gasoline due to their high oxygen content. Furthermore, lower alcohols have very high HoV

which causes a reduction in temperature in the intake manifold in port fuel injection systems (improved volumetric efficiency) and charge cooling effect in direct injection SI engines [120]. Also, excellent anti-knock characteristic of lower alcohols allows engine to operate at higher compression ratios which increases the power-output notably. Thus, considering higher HoV, more complete combustion and higher octane value of lower alcohols, it is possible to obtain even better brake specific fuel consumption (BSFC) with blends of lower alcohols than gasoline. Higher alcohols not only exhibit very comparative advantages but also have closer LHV to gasoline due to the longer hydrocarbon chain and less oxygen content [119].

2.4.4. Alcohol effect on water tolerance

C1 to C3 alcohols are completely miscible in water, but miscibility decreases with higher alcohols [119]. Gasoline and water are not soluble in each other; however, when an alcohol is blended into gasoline, some measurable water can also dissolve [115]. Based on ASTM D8418, water tolerance is defined as the ability to absorb small quantities of water without creating a separate phase in the fuel. Water can enter the fuel system a variety of ways. If water tolerance of a fuel is sufficiently high to absorb all the available water at a given ambient temperature, no secondary phase forms. A trace amount of water in a fuel will have no notable adverse effects on engine components and acts as an inert diluent in the combustion process and only acts to decrease fuel economy [119]. However, water as a separate phase can have negative impacts. If lower alcohols with high affinity to water are blended with gasoline, after phase separation, water starts absorbing the alcohol from the blend. As a result, the octane value of the fuel blend will decrease, a part of oxygen content will be gone, and volatility will be changed because of lower oxygenate content. Furthermore, the separated phase is corrosive to engine parts and its presence in the combustion process can damage the engine because it makes the fuel- air mixture leaner which

requires a higher temperature to combust [109]. However, phase separation in case of higher alcohols can be less damaging because the separated phase mostly consists of water which goes to the bottom of the fuel tank due to its higher density and when pumped into the engine and can stop the engine from running, but with no significant damage to the engine. Therefore, a fuel with a high water tolerance at low temperatures is desirable. Solubility of water in alcohol-gasoline blends depends on parameters such as the temperature, humidity, fuel (both gasoline fuel and alcohol) composition, and co-solvent [11]. For instance, fuels containing more aromatics and olefins are more miscible in water due to the Pi-bonding in their structures [109].

Although methanol is the most polar of the alcohols, methanol blends with gasoline have very low water tolerances. This behavior is attributed to the highly hygroscopic nature of methanol such that it is quickly absorbed by water and phase separation occurs. However, ethanol has a more moderate hygroscopicity which results in a better water tolerance compared to methanol. Water tolerance of alcohol blends increases rapidly from methanol to propanol, but 1-butanol and t-butanol provide almost the same water tolerance as propanol [119, 121]. However, i-butanol blends have lower water tolerance compared to ethanol blends with the same blending ratio [122].

2.4.5. Alcohol effect on viscosity and density

Density is directly related to the amount of fuel injected to the cylinder so that using fuels with higher densities lead to higher amounts of injected fuel and therefore higher engine power [109].

Specific gravity of the gasoline increased with addition of alcohols (especially higher alcohols) which is a positive point [122]. The viscosity of a fuel needs to be within an acceptable range. If the viscosity of a fuel is high, larger droplets are formed during injection which results in a poor fuel atomization that increases the spray tip penetration and reduces the spray angle and

hence leads to a high exhaust emissions and engine deposits [11]. Moreover, high viscosity can be problematic at lower temperatures because of high resistance to flow [109]. In contrast, if the viscosity of a fuel is low, poor lubrication (engine parts' wearing) and injector leakage (waste of fuel and power output reduction) are possible consequences [11]. Viscosity of blends increases with increase in alcohol content with a non-linear trend and this increasing trend is more accentuated in case of higher alcohols [122].

2.5. Alcohol combustion chemistry

A detailed understanding of alcohol combustion chemistry is very informative in terms of fuel's ignition delay time, laminar flame speed, and emissions characteristics. These combustion features were analyzed by pyrolysis and oxidation reactors, shock tubes, rapid compression machines, and research engines. A comprehensive review on recent experimental studies on reaction kinetics under conditions relevant to ignition and combustion of alcohols was provided by Sarathy et al. [117].

2.6. Combustion and emission characteristics of alcohols

The key motivation for advancements in engine technologies has always been the increasingly-strict exhaust-emission regulations imposed to enhance air quality and improve human health. Given the stringent emission standards, refineries use oxygenates such as alcohols in their fuels to reduce contribution to harmful exhaust emissions while improving combustion characteristics [118]. Combustion and emissions of alcohols and alcohol-gasoline blends have been widely investigated. In general, use of alcohols has positive impact on exhaust emissions, brake thermal efficiency, heat release rate (HRR), and cylinder gas pressure [123].

Soot emissions are particularly damaging because particle sizes are below 10 μm which can penetrate deeper into the lungs [124]. Use of alcohols can cause a reduction in soot emissions,

but the exact chemical mechanism has not been understood yet [125]. Generally, it is believed that oxygen atoms isolate bonded carbons from the active radical pool responsible for soot formation. Although fuel composition has the most important effect on soot formation [126], other factors such as HoV, ignition property, boiling characteristics, and viscosity are also effective [127].

The oxides of nitrogen that are produced during combustion are NO, NO_2, and N_2O and are referred to as NO_x. NO_x emissions cause acid rain and eventual acidification of lakes and streams. In addition, NO_x can react with volatile organic compounds to form ozone which is a major cause of urban smog [124]. NO is the major product of combustion and is produced mainly by two mechanisms: Zel'dovich NO (thermal route) and Fenimore NO_x (prompt route). NO is the only oxide of nitrogen formed by Zel'dovich route; however, the Fenimore NO_x mechanism can produce NO, N_2O, and/or NO_2 [128]. The Zel'dovich mechanism consists of three reactions and the rate-limiting reaction is the one in which the nitrogen bond must be broken. Therefore, NO can be produced via Zel'dovich route only when combustion temperature exceeds 1800 K [129]. Favorable conditions for Zel'dovich NO formation are a slightly lean regime and high peak flame temperature [130]. In the Fenimore NO_x route, CH radicals are initiators and react with nitrogen molecules. Thus, hydrocarbons such as straight chain alkanes have more potential to produce NO_x via this mechanism. This mechanism consists of more reactions compared to Zel'dovich and is not strictly limited to high temperature conditions. Favorable conditions for this mechanism are rich regime and low to medium temperatures [131]. Since alcohols have lower energy content compared to the corresponding alkane fuels, the peak flame temperature would be lower under the same condition which results in lower NO_x emissions through the thermal mechanism [132]. Furthermore, presence of hydroxyl group reduces the number of CH radicals which are initiators for Fenimore NO_x mechanism [125]. Therefore, alcohols produce less NO compared to their

corresponding alkanes. To accurately address the effect of alcohols on NO_x emissions, some issues must be considered. The high octane value of alcohols allows a higher compression ratio to be used resulting in a higher end-gas temperature and pressure. The high temperature at the end of the compression stroke provides an appropriate situation for Zel'dovich NO formation. In contrast, high HoV of alcohol fuel have charge cooling effect in direct injection systems which can reduce NO_x emission [120]. Furthermore, engine speed and load are also effective by changing air-fuel ratio in the cylinder.

Carbon monoxide at adequately high levels can be deadly by reducing the oxygen-carrying capacity of the blood. CO emissions are controlled primarily by the air-fuel equivalence ratio. Unburned hydrocarbons (UHC) emissions are mainly caused by the unburned air-fuel mixture because of poor mixing and incomplete combustion. Since both CO and UHC emissions represent incomplete combustion and lost chemical energy, improving the combustion process can cause reduction in both [133]. Oxygen content of alcohols makes the combustion more complete and can reduce CO and UHC emissions, but design and operating factors such as air-fuel ratio, speed, and load can make differences. For example, effect of alcohols on CO and UHC emissions reduction is more notable during the open-loop mode (fuel rich regime) than closed-loop mode (stoichiometric ratio) [133, 134].

CO_2 emissions highly depend on hydrogen-carbon ratio of the fuel and engine efficiency [38]. Thus, higher hydrogen-to-carbon ratio of alcohols compared to gasoline may reduce CO_2 emissions under the same condition, but other effective parameters must be considered as well to make a correct conclusion [133].

Use of alcohols in gasoline changes combustion pathway toward production of oxygenates such as formaldehyde, acetaldehyde and ketones. Potential increase in such oxygenate emissions is an ongoing concern although these are not regulated emissions [135].

2.6.1. General effects of alcohols on combustion and emission characteristics

For this project, an extensive review was conducted on the effect of C1-C4 alcohol addition to the gasoline on engine performance and emissions and a brief conclusion is provided here:

- The major attraction of C1-C4 alcohols are their high octane ratings. These alcohols exhibit low reactivity at low temperatures because of hydroxyl group.
- Although C1-C4 alcohols have lower LHVs relative to the gasoline, addition of alcohols can increase the brake thermal efficiency for the following reasons: combustion of these alcohols usually completes earlier than gasoline due to the higher laminar flame speeds which decreases heat losses from the cylinder; oxygen content contributes to a more complete combustion; due to the high HoV, alcohols absorb more heat from the cylinder in the compression stroke decreasing required work for compression; higher octane rating of alcohols allows higher CR to be used.
- Peak pressure (PP) and peak heat release rate of gasoline blends containing C1-C4 alcohols usually occur sooner than the gasoline due to the faster flame propagation speed. Generally, if the engine is tuned for alcohols blends, the magnitudes of PP and peak HRR are also higher.
- Lower LHV of alcohol blends usually increases the BSFC. However, optimization of engine parameters for alcohol blends especially CR and spark timing corresponding to maximum brake torque may result in a better BSFC than gasoline.

- High HoV of alcohols has the charge cooling effect in the intake manifold which usually improves the volumetric efficiency in comparison to the gasoline.
- CO and UHC emissions are usually reduced for following reasons: lower stoichiometric air/fuel and C/H ratios of alcohols which reduces the demand for oxygen and avoid formation of fuel-rich zones; smaller number of C–C bond which restrain the formation of incomplete resultants; oxygen content increases the oxygen-to-fuel ratio in the fuel-rich regions and accordingly a more complete combustion occurs; the concentration of the higher boiling point gasoline fractions in the fuel is reduced.
- CO_2 emissions are usually decreased because alcohol blends contain lower carbon atom. However, a more complete combustion may even increase the CO_2 compared to the gasoline.
- Effect of alcohol addition to the gasoline on NO_x is not clear because lower LHV and higher HoV of alcohols usually results in lower EGT which can reduce the NO_x emissions. However, more oxygen is available for NO_x production. In addition, optimizing engine parameters to gain a higher efficiency with alcohol blends may have the penalty of NO_x emissions increase.
- Generally, addition of alcohols reduces PM emissions because of aromatic dilution effect and oxygen content which can remove a great deal of carbon atoms from radical pools responsible for soot formation.
- Unregulated carbonyl emissions are usually increased with use of alcohol-gasoline blends.

References

1- Bergthorson, J. M., & Thomson, M. J. (2015). A review of the combustion and emissions properties of advanced transportation biofuels and their impact on existing and future engines. Renewable and Sustainable Energy Reviews, 42, 1393-1417.

2- Reddy, H. K., Muppaneni, T., Rastegary, J., Shirazi, S. A., Ghassemi, A., & Deng, S. (2013). ASI: Hydrothermal extraction and characterization of bio-crude oils from wet chlorella sorokiniana and dunaliella tertiolecta. Environmental Progress and Sustainable Energy, 32(4), 910–915.

3- Kirchstetter, T. W., Singer, B. C., Harley, R. A., Kendall, G. R., & Ghan, W. (1996). Impact of oxygenated gasoline use on California light-duty vehicle emissions. Environmental Science and Technology, 30(2), 661–670.

4- Surisetty, V. R., Dalai, A. K., & Kozinski, J. (2011). Alcohols as alternative fuels: An overview. Applied Catalysis A: General. 404, 1-11.

5- Christensen, E., Yanowitz, J., Ratcliff, M., & McCormick, R. L. (2011). Renewable oxygenate blending effects on gasoline properties. Energy and Fuels, 25(10), 4723–4733.

6- U.S. Environmental Protection Agency. Renewable Fuel Standard Program (RFS2) Regulatory Impact Analysis. EPA-42-R-10-006, February 2010.

7- Lee, S. K., Chou, H., Ham, T. S., Lee, T. S., & Keasling, J. D. (2008). Metabolic engineering of microorganisms for biofuels production: from bugs to synthetic biology to fuels. Current Opinion in Biotechnology, 19(6), 556-63.

8- Surisetty, V. R., Dalai, A. K., & Kozinski, J. (2011). Alcohols as alternative fuels: An overview. Applied Catalysis A: General. 404, 1-11.

9- Hansen, A. C., Zhang, Q., & Lyne, P. W. L. (2005). Ethanol-diesel fuel blends - A review. Bioresource Technology, 96(3), 277–285.

10- Agarwal, A. K. (2007). Biofuels (alcohols and biodiesel) applications as fuels for internal combustion engines. Progress in Energy and Combustion Science.33. 233–271.

11- Lee, S. K., Chou, H., Ham, T. S., Lee, T. S., & Keasling, J. D. (2008). Metabolic engineering of microorganisms for biofuels production: from bugs to synthetic biology to fuels. Current Opinion in Biotechnology, 19(6), 556-63.\

12- Bergthorson, J. M., & Thomson, M. J. (2015). A review of the combustion and emissions properties of advanced transportation biofuels and their impact on existing and future engines. Renewable and Sustainable Energy Reviews, 42, 1393-1417.

13- Yan, Y., & Liao, J. C. (2009). Engineering metabolic systems for production of advanced fuels. Journal of Industrial Microbiology and Biotechnology. 6(4), 471-479.

14- Mainguet, S. E., & Liao, J. C. (2010). Bioengineering of microorganisms for C3 to C5 alcohols production n. Biotechnology JournaL, 5(12), 1297–1308.

15- Dahmen, M., & Marquardt, W. (2016). Model-Based Design of Tailor-Made Biofuels. Energy and Fuels, 30(2), 1109–1134.

16- Andersen, V. F., Anderson, J. E., Wallington, T. J., Mueller, S. A., & Nielsen, O. J. (2010). Vapor pressures of alcohol-gasoline blends. In Energy and Fuels, 24, 3647–3654.

17- Ratcliff, M. A., Luecke, J., Williams, A., Christensen, E., Yanowitz, J., Reek, A., & McCormick, R. L. (2013). Impact of higher alcohols blended in gasoline on light-duty vehicle exhaust emissions. Environmental Science and Technology, 47(23), 13865–13872.

18- Lapuerta, M., García-Contreras, R., Campos-Fernández, J., & Dorado, M. P. (2010). Stability, lubricity, viscosity, and cold-flow properties of alcohol-diesel blends. Energy and Fuels, 24(8), 4497–4502.

19- Gautam M, Martin DW, Carder D. Emissions characteristics of higher alcohol/gasoline blends. Proc Inst Mech Eng Part A J Power Energy 2000;214:165–82. doi:10.1243/0957650001538263.

20- Arapatsakos,C., Karkanis, A.N., Panagiotis D. Sparis, P.D. (2003), Behavior of a Small Four-Stroke Engine Using as Fuel Methanol - Gasoline Mixtures. SAE International. doi:10.4271/2003-32-0024.

21- Abu-Zaid, M., Badran, O., Yamin, J.(2004). Effect of Methanol Addition on the Performance of Spark Ignition Engines. Energy & Fuels, 18 (2), 312-315.

22- Geng, P., Zhang, H., & Yang, S. (2015). Experimental investigation on the combustion and particulate matter (PM) emissions from a port-fuel injection (PFI) gasoline engine fueled with methanol-ultralow sulfur gasoline blends. Fuel, 145, 221–227. http://doi.org/10.1016/j.fuel.2014.12.067

23- Bilgin, A., & Sezer, I. (2008). Effects of methanol addition to gasoline on the performance and fuel cost of a spark ignition engine. Energy and Fuels, 22(4), 2782–2788. http://doi.org/10.1021/ef8001026

24- Yanju,W., Shenghua,L., Hongsong, L., Rui,y., Jie, L., Ying, W.(2008).Effects of Methanol/Gasoline Blends on a Spark Ignition Engine Performance and Emissions .Energy & Fuels 2008, 22, 1254–1259.

25- Çelik, M.B., Özdalyan, B., Alkan, F. (2011) The use of pure methanol as fuel at high compression ratio in a single cylinder gasoline engine. Fuel.90 (4):1591–8.

26- Chmielniak, T., & Sciazko, M. (2003). Co-gasification of biomass and coal for methanol synthesis. Applied Energy, 74(3–4), 393–403. https://doi.org/10.1016/S0306-2619(02)00184-8

27- Olah, G. A., Goeppert, A., & Prakash, G. K. S. (2009). Beyond Oil and Gas: The Methanol Economy: Second Edition. Beyond Oil and Gas: The Methanol Economy: Second Edition. https://doi.org/10.1002/9783527627806

28- Hamelinck, C. N., & Faaij, A. P. C. (2002). Future prospects for production of methanol and hydrogen from biomass. Journal of Power Sources, 111(1), 1–22. https://doi.org/10.1016/S0378-7753(02)00220-3

29- Lange, J.-P. (1997). Perspectives for Manufacturing Methanol at Fuel Value. Industrial & Engineering Chemistry Research, 36(10), 4282–4290. https://doi.org/10.1021/ie9607762

30- Lange, J. P. (2001). Methanol synthesis: A short review of technology improvements. Catalysis Today, 64(1–2), 3–8. https://doi.org/10.1016/S0920-5861(00)00503-4

31- Xu, J. G., & Froment, G. F. (1989). Methane Steam Reforming, Methanation and Water-Gas Shift .1. Intrinsic Kinetics. Aiche Journal, 35(1), 88–96. https://doi.org/10.1002/aic.690350109

32- Watanabe, H., & Otaka, M. (2006). Numerical simulation of coal gasification in entrained flow coal gasifier. Fuel, 85(12–13), 1935–1943. https://doi.org/10.1016/j.fuel.2006.02.002

33- Park, D., & Lee, J. (2013). Biological conversion of methane to methanol. Korean Journal of Chemical Engineering, 30(5), 977–987. https://doi.org/10.1007/s11814-013-0060-5

34- Xin, J., Cui, J., Niu, J., Hua, S., Xia, C., Li, S., & Zhu, L. (2004). Production of methanol from methane by methanotrophic bacteria. Biocatalysis and Biotransformation, 22(3), 225–229. https://doi.org/10.1080/10242420412331283305

35- Trudewind, C. A., Schreiber, A., & Haumann, D. (2014). Photocatalytic methanol and methane production using captured CO2 from coal-fired power plants. Part i - A Life Cycle Assessment. Journal of Cleaner Production, 70, 27–37. https://doi.org/10.1016/j.jclepro.2014.02.014

36- Patel, S. K. S., Mardina, P., Kim, S. Y., Lee, J. K., & Kim, I. W. (2016). Biological methanol production by a type II methanotroph methylocystis bryophila. Journal of Microbiology and Biotechnology, 26(4), 717–724. https://doi.org/10.4014/jmb.1601.01013

37- Obert, R., & Dave, B. C. (1999). Enzymatic conversion of carbon dioxide to methanol: Enhanced methanol production in silica sol-gel matrices [5]. Journal of the American Chemical Society. https://doi.org/10.1021/ja991899r

38- Ganesh, I. (2014). Conversion of carbon dioxide into methanol - A potential liquid fuel: Fundamental challenges and opportunities (a review). Renewable and Sustainable Energy Reviews, 31, 221–257. https://doi.org/10.1016/j.rser.2013.11.045

39- Jadhav, S. G., Vaidya, P. D., Bhanage, B. M., & Joshi, J. B. (2014). Catalytic carbon dioxide hydrogenation to methanol: A review of recent studies. Chemical Engineering Research and Design. https://doi.org/10.1016/j.cherd.2014.03.005

40- Wang, W. H., Himeda, Y., Muckerman, J. T., Manbeck, G. F., & Fujita, E. (2015). CO2 Hydrogenation to Formate and Methanol as an Alternative to Photo- and Electrochemical CO2 Reduction. Chemical Reviews. https://doi.org/10.1021/acs.chemrev.5b00197

41- Masum BM, Masjuki HH, Kalam MA, Rizwanul Fattah IM, M Palash S, Abedin MJ. Effect of ethanol-gasoline blend on NOx emission in SI engine. Renew Sustain Energy Rev 2013;24:209–22. doi:10.1016/j.rser.2013.03.046.

42- Bielaczyc, P., Szczotka, A., Woodburn, J. A Study of Gasoline-Ethanol Blends Influence on Performance and Exhaust Emissions from a Light- Duty Gasoline Engine.SAE Technical Paper, (2012-01-1052).

43- Szulczyk KR, McCarl BA, Cornforth G. Market penetration of ethanol. Renew Sustain Energy Rev 2010;14:394–403. doi:10.1016/j.rser.2009.07.007.

44- Schifter, I., Diaz, L., Rodriguez, R., G??mez, J. P., & Gonzalez, U. (2011). Combustion and emissions behavior for ethanol-gasoline blends in a single cylinder engine. Fuel, 90(12), 3586–3592. https://doi.org/10.1016/j.fuel.2011.01.034.

45- Bergthorson, J. M., & Thomson, M. J. (2015). A review of the combustion and emissions properties of advanced transportation biofuels and their impact on existing and future engines. Renewable and Sustainable Energy Reviews, 42, 1393-1417.

46- Wallner, T. and Miers, S., .Combustion Behavior of Gasoline and Gasoline/Ethanol Blends in a Modern Direct-Injection 4-Cylinder Engine.2008. SAE Technical Paper No. 2008-01-0077.

47- Demirbas A. Competitive liquid biofuels from biomass. Appl Energy 2011;88:17–28. doi:10.1016/j.apenergy.2010.07.016.

48- Koç, M., Sekmen, Y., Topgu¨l, T., & Yu¨ cesu, H. S. (2009). The effects of ethanol-unleaded gasoline blends on engine performance and exhaust emissions in a spark-ignition engine. Renewable Energy, 34(10), 2101–2106.

49- Kumar, A., Khatri, D. S., & Babu, M. K. G. (2009). An Investigation of Potential and Challenges with Higher Ethanol-gasoline Blend on a Single Cylinder Spark Ignition Research Engine. SAE Technical Paper, (2009-01–0137). https://doi.org/10.4271/2009-01-0137

50- Demirbas A. Competitive liquid biofuels from biomass. Appl Energy 2011;88:17–28. doi:10.1016/j.apenergy.2010.07.016.

51- Williams PRD, Cushing CA, Sheehan PJ. Data available for evaluating the risks and benefits of MTBE and ethanol as alternative fuel oxygenates. Risk Anal 2003;23:1085–115. doi:10.1111/1539-6924.00384.

52- Wu T-N, Chang C-P, Wu T-S, Shen Y-H. Emission Characteristics of Ethanol Blending Fuels from a Laboratory Gasoline Engine. Sustain. Dev. Urban Infrastructure, Pts 1-3, vol. 253–255, 2013, p. 2227–30. doi:10.4028/www.scientific.net/AMM.253-255.2227.

53- Nigam PS, Singh A. Production of liquid biofuels from renewable resources. Prog Energy Combust Sci 2011;37:52–68. doi:10.1016/j.pecs.2010.01.003.

54- Shen CR, Liao JC. Metabolic engineering of Escherichia coli for 1-butanol and 1-propanol production via the keto-acid pathways. Metab Eng 2008;10:312–20. doi:10.1016/j.ymben.2008.08.001.

55- Rajesh Kumar, B., & Saravanan, S. (2016). Use of higher alcohol biofuels in diesel engines: A review. Renewable and Sustainable Energy Reviews. 60. 84-115

56- Sivasubramanian H, Pochareddy YK, Dhamodaran G, Esakkimuthu GS. Performance, emission and combustion characteristics of a branched higher mass, C3 alcohol (isopropanol) blends fuelled medium duty MPFI SI engine. Eng Sci Technol an Int J 2017;20:528–35. doi:10.1016/j.jestch.2016.11.013.

57- Bustard MT, McEvoy EM, Goodwin J a, Burgess JG, Wright PC. Biodegradation of propanol and isopropanol by a mixed microbial consortium. Appl Microbiol Biotechnol 2000;54:424–31. doi:10.1007/s002530000398.

58- Inokuma K, Liao JC, Okamoto M, Hanai T. Improvement of isopropanol production by metabolically engineered Escherichia coli using gas stripping. J Biosci Bioeng 2010;110:696–701. doi:10.1016/j.jbiosc.2010.07.010.

59- Liu K, Atiyeh HK, Stevenson BS, Tanner RS, Wilkins MR, Huhnke RL. Continuous syngas fermentation for the production of ethanol, n-propanol and n-butanol. Bioresour Technol 2014;151:69–77. doi:10.1016/j.biortech.2013.10.059.

60- Atsumi S, Liao JC. Directed evolution of Methanococcus jannaschii citramalate synthase for biosynthesis of 1-propanol and 1-butanol by Escherichia coli. Appl Environ Microbiol 2008;74:7802–8. doi:10.1128/AEM.02046-08.

61- Srirangan K, Liu X, Westbrook A, Akawi L, Pyne ME, Moo-Young M, et al. Biochemical, genetic, and metabolic engineering strategies to enhance coproduction of 1-propanol and ethanol in engineered Escherichia coli. Appl Microbiol Biotechnol 2014;98:9499–515. doi:10.1007/s00253-014-6093-9.

62- Kusakabe T, Tatsuke T, Tsuruno K, Hirokawa Y, Atsumi S, Liao JC, et al. Engineering a synthetic pathway in cyanobacteria for isopropanol production directly from carbon dioxide and light. Metab Eng 2013;20:101–8. doi:10.1016/j.ymben.2013.09.007.

63- Hirokawa Y, Suzuki I, Hanai T. Optimization of isopropanol production by engineered cyanobacteria with a synthetic metabolic pathway. J Biosci Bioeng 2015;119:585–90. doi:10.1016/j.jbiosc.2014.10.005.

64- Hanai T, Atsumi S, Liao JC. Engineered synthetic pathway for isopropanol production in Escherichia coli. Appl Environ Microbiol 2007;73:7814–8. doi:10.1128/AEM.01140-07.

65- C. Jin, M. Yao, H. Liu, C.F.F. Lee, J. Ji, Progress in the production and application of n-butanol as a biofuel, Renew. Sustain. Energy Rev. 15 (2011) 4080–4106. doi:10.1016/j.rser.2011.06.001.

66- Cooney C, Wallner T, McConnell S, Gillen JC, Abell C, Miers SA, et al. Effects of Blending Gasoline With Ethanol and Butanol on Engine Efficiency and Emissions Using a Direct-

Injection, Spark-Ignition Engine. ASME Conf Proc 2009;2009:157–65. doi:10.1115/ICES2009-76155.

67- C. Regalbuto, M. Pennisi, B. Wigg, D. Kyritsis, Experimental Investigation of Butanol Isomer Combustion in Spark Ignition Engines, SAE Tech. Pap. 2012-01-1271. 165 (2012) 612–626. doi:10.4271/2012-01-1271.

68- S.S. Merola, G. Valentino, C. Tornatore, L. Marchitto, In-cylinder spectroscopic measurements of knocking combustion inaSI engine fuelled with butanol-gasoline blend, Energy. 62 (2013) 150–161. doi:10.1016/j.energy.2013.05.056.

69- H. Wei, D. Feng, J. Pan, A. Shao, M. Pan, Knock characteristics of SI engine fueled with n-butanol in combination with different EGR rate, Energy. 118 (2017) 190–196. doi:10.1016/j.energy.2016.11.134.

70- Z. Chen, F. Yang, S. Xue, Z. Wu, J. Liu, Impact of higher n-butanol addition on combustion and performance of GDI engine in stoichiometric combustion, Energy Convers. Manag. 106 (2015) 385–392. doi:10.1016/j.enconman.2015.09.051.

71- A. Irimescu, Fuel conversion efficiency of a port injection engine fueled with gasoline-isobutanol blends, Energy. 36 (2011) 3030–3035. doi:10.1016/j.energy.2011.02.047.

72- A. Elfasakhany, Experimental investigation on SI engine using gasoline and a hybrid iso-butanol/gasoline fuel, Energy Convers. Manag. 95 (2015) 398–405. doi:10.1016/j.enconman.2015.02.022.

73- S.G. Davis, C.K. Law, Determination of and Fuel Structure Effects on Laminar Flame Speeds of C1 to C8 Hydrocarbons, Combust. Sci. Technol. 140 (1998) 427–449. doi:10.1080/00102209808915781.

74- Ji, C., Sarathy, S. M., Veloo, P. S., Westbrook, C. K., & Egolfopoulos, F. N. (2012). Effects of fuel branching on the propagation of octane isomers flames. Combustion and Flame, 159(4), 1426–1436. http://doi.org/10.1016/j.combustflame.2011.12.004

75- J.T. Moss, A.M. Berkowitz, M.A. Oehlschlaeger, J. Biet, V. Warth, P.A. Glaude, F. Battin-Leclerc, An experimental and kinetic modeling study of the oxidation of the four isomers of butanol., J. Phys. Chem. A. 112 (2008) 10843–10855. doi:10.1021/jp806464p.

76- W. Liu, A.P. Kelley, C.K. Law, Non-premixed ignition, laminar flame propagation, and mechanism reduction of n-butanol, iso-butanol, and methyl butanoate, Proc. Combust. Inst. 33 (2011) 995–1002. doi:10.1016/j.proci.2010.05.084.

77- Y.N. Zheng, L.Z. Li, M. Xian, Y.J. Ma, J.M. Yang, X. Xu, D.Z. He, Problems with the microbial production of butanol, J. Ind. Microbiol. Biotechnol. 36 (2009) 1127–1138. doi:10.1007/s10295-009-0609-9.

78- E.M. Green, Fermentative production of butanol-the industrial perspective, Curr. Opin. Biotechnol. 22 (2011) 337–343. doi:10.1016/j.copbio.2011.02.004.

79- S. Begum, Y. Dahman, Enhanced biobutanol production using novel clostridial fusants in simultaneous saccharification and fermentation of green renewable agriculture residues, Biofuels, Bioprod. Biorefining. 9 (2015) 529–544. doi:10.1002/bbb.1564.

80- D.R. Woods, The genetic engineering of microbial solvent production, Trends Biotechnol. 13 (1995) 259–264. doi:10.1016/S0167-7799(00)88960-X.

81- E. Galloni, G. Fontana, S. Staccone, F. Scala, Performance analyses of a spark-ignition engine firing with gasoline-butanol blends at partial load operation, Energy Convers. Manag. 110 (2016) 319–326. doi:10.1016/j.enconman.2015.12.038.

82- L.K. Bowles, W.L. Ellefson, Effects of butanol on Clostridium acetobutylicum, Appl. Environ. Microbiol. 50 (1985) 1165–1170.

83- B. Deng, J. Yang, D. Zhang, R. Feng, J. Fu, J. Liu, K. Li, X. Liu, The challenges and strategies of butanol application in conventional engines: The sensitivity study of ignition and valve timing, Appl. Energy. 108 (2013) 248–260. doi:10.1016/j.apenergy.2013.03.018.

84- T. Lütke-Eversloh, H. Bahl, Metabolic engineering of Clostridium acetobutylicum: Recent advances to improve butanol production, Curr. Opin. Biotechnol. 22 (2011) 634–647. doi:10.1016/j.copbio.2011.01.011.

85- O. V. Berezina, N. V. Zakharova, A. Brandt, S. V. Yarotsky, W.H. Schwarz, V. V. Zverlov, Reconstructing the clostridial n-butanol metabolic pathway in Lactobacillus brevis, Appl. Microbiol. Biotechnol. 87 (2010) 635–646. doi:10.1007/s00253-010-2480-z.

86- C.A. Tomas, J. Beamish, E.T. Papoutsakis, Transcriptional Analysis of Butanol Stress and Tolerance in Clostridium acetobutylicum, J. Bacteriol. 186 (2004) 2006–2018. doi:10.1128/JB.186.7.2006-2018.2004.

87- J.R. Borden, E.T. Papoutsakis, Dynamics of genomic-library enrichment and identification of solvent tolerance genes for Clostridium acetobutylicum, Appl. Environ. Microbiol. 73 (2007) 3061–3068. doi:10.1128/AEM.02296-06.

88- T.C. Ezeji, N. Qureshi, H.P. Blaschek, Butanol fermentation research: Upstream and downstream manipulations, Chem. Rec. 4 (2004) 305–314. doi:10.1002/tcr.20023.

89- T.C. Ezeji, N. Qureshi, H.P. Blaschek, Acetone butanol ethanol (ABE) production from concentrated substrate: Reduction in substrate inhibition by fed-batch technique and product inhibition by gas stripping, Appl. Microbiol. Biotechnol. 63 (2004) 653–658. doi:10.1007/s00253-003-1400-x.

90- T.C. Ezeji, N. Qureshi, H.P. Blaschek, Bioproduction of butanol from biomass: from genes to bioreactors, Curr. Opin. Biotechnol. 18 (2007) 220–227. doi:10.1016/j.copbio.2007.04.002.

91- P. Izák, K. Schwarz, W. Ruth, H. Bahl, U. Kragl, Increased productivity of Clostridium acetobutylicum fermentation of acetone, butanol, and ethanol by pervaporation through supported ionic liquid membrane, Appl. Microbiol. Biotechnol. 78 (2008) 597–602. doi:10.1007/s00253-008-1354-0.

92- T. Ezeji, N. Qureshi, H.P. Blaschek, Butanol production from agricultural residues: Impact of degradation products on Clostridium beijerinckii growth and butanol fermentation, Biotechnol. Bioeng. 97 (2007) 1460–1469. doi:10.1002/bit.21373.

93- S. Atsumi, A.F. Cann, M.R. Connor, C.R. Shen, K.M. Smith, M.P. Brynildsen, K.J.Y. Chou, T. Hanai, J.C. Liao, Metabolic engineering of Escherichia coli for 1-butanol production, Metab. Eng. 10 (2008) 305–311. doi:10.1016/j.ymben.2007.08.003.

94- C.R. Shen, E.I. Lan, Y. Dekishima, A. Baez, K.M. Cho, J.C. Liao, Driving forces enable high-titer anaerobic 1-butanol synthesis in Escherichia coli, Appl. Environ. Microbiol. 77 (2011) 2905–2915. doi:10.1128/AEM.03034-10.

95- Zhao, F., Lai, M. C., & Harrington, D. L. (1999). Automotive spark-ignited direct-injection gasoline engines. Progress in Energy and Combustion Science, 25(5), 437–562.

96- Yao, M., Zheng, Z., & Liu, H. (2009). Progress and recent trends in homogeneous charge compression ignition (HCCI) engines. Progress in Energy and Combustion Science. 35(5). 398–437.

97- Myung, C. L., & Park, S. (2012). Exhaust nanoparticle emissions from internal combustion engines: A review. International Journal of Automotive Technology. 13(1). 9−22.

98- Reitz, R.D. (2013). Directions in internal combustion engine research. Combustion and Flame. 160(1).1-8.

99- Alagumalai, A. (2014). Internal combustion engines: Progress and prospects. Renewable and Sustainable Energy Reviews. 38. 561–571.

100- Alkidas, A. C. (2007). Combustion advancements in gasoline engines. Energy Conversion and Management, 48(11), 2751–2761.

101- Yacoub,Y., Bata, R., Gautam, M. (1998). The performance and emission characteristics of C1-C5 alcohol-gasoline blends with matched oxygen content in a single-cylinder spark ignition engine. Proceedings of the Institution of Mechanical Engineers, Part A: Journal of Power and Energy, 212 (5), 363-379.

102- Lignola, P.G., Reverchon, E. (1987). Cool flames. Progress in Energy and Combustion Science. 13(1),75-96.

103- Westbrook, C. K., Pitz, W. J., Herbinet, O., Curran, H. J., & Silke, E. J. (2009). A comprehensive detailed chemical kinetic reaction mechanism for combustion of n-alkane hydrocarbons from n-octane to n-hexadecane. Combustion and Flame, 156(1), 181–199.

104- Westbrook, C. K., Pitz, W. J., Herbinet, O., Curran, H. J., & Silke, E. J. (2009). A comprehensive detailed chemical kinetic reaction mechanism for combustion of n-alkane hydrocarbons from n-octane to n-hexadecane. Combustion and Flame, 156(1), 181–199.

105- Battin-Leclerc, F. (2008). Detailed chemical kinetic models for the low-temperature combustion of hydrocarbons with application to gasoline and diesel fuel surrogates. Progress in Energy and Combustion Science. 34(4). 440–498.

106- Gibson, C., Gray, P., Griffiths, J. F., & Hasko, S. M. (1985). Spontaneous ignition of hydrocarbon and related fuels: A fundamental study of thermokinetic interactions. Symposium (International) on Combustion, 20(1), 101–109.

107- Canakci, M., Ozsezen, A. N., Alptekin, E., & Eyidogan, M. (2013). Impact of alcohol-gasoline fuel blends on the exhaust emission of an SI engine. Renewable Energy, 52, 111–117.

108- Anderson, J.E., Leone, T.G., Shelby, M.H., Wallington, T.J., Bizub, J.J., Foster, M., et al.(2012) Octane numbers of ethanol–gasoline blends: measurements and novel estimation method from molar composition. SAE Technical Paper 2012-01- 1274; 2012. doi:http://dx.doi.org/10.4271/2012-01-1274.

109- Anderson, J. E., Kramer, U., Mueller, S. A., & Wallington, T. J. (2010). Octane numbers of ethanol- and methanol-gasoline blends estimated from molar concentrations. Energy and Fuels, 24(12), 6576–6585.

110- Foong, T.M., Morganti, K.J., Brear, M.J., da Silva, G., Yang, Y., Dryer, F.L..(2013). The effect of charge cooling on the RON of ethanol/gasoline blends. SAE International Journal of Fuels and Lubricants .6.34–43.

111- Francis M. Haas, Marcos Chaos, & Frederick L. Dryer. (2009). Low and intermediate temperature oxidation of ethanol and ethanol--PRF blends: An experimental and modeling study. Combustion and Flame, 156(12), 2346–2350.

112- Qi, D. H., Liu, S. Q., Liu, J. C., Zhang, C. H., & Bian, Y. Z. (2005). Properties, performance, and emissions of methanol-gasoline blends in a spark ignition engine. Proceedings of the Institution of Mechanical Engineers Part D-Journal of Automobile Engineering, 219(D3), 405–412. http://doi.org/10.1243/095440705x6659

113- Cai, L., Uygun, Y., Togbe, C., Pitsch, H., Olivier, H., Dagaut, P., & Sarathy, S. M. (2015). An experimental and modeling study of n-octanol combustion. Proceedings of the Combustion Institute, 35(1), 419–427. http://doi.org/10.1016/j.proci.2014.05.088

114- Ji, C., Sarathy, S. M., Veloo, P. S., Westbrook, C. K., & Egolfopoulos, F. N. (2012). Effects of fuel branching on the propagation of octane isomers flames. Combustion and Flame, 159(4), 1426–1436. http://doi.org/10.1016/j.combustflame.2011.12.004

115- Heufer, K. A., Bugler, J., & Curran, H. J. (2013). A comparison of longer alkane and alcohol ignition including new experimental results for n-pentanol and n-hexanol. Proceedings of the Combustion Institute, 34(1), 511–518. http://doi.org/10.1016/j.proci.2012.05.103

116- Mužíková, Z., Pospíšil, M., & Šebor, G. (2009). Volatility and phase stability of petrol blends with ethanol. Fuel, 88(8), 1351–1356. http://doi.org/10.1016/j.fuel.2009.02.003

117- Chevron. "Motor Gasoline Technical Review", Chevron Product Company, USA, Downloaded November 2016, http://www.chevron.com/

118- U.S. Environmental Protection Agency. Renewable Fuel Standard Program (RFS2) Regulatory Impact Analysis. EPA-42-R-10-006, February 2010.

119- Sholes , Kevin R. AU - Odaka , Matsuo AU - Goto , Yuichi AU - Ishii , Hajime AU - Suzuki , Hisakazu JO – (2002)- SAE International T1 - Study of the Effect of Boiling Point on Combustion and PM Emissions in a Compression Ignition Engine Using Two-Component n-Paraffin Fuels PY

120- Smith, B. L., & Bruno, T. J. (2007). Improvements in the measurement of distillation curves. 3. Application to gasoline and gasoline + methanol mixtures. Industrial and Engineering Chemistry Research, 46(1), 297–309.

121- Smith, B. L., Ott, L. S., & Bruno, T. J. (2008). Composition-explicit distillation curves of diesel fuel with glycol ether and glycol ester oxygenates: Fuel analysis metrology to enable decreased particulate emissions. Environmental Science and Technology, 42(20), 7682–7689.

122- Christensen, E., Yanowitz, J., Ratcliff, M., & McCormick, R. L. (2011). Renewable oxygenate blending effects on gasoline properties. Energy and Fuels, 25(10), 4723–4733.

123- Andersen, V. F., Anderson, J. E., Wallington, T. J., Mueller, S. A., & Nielsen, O. J. (2010). Distillation Curves for Alcohol-Gasoline Blends. In Energy and Fuels (Vol. 24, pp. 2683–2691).

124- Sarathy, S. M., OBwald, P., Hansen, N., & Kohse-HBinghaus, K. (2014). Alcohol combustion chemistry. Progress in Energy and Combustion Science. 44. 40-102. http://doi.org/10.1016/j.pecs.2014.04.003

125- Gautam, M., & Martin II, D. W. (2005). Combustion characteristics of higher-alcohol/gasoline blends. Proceedings of the Institution of Mechanical Engineers, Part A: Journal of Power and Energy, 214(5), 497–511. http://doi.org/10.1243/0957650001538047

126- Wallner T, Ickes A, Lawyer K. Analytical assessment of C2-C8 alcohols as spark-ignition engine fuels. Lect. Notes Electr. Eng., vol. 191 LNEE, 2013, p. 15–26. doi:10.1007/978-3-642-33777-2_2.

127- Costagliola, M.A., De Simio, L., S., Iannaccone, M., Prati, V., Combustion efficiency and engine out emissions of a S.I. engine fueled with alcohol/gasoline blends, Applied Energy, 111, 1162-1171.

128- Peng C, Lewis KC, Stein FP. Water solubilities in blends of gasoline and oxygenates. Fluid Phase Equilib 1996;116:437–44. doi:10.1016/0378-3812(95)02916-8.

129- Pereira CC, Pasa VM. Effect of alcohol and copper content on the stability of automotive gasoline. Energy & Fuels. 2005 Mar 16;19(2):426-32.

130- Muharrem Eyidogan, Ahmet Necati Ozsezen, Mustafa Canakci, Ali Turkcan, Impact of alcohol–gasoline fuel blends on the performance and combustion characteristics of an SI engine, Fuel, Volume 89, Issue 10, October 2010, Pages 2713-2720, ISSN 0016-2361, http://dx.doi.org/10.1016/j.fuel.2010.01.032

131- Kohse-Höinghaus, K., Oßwald, P., Cool, T. A., Kasper, T., Hansen, N., Qi, F., … Westmoreland, P. R. (2010). Biofuel combustion chemistry: From ethanol to biodiesel. Angewandte Chemie - International Edition. http://doi.org/10.1002/anie.200905335

132- Schofield, K. (2012). Large scale chemical kinetic models of fossil fuel combustion: Adequate as engineering models-no more, no less. Energy and Fuels, 26(9), 5468–5480.

133- Williams, P. R. D., Inman, D., Aden, A., & Heath, G. A. (2009). Environmental and sustainability factors associated with next-generation biofuels in the U.S.: What do we really know? Environmental Science and Technology.43 (13). 4763-4775. http://doi.org/10.1021/es900250d

134- Serinyel, Z., Black, G., Curran, H. J., & Simmie, J. M. (2010). A Shock Tube and Chemical Kinetic Modeling Study of Methy Ethyl Ketone Oxidation. Combustion Science and Technology, 182(4–6), 574–587. http://doi.org/10.1080/00102200903466129

135- Bowman,C.T. (1992).Control of combustion-generated nitrogen oxide emissions: Technology driven by regulation, Symposium (International) on Combustion, 24 (1), 1992, 859-878. http://dx.doi.org/10.1016/S0082-0784(06)80104-9

136- Turns, S. R. (1995). Understanding NOx formation in nonpremixed flames: Experiments and modeling. Progress in Energy and Combustion Science, 21(5), 361–385. http://doi.org/10.1016/0360-1285(94)00006-9

137- Law, C.K. (2006). Combustion Physics. Cambridge University Press.

138- Moskaleva,L. and Lin, M. (2000). The spin-conserved reaction CH+N2 → H+NCN: A major pathway to prompt NO studied by quantum/statistical theory calculations and kinetic modeling of rate constant. Proceedings of the Combustion Institute. 28(2). 2393–2401.

139- Watson, G. M. G., Versailles, P., & Bergthorson, J. M. (2016). NO formation in premixed flames of C1-C3 alkanes and alcohols. Combustion and Flame, 169, 242–260. http://doi.org/10.1016/j.combustflame.2016.04.015

140- Gravalos, I., Moshou, D., Gialamas, T., Xyradakis, P., Kateris, D., & Tsiropoulos, Z. (2013). Emissions characteristics of spark ignition engine operating on lower higher molecular mass alcohol blended gasoline fuels. Renewable Energy, 50, 27–32. http://doi.org/10.1016/j.renene.2012.06.033

141- Gautam, M., Martin II, D. W., & Carder, D. (2000). Emissions characteristics of higher alcohol/gasoline blends. Proceedings of the Institution of Mechanical Engineers, Part A: Journal of Power and Energy, 214(2), 165–182. http://doi.org/Doi 10.1243/0957650001538263

142- Lynd, L. R. (1996). OVERVIEW AND EVALUATION OF FUEL ETHANOL FROM CELLULOSIC BIOMASS: Technology, Economics, the Environment, and Policy. Annual Review of Energy and the Environment, 21(1), 403–465. http://doi.org/10.1146/annurev.energy.21.1.403

3 Development and Application of a Fuel Property Database for Mono-Alcohols as Fuel Blend Components for Spark Ignition Engines [*]

3.1. Summary

Alcohols are attractive as fuels for spark ignition engines due to their high octane values and potentially positive influence on performance and emission. Although methanol, ethanol, and butanol have been widely studied, many other alcohols could be considered for use as fuels or in fuel blends. However, it is not possible to experimentally investigate the fuel potential of all of these molecules. The goals of this study were to develop a systematic product design methodology and to use that approach to identify alcohols that might be suitable for blending with gasoline for use in SI engines. A detailed database was developed with 13 fuel properties of all possible molecular structures of saturated linear, branched, and cyclic alcohols (C1-C10) with one hydroxyl group. Where available, fuel property data were obtained from literature reports. Property estimation methods were exploited for compounds without property data. An initial decision framework for removing problematic compounds was devised and applied. Next, the database and decision framework were used to evaluate alcohols suitable for blending in gasoline for spark ignition engines. Three scenarios were considered: (a) low-range (up to 15 vol%) blends with minimal constraints; (b) ideal low-range blends; and (c) high-range (greater than 40 vol%) blends. The two low-range blend cases resulted in the identification of 48 and 46 alcohols as good candidates for blending with gasoline. In the case of high-range blending, only six alcohols were

[*] *Submitted as "Development and Application of a Fuel Property Database for Mono-Alcohols as Fuel Blend Components for Spark Ignition Engines" by Saeid Aghahossein Shirazi, Thomas D. Foust and Kenneth F. Reardon.*

found to be suitable: 1-propanol, 1-butanol, 2-methyl-1-propanol (iso-butanol), 2-methyl-2-pentanol, 3-methyl-3-pentanol, and (1-methylcyclopropyl)methanol. The complete database is a resource for other fuel development objectives. The approach used in this study could be modified for the evaluation of other classes of fuel molecules and for other engine types and fuel blending goals.

3.2. Introduction

Gasoline is the most common transportation fuel for spark ignition (SI) engines derived from different cuts within the distillation column of a petroleum refinery [1]. At least for the near future, it remains the most cost-effective fuel [2]. However, the uncertainty for petroleum supplies, oil price fluctuation, and adverse environmental impacts associated with using fossil fuels are motivations for supplementing the gasoline fuel supply with renewable and sustainable sources of energy [3]. Biofuels have the capability to replace a substantial fraction of fossil fuels [4]. Among biofuels, alcohols (mainly ethanol) and biodiesels (fatty acid methyl esters) have been commercialized broadly as gasoline and diesel blending agents, respectively [5].

Given increasingly stringent emissions standards, it is vital to find alternative, low-emission fuels along with improvements in engine technologies. The "substantially similar" rule published by EPA stated that alcohols can be blended with gasoline up to an oxygen content of 3.7 mass% [6]. Alcohols are particularly attractive as fuels for spark ignition engines due to the high research octane (RON) values and the potentially positive influence on performance and emission [7]. The term “lower alcohols” is used to refer to methanol and ethanol, while “higher alcohols” typically refers to any linear or branched non-cyclic saturated alcohol with higher molecular weight; here we include cyclic alcohols in the “higher” alcohol class. Several review articles have summarized the general reduction of engine emissions and positive effects on knock performance

and thermal efficiency that can be achieved by using alcohols in the fuel blends [2, 7, 8]. These reviews noted that the impact of alcohols on engine performance and emissions is very dependent on the alcohol properties and engine type hence having a database that categories the properties of alcohols will be very useful. The oxygen content of alcohols can lead to a more homogenous and complete combustion which will lead to reduced soot formation, given appropriate combustion conditions. In general, soot emission decreases with alcohol-gasoline blends because the oxygen atoms reduce the number of carbon atoms that are active in the radical pool responsible for soot formation [2]. However, in vehicles in actual driving conditions, many factors such as engine type and operating loads can complicate this effect such that alcohols blended with gasoline have been shown to increase or decrease soot emissions in vehicle tests. The more complete combustion attained with alcohol-gasoline blends leads to reductions in CO and unburned hydrocarbon (UHC) emissions [7]. In addition to reduced emissions, alcohols have the potential to increase thermal efficiency due to their high heat of vaporization (HoV) and to diminish the Brake Specific Fuel Consumption (BSFC) because a higher compression ratio can be used [9].

Systematic product design methodologies are new approaches to avoid expensive and time-consuming trial-and-error experimental methods. In these approaches, computational methods are used to first generate possible molecules and then to narrow down potential candidates to a reasonable number for experimentation. These methodologies have been used in several fuel development projects. Dahmen and Wolfgang [10] introduced a framework for model-based fuel design. In their study, a potential product spectrum from bio-derived intermediates (mainly lignocellulosic biomass fermentation products) was created and then screened for biofuel candidates with the help of computational property predictions for use in spark ignition and compression ignition engines. A fuel design framework was developed by Hechinger et al. [11]

combining generation of molecular structures with a stepwise reduction to find promising candidates based on fuel-relevant properties. Ulonska et al. [12] presented a methodology to find the most promising platform chemicals gained by fermentation of lignocellulosic biomass for biofuel production. Yunus et al. [13] developed a computer-aided methodology to design different tailor-made gasoline blends that match the constraints for target properties using rigorous models. Hashim et al. [14] developed an integrated computational and experimental technique to design low cost/low emission, tailor-made diesel-like biofuel blends from palm oil that satisfy specified target properties. Phoon et al. [15] formulated green diesel blend candidates that meet the property constraints for a diesel-like fuel by an implementation of the decomposition-based computer-aided approach. Simasatitkul et al. [16] developed a systematic design methodology to produce possible products from a bio-based renewable source. As a part of their work, an economic analysis was implemented to find the most cost-effective production process. The application of the methodology was demonstrated for biodiesel and fatty alcohol production. Hada et al. [17] employed chemometric techniques to identify novel additives to compensate for the poor low-temperature flow properties and oxidative stability of biodiesel. Finally, Kashinath et al. [18] presented a computer-aided technique to design economically and environmentally sustainable tailor-made sets of feasible mixtures presenting green-diesel blends that meet the desirable constraints for target properties. These examples illustrate the potential of molecular design methodologies for fuel applications; however, most have been developed for diesel fuels.

While lower alcohols have been intensively studied for gasoline blending, the potential of higher and cyclic alcohols have been less examined as fuels or fuel blend components for SI engines. The goals of this study were to develop a systematic product design methodology and to use it to identify alcohols that might be advantaged for blending with gasoline for use in SI engines.

To accomplish these goals, all possible structures of linear, branched, and cyclic alcohol molecules (C1-C10) with one hydroxyl group and no double bond were generated computationally. For each alcohol, toxicity and 13 fuel properties were determined through literature/databases or predictive models. Subsequently, a two-stage screening procedure was used to find the most promising alcohol molecules suitable for blending with gasoline for three scenarios. The open design approach used here is different than other approaches in that it was based only on fuel properties and was not biased by considerations of alcohol production methods or current availability.

3.3. Methods

3.3.1. Database development

The structures of all possible isomers of linear, branched, and cyclic saturated mono-alcohols from C1 to C10 were generated using the molecular structure generator Molgen [19]. Toxicity information and thirteen physiochemical properties important for SI engine performance were then obtained for each of these alcohols: boiling point, melting point, peroxide-forming potential, water solubility, anaerobic biodegradability, research octane number (RON), vapor pressure, flash point, viscosity, density, surface tension, lower heating value (LHV), and HoV. Where available, property data were obtained from literature reports and databases of experimental values. If measured values were not available, predictive models based on the chemical behavior of similar classes of molecules methods were exploited. EPI Suite^{TM} [20] is a series of quantitative structure-activity relationship models based on the regression of experimental data to predict the effect of chemical structures on the modeled parameter. Boiling and melting points, vapor pressures, water solubility, anaerobic biodegradability (BIOWIN7), viscosity, density, surface tension, and flash point were predicted via EPI Suite^{TM}. BIOWIN7 is a model that predicts the probability of rapid anaerobic biodegradability in the presence of heterogeneous microorganisms.

The LHV was predicted by a model suggested by Hechinger et al [21]. The HoV was estimated via ACD Structure Elucidator v15.01 (Advanced Chemistry Development, Inc.) [22]. A group contribution modeling method based on the assumption of functional group additivity for derived cetane number (DCN) prediction [23] in combination with the relationship between DCN and RON [24] was used to estimate RON for the proposed alcohols. Known peroxide-forming alcohols from a published list [25] were eliminated, and secondary alcohols were removed since they are potential peroxide formers. Material safety data sheets were used to establish physical and health hazard categories.

3.3.2. First-stage database screening

The objective of the initial database screening was to eliminate any problematic alcohols that would be unsuitable for any fuel application in SI engines. To pass this stage, alcohols were required to satisfy the property constraints shown in Table 3.1 for boiling point, melting point, RON, peroxide formation, and anaerobic biodegradability. The property ranges were then applied sequentially in a decision process (Figure 3.1).

The United States Occupational Health and Safety Administration (OSHA) has published the Hazard Communication Standard (HCS), which defines a set of physical and health hazard categories [26]. Fire and explosion hazards were not included in the screening because the infrastructure for handling SI fuels is designed for gasoline, and alcohols are less flammable and explosive. Reproductive toxicity and carcinogenicity were considered for the initial screening. However, none of the alcohols are known or suspected carcinogens or reproductive toxins. Other classes of OSHA hazards are noted in the database but were not used as screening criteria.

In addition, other fuel properties, namely corrosion potential, stability, solubility, and flash point were not considered in this initial screen. Since methanol and ethanol, which are more

corrosive than the other alcohols, are already in the market, corrosion was not used as an initial elimination criterion. The stability and solubility of any new molecule in a hydrocarbon blend is a critical concern. However, since methanol and ethanol have lower stability and solubility in gasoline than higher alcohols [27], it is not necessary to consider the stability and solubility factor in this screening. The flash point is a strong indication of flammability and is important for safety during storage and distribution. Since the flash point of gasoline is usually less than 40 °C and the infrastructure is compatible with that value, it is not necessary to consider this as one of the factors for screening of these less-flammable alcohols [28].

Table 3.1. Property values used in the first-stage screening.

Property	**Required range**	**Comments**
Boiling point	25 – 190 °C	Ensure liquid at room temperature; compatibility with ASTM D4814
Melting point	≤ –10 °C	Guarantee fluidity in the terminal environment
RON	≥ 98	SI engines require a finished fuel with high RON to demonstrate a high efficient performance.
Peroxide formation		Molecules with known peroxide formation (List B of peroxide former compounds) present safety risks; Secondary alcohols are likely peroxide formers
Anaerobic biodegradation probability	≥ 0.2	Rejected if less than 0.2 with the water solubility greater than or equal to 10,000 mg/L

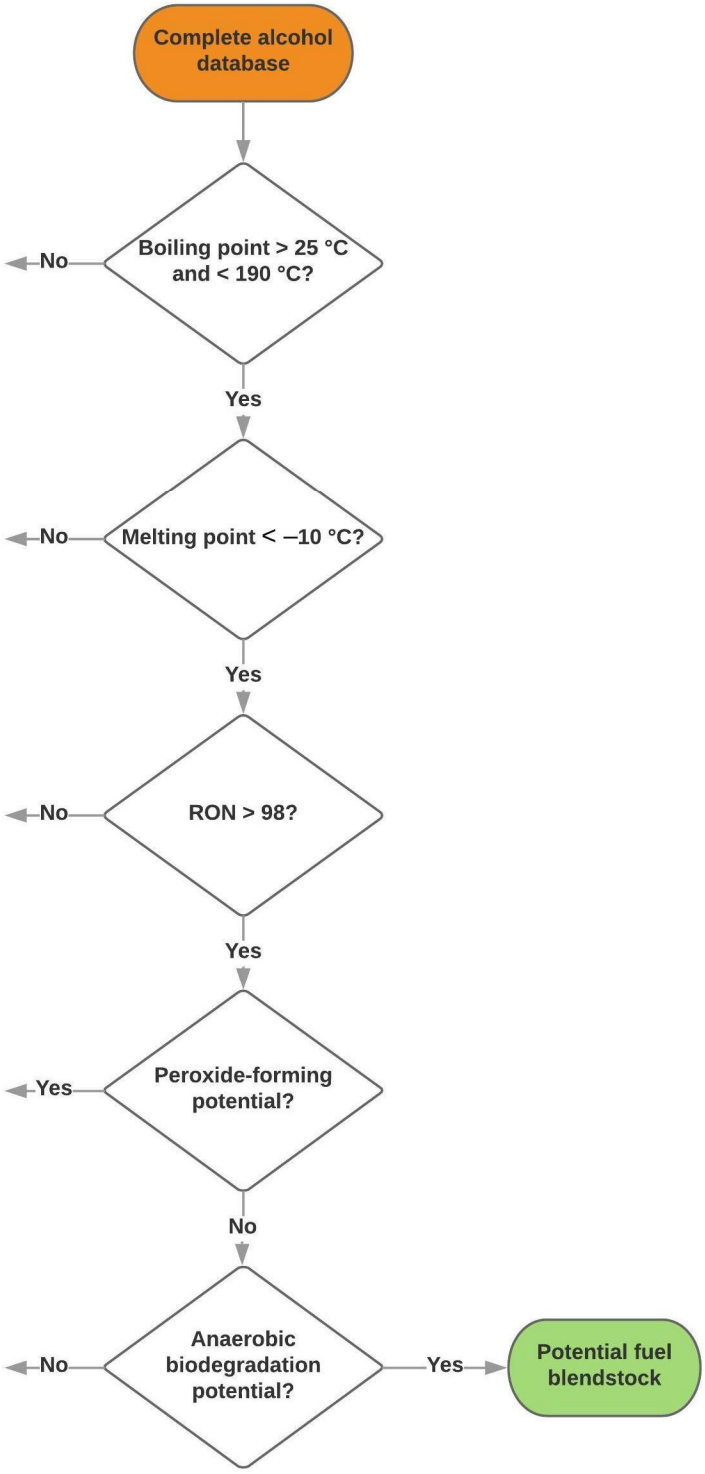

Figure 3.1. Decision framework for the first-stage screening of the alcohol database.

3.3.3 Additional screening criteria for low- and high-range blending

The utility of the database and methodology was explored with three scenarios, each implemented as a second stage of screening. The goal of the first scenario was to identify alcohols suitable for blending with gasoline at levels up to 15 vol% ("low range") using minimal constraints. The second scenario again dealt with low-range blends but added more stringent requirements related to volatility. The goal of the third scenario was to identify alcohols that could be blended with gasoline at levels greater than 40 vol% ("high range"). All cases started from the list of alcohols that passed the initial screen. The property constraints for each scenario are shown in Table 3.2 and summaries of the screening process for each scenario are depicted in Figure 3.2.

Table 3.2. Property values used for screening in the three scenarios. All fuel candidates passed the initial screening prior to these requirements.

	Requirements			
Property	**Low-range blends: basic**	**Low-range blends: stringent**	**High-range blends**	**Comments**
Reid vapor pressure		Rejected if RVP blending value > 0	Rejected if RVP < 0.5 kPa	Low range: avoid high evaporative emissions High range: avoid cold start problems
Boiling point			Rejected if >165 °C	Compatibility with T90 of ASTM D4814
Melting point			Rejected if > -20 °C	
LHV	Rejected if LHV < 25 MJ/kg		Rejected if < 30 MJ/kg	Avoid high fuel consumption
Kinematic viscosity			Rejected if > 5 mm^2/s	Avoid large droplets

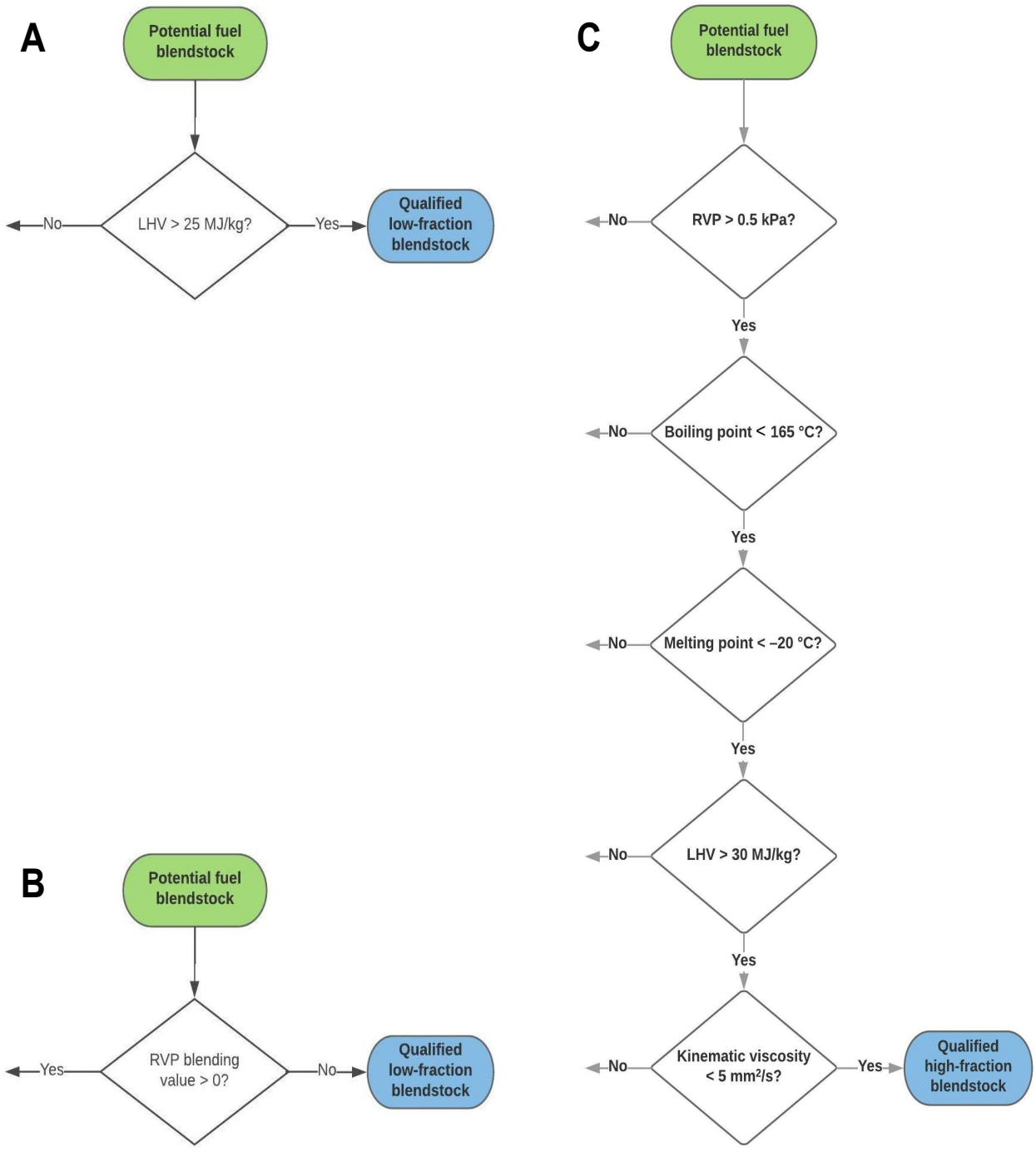

Figure 3.2. Decision framework for the screening of the alcohol database. A: Base-case low-range blends (Scenario 1). B: Ideal low-range blends (Scenario 2). C: High-range blends (Scenario 3).

3.4. Results and Discussion

3.4.1. Characteristics of the alcohol database

The compelete database of C1-C10 linear, branched and cyclic saturated mono-alcohols contains 943 species. For each alcohol, fuel-relevant physiochemical properties were obtained as experimental data from literature and databases or through the use of predictive models. Many of the higher non-cyclic and cyclic alcohols appear never to have been synthesized and/or purified, and thus no experimental data are available. For those species, properties were estimated via group contribution methods [20-24] based on the molecular structure, as described in Section 3.1.1. The complete database is available at http://projects-web.engr.colostate.edu/co-optima/alcohol-database-CSU.xlsx .

3.4.2. Initial database screening

3.4.2.1. Rationale for first-stage screening

Any alternative fuel that is introduced into existing engines and infrastructure must fit within standard fuel property ranges for petroleum-based transportation fuels to avoid prohibitive capital investments for replacing the current infrastructure [29]. The initial screening was designed to eliminate any fuel molecules with unacceptable properties. The rationale for each criterion in the initial screening is discussed below.

Melting and boiling points: The melting point is important to determine if the fuel can be handled in the terminal environment, especially in winter. Since gasolines typically have a cloud point below -50 °C, a melting point criterion of less than -10 °C is a reasonable window for selecting alcohols. The boiling point is also a key specification for SI engine fuels. For gasoline and other fuel mixtures, the distillation curve is used instead of boiling point [30]. To identify a reasonable range of alcohol boiling points, we focused on specific ranges of the distillation curve.

The front-end volatility (T0 to T20) is of importance for cold start, mid-range volatility (T20 to T90) is vital for warming up, and tail-end volatility (T90 to end point) is essential for performance when the engine is hot [31]. Typical gasoline is composed of compounds with boiling points ranging from 20 to 225 °C [32]. The ASTM D4814 [33] sets maximum levels for T10, T90, and end-point distillation temperatures, and a range for T50 to guarantee smooth drivability and elimination of cold-start and oil dilution problems. Therefore, the lower boiling limit was defined as 25 °C, to ensure the liquid phase at room temperature, and the upper limit was chosen to be 190 °C, which is the maximum allowed temperature for T90 in the ASTM D4814. No non-cyclic alcohol smaller than C9 was rejected for boiling point constraints. Other than 2-methyl-2-propanol, 2,2-dimethyl-1-propanol, 2-methyl-2-butanol,and 3,3-dimethyl-2-butanol, which have unusually high melting points, no non-cyclic alcohol smaller than C7 was found with a melting point higher than the defined limit. Most of non-cyclic higher molecular weight alcohols were rejected due to their high boiling and melting points. Most cyclic alcohols suffer from weak fluidity (high melting point) and high boiling points.

Ignition properties: The fuel for SI engines must be resistant to autoignition to avoid knocking, a sharp rise in pressure that is not timed properly with the combustion event can damage the engine. The risk of knock is accentuated in downsized and turbocharged engines [34]. The octane rating is an index to measure the ignition quality of a fuel. Fuels with a high octane number are desired because they avoid knocking in SI engines, and because such fuels allow a higher compression ratio to be used, resulting in higher engine power output. RON is always greater than MON, and the difference between them is the sensitivity (S), an important parameter in modern engines. It was shown that the anti-knock quality of a fuel is best characterized by the Octane Index (OI) [35]. The OI is defined as $OI = RON - K \times S$, in which K is an empirical engine parameter.

This index combines fuel sensitivity and engine conditions to more accurately describe autoignition than RON or MON alone. However, since K for normally aspirated port fuel injection SI engines is about zero [36] and MON is difficult to predict, RON was used in this study as the criterion for knock resistance. RON generally increases when the fuel contains molecules with methyl branching, double bonds, aromatic rings [29], and oxygen content [37].

Blending gasoline with lower alcohols substantially increases the octane value without adversely affecting the three-way catalytic converter [38]. For example, the addition of ethanol to lead-free gasoline increases the RON by 5 units for each 10% ethanol addition [38]. When lower alcohols are blended with gasoline, oxygenated molecules act as a sink of reactive species (OH radicals) that reduce the chain branching reactions of hydrocarbon fuel under the low-temperature combustion regime that control autoignition in a SI engine and eventually retards ignition of the blend [39]. Propanol and butanol isomers similarly increase the octane value, but n-pentanol is the smallest higher alcohol that exhibits significant low-temperature chemistry and decreases the inhibiting effect of the hydroxyl group on low-temperature reactions due to the larger hydrocarbon chain [2]. However, some of highly branched higher alcohols have high octane numbers and have been considered as potential gasoline additives [29]. Since modern SI engines require a finished fuel with high RON to achieve high efficient performance, a cut-off of 98 RON was selected. Most of the non-cyclic higher molecular weight alcohols did not pass this threshold (and were also rejected due to their high boiling and melting points). However, some of highly branched larger alcohols with appropriate fluidity passed the octane rating requirement.

Peroxide formation: The OSHA HCS categories describe the intrinsic hazards associated with materials, but changes that may occur over time, such as peroxide forming potential, are not addressed. Peroxides are a class of highly reactive (unstable) chemicals that can be formed during

storage of certain compounds [40]. Therefore, alcohols that exhibit peroxide formation during storage must be avoided as fuel blending components. Eight of the original set of alcohols are known peroxide formers and were eliminated. Since secondary alcohols can form peroxides, especially when the concentration is high [25], these alcohols cannot be distilled or evaporated without first testing for the presence of peroxides at least every six months. Hence, all secondary alcohols were also removed as potential peroxide formers.

Anaerobic biodegradation: There is always the risk for release of fuels to the environment; hence, it is important for a fuel to be biodegradable and present little opportunity for impacting human health or the environment. Biodegradability is a measure of the rate at which compounds can be broken down through the actions of microorganisms. Fuel spills commonly occur in groundwater and surface water sites where the contact with atmosphere is limited; thus, anaerobic biodegradability is an important factor. Compounds that are both difficult to degrade anaerobically and highly soluble in water present a risk to the environment. Since there is no standard for acceptable levels of anaerobic biodegradability, alcohols with an anaerobic biodegradation probability (BIOWIN7) greater than 0.2 and water solubility greater than 10,000 mg/L were rejected. Seven alcohols, all either C6 or C7 non-cyclic alcohols, were eliminated based on these criteria.

3.4.2.2. Outcome of initial screening

Following the screening procedure illustrated in Figure 3.1, a reduced database of 49 alcohols (34 non-cyclic and 15 cyclic alcohols) was obtained (Table S3.1). All of the cyclic alcohols that passed the initial screening contain rings with three to six carbons, but not more.

A similar study [41] was conducted as a part of the DOE Co-Optimization of Fuels and Engines Program (Co-Optima) [42]. In that work, 470 molecules (with known production

pathways from biomass) representing 14 chemical families (including alcohols) were assessed for their potential as SI engine fuels or blendstocks. The screening limits used were same as our initial screening criteria for melting point, toxicity, biodegradation, and ignition quality. However, for boiling point, 20°C and 165 °C were used as lower and upper limits, respectively. In addition, only known rapid peroxide formers were removed, while in our methodology, we stringently screened out secondary alcohols as well. The Thrust I study yielded a set of 41 blendstocks including nine alcohols (methanol, ethanol, 1-propanol, 2-propanol, 1-butanol, 2-butanol, iso-butanol, 2-methyl-2-pentanol, and 2-pentanol). Seven of these alcohols also passed our initial screening; the exceptions are 2-propanol and 2-pentanol, which were removed in our study because they are secondary alcohols and thus potential peroxide formers.

3.4.3. Scenario 1: Low-range alcohol blends, base case

At low blending ratios, the effect of the alcohol on combustion-related properties (e.g., LHV, density, and viscosity) is not significant. However, volatility, hygroscopicity, and miscibility are affected at this level of alcohol content and have direct impacts on evaporative emissions, handling, and storage. Thus, in order to find ideal potential blendstocks some restrictions must be applied on these properties. In case of alcohols, the oxygen content (molar fraction) directly affects these properties. Alcohols with high oxygen content are known to cause an increase in the RVP of the blend when relatively low concentrations of these alcohols are used [43]. In addition, low LHV and phase separation in the presence of water is another problematic issue with such alcohols. However, ethanol has been already introduced to the market and blended at 10 vol % in nearly the entire US gasoline supply. Therefore, in the first scenario with a realistic approach, only methanol is removed given its lower LHV relative to ethanol. This results in a list of 48 alcohols: namely, all of those that passed the first-stage screening except methanol.

3.4.4. Scenario 2: Low-range alcohol blends, stringent case

3.4.4.1. Rationale for screening

The criterion applied for Scenario 2 is that the RVP blending value cannot be larger than zero (Table 3.2, Figure 3.2). Vapor pressure is the most critical property for SI engine fuels [44] and directly impacts cold-start and warm-up drivability. If the vapor pressure is low, an engine may have to be cranked a long time before it starts or even may not start. The vapor pressure should be high enough to avoid cold-start problems while not so high as to cause vapor lock and evaporative emissions [44]. While the pure component RVP of all of the alcohols is less than that of gasoline, addition of alcohols to gasoline may form near-azeotropic mixtures with non-ideal behavior and higher volatility. Because the volatility of a blend depends both on the alcohol and the blending level, we defined the RVP blending value as difference between RVP of the blend and that of base gasoline. The requirement for this scenario is that the RVP blending value be zero or less for blends in this low range.

Andersen et al. [43] demonstrated that gasoline blends with methanol, ethanol, and propanol isomers have RVP blending values greater than zero over certain concentration ranges. However, that study and one from Christensen et al. [45] showed that higher alcohols led to RVP blending values less than zero, regardless of alcohol concentration. The trend of the RVP blending value with alcohol carbon number for 5 and 10 vol% blends in gasoline (Figure S3.1) demonstrates that C5 and higher mono-alcohols always have negative RVP blending values. All C4 alcohols except 2-methyl-2-propanol (tert-butanol) also have negative RVP blending values.

No lower bound for vapor pressure was applied because there is no standard minimum limit identified for gasoline-like fuels, and the effect of a low level of a low vapor pressure alcohol would not have a detrimental effect on the RVP of the blend.

The near-azeotropic behavior of alcohol-gasoline blends is also evident as a localized plateau region in the distillation curve and is more accentuated in blends containing lower alcohols due to their higher polarity. The lower alcohols reduce the front-end distillation temperatures significantly, which affects the composition of the first 50% evaporated fraction. In contrast, higher alcohols increase the front-end distillation temperatures due to their higher boiling points and lower vapor pressure. The tail-end volatility for blends of gasoline with both lower and higher alcohols tends to be lower than that of the base gasoline [46]. In the distillation curve, changes in T10 are considerable when high concentrations of lower (more polar) alcohols are used. T50 is always significantly affected by the presence of alcohols with high to moderate polarity. The changes in T90 compared to the base gasoline are negligible [46]. Alcohols with polarity high enough to cause the distillation curve of the blend to be sub-optimal are a concern. However, with the limit for RVP blending value, these species are already removed.

Other essential properties at low blending levels are hygroscopicity and miscibility in gasoline. Lower alcohols are hygroscopic and absorb moisture from the atmosphere when staying in a fuel tank for a long time. Phase separation (immiscibility) occurs when an alcoholic blend contains more water than its water tolerance at a given temperature. It usual happens at low temperatures and leads to the generation of a corrosive mixture at the bottom of the tank, which causes corrosion to the fuel injection system [47]. In contrast, higher alcohols are less hygroscopic because the hydrocarbon chain is larger [48]. However, since these issues are satisfied in parallel with the cutoff criterion set for RVP blending value, no separate limits were used for hygroscopicity or miscibility of alcohols in gasoline.

No other constraints were applied for low-range blends because it was assumed that the low concentration of the alcohol component would not significantly change parameters other than

those considered here.

3.4.4.2. Candidate alcohols for low-range blends

Following the application of the screening criteria for this scenario, a set of 46 alcohols was obtained that have the potential to be used in this ideal low-range blending scenario (Tables 3.3 and S3.2). 1-Butanol was the only linear alcohol that qualified, while many branched higher alcohols with six to ten carbons were found to be suitable. Several C7-C8 cyclic alcohols containing rings with three to six carbons, but not more, also qualified. Several C7-C8 cyclic alcohols containing rings with three to six carbons, but not more, also qualified.

Notably, methanol and ethanol are not among these alcohols. The screening rules were set to identify blending alcohols with ideal physical and chemical characteristics, and do not take into account practical issues such as availability. Methanol and ethanol were removed because they increase vapor pressure at low concentrations [43], and also reduce the front-end distillation temperatures significantly [46]. The latter phenomenon affects the first 50% evaporated fraction, resulting in cold start problems [46]. The latter phenomenon affects the first 50% evaporated fraction, resulting in cold start problems [46]. In addition to those criteria, methanol and ethanol are relatively insoluble in gasoline in the presence of water leading to phase separation at low temperatures and subsequently corrosion. This problem can be minimized by using additives [49]. Two of the 46 candidate alcohols, 1-butanol and 2-methyl-1-propanol (iso-butanol), have been studied previously for blending with gasoline in this concentration range [50-56]. Table 3.4 provides a summary of these studies on the performance and emission characteristics of various SI engines fueled with these blends. No reports could be found in the literature on studies involving the other alcohols identified in this screening.

Table 3.3. List of alcohols with potential to be blended at low (<15%) range in gasoline.

Linear and branched alcohols		Cyclic alcohols
1-Butanol	2,3,4-Trimethyl-3-pentanol	(1-Methylcyclopropyl)methanol
2-Methyl-1-propanol	2,4,4-Trimethyl-2-pentanol	(2,2-Dimethylcyclopropyl)methanol
2-Methyl-2-pentanol	2,3,4-Trimethyl-2-pentanol	2-Cyclopentylethanol
3-Methyl-3-pentanol	2,3,4-Trimethyl-1-pentanol	2-Cyclopropyl-2-butanol
2,2-Dimethyl-1-butanol	3-Ethyl-2-methyl-3-pentanol	(1-Ethylcyclobutyl)methanol
2,3-Dimethyl-1-butanol	3,4,4-Trimethyl-1-hexanol	1,3-Dimethylcyclopentanol
3,3-Dimethyl-1-butanol	2,5,5-Trimethyl-1-hexanol	1,2-Dimethylcyclopentanol
4,4-Dimethyl-1-pentanol	4,5,5-Trimethyl-1-hexanol	2-Cyclobutyl-2-propanol
3,3-Dimethyl-1-pentanol	3,5,5-Trimethyl-3-hexanol	Cyclohexylmethanol
2-Ethyl-2-methyl-1-butanol	3-Ethyl-2,4-dimethyl-3-pentanol	1-Isopropylcyclopentanol
2,3,3-Trimethyl-1-butanol	2,4,6-Trimethyl-4-heptanol	2-Cyclopropyl-3-methyl-2-butanol
2,2,3-Trimethyl-1-butanol	2,3,4,5-Tetramethyl-3-hexanol	2-Cyclopropyl-2-pentanol
3,4-Dimethyl-3-hexanol	4-Ethyl-2,3-dimethyl-3-hexanol	(2,3,4-Trimethylcyclobutyl)methanol
2,2-Dimethyl-1-hexanol	3-Isopropyl-2,4-dimethyl-3-pentanol	3-Cyclopropyl-3-pentanol
2,4,4-Trimethyl-1-pentanol	3-Methyl-2-(2-methyl-2-propanyl)-1-pentanol	1-Cyclopentyl-2-propanol
2,2,4-Trimethyl-1-pentanol		

Table3.4. Summary of investigations that used low-range blends of n-butanol (nB) and iso-butanol (iB) with gasoline (G) in SI engines. All performance evaluates were relative to the base gasoline used. ▲: increase; ▼: decrease; BS NO_x: brake-specific NO_x emissions; BS soot: brake-specific soot emissions; BS CO: brake-specific CO emissions; BS UHC: brake-specific UHC emissions; BS CO_2: brake-specific CO_2 emissions; 4S: Four-stroke; ED: Engine displacement; PFI: Port fuel injection; DI: Direct injection; RP: Rated power; CR: Compression ratio; AC: Air-cooled; HRR: Heat-release rate; BP: Brake power; T: Torque; BTE: Brake thermal efficiency; BSFC: Brake-specific fuel consumption; EGT: Exhaust gas temperature; PP:L Peak pressure; EGR: Exhaust gas recirculation; VE: Volumetric efficiency; GE: Global efficiency; n/a: not available.

Fuel	Blends tested	Engine	Test conditions	Performance	BS NO_x	BS soot	BS CO	BS UHC	BS CO2	Ref.
G + nB	G100 nB3-G97 nB7-G93 nB10-G90	1-cylinder, 4S, AC, Carbureted, CR: 7, RP: 1.5 kW	2600 – 3400 rpm	EGT, T, BP, VE, PP ▼ with increase in nB content	n/a	n/a	▼ with increase in nB content	▼ with increase in nB content	▼ with nB blends but ▲ with increase in nB content	[48]
G + iB	G100 iB3-G97 iB7-G93 iB10-G90	1-cylinder, 4S, AC, Carbureted, CR: 7, RP: 1.5 kW	2600 – 3400 rpm	EGT, T, BP, VE, PP ▼ with increase in iB content	n/a	n/a	▼ with increase in iB content	▼ with iB (2600 – 2800 rpm) but ▲ at higher engine speeds	▼ with increase in iB content	[49]
G + nB + iB	G100 iB1.5-nB1.5-G97 iB3.5-nB3.5-G93 iB5-nB5-G90	1-cylinder, 4S, AC, Carbureted, CR: 7, RP: 1.5 kW	2600 – 3400 rpm	EGT, T, BP, VE, PP ▼ with dual-alcohol blends	n/a	n/a	▼ with dual alcohol blends up to 3000 rpm but ▲ at higher engine speeds	▼ with dual alcohol blends	▼ with dual alcohol blends	[50]
G + nB	G100 nB10-G90 nB20-G80	4-cylinder, 4S, DI, ED: 1.8 l, CR: 9.6	200 rpm, T: 210 Nm, variable EGR rate (0 to 20%)	BSFC ▲ with increase in nB content; HRR ▲ with nB	n/a	lower peak particle number with nB blends	n/a	▼with nB	n/a	[51]
G + nB	G100 nB10-G90	PFI, ED: 1.6 L, CR: 10.5	variable torques (20 to 80 Nm), 1750 to 3000 rpm	GE ▲ with nB	▼ with nB	▼ with nB	▼ with nB	▼ with nB	n/a	[52]
G + nB	G100 nB10-G90	4-cylinder, 4S, CR: 11.1, RP: 55 kW	1000 to 4000 rpm	EGT, BSFC ▲ with nB BTE ▼ with nB	n/a	n/a	▼with nB	▼with n-butanol	▲ with nB	[54]

3.4.5. Scenario 3: High-range alcohol blends

3.4.5.1. Rationale for screening

To create a gasoline blend with more than 40 vol% alcohol, fuel properties beyond RVP considered for the lower-range blends must be taken into consideration because the alcohol's characteristics exert a larger influence on the blend properties. Thus, requirements on the vapor pressure, boiling point, melting point, lower heating value, and kinematic viscosity were applied to identify appropriate alcohols for high-range blends.

Vapor pressure: Higher alcohols have very low vapor pressure and using a high portion of single higher alcohols can result in cold start problems. Thus, in the screening for high range blends, alcohols with vapor pressure less than 0.5 kPa at 25 °C were eliminated. Only nine non-cyclic alcohols and one cyclic alcohol passed this constraint.

Boiling point and melting point: The upper boiling limit used in the initial screening is 190 °C, which is the T90 limit for finished gasoline based on ASTM D4814. However, some alcohols would cause the gasoline blend to fail the T90 requirement even at low blending levels. Therefore, for the high blend level case, a boiling point cutoff of 165 °C was applied. This eliminated 23 non-cyclic and 17 cyclic alcohols from consideration. Similarly, the initial fluidity constraint (melting point) was tightened to be -20 °C, which removed 35 non-cyclic and 29 cyclic alcohols.
Heating value: The power output of an engine depends on the heating value of a fuel which directly has influence on the fuel consumption [57]. The use of higher alcohols instead of lower alcohols can improve the consumption due to the higher calorific values [7]. Therefore, for blends with a high proportion of alcohols, molecules with low calorific value must be avoided. Since the calorific value of gasoline is about 45 MJ/kg, alcohols with lower heating value (LHV) less than 30 MJ/kg were eliminated for high range blends to avoid high fuel consumption.

Kinematic viscosity: The low viscosity of lower alcohols results in lubrication problems in conventional port fuel injection systems leading to wearing of the engine parts. However, the higher viscosity of larger alcohols has conflicting influences: it can be problematic due to the formation of larger droplet size, especially in direct injection systems, and be beneficial by offering better lubrication and less wear on engine parts [58]. An upper limit (kinematic viscosity of 5 mm^2/s) close to the maximum limit for diesel-like fuels (4.1 mm^2/s) in ASTM D975 [59] was used to eliminate candidate alcohols because there is no viscosity standard for SI fuels, direct injection SI systems have a similar mechanism as compression ignition engines, and gasoline has a relatively low viscosity (about 0.8 mm^2/s). Based on this consideration, seven non-cyclic alcohols and 20 cyclic alcohols were eliminated because of their high viscosity.

3.4.5.2. Candidate alcohols for high-range blends

Following the screening procedure (Figure 3.2), a reduced database of six alcohols was obtained for use in high-range blending scenarios (Tables 3.5 and S3.3). These are 1-propanol, 1-butanol, 2-methyl-1-propanol (iso-butanol), 2-methyl-2-pentanol, 3-methyl-3-pentanol, and (1-methylcyclopropyl)methanol. 1-propanol, 1-butanol, and iso-butanol are non-cyclic C4 alcohols, 2-methyl-2-pentanol is a C6 non-cyclic alcohol, and (1-methylcyclopropyl)methanol is a C5 cyclic alcohol with a three-carbon ring.

Among these alcohols, only 1-propanol, 1-butanol, and 2-methyl-1-propanol have been used as blending components with gasoline at this high range (40 vol% or greater) [60-66]. A summary of studies involving such blends is presented in Table 3.6.

3.4.6. Considerations for use of the database and product design methodology

While the systematic product design methodology and thee scenarios presented here is intended to provide both an approach and results that will be useful for others, we note that

elimination of an alcohol during screening does not necessarily mean that the molecule is unsuitable for blending with gasoline, especially at low levels (Scenario 2), but rather than other alcohols have better (known or estimated) technical properties.

It is important to note that the outcomes of these scenarios are dependent on several factors. One of the most important of those is the accuracy of the property values used in the screening, especially those estimated from group contribution methods. Since no measured data are available for many of the alcohols considered in this study, reliance on estimated values was a necessity. For any alcohol with one or more property values near a criterion threshold, it may be of interest to obtain measured values. Our property database is publicly accessible (http://projects-web.engr.colostate.edu/co-optima/alcohol-database-CSU.xlsx) and can be updated as new information becomes available.

Table 3.5. Characteristics of six alcohols identified for high-range gasoline blends.

Property	1-Propanol	1-Butanol	2-Methyl-1-propanol	2-Methyl-2-pentanol	3-Methyl-3-pentanol	(1-Methylcyclo-propyl)methanol
Molecular weight (g/mol)	6.1	74.12	74.12	102.17	102.17	86.13
C (wt%)	59.96	64.82	64.82	70.53	70.53	69.72
H (wt%)	13.42	13.60	13.60	13.81	13.81	11.70
O (wt%)	26.62	21.59	21.59	15.66	15.66	18.57
Boiling point (°C)	97.2	117.7	107.8	121.1	122.40	128
Melting point (°C)	-126.1	-89.80	-108	-103	-23.60	-31.42
Water Solubility at 25 °C (g/L)	1000	63.20	85	32.4	42.60	46.49 [a]
Anaerobic Biodegradation Probability (Biowin7)	0.94 [a]	0.65 [a]	0.67 [a]	0.31 [a]	0.32 [a]	0.341 [a]
Research octane number (RON)	104	98	105	99.16 [a]	98.56 [a]	99.73 [a]
Flash point (°C)	15.00	28.88	27.78	21.1	156.00	48.4 [a]
Vapor pressure at 25°C (mmHg)	20.99	6.7	10.5	8.59	5.56	4.35 [a]
Viscosity at 25 °C (cP)	1.96	2.55	3.37	3.35 [a]	3.57 [a]	3.1 [a]
Density at 25 °C (g/cm^3)	0.80	0.81	0.8	0.81	0.83	0.042 [a]
Kinematic Viscosity at 25 °C (mm^2/s)	2.44	3.15	4.2	4.14 [a]	4.3 [a]	3.1 [a]
Surface tension at 25 °C (dyne/cm)	23.32	24.93	22.54	22.92	23.26	28.69 [a]
Heat of evaporation (kJ/mol)	47.45	17	41.8 [a]	39.6 [a]	55.70	42.7 [a]
Lower heating value (MJ/Kg)	31.57	33.09	33.11	36.42 [a]	36.42 [a]	36.14 [a]

a: Predicted via group contribution methods

Table 3.6. Summary of investigations that used high-range blends of 1-propanol (P), n-butanol (nB) and iso-butanol (iB) with gasoline (G) in SI engines. All performance evaluates were relative to the base gasoline used. ▲: increased; ▼: decreased; ⇔: no change; BS NO_x: brake-specific NO_x emissions; BS soot: brake-specific soot emissions; BS CO: brake-specific CO emissions; BS UHC: brake-specific UHC emissions; 4S: Four-stroke; ED: Engine displacement; PFI: Port fuel injection; DI: Direct injection; RP: Rated power; RT: Rated torque; CR: Compression ratio; AC: Air-cooled; HRR: Heat release rate; BP: Brake power; T: Torque; BTE: Brake thermal efficiency; BSFC: Brake specific fuel consumption; EGT: Exhaust gas temperature; PP: Peak pressure; EGR: Exhaust gas recirculation; VE: Volumetric efficiency; DOI: Duration of injection; FCE: Fuel conversion efficiency; GE: Global efficiency; n/a: not available.

Fuel	Blends tested	Engine	Test conditions	Performance	BS NO_x	BS Soot	BS CO	BS UHC	Ref.
G + P	G60-P40 P100	3-Cylinder, ED: 796 cc, PFI, CR: 9.4:1, RP: 26.5 kW, EGR	Full load, 3000 rpm, variable spark timing and EGR rate (0 and 10%)	n/a	n/a	▲ with P40 and P100	▼ with P40 ▲ with P100	▼ with P40 and P100	[60]
G + nB	G100 nB20-G80 nB40-G60	1-cylinder, PFI, ED: 399 cc, CR:10	Full load, 2000 rpm, two injection timings (closed intake valve and open intake valve)	DOI ▲ with nB	▼with nB	n/a	n/a	▼ with nB	[61]
G + nB	G100 nB20-G80 nB60-G40 nB100	Waukesha CFR engine, 1-cylinder, CR: 5.4–18.5, ED: 611 cm^3	variable loads, 900 rpm, variable spark timing, two CRs (8 & 10)	GE▲ with nB PP ▲ with increase in nB content	n/a	n/a	n/a	n/a	[62]
G + nB	G100 nB5-G95 nB10-G90 nB20-G80 nB50-G50 nB75-G25	Zen/Maruti Suzuki, 4-cylinder, 4S, PFI, ED: 0.99 L, RP: 40 PS, CR: 8.8	variable torque (0–66 Nm), 1500–4500 rpm	BSFC slightly ▲ with nB blends BTE ▼ with nB especially for lower engine speeds EGTslightly ▼ with nB blends	▼ with nB blends	n/a	▼ with nB blends	<=> with nB5 and nB10; ▼ with nB50 and nB75	[63]
G + iB	G100 iB50-G50 iB100	PFI passenger car, RP: 85 kW, ED: 1998 cm^3, CR: 9.2	variable loads, 1000 to 6000 rpm	BP <=> FCE (at full load)▼ with iB100 but▲ with iB50 FCE (at part load)▼ with iB100 but<=> with iB50	n/a	n/a	n/a	n/a	[64]
G + nB + iB	G100 nB85-G15 iB85-G15	GM L850, 4-cylinder, DI, EGR, ED: 2.19 L, CR:12, RP: 114 kW	variable loads, 1000 to 4000 rpm, torque: 25 to 150 Nm	BTE ▲ with both n-butanol and iso-butanol blends (but for nB85 at IMEP of 8.5 bar) PP almost <=>	no specific trend	n/a	▼with both n-butanol and iso-butanol blends	▲ with both n-butanol and iso-butanol blends	[65]

A second factor is that we have screened the alcohols based on pure component values rather than on the property of their blends with gasoline, with the exception of the RVP blending value criterion used for Scenario 2. This was done because alcohol-gasoline blend properties are available for only a few alcohols (mostly non-cyclic C1 to C4 alcohols) and the approaches for estimating blend properties (e.g., statistical associating fluid theory [67, 68, 69]) require parameters that are not straightforward to estimate for a blend involving a mixture as complex as gasoline. For some fuel characteristics, such as the RVP and distillation curve, studies have shown the extent of nonlinear effects and the trends with molecular weight [43, 46]. Non-idealities are likely to be less for higher alcohols than for methanol and ethanol in blends.

Finally, the criteria selected for the initial screening and for each scenario have a strong influence on the outcome of the screening. We carefully considered the specific criteria and justified them in the context of accepted fuel property values. Naturally, other investigators may choose different criteria for these or other goals.

Several factors were not considered in this screening approach. The first is cost, which was deliberately omitted because the current prices for any chemical primarily reflect the market size. Many of the alcohols are not currently available for purchase, but this does not mean that they cannot be synthesized by biological, chemical, or hybrid approaches. We suggest that it is of interest to first consider the promise of a candidate alcohol for gasoline blending, and then to consider whether it can be produced at an acceptable cost. Similarly, sustainability evaluations (e.g., life cycle assessment for greenhouse gas emissions and water use, energy return on investment) were not taken into consideration because those require a known production pathway.

One important fuel property that was not incorporated into the screening frameworks used here is heat of vaporization. Alcohols have a high HoV, which has different effects in different

engine types. In direct injection engines, the high HoV of a fuel results in charge cooling and consequently lower peak temperature and lower NO_x emission; in addition, charge cooling contributes to a better knock performance of the engine. In the port fuel injection system, this property makes the temperature on the intake manifold lower and accordingly increases fuel density; hence, more mass of fuel can be trapped inside the cylinder which increases the volumetric efficiency [8]. Regardless of the fuel injection approach, the high heat of vaporization can cause cold start/run problems [70]. Therefore, blends containing alcohols must be richer when compared to straight gasoline to start cold engines during open loop operation because sufficient fuel needs to vaporize to form a combustible air/fuel mixture [71]. Soot emissions generally decrease because the oxygen molecules reduce the number of carbon atoms that are active in the radical pool responsible for soot formation [2]. However, in certain operation conditions in direct injection engines, soot emission can be increased due to the high heat of vaporization of lower alcohols. The high heat of vaporization retards the evaporation of the fuel inside the chamber; thus, at higher speeds of engine, there would not be enough time for fuel droplets to get evaporated which results in soot emission [10]. Unburned hydrocarbon emissions are mainly caused by the unburned air-fuel mixture as a result of poor mixing and incomplete combustion. The high heat of vaporization of lower alcohols in direct injection engines can be one of the main reasons for poor mixing [7]. Although HoV is a very important characteristic of a fuel, it was not used as a screening criterion because its values for alcohols are far greater than that of gasoline and these greater values can have both positive and negative impacts depending on the system and engine load [72].

3.5. Conclusions

With this systematic product design methodology and three scenarios in which we identified alcohols suitable for low- and high-range blending, we developed a database of 13 fuel

properties of all saturated C1-C10 linear, branched, and cyclic mono-alcohols, and subsequently narrowed the potential gasoline blending candidates to select the most promising ones. An initial decision framework was used to screen unsuitable compounds, and then more stringent constraints were considered for three scenarios of low- and high-range blends of alcohol in gasoline. Forty-eight and 46 alcohols were identified as good candidates for blending with gasoline a levels up to 15 vol%, depending on whether a stringent requirement was imposed on the increased volatility of the blend over the base gasoline. The more challenging requirements for blending at more than 40 vol% resulted in a much shorter list of six alcohols: 1-propanol, 1-butanol, 2-methyl-1-propanol (iso-butanol), 2-methyl-2-pentanol, 3-methyl-3-pentanol, and (1-methylcyclopropyl)methanol were identified as most promising alcohol molecules for blending with gasoline at high concentrations. The approach used in this study could be modified for the evaluation of other classes of fuel molecules (e.g., esters, ketones, ethers) and for other engine types and fuel blending goals.

Using the lists of alcohols for these three scenarios, new research could focus on how and from what feedstocks these molecules can be produced, and on fuel characterization tests, combustion and emission characteristics, and technoeconomical and environmental assessments. All of those are necessary to fully understand whether these alcohols have the necessarily

References

1. Westbrook CK. Biofuels combustion. Annu Rev Phys Chem 2013;64:201–19. doi:10.1146/annurev-physchem-040412-110009.
2. Bergthorson JM, Thomson MJ. A review of the combustion and emissions properties of advanced transportation biofuels and their impact on existing and future engines. Renew Sustain Energy Rev 2015;42:1393–417. doi:10.1016/j.rser.2014.10.034.
3. Amin S. Review on biofuel oil and gas production processes from microalgae. Energy Convers Manag 2009;50:1834–40. doi:10.1016/j.enconman.2009.03.001.
4. Perlack RD, Wright LL, Turhollow AF, Graham RL, Stokes BJ, Erbach DC. Biomass as Feedstock for a Bioenergy and Bioproducts Industry : The Technical Feasibility of a Billion-Ton Annual Supply. Agriculture 2005;DOE/GO-102:78. doi:10.2172/885984.
5. Reddy HK, Muppaneni T, Rastegary J, Shirazi SA, Ghassemi A, Deng S. ASI: Hydrothermal extraction and characterization of bio-crude oils from wet Chlorella sorokiniana and Dunaliella tertiolecta. Environ Prog Sustain Energy 2013;32:910–5. doi:10.1002/ep.11862.
6. Regulation of fuels and fuel additives: Changes to renewable fuel standard program. Fed Regist 2011;76:18066. doi:10.1080/19388078109557636.
7. Sharudin H, Abdullah NR, Mamat AMI, Ali OM, Mamat R. An overview of spark ignition engine operating on lower-higher molecular mass alcohol blended gasoline fuels. J Teknol 2015;76:101–5. doi:10.11113/jt.v76.5547.
8. Costagliola MA, De Simio L, Iannaccone S, Prati M V. Combustion efficiency and engine out emissions of a S.I. engine fueled with alcohol/gasoline blends. Appl Energy 2013;111:1162–71. doi:10.1016/j.apenergy.2012.09.042.

9. Eyidogan M, Ozsezen AN, Canakci M, Turkcan A. Impact of alcohol-gasoline fuel blends on the performance and combustion characteristics of an SI engine. Fuel 2010;89:2713–20. doi:10.1016/j.fuel.2010.01.032.
10. Dahmen M, Marquardt W. Model-Based Design of Tailor-Made Biofuels. Energy and Fuels 2016;30:1109–34. doi:10.1021/acs.energyfuels.5b02674.
11. Hechinger M, Dahmen M, Victoria Villeda JJ, Marquardt W. Rigorous Generation and Model-Based Selection of Future Biofuel Candidates. Comput Aided Chem Eng 2012;31:1341–5. doi:10.1016/B978-0-444-59506-5.50099-7.
12. Ulonska K, Ebert BE, Blank LM, Mitsos A, Viell J. Systematic Screening of Fermentation Products as Future Platform Chemicals for Biofuels. Comput Aided Chem Eng 2015;37:1331–6. doi:10.1016/B978-0-444-63577-8.50067-X.
13. Yunus NA, Gernaey K V., Woodley JM, Gani R. A systematic methodology for design of tailor-made blended products. Comput Chem Eng 2014;66:201–13. doi:10.1016/j.compchemeng.2013.12.011.
14. Hashim H, Narayanasamy M, Yunus NA, Shiun LJ, Muis ZA, Ho WS. A cleaner and greener fuel: Biofuel blend formulation and emission assessment. J Clean Prod 2017;146:208–17. doi:10.1016/j.jclepro.2016.06.021.
15. Phoon LY, Hashim H, Mat R, Mustaffa AA. Tailor-Made Green Diesel Blends Design using a Decomposition-Based Computer-Aided Approach. Comput Aided Chem Eng 2015;37:1085–90. doi:10.1016/B978-0-444-63577-8.50026-7.
16. Simasatitkul L, Arpornwichanop A, Gani R. Design methodology for bio-based processing: Biodiesel and fatty alcohol production. Comput Chem Eng 2013;57:48–62. doi:10.1016/j.compchemeng.2013.01.018.

17. Hada S, Solvason CC, Eden MR. Molecular Design of Biofuel Additives for Optimization of Fuel Characteristics. vol. 29. 2011. doi:10.1016/B978-0-444-54298-4.50105-7.
18. Ariffin Kashinath SA, Abdul Manan Z, Hashim H, Wan Alwi SR. Design of green diesel from biofuels using computer aided technique. Comput Chem Eng 2012;41:88–92. doi:10.1016/j.compchemeng.2012.03.006.
19. Gugisch R, Kerber A, Kohnert A, Laue R, Meringer M, Rücker C, et al. MOLGEN 5.0, A Molecular Structure Generator. Adv. Math. Chem. Appl. Revis. Ed., vol. 1, 2016, p. 113–38. doi:10.1016/B978-1-68108-198-4.50006-0.
20. Toxics P. Estimation Program Interface (EPI) Suite. Program 2011:2–5.
21. Hechinger M, Voll A, Marquardt W. Towards an integrated design of biofuels and their production pathways. Comput Chem Eng 2010;34:1909–18. doi:10.1016/j.compchemeng.2010.07.035.
22. ACD/Structure Elucidator, version 15.01, Advanced Chemistry Development, Inc., Toronto, ON, Canada, www.acdlabs.com, 2015.
23. Dahmen M, Marquardt W. A Novel Group Contribution Method for the Prediction of the Derived Cetane Number of Oxygenated Hydrocarbons. Energy and Fuels 2015;29:5781–801. doi:10.1021/acs.energyfuels.5b01032.
24. Perez PL, Boehman AL. Experimental investigation of the autoignition behavior of surrogate gasoline fuels in a constant-volume combustion bomb apparatus and its relevance to HCCI combustion. Energy and Fuels 2012;26:6106–17. doi:10.1021/ef300503b.
25. Kelly RJ. Review of Safety Guidelines for Peroxidizable Organic Chemicals. Chemical Health & Safety- American Chemical Society 1996;4(5);28-36.
26. The United States Occupational Health and Safety Administration (OSHA).

https://www.osha.gov/dsg/hazcom/; [accessed 04.05.18].

27. Lapuerta M, García-Contreras R, Campos-Fernández J, Dorado MP. Stability, lubricity, viscosity, and cold-flow properties of alcohol-diesel blends. Energy and Fuels 2010;24:4497–502. doi:10.1021/ef100498u.
28. Patel SJ, Ng D, Mannan MS. QSPR flash point prediction of solvents using topological indices for application in computer aided molecular design. Ind Eng Chem Res 2009;48:7378–87. doi:10.1021/ie9000794.
29. Lee SK, Chou H, Ham TS, Lee TS, Keasling JD. Metabolic engineering of microorganisms for biofuels production: from bugs to synthetic biology to fuels. Curr Opin Biotechnol 2008;19:556–63. doi:10.1016/j.copbio.2008.10.014.
30. Smith BL, Bruno TJ. Improvements in the measurement of distillation curves. 3. Application to gasoline and gasoline + methanol mixtures. Ind Eng Chem Res 2007;46:297–309. doi:10.1021/ie060937u.
31. Smith BL, Ott LS, Bruno TJ. Composition-explicit distillation curves of diesel fuel with glycol ether and glycol ester oxygenates: Fuel analysis metrology to enable decreased particulate emissions. Environ Sci Technol 2008;42:7682–9. doi:10.1021/es800067c.
32. Song C. An overview of new approaches to deep desulfurization for ultra-clean gasoline, diesel fuel and jet fuel. Catal Today 2003;86:211–63. doi:10.1016/S0920-5861(03)00412-7.
33. ASTM D4814-06. Standard Specification for Automotive Spark-Ignition Engine Fuel. doi: 10.1520/D4814-06.
34. Kalghatgi GT. Developments in internal combustion engines and implications for combustion science and future transport fuels. Proc Combust Inst 2015;35:101–15. doi:10.1016/j.proci.2014.10.002.

35. Kalghatgi GT. Fuel Anti-Knock Quality - Part I. Engine Studies. SAE Tech Pap Ser 2001. doi:10.4271/2001-01-3584.
36. Yates ADB, Swarts A, Viljoen CL. Correlating auto-ignition delays and knock-limited spark-advance data for different types of fuel. SAE Tech Pap 2005. doi:10.4271/2005-01-2083.
37. Yacoub Y, Bata R, Gautam M. The performance and emission characteristics of C1-C5 alcohol-gasoline blends with matched oxygen content in a single-cylinder spark ignition engine.1998.Proceedings of the Institution of Mechanical Engineers, Part A: Journal of Power and Energy 1998;212(5), 363-379. doi: 10.1243/0957650981536934.
38. Canakci M, Ozsezen AN, Alptekin E, Eyidogan M. Impact of alcohol-gasoline fuel blends on the exhaust emission of an SI engine. Renew Energy 2013;52:111–7. doi:10.1016/j.renene.2012.09.062.
39. Haas FM, Chaos M, Dryer FL. Low and intermediate temperature oxidation of ethanol and ethanol-PRF blends: An experimental and modeling study. Combust Flame 2009;156:2346–50. doi:10.1016/j.combustflame.2009.08.012.
40. Fodor GE, Naegeli DW, Kohl KB. Peroxide formation in jet fuels. Energy & Fuels 1988;2:729–34. doi:10.1021/ef00012a002.
41. Farrell J, Holladay J, and Wagner R. Fuel Blendstocks with the Potential to Optimize Future Gasoline Engine Performance: Identification of Five Chemical Families for Detailed Evaluation. Technical Report. U.S. Department of Energy, Washington, DC. 2018. DOE/GO-102018-4970.
42. McCormick RL, Fioroni G, Fouts L, Christensen E, Yanowitz J, Polikarpov E, Albrecht K, Gaspar DJ, Gladden J, George A. Selection criteria and screening of potential biomass-derived streams as fuel blendstocks for advanced spark-ignition engines. SAE International Journal of

Fuels and Lubricants. 2017 Mar 28;10(2017-01-0868):442-60.

43. Andersen VF, Anderson JE, Wallington TJ, Mueller SA, Nielsen OJ. Vapor pressures of alcohol-gasoline blends. Energy and Fuels, vol. 24, 2010, p. 3647–54. doi:10.1021/ef100254w.
44. Gibbs L, Anderson B, Barnes K, Engeler G, Freel J, Horn J, Ingham M, Kohler D, Lesnini D, MacArthur R, Mortier M. Motor gasolines technical review. Chevron Products Company, San Ramon, CA. 2009.
45. Christensen E, Yanowitz J, Ratcliff M, McCormick RL. Renewable oxygenate blending effects on gasoline properties. Energy and Fuels 2011;25:4723–33. doi:10.1021/ef2010089.
46. Andersen VF, Anderson JE, Wallington TJ, Mueller SA, Nielsen OJ. Distillation curves for alcohol-gasoline blends. Energy and Fuels, vol. 24, 2010, p. 2683–91. doi:10.1021/ef9014795.
47. Hansen AC, Zhang Q, Lyne PWL. Ethanol-diesel fuel blends - A review. Bioresour Technol 2005;96:277–85. doi:10.1016/j.biortech.2004.04.007.
48. Rajesh Kumar B, Saravanan S. Use of higher alcohol biofuels in diesel engines: A review. Renew Sustain Energy Rev 2016;60:84–115. doi:10.1016/j.rser.2016.01.085.
49. Yanju W, Shenghua L, Hongsong L, Rui Y, Jie L, Ying W. Effects of Methanol/Gasoline Blends on a Spark Ignition Engine Performance and Emissions. Energy & Fuels 2008;22:1254–9. doi:10.1021/ef7003706.
50. Elfasakhany A. Experimental study on emissions and performance of an internal combustion engine fueled with gasoline and gasoline/n-butanol blends. Energy Convers Manag 2014;88:277–83. doi:10.1016/j.enconman.2014.08.031.
51. Elfasakhany A. Experimental investigation on SI engine using gasoline and a hybrid iso-butanol/gasoline fuel. Energy Convers Manag 2015;95:398–405. doi:10.1016/j.enconman.2015.02.022.

52. Elfasakhany A. Experimental study of dual n-butanol and iso-butanol additives on spark-ignition engine performance and emissions. Fuel 2016;163:166–74. doi:10.1016/j.fuel.2015.09.059.
53. Zhang Z, Wang T, Jia M, Wei Q, Meng X, Shu G. Combustion and particle number emissions of a direct injection spark ignition engine operating on ethanol/gasoline and n-butanol/gasoline blends with exhaust gas recirculation. Fuel 2014;130:177–88. doi:10.1016/j.fuel.2014.04.052.
54. Costagliola MA, De Simio L, Iannaccone S, Prati M V. Combustion efficiency and engine out emissions of a S.I. engine fueled with alcohol/gasoline blends. Appl Energy 2013;111:1162–71. doi:10.1016/j.apenergy.2012.09.042.
55. Wallner T, Miers SA, McConnell S. A Comparison of Ethanol and Butanol as Oxygenates Using a Direct-Injection, Spark-Ignition Engine. J Eng Gas Turbines Power 2009;131:32802. doi:10.1115/1.3043810.
56. Varol Y, Oner C, Oztop HF, Altun S. Comparison of Methanol, Ethanol, or n-Butanol Blending with Unleaded Gasoline on Exhaust Emissions of an SI Engine. Energy Sources Part A Recover Util Environ Eff 2014;36:938–48. doi:10.1080/15567036.2011.572141.
57. Demirbas A. Relationships derived from physical properties of vegetable oil and biodiesel fuels. Fuel 2008;87:1743–8. doi:10.1016/j.fuel.2007.08.007.
58. Surisetty VR, Dalai AK, Kozinski J. Alcohols as alternative fuels: An overview. Appl Catal A Gen 2011;404:1–11. doi:10.1016/j.apcata.2011.07.021.
59. ASTM: D975-15b. Standard Specification for Diesel Fuel Oils. 2015. doi:10.1520/D0975-12A.2.
60. Gong J, Cai J, Tang C. A Comparative Study of Emission Characteristics of Propanol Isomers/Gasoline Blends Combined with EGR. SAE Int J Fuels Lubr 2014;7:2014-01–1454.

doi:10.4271/2014-01-1454.

61. Merola SS, Tornatore C, Marchitto L, Valentino G, Corcione FE. Experimental investigations of butanol-gasoline blends effects on the combustion process in a SI engine. Int J Energy Environ Eng 2012;3:1–14. doi:10.1186/2251-6832-3-6.
62. Szwaja S, Naber JD. Combustion of n-butanol in a spark-ignition IC engine. Fuel 2010;89:1573–82. doi:10.1016/j.fuel.2009.08.043.
63. Singh SB, Dhar A, Agarwal AK. Technical feasibility study of butanol-gasoline blends for powering medium-duty transportation spark ignition engine. Renew Energy 2015;76:706–16. doi:10.1016/j.renene.2014.11.095.
64. Irimescu A. Performance and fuel conversion efficiency of a spark ignition engine fueled with iso-butanol. Appl Energy 2012;96:477–83. doi:10.1016/j.apenergy.2012.03.012.
65. Cooney C, Wallner T, McConnell S, Gillen JC, Abell C, Miers SA, et al. Effects of Blending Gasoline with Ethanol and Butanol on Engine Efficiency and Emissions Using a Direct-Injection, Spark-Ignition Engine. ASME Conf Proc 2009;2009:157–65. doi:10.1115/ICES2009-76155.
66. Venugopal T, Ramesh A. Effective utilisation of butanol along with gasoline in a spark ignition engine through a dual injection system. Appl Therm Eng 2013;59:550–8. doi:10.1016/j.applthermaleng.2013.06.026.
67. Tamouza S, Passarello JP, Tobaly P, De Hemptinne JC. Group contribution method with SAFT EOS applied to vapor liquid equilibria of various hydrocarbon series. Fluid Phase Equilib., vol. 222–223, 2004, p. 67–76. doi:10.1016/j.fluid.2004.06.038.
68. Tihic A, von Solms N, Michelsen ML, Kontogeorgis GM, Constantinou L. Analysis and applications of a group contribution sPC-SAFT equation of state. Fluid Phase Equilib

2009;281:60–9. doi:10.1016/j.fluid.2009.04.003.

69. Lubarsky H, Polishuk I, Nguyenhuynh D. Implementation of GC-PPC-SAFT and CP-PC-SAFT for predicting thermodynamic properties of mixtures of weakly- and non-associated oxygenated compounds. J Supercrit Fluids 2016;115:65–78. doi:10.1016/j.supflu.2016.04.013.
70. Thewes M, Müther M, Brassat A, Pischinger S, Sehr A. Analysis of the Effect of Bio-Fuels on the Combustion in a Downsized DI SI Engine. SAE Int J Fuels Lubr 2012;5:274–88. doi:10.4271/2011-01-1991.
71. Gautam M, Martin II DW. Combustion characteristics of higher-alcohol/gasoline blends. Proc Inst Mech Eng Part A J Power Energy 2005;214:497–511. doi:10.1243/0957650001538047.
72. Sharudin H, Abdullah NR, Mamat AMI, Ali OM, Mamat R. An overview of spark ignition engine operating on lower-higher molecular mass alcohol blended gasoline fuels. J Teknol 2015;76:101–5. doi:10.11113/jt.v76.5547.

4 Dual-Alcohol Blending Effects on Gasoline Properties [*]

4.1. Summary

Biofuels can contribute to reducing greenhouse gas emissions from the transportation sector. While the use of a neat alcohol as a fuel for spark-ignition engines would displace large amounts of petroleum, neat alcohols cannot provide the distillation temperature range required for smooth driveability and often exhibit high enthalpies of vaporization and low vapor pressures, which create cold-start problems. Gasoline blends containing high concentrations of single alcohols also have shortcomings. Blends of lower alcohols (methanol and ethanol) exhibit azeotropic behavior, lower calorific value, and low stability, while the low volatility of higher alcohols significantly limits the maximum fraction at which they can be blended. One way to circumvent these issues is to use a dual-alcohol approach, mixing lower and higher alcohols with gasoline to obtain a blend with a vapor pressure close to that of the base gasoline. The goal of this study was to evaluate the fuel potential of dual alcohol blends experimentally and with a model that provided insights into the azeotropic volatility behavior and mixing/sooting potential of the blends. Ten dual-alcohol blends were tested at blending ratios from 10 to 80 vol%, with methanol and ethanol used as the lower alcohols, and iso-butanol and 3-methyl-3-pentanol as the higher alcohols. The corresponding single alcohol-gasoline blends were also evaluated.

To be submitted as "Dual-Alcohol Blending Effects on Gasoline Properties" by Saeid Aghahossein Shirazi, Bahareh Abdollahipoor, Jake Martinson, Bret Windom and Kenneth F. Reardon. The study presented in this chapter was designed and conducted by me except for the distillation and modeling sections. In these sections, I contributed to the distillation curve testing and composition analysis, interpretation of the results, and the writing.

For each blend, Reid vapor pressure, vapor lock protection potential, distillation curve, lower heating value, kinematic viscosity, and water tolerance at three temperatures were measured. A droplet evaporation model was also applied. The results of this study show that it is advantageous to use dual-alcohol blends containing up to 40 vol% because they have the characteristics necessary for good performance in existing spark-ignition engines, particularly in terms of volatility, kinematic viscosity, and water tolerance. This study is the first to characterize matched vapor pressure, dual-alcohol blends over a wide blending range as drop-in fuels for conventional spark ignition engines. Furthermore, this was the first investigation of the fuel potential of 3-methyl-3-pentanol in single- and dual-alcohol blends and iso-butanol in dual-alcohol blends.

4.2. Introduction

Overreliance on fossil fuels can lead to serious environmental issues. Biofuels have attracted widespread attention due to their capacity to curb the demand for fossil fuels and play a vital role in reducing greenhouse gas emissions [1]. Among biofuels, bio-alcohols are considered to be a promising alternative fuel for use in spark ignition (SI) engines [2]. United States of America and Brazil, as leading countries in the biofuel, have replaced a great share of their gasoline with bio-ethanol. In the United States, in 2011, the U.S. Environmental Protection Agency (EPA) granted a partial waiver for use of fuel blend of 15% ethanol and 85% gasoline in passenger cars, light-duty trucks, and flexible-fuel vehicles starting from model year 2001 [3]. In addition, the use of a blend of gasoline and denatured ethanol containing up to 85 percent ethanol is allowed only in flex fuel vehicles [3].

Alcohols have the potential to replace traditional octane enhancing strategies minimizing environmental/health impacts while reducing greenhouse gas emissions by closing the carbon

cycle and improving energy conversion efficiencies. Conventionally, low molecular weight alcohols such as methanol and ethanol are blended with gasoline. The production processes for these alcohols from renewable sources are well-established, and they are produced at relatively low cost [4]. Blending these alcohols with gasoline enhances the anti-knock properties of the fuel blends and can reduce a refinery's production costs for high-grade gasoline [5]. The high oxygen content of low molecular weight alcohols results in cleaner combustion, especially with regard to emission of CO and unburned hydrocarbons [4-7]. Low molecular weight alcohols exhibit faster laminar flame speeds than gasoline, which can improve the combustion process [8]. Furthermore, the heat of vaporization (HoV) of these low molecular weight alcohols is significantly higher than that of gasoline, leading to improved thermal efficiencies through the charge cooling phenomenon in both port fuel and direct injected SI engines. In addition, charge cooling can help lower peak combustion temperatures, reducing NO_x emissions [9-12].

However, there are limitations with blending low molecular weight alcohols with gasoline. Both methanol and ethanol can form positive azeotropes with hydrocarbons compounds in gasoline. Consequently, the vapor pressure of the blend is significantly higher, contributing to evaporative emissions problems [2]. In addition, low molecular weight alcohols can promote phase separation in the presence of water, especially in cold environments, due to their hygroscopicity and water solubility. This can result in separated alcohol/water mixtures that can be corrosive to the engine and the fuel delivery system [6]. Stemming from the large oxygen mass fraction of methanol and ethanol, their lower heating value (LHV) and stoichiometric air-fuel ratios are lower than gasoline. Both of these factors contribute to increased brake-specific fuel consumption (BSFC), especially if the engine is not tuned to maximize the conversion efficiency for the blended fuel [1, 2, 6, 7, 13]. Also, the high HoV of lower alcohols can cause cold start problems under

certain operating conditions [14] and can influence the fuel atomization evaporation/mixing phenomenon in direct injection engines, which has implications for particulate matter (PM) formation [15-17].

Considering these limitations, expensive upgrades to existing vehicle architectures and refueling infrastructure are likely to be required to increase the use of low molecular weight alcohols [6]. An alternative approach to increasing the fraction of biofuel in a gasoline blend is to co-blend higher alcohols (any saturated mono-alcohol with three or more carbon atoms). Higher alcohols are effective options as co-solvents with lower alcohols in gasoline because (1) higher alcohols can be produced from renewable feedstocks through either fermentation or catalytic conversion of syngas, although the cost of production is currently higher than lower alcohols [18], (2) they are less corrosive to materials in the fuel delivery and injection systems compared to lower alcohols [1], (3) higher alcohols can increase the water tolerance of alcohol-gasoline blends, especially compared to methanol blends with gasoline [19, 20], (4) they exhibit better lubrication and contribute to less engine wear as a result of their higher viscosity [6], (5) they have a higher LHV than lower alcohols as a result of decreased oxygen mass fraction which results in better fuel economy [7], and (6) their lower vapor pressures and reduced azeotropic activity can mitigate many of the evaporation-driven concerns associated with lower alcohols [21].

Andersen et al. [22] described the concept of mixing a lower alcohol and a higher alcohol (ethanol and 1-butanol) in gasoline to obtain an alcohol-gasoline blend with a Reid vapor pressure (RVP) matching that of the base gasoline. A few studies have been conducted to test dual-alcohol blends using this approach. Siwale et al. [23] compared M70 (methanol 70 vol%+ gasoline 30 vol%) with a blend containing 53 vol% methanol, 17 vol% n-butanol and 30 vol% gasoline. The dual-alcohol blend was recommended in preference to M70 due to the shortened combustion

duration, better volumetric efficiency, higher energy content, and better brake thermal efficiency, while the RVP was matched to that of gasoline. Ratcliff et al. [24] compared the effects on light-duty vehicle exhaust emissions of four blends with 5.5 wt% oxygen, a dual-alcohol blend (12% i-butanol-7% ethanol) and three single-alcohol gasoline blends (16 vol% ethanol, 17 vol% n-butanol, and 21 vol% i-butanol). The emissions of the dual-alcohol blend had the lowest levels of NO_x, non-methane organic gas, and unburned alcohols.

To date, no study has been conducted to characterize matched-RVP, dual-alcohol blends over a wide blending volume range to examine their potential as drop-in fuel for conventional spark ignition engines. The goal of this study was to characterize important physiochemical properties of dual-alcohol gasoline blends and to assess how these blends are compatible with the current standard specification for automotive spark ignition engine fuel (ASTM D4814). Properties of dual-alcohol blends were also compared to the base gasoline and corresponding single alcohol-gasoline blends. The two higher alcohols used in the dual-alcohol blends were iso-butanol and 3-methyl-3-pentanol (3M3P), identified as promising higher alcohols for blending with gasoline in our previous study [25]. In addition to fuel property determination, an advanced distillation apparatus was used to obtain distillation curves and distillate composition for all blends. A distillation-based droplet evaporation model validated with the experimental data was used to provide insights on volatility differences and the in-cylinder mixing potential between the dual-alcohol blends, single alcohol blends, and gasoline.

4.3. Materials and methods

4.3.1. Test fuels

The base gasoline used was an unleaded test gasoline (UTG-96) from Phillips 66. The measured RVP of the gasoline was 52 kPa. Methanol (99.9%, Certified ACS) and ethanol (200

proof) were obtained from Fisher Scientific. Iso-butanol (≥ 99 %, FG) and 3-methyl-3-pentanol (≥ 99 %, FG) were obtained from Sigma-Aldrich. A total of 25 gasoline alcohol blends as well as the neat gasoline were tested in this study. Total alcohol blending volumes spanning from 10–80 vol% were considered in order to investigate the effect of increased alcohol usage on the fuel specifications.

Dual-alcohol blends were selected to control RVP with the intent to reduce the issues associated with the increased volatility of single alcohol-gasoline blends. The concentration of lower and higher alcohols in each dual-alcohol blend was obtained by using the equation proposed by Anderson et al. [22] aiming to match the RVP of the blend with that of base gasoline:

$$C_i = \left(\frac{RVP_G - RVP_j(@C_t)}{RVP_i(@C_t) - RVP_j(@C_t)}\right) \times C_t \qquad \text{Eq.4.1}$$

Here, C_i is the volume fraction of alcohol i, C_t is the total alcohol volume fraction, RVP_G is the RVP of the base gasoline, and $RVP_i(@Ct)$ and $RVP_j(@Ct)$ are RVPs of the single alcohol gasoline blends i and j each at a blending ratio of C_t, respectively. Volumetric concentrations of lower and higher alcohols for each dual-alcohol blend are presented in Table 4.1. In this work, G, M, E, B, and H represent gasoline, methanol, ethanol, iso-butanol, and 3M3P, respectively. Since 3M3P is a hexanol isomer, it is represented by the letter "H". Each blend is abbreviated with an alphanumeric code in which the letter (or letters) represents the alcohol (or alcohols) used in the blend and the number represents the total alcohol volume fraction. For instance, H10 consists of 10 vol% 3M3P and 90 vol% gasoline while MB80 consists of 80 vol% total alcohol (74 vol% methanol + 6 vol% iso-butanol) and 20 vol% gasoline.

In general, ethanol is a superior fuel to methanol due to the lower RVP, lower corrosivity, better water tolerance, and higher heating value [6]. Therefore, ethanol was used to make dual-

alcohol blends for blending ratios of 10, 20 and 40 vol%. However, since the RVPs of E60 and E80 are less than the RVP of the base gasoline, it is no longer possible to make matched-RVP dual-alcohol blends with ethanol. Thus, methanol was used for the higher blending ratios (60% and 80%). Comparison of the dual-alcohol blends containing 60% or more total alcohol were compared to corresponding methanol (single-alcohol) blends.

Table 4.1 List of test blends. M: methanol. E: ethanol. B: i-butanol. H: 3-methyl-3-pentanol.

Total alcohol volume fraction (vol%)	Methanol blends	Ethanol blends	Iso-butanol blends	3M3P blends	Dual-alcohol blends containing iso-butanol (lower alcohol vol% + iso-butanol vol%)	Dual-alcohol blends containing 3M3P (lower alcohol vol% +3M3P vol%)
10	–	E10	B10	H10	EB10 (E 2.7 vol% +B 7.3 vol%)	EH10 (E 3.3 vol% +H 6.7 vol%)
20	–	E20	B20	H20	EB20 (E 8.9 vol% +B 11.1 vol%)	EH20 (E 11.5 vol% +H 8.5 vol%)
40	–	E40	B40	H40	EB40 (E 33.1 vol% +B 6.9 vol%)	EH40 (E 36.3 vol% +H 3.7 vol%)
60	M60	–	B60	H60	MB60 (M 34.5vol% +B 25.5 vol%)	MH60 (M 37.8 vol% +H 22.2 vol%)
80	M80	–	B80	H80	MB80 (M 74 vol% +B 6 vol%)	MH80 (M 75 vol% +H 5 vol%)

4.3.2. Methods

The test fuel blends were prepared and kept in a freezer to minimize evaporative losses. The Reid vapor pressure, vapor lock protection potential, temperature dependent water tolerance, LHV, density, and viscosity were characterized for each fuel. These properties were measured three times for each sample. Reid vapor pressure and vapor lock protection potential were measured using the Grabner Instruments Minivap VPXpert vapor pressure analyzer according to ASTM 5191 [26] and ASTM D5188 [27], respectively. RVP was measured for single alcohol-gasoline blends at 1, 2, 3, 5, 10, 15, 20, 30, …, 90, and 100 vol%. For dual-alcohol blends, RVP was measured at 10, 20, 40, 60, and 80 vol%. Water tolerance was measured at three target temperatures, +10, 0, and –10 °C, by gradually adding water to the tempered blend until phase separation was observed. The water tolerance was defined as the percent volume of water added over the total volume of the blend. The LHV was measured with an IKA C200 calorimeter according to ASTM D240-14 [28]. An Anton-Paar SVM 3000 viscometer-densitometer was used to measure viscosity and density.

A custom-built Advanced Distillation Curve (ADC) apparatus was employed to conduct the distillation curve measurements at 84.3 kPa. The ADC apparatus and method are comprehensively described elsewhere [29]. The distillation was conducted two times for each sample. Moreover, to scrutinize the effect of replacing a portion of ethanol with a higher alcohol on the composition evolution during the distillation, distillate samples were taken for analysis at the first drop, 10, 20, 30, 40, 50, 60, 70, 80, and 90 vol% distilled only for the most promising dual-alcohol blends (10, 20 and 40 vol%) in addition to corresponding ethanol blends and gasoline for comparison. Detailed hydrocarbon analysis was applied to quantify the sampled distillate composition according to ASTM D6729 [30] using an HP 5890 Series II GC-FID equipped with 100-m long Petrocol DH fused-silica capillary column coated with polydimethyl siloxane. Chromatogram peak areas were converted to the mass concentrations following calibration. Average molecular weight was calculated using the mass fraction and the molecular weight of each component.

4.3.3 Droplet evaporation model

In this study, droplet evaporation model developed by Burke et al. [31] was used to simulate the evaporation of fuel droplets to obtain thermodynamically driven evaporation times. The evaporation time can be used to estimate differences in mixing time scales between two fuel mixtures and the potential of the blends to form PM [32]. This model uses the same algorithm as distillation model developed by Backhaus [33], but to model the distillation of the fuels as droplets, the D^2 law and appropriate energy and mass conservation equations are incorporated. In these models, the UNIFAC group contribution was utilized to take the non-ideality into account. The complex fuel was simulated using 54 components. The list of the simplified composition for gasoline UTG-96 is available in the supplementary materials (Table S4.1). Using the simplified

composition, a mass fraction weighted average approach described in [34] was used to determine properties of fuels.

4.4. Results and discussion

4.4.1. Volatility

4.4.1.1. Reid vapor pressure

The RVPs of all tested alcohols and blends with gasoline are shown in Tables 4.2, 4.3 and Figure 4.1. Since the desirable volatility of a SI engine fuel is different for each season and location, ASTM D4814 specifies six vapor pressure/distillation and vapor lock protection classes as shown in Table S4.2.

Table 4.2 Properties of pure alcohols. Values are shown as the mean +/- one standard deviation of triplicate measurements. [a] Obtained from [25]. [b] Obtained from [35].

Alcohol	RVP (kPa)	Boiling point (°C) [a]	HoV at 25 °C (kJ/kg) [b]	LHV (kJ/g)	ρ (g/cm^3)	μ (cP)	ν (mm^2/s)
Methanol	30 ± 0.35	64.70	1169.3	22 ± 0.28	0.79 ± 0	0.55 ± 0.1	0.7 ± 0.1
Ethanol	15 ± 0.41	78.20	924.1	29 ± 0.31	0.79 ± 0	1.1 ± 0.2	1.5 ± 0.2
Iso-butanol	2 ± 0.02	107.80	701.9	36 ± 0.38	0.80 ± 0	4.1 ± 0.1	5.1 ± 0.1
3-methyl-3-pentanol	1 ± 0.3	122.40	474.0	38 ± 0.04	0.83 ± 0	5.4 ± 0.3	6.6 ± 0.3

Table 4.3 Measured properties of tested fuels. Error ranges correspond to +/- one standard deviation of multiple measurements. RVP: Reid vapor pressure. IBP: Initial boiling point. EP: end-point. ρ: Density @ 20 °C. μ: Dynamic viscosity @ 20°C. ν: Kinematic viscosity @ 20 °C. WT: water tolerance (v/v%). M: methanol. E: ethanol. B: i-butanol. H: 3-methyl-3-pentanol.

Fuel	RVP (kPa)	$T_{v/l=20}$ (°C)	IBP (°C)	T10 (°C)	T50 (°C)	T90 (°C)	LHV (kJ/g)	ρ (g/cm^3)	μ (cP)	ν (mm^2/s)	WT(v/v%)		
											+10 °C	0 °C	−10 °C
Gasoline	52 ± 0.83	66 ± 0.66	52 ± 0.2	73 ± 0	105 ± 0.04	153 ± 4.9	46 ± 0.2	0.74 ± 0	0.37 ± 0.03	0.50 ± 0.03	0 ± 0	0 ± 0	0 ± 0
E10	60 ± 0.25	57 ± 0.17	49 ± 0.96	61 ± 0.1	103 ± 0.34	142 ± 1.6	44 ± 0.6	0.74 ± 0	0.39 ± 0.01	0.53 ± 0.01	0.3 ± 0.004	0.2 ± 0.002	0.2 ± 0.001
B10	51 ± 0.1	67 ± 0.31	56± 1.9	75 ± 1	100 ± 2	144 ± 12	45 ± 0.22	0.77 ± 0	0.55 ± 0.01	0.71 ± 0.01	0 ± 0	0 ± 0	0 ± 0
H10	50 ± 0.1	69 ± 0.86	56 ± 1.4	78 ± 0.8	106 ± 0.75	146 ± 5.6	45 ± 0.11	0.75 ± 0	0.43 ± 0.01	0.58 ± 0.02	0 ± 0	0 ± 0	0 ± 0
EB10	53 ± 0.1	62 ± 0.24	51 ± 0.53	71 ± 0.03	101 ± 1	143 ± 0.57	44 ± 0.15	0.75 ± 0	0.44 ± 0.04	0.58 ± 0.05	0 ± 0	0 ± 0	0 ± 0
EH10	56 ± 0.1	62 ± 0.42	48 ± 0.97	66 ± 0.54	103 ± 0.82	144 ± 0.74	44 ± 0.05	0.75 ± 0	0.44 ± 0.01	0.59 ± 0.02	0 ± 0	0 ± 0	0 ± 0
E20	58 ± 0.41	57 ± 0	47 ± 0.01	60 ± 0.29	74 ± 0.12	144 ± 3	42 ± 0.13	0.75 ± 0	0.47 ± 0.01	0.62 ± 0.01	0.7 ± 0.003	0.6 ± 0.004	0.5 ± 0
B20	48 ± 0.2	68 ± 0.46	54 ± 0.4	74 ± 1	96± 0	135 ± 3	44 ±0.43	0.75 ± 0	0.53 ± 0.01	0.70 ± 0.01	0.02 ± 0.004	0.02 ± 0.004	0.007 ± 0
H20	47 ± 0.45	71 ± 0.24	56± 0.11	82 ± 0.6	108 ± 0.72	138 ± 2.1	44 ± 0.35	0.75 ± 0	0.50 ± 0.01	0.67 ± 0.02	0 ± 0	0 ± 0	0 ± 0
EB20	53 ± 0.16	62 ± 0.59	50 ± 0.8	65 ± 0.26	89 ± 0.2	134 ± 0.8	43 ± 0.42	0.75 ± 0	0.51 ± 0	0.68 ± 0	0.02 ± 0.001	0.02 ± 0.006	0.01 ± 0.002
EH20	56 ± 0.18	60 ± 0.51	49 ± 0.87	63 ± 0.59	94 ± 0.52	137 ± 0.84	43 ± 0.45	0.75 ± 0	0.48 ± 0.01	0.64 ± 0.02	0.6 ± 0.002	0.5 ± 0.008	0.4 ± 0.002
E40	54 ± 0.13	60 ± 0.17	50 ± 0.74	62 ± 0.57	73 ± 0.84	140 ± 0.53	39 ± 0.37	0.77 ± 0	0.67 ± 0.01	0.88 ± 0.01	2.6 ± 0.004	2.3 ± 0.008	2.1 ± 0.007
B40	42 ± 0.16	75 ± 0.39	55 ± 0.16	79 ± 1	97 ± 1	110 ± 2	42 ± 0.45	0.77 ± 0	0.83 ± 0.01	1.09 ± 0.01	0.2 ± 0.003	0.1 ± 0.001	0 ± 0
H40	40 ± 0.1	79 ± 0.69	62 ± 0.4	91 ± 0.08	112 ± 0.26	128 ± 0.22	43 ± 0.64	0.77 ± 0	0.74 ± 0.01	0.95 ± 0.01	0 ± 0.000	0 ± 0	0.0 ± 0.0
EB40	52 ± 0.04	61 ± 0.22	50 ± 0.18	65 ± 0	76 ± 0.39	108 ± .07	39 ± 0.39	0.77 ± 0	0.72 ± 0.01	0.94 ± 0.01	3.2 ± 0.003	3 ± 0.002	2.6 ± 0.009
EH40	54 ± 0.15	60 ± 0.26	48 ± 0.68	63 ± 0.83	74 ± 0.73	126 ± 0.97	39 ± 0.06	0.76 ± 0	0.65 ± 0.01	0.85 ± 0.01	3.0 ± 0.003	2.7 ± 0.006	2.4 ± 0.003
M60	67 ± 0.53	52 ± 0.21	44 ± 0.13	54 ± 0.75	60 ± 0.9	62 ± 0.75	31 ± 0.35	0.77 ± 0	0.53 ± 0.04	0.69 ± 0.05	0.6 ± 0.003	0.3 ± 0.002	0.1 ± 0.004
B60	33 ± 0.35	83 ± 0.29	69 ± 0.1	88 ± 0.6	101 ± 0.25	106 ± 0.25	39 ± 0.41	0.78 ± 0	1.50 ± 0.01	1.92 ± 0.01	2.4 ± 0.001	1.8 ± 0.004	1.6 ± 0
H60	29 ± 0.16	87 ± 0.9	74 ± 1.6	102 ± 0.27	116 ± 0.51	124 ± 0.03	41 ± 0.08	0.79 ± 0	1.22 ± 0.01	1.54 ± 0.01	0 ± 0	0 ± 0	0 ± 0
MB60	57 ± 0.2	56 ± 0.12	49 ± 0.31	60 ± 0.06	72 ± 0.13	106 ± 0.48	34 ± 0.17	0.77 ± 0	0.75 ± 0.05	0.97 ± 0.07	4.4 ± 0.004	4 ± 0.004	3.5 ± 0.004
MH60	58 ± 0.17	56 ± 0.16	46 ± 0.32	58 ± 0.81	69 ± 1	124 ± 0.53	34 ± 1.2	0.78 ± 0	0.78 ± 0.03	1.00 ± 0.03	4.2 ± 0.002	3.8 ± 0.007	3.4 ± 0.002
M80	55 ± 0.15	57 ± 0.05	49 ± 0.19	58 ± 0.13	61 ± 0.01	62 ± 0.6	26 ± 0.98	0.78 ± 0	0.55 ± 0.01	0.70 ± 0.01	3.1 ± 0.004	2.7 ± 0.003	2.2 ± 0.005
B80	20 ± 0.43	90 ± 0	83 ± 1.2	99 ± 0.2	105 ± 0.08	107 ± 0.3	37 ± 1.1	0.79 ± 0	2.38 ± 0.01	3.02 ± 0.01	3.5 ± 0.004	2.9 ± 0.002	2.7 ± 0.005
H80	16 ± 0.7	86 ± 1.2	91 ± 0.49	111 ± 0.13	118 ± 0.16	122 ± 0.51	40 ± 0.23	0.81 ± 0	2.23 ± 0.02	2.76 ± 0.03	0.003 ± 0.003	0.002 ± 0	0.001 ± 0
MB80	54 ± 0.13	57 ± 0.09	50 ± 0.51	59 ± 0.21	63 ± 0.05	72 ± 2.9	28 ± 0.06	0.78 ± 0	0.57 ± 0.02	0.73 ± 0.02	3.5 ± 0.003	2.9 ± 0	2.2 ± 0.006
MH80	53 ± 1.7	57 ± 0.12	51 ± 0.55	60 ± 0.99	63± 0.52	117 ± 0.64	28 ± 0.1	0.78 ± 0	0.58 ± 0.02	0.74 ± 0.02	4 ± 0.003	3.4 ± 0.009	2.9 ± 0.003

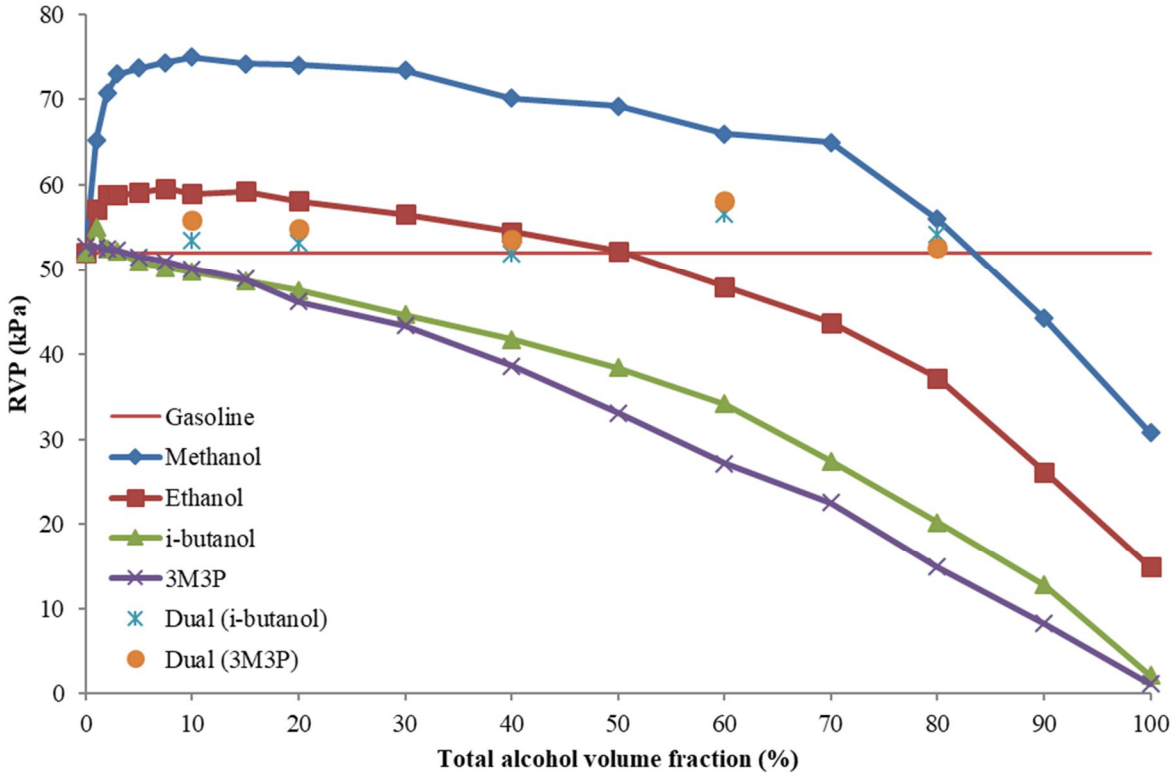

Figure 4.1. RVPs of test fuels plotted versus total alcohol volume fraction. The average standard error for all data points is 0.3.

The RVP of methanol and ethanol gasoline blends are highly affected by non-ideal vapor liquid equilibrium mixture behavior (Figure 4.1). While the RVPs of pure methanol and ethanol are lower than that of the gasoline, formation of positive azeotropes in the mixture of lower alcohols and gasoline results in higher vapor pressures than the gasoline below 80 vol% methanol and 50 vol% ethanol. The highest RVP (74.21 kPa) was observed for a blend containing 10 vol% methanol. Among ethanol blends, the highest RVP was observed for E15 (59.22 kPa). All blends with only methanol and ethanol qualified under ASTM D4814 in these volatility classes: Class

AA for blends containing more than 50% and 80% ethanol and methanol; Class A for ethanol blends with less than 50% ethanol; Class C for methanol blends with less than 50% methanol; and Class B for methanol blends containing 50% to 80% methanol.

There is a clear trend of decreasing RVP with the increase in alcohol concentration for the blends containing only a higher alcohol (i.e., i-butanol and 3M3P) except for the blend containing 1 vol% of i-butanol (Figure 4.1). This confirms that as the length of hydrocarbon chain is increased, the azeotropic effect of hydroxyl group is dissipated such that the higher alcohol blends behave as ideal mixtures. All the blends containing a single higher alcohol qualified under ASTM D4814 for all classes due to their low RVP values, especially at high blending ratios. Since gasoline is very volatile, lowering the RVP of gasoline to a certain point is generally desired because it is expensive to produce a low RVP gasoline [36]. Therefore, the use of higher alcohols can be advantageous. However, cold starting requires a minimum vapor pressure especially when considering high HoV fuels containing alcohols. Although no minimum limit is specified in the ASTM D4814 for vapor pressure, the low RVPs of blends containing a high concentration of higher alcohols are not desirable because it may cause cold start problems.

All dual-alcohol blends had an RVP within 9% of that of the base gasoline, regardless of total alcohol concentration (Table 4.3). A small number of the measured values were slightly higher than the target gasoline RVP, which may be due to non-linear blending effects that are not accounted for in Eqn. 1. Nevertheless, Eq. 4.1 proved to be a good predictor of RVP for the dual-alcohol blended fuels.

4.4.1.2. Vapor lock protection potential

The best index to assess hot fuel handling problems is vapor lock protection potential ($T_{V/L=20}$), which is the temperature at which a fuel forms a volumetric vapor-liquid ratio of 20 at

atmospheric pressure. Six vapor lock protection classes for minimum $T_{V/L=20}$ are specified in ASTM D4814; fuels with a greater vapor lock protection potential have greater protection against vapor lock. All tested blends met ASTM specifications for all volatility classes except for M60 with a $T_{V/L=20}$ of 51.53 °C, which qualifies for all classes other than Class 1 (min $T_{V/L=20}$ of 54). Blends containing high concentration of single higher alcohols (60 and 80 vol%) show the highest (i.e., safest) $T_{V/L=20}$ due to their very low volatility. The lowest vapor lock index belonged to M60, followed by the low content ethanol blends (E10 and E20) because of the azeotrope-driven volatility of these blends. Dual-alcohol blends containing up to 40 vol% of total alcohol successfully maintained vapor lock indices close to that of gasoline. For the dual-alcohol blends with higher blending ratios (60 and 80 vol%), $T_{V/L=20}$ was reduced due to the high concentration of methanol in these blends, but still maintain values high enough to meet all ASTM class requirements.

4.4.1.3. Distillation curve

ASTM D4814 sets acceptable boundaries for distillation temperatures for fuels used in SI engines. To ensure that a fuel provides an appropriate volatility, this standard specifies maximum limits on T10, T50, T90, and end-point and minimum limits for T50 for six distillation classes. Distillation curves are available in supplemental materials (Figures S4.1 to S4.5, sorted by total initial alcohol content). Also, distillation temperatures at 84.3 kPa (initial boiling point, T10, T50, and T90) for each blend are listed in Table 4.3. The distillation curve of the unblended gasoline demonstrates smooth and steadily increasing temperatures. Addition of lower alcohols (methanol and ethanol) to gasoline increased the volatility through the formation of positive azeotropes and causes a reduction in the front end (T0-T20) and midrange (T20-T90) distillation temperatures. For the blends of single lower alcohols, once the alcohol evaporates, a relatively sharp rise in

boiling temperatures was observed as the distillation curves approach boiling temperatures of the gasoline. This behavior was observed in low to medium (10 to 40 vol%) blending ratios. For higher blending ratios, the suppressed boiling temperature behavior exists throughout the entirety of the measured distillation, resulting in nearly isothermal boiling temperatures. The end-point temperature decreased in the alcohol blends due to the dilution of heavy hydrocarbons.

In contrast to the lower alcohols, the blends of higher alcohols exhibited little to no azeotropic behavior. In the early stages, the distillation curves of these blends are located on the top of the distillation curve of the base gasoline due to their high boiling points and low RVPs. Once the alcohol was evaporated, the distillation temperatures converged to that of the gasoline. As the concentration of the higher alcohol in the blend increases, the point at which the distillation temperatures approach that of the gasoline occurs at higher distilled volume fractions. The temperatures at the tail end of the distillation curve for the high alcohol fuel blends are lower than those of gasoline due to dilution of the heavy petroleum fraction. In all blending ratios, 3M3P reduces the volatility of the gasoline more so than iso-butanol owing to its higher boiling point, lower RVP, and reduced polarity.

Distillation curves for the dual-alcohol blends lied between the curves of the corresponding single-alcohol blends. At the beginning of the distillation, temperatures were closer to that of the corresponding single-lower alcohol blend while at higher volume fractions, once most of the lower alcohol was evaporated, there was a sharp rise in boiling temperatures as the distillation curve converges to that of the blend containing a single higher alcohol. The blends containing methanol and 3M3P (MH60 and MH80) provided the clearest example of this trend as it was comprised of the alcohol combination with the widest range in RVP, and the most and least polar alcohols used in this study.

The distillation temperatures were also compared to the ASTM D4814 limits to investigate the compatibility of these blends with the current standards. In this study, distillation curves were obtained at 84.3 kPa, while ASTM D8418 sets limits at 1 atm. Therefore, temperature measurements were corrected to 101.3 kPa using the Sydney-Young equation as stated in ASTM D86 [37]. Corrected temperatures for 1 atm are available in Table S4.3. The maximum limit for T10 is 70 °C for Class AA, while its value is 50 °C for Class E (Table S4.2). The T10 for the gasoline used in this study was 77.9 °C, which is not within the acceptable range. GC-FID analysis of the gasoline revealed high concentrations of heavy olefins and aromatics. The relatively low RVP and high molecular weight of these compounds led to the high T10 for the gasoline. Therefore, none of the higher alcohol blends passed the T10 requirements with this low-volatile gasoline because they tend to increase the T10 of the fuel. All blends with single lower alcohols and some dual-alcohol blends (EH20, EG40, MB60, MH60, MB80, and MH80) have T10 values that meet ASTM D4814 class specifications. The ASTM D4814 allowable minimum T50 value is 77 °C for all classes. The ASTM D4814 maximum for T50 varies from 110 °C for Class E to 120 °C for Class AA. Five blends, each containing methanol, do not meet the minimum T50 (M60, M80, MH60, MB80, and MH80). Two 3M3P blends exceeded the maximum T50 requirement (H60 and H80) because of the high boiling temperature of 3M3P. The tail-end volatilities (T90-end point) for all blends are below that of gasoline, all passing the T90 maximum requirement. Considering all these limitations together, using this gasoline, which was not qualified itself due to the high T10, only six blends (E10, E20, EH20, E40, EH40, MB60) qualified for distillation curve Class AA.

4.4.1.4. Distillate Composition

The presence of alcohol(s), in particular ethanol, suppressed the distillation of aromatic species, as is apparent from the sharp rise in aromatic concentration once ethanol was evaporated (Figure 4.2). This sharp rise occurred later during the distillation for the blends containing higher concentrations of ethanol. This aromatic enrichment occurred because ethanol evaporated early, delaying the evaporation of the heavier aromatics. Previous work has shown that azeotropes formed with ethanol can play a minor role in the observed aromatic enrichment [38]. In most of the blends containing only ethanol, the mass fraction of aromatics at the late stages of the distillation (e.g., 90 vol%) are very similar to the neat gasoline despite having a much lower total fraction of aromatics than the base gasoline due to dilution. Comparing the dual-alcohol blends with the ethanol-only blends, the dual-alcohol blends (especially those with 3M3P) resulted in 4.2-30.3 % lower aromatic concentrations compared to gasoline at the 90 vol% distilled point. Since aromatics generally have shorter kinetic pathways to soot compared to other types of hydrocarbons present in gasoline [29], there is an increased susceptibility of PM formation when aromatics make up the heavy fraction of the fuel. Thus, oxygenated blends, especially dual-alcohol blends, may lead to an increase in PM emissions. It is worth noting that it is only one of many parameters that can affect the level of PM emissions. Other factors, including engine parameters, test conditions, fuel spray break-up, and air mixing, could potential modulate the formation of PM in oxygenated blends.

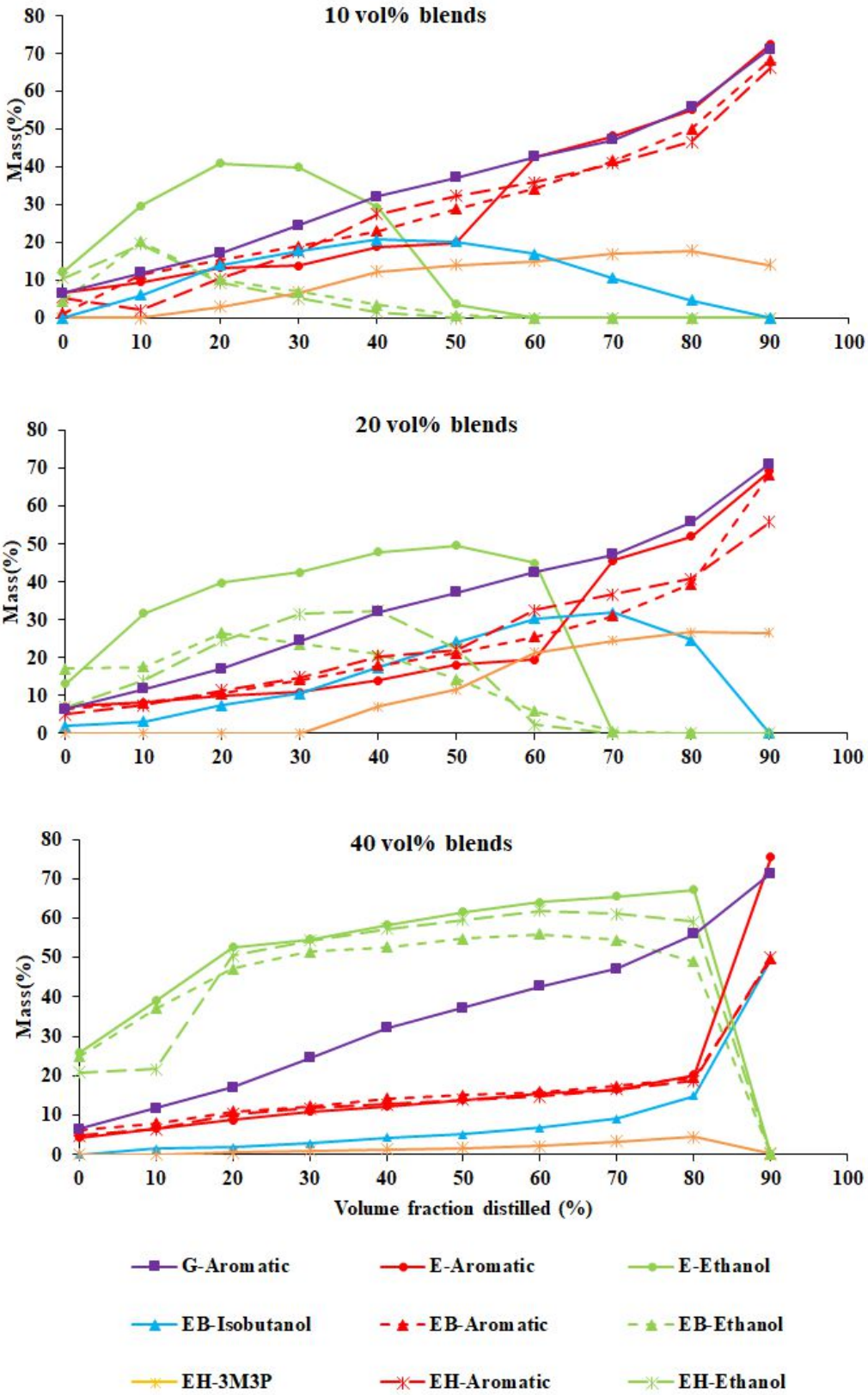
10 vol% blends
20 vol% blends
40 vol% blends
Mass(%)
Volume fraction distilled (%)
G-Aromatic
E-Aromatic
E-Ethanol
EB-Isobutanol
EB-Aromatic
EB-Ethanol
EH-3M3P
EH-Aromatic
EH-Ethanol

Figure 4.2. Distillate composition analysis for gasolines and blends containing up to 40% alcohol. The average coefficient of variation of all data points is ±2.5% for aromatics and ±3.7% for oxygenates from triplicate tests. G-Aromatic: Mass percent of aromatics in gasoline. E-Aromatic: Mass percent of aromatics in ethanol blends. EB-Aromatic: Mass percent of aromatics in dual-alcohol blends containing i-butanol. EH-Aromatic: Mass percent of aromatics in dual-alcohol blends containing 3M3P. E-Ethanol: Mass percent of ethanol in ethanol blends. EB-Ethanol: Mass percent of aromatics in dual-alcohol blends containing i-butanol. EH-Ethanol: Mass percent of aromatics in dual-alcohol blends containing 3M3P. EB- Isobutanol: Mass percent of i-butanol in dual-alcohol blends containing i-butanol. EH-3M3P: Mass percent of 3M3P in dual-alcohol blends containing 3M3P.

4.4.1.5. Distillation model validation

The distillation model accurately predicted the temperature inflection points for each of the mixtures and the corresponding composition changes, as seen in comparisons of distillation curves and molecular weight (Figures S4.6-S4.11). The overall agreement validates the accuracy of the distillation model and its use to predict droplet evaporation [31].

4.4.1.6. Droplet lifetime

Many parameters such as the injector's nozzle design, operational conditions, and physical properties of a fuel can influence spray atomization and droplet size distributions. In particular, density, viscosity, and surface tension are known to be important factors that describe the atomization of a liquid fuel. The specific gravity of the gasoline increased with the addition of alcohols, especially with higher alcohols (Table 4.3). The densities of the dual alcohol blends lied between the density of corresponding higher and lower alcohol blends. The kinematic viscosity was increased with increase in alcohol content (Figure 4.3). The kinematic viscosity for the single

higher alcohol blends (iso-butanol and 3M3P) increased more rapidly in a non-linear fashion compared to the blends containing only a single lower alcohol. The dual-alcohol blends exhibited viscosities closer to that of gasoline. Fuels with higher density and viscosity form larger droplet sizes, which can cause poor fuel atomization and may result in a heterogeneous mixture and accordingly more susceptibility to PM emissions [39]. The surface tensions of the blends were predicted by the DIPPR database [35] and the results were very close to the value for gasoline. Accounting for these differences in physical properties, a model developed by Elkotb [40, 41] was exploited to estimate the droplet size of all the fuel blends (relative to that of gasoline).

$$\text{Sauter Mean Diameter} = 3.085 v_l^{0.385} \sigma_l^{0.737} \rho_l^{0.737} \rho_g^{0.06} \Delta P_l^{-0.54} \quad \text{Eq. 4.2}$$

In Eqn. 4.2, v_l is the viscosity of liquid, ρ_l and ρ_l are the gas and liquid density, σ_l is the surface tension of liquid, and ΔP_l *is* the difference between injection pressure and ambient pressure. For an initial droplet diameter of gasoline of 25 μm, which is in the usual range for mean droplet diameters observed in traditional DISI injector technology [42], and maintaining the same ΔP_l for all blends, the initial droplet sizes of all other blends were determined relative to that of gasoline with Eq. 4.2 and the physical properties listed in Table 4.4. The droplet evaporation model was then used with the calculated droplet sizes for each blend at constant ambient temperature (323 K) and standard atmospheric pressure to determine the influence of droplet size on droplet evaporation lifetimes. In addition to droplet evaporation lifetimes, the transient HoV, surface temperature, and total oxygenate concentration profiles for gasoline and the blends were obtained (Figures S4.12-S4.14).

Regardless of total alcohol concentration, the dual-alcohol blends had longer droplet evaporation times compared to gasoline because of the higher HoV and larger initial droplet sizes (Figure 4.4). This difference is more accentuated for blends with higher blending ratios (17.1 and

8.4% increase relative to gasoline for EB40 and EH40, respectively). The dual-alcohol blends containing iso-butanol experienced had slower evaporation because of the higher HoV of iso-butanol relative to 3M3P. The only oxygenated blend that exhibited shorter evaporation time than the gasoline is E10, which can be attributed to the high vapor pressure of this blend. In the case of E20 and E40, the reduced RVP, increased HoV, and increase in droplet size compared to E10 lead to longer evaporation times relative to gasoline. The blends containing only ethanol were predicted to have ~14% shorter evaporation time on average compared to the corresponding dual-alcohol blends because of their higher volatility, regardless of slightly higher HoV values. The exception is E40, which has a longer evaporation time than EH40 because the difference in HoV between E40 and EH40 is high enough to overcome the differences in volatility. Interestingly, this is not the case with EB40 because iso-butanol has a higher HoV than 3M3P. These results indicate that once the multiple changes in properties responsible for droplet atomization and vaporization have been considered, fuels containing alcohol(s) may in fact possess slower in-cylinder evaporation behaviors and thus could be more prone to form inhomogeneous charges that could contribute to PM emissions, although engine testing and emission measurements are required to assess this.

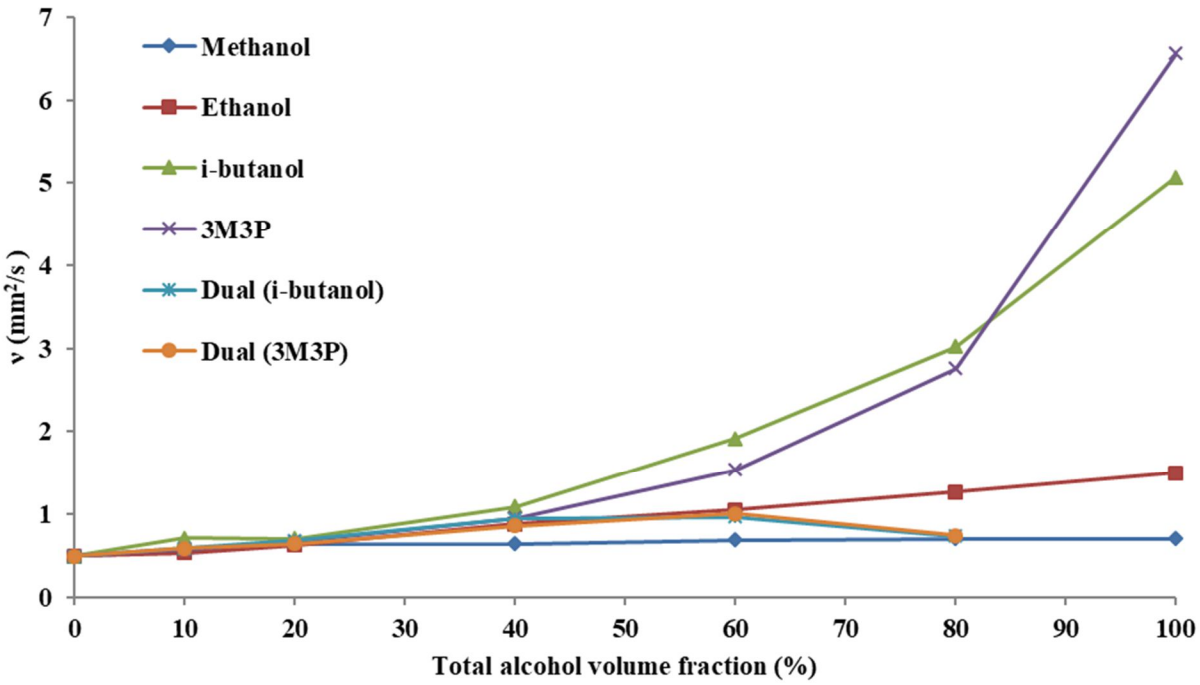

Figure 4.3 Kinematic viscosity at 20 °C plotted versus total alcohol volume fraction. The average standard error for all data points is 0.2.

Table 4.4. Physical properties and corresponding droplet sizes obtained from Elkotb model [40] for test fuels. [a] Predicted by the DIPPR databases [35].

Fuel	ρ (g/cm^3)	Surface tension [a] (N/m)	ν (mm^2/s)	Initial droplet size (μm)
Gasoline	0.74	0.0228	0.50	25.00
E10	0.74	0.0227	0.53	25.71
EB10	0.75	0.0228	0.58	26.91
EH10	0.75	0.0228	0.59	27.12
E20	0.75	0.0227	0.62	27.52
EB20	0.75	0.0227	0.68	28.56
EH20	0.75	0.0228	0.64	27.94
E40	0.77	0.0225	0.88	31.96
EB40	0.77	0.0226	0.94	32.80
EH40	0.76	0.0226	0.85	31.27

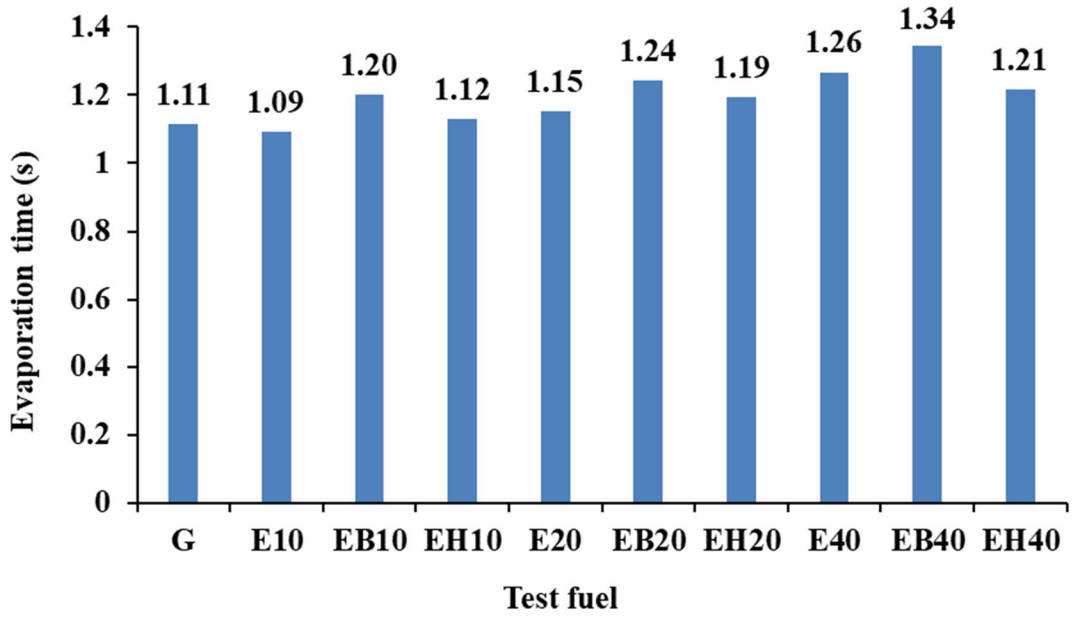

Figure 4.4 Droplet evaporation time for gasoline and alcohol blends obtained from droplet evaporation model for a constant ambient pressure and temperature of 1 atm and 323 K.

4.4.2. Water tolerance

Gasoline and water are immiscible; however, when an alcohol is blended into gasoline, some amount of water can also dissolve [18]. If the water tolerance of a fuel is sufficiently high to absorb the water which is in contact with the fuel at a given ambient temperature, no secondary corrosive phase forms. Among blends containing single alcohols, ethanol blends exhibited the highest water tolerance followed by i-butanol, methanol, and 3M3P at 10 °C (Figure 4.5). Although methanol is the most polar alcohol, the results showed a very low water tolerance for the blends containing methanol. This behavior can be explained by the high hydrophilicity of methanol such that it is quickly absorbed by the water that is in contact with the fuel. Ethanol is hygroscopic than the higher alcohols but not as hydrophilic as methanol, which explains why the ethanol blends showed the best water tolerance behavior. Of the higher alcohols, i-butanol had relatively good

water tolerance, especially at moderate to high blending ratios, while 3M3P had the lowest, even at high blending ratios, due to its lower polarity and longer hydrocarbon chain.

In case of the dual-alcohol blends, the concentration of the higher alcohols and total alcohol fraction were not high enough at the 10 vol% blending ratio to significantly improve the water tolerance of the gasoline. Among the 20 vol% blends, EH20 performed approximately as well as E20, while EB20 exhibited negligible water tolerance. This can be attributed to the higher concentration of ethanol in EH20 (11.5% in EH20 vs. 8.9% in EB20) as well as the lower polarity, and longer hydrocarbon chain of 3M3P. Interestingly, at blending ratios of 40 vol%, the water tolerance of both dual-alcohol blends exceeded that of ethanol owing to the influence of the higher alcohols. At 60 vol%, the dual-alcohol blends significantly improved the water tolerance compared to M60 (p-value = 0.0009) (recall that methanol is the lower alcohol in the 60 and 80 vol% dual-alcohol blends). Although the concentration ratio of the higher alcohols relative to the lower alcohol is very low in the 80 vol% blends, the dual-alcohol blends still had 15.3% higher water tolerance than M80.

A decrease of temperature from +10 to -10 °C led to an average decrease of 0.34 v/v % in the water tolerance, suggesting that diurnal and seasonal temperature variation may influence stability. It is worth noting that the solubility of water in alcohol-gasoline blends also depends on other parameters, including humidity and fuel (both gasoline fuel and alcohol) composition [43]. Fuels containing higher fractions of aromatics and olefins are more miscible with water due to the pi-bond in their structures [44].

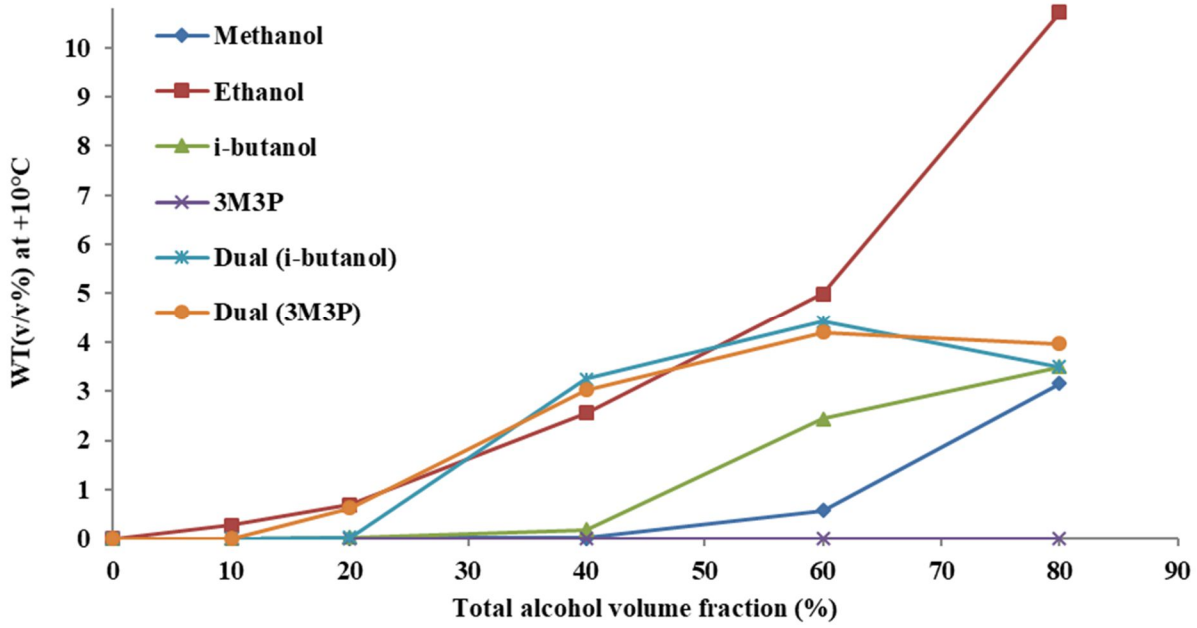

Figure 4.5. Water tolerance at +10 °C plotted versus total alcohol volume fraction. WT: Water tolerance. The average standard error for all data points is ± 0.002.

4.4.3. Lower heating value

Figure 4.6 depicts the measured LHV for the alcohol-gasoline blends as a function of the alcohol blending ratio. An approximately linear trend of decreasing LHV with decreasing carbon chain length can be observed for the alcohols investigated in this study due to the increase in oxygen content, with the lowest reduction in LHV from that of the gasoline observed for the 3M3P blends followed by iso-butanol, ethanol, and methanol. Applying the dual-alcohol approach did not increase the LHV of the blends notably, especially at high blending ratios. Up to 40 vol%, the LHVs of dual-alcohol blends were only an average of 0.9% higher than the ethanol blends because ethanol was the dominant alcohol component in dual-alcohol blends. At blending ratios higher than 40%, ethanol was replaced by methanol in the dual-alcohol blends and the LHV of the dual-alcohol blends dropped dramatically. Although the lower LHV combined with higher

stoichiometric air-fuel ratio of these alcohols compared to gasoline may adversely impact the fuel economy, the excellent anti-knock characteristics of these alcohols as well as their potential for charge cooling may allow the engine to operate at higher compression ratios and maximum pressures, which would increase the power-output notably. Thus, considering the higher HoV, more complete combustion, and higher octane value of these alcohols, it may be possible to obtain even better BSFC using these blends.

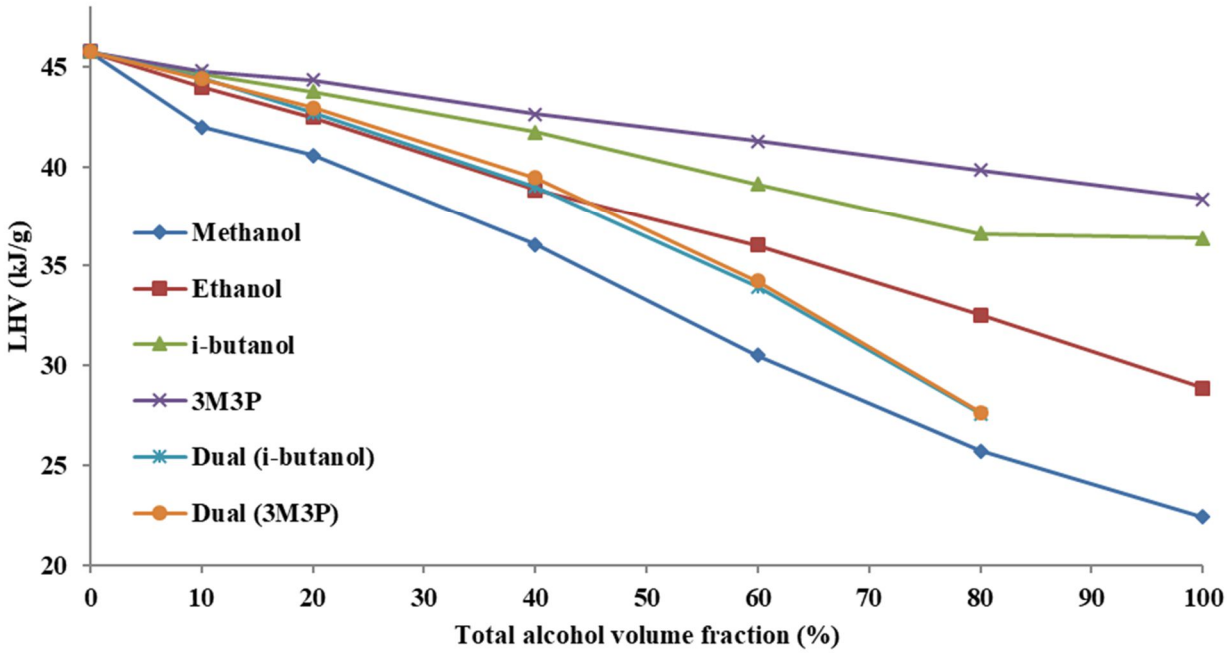

Figure 4.6. LHV as a function of total alcohol volume fraction for the tested blends. The average standard error for all data points is 0.37.

4.5. Conclusions

Regardless of total alcohol concentration, properly designed dual-alcohol blends could successfully keep the RVP very close to that of gasoline. Therefore, using higher alcohols as co-solvents in blends of gasoline with lower alcohols seems to be a viable option for controlling the RVP which can mitigate limitations associated with both high and low volatilities of gasoline

blends containing a single alcohol. Results showed that it may be advantageous to use dual-alcohol blends containing up to 40 vol% as they minimize the limitations of single-alcohol blends, in particular volatility, while exhibiting satisfactory properties for an acceptable performance in existing spark ignition engines particularly in terms of volatility, kinematic viscosity, and water tolerance. For the first time, the fuel potential of 3-methyl-3-pentanol in single- and dual-alcohol blends and iso-butanol in dual-alcohol blends was evaluated. Both iso-butanol and 3-methyl-3-pentanol exhibit promising properties as blendstocks for being used along with ethanol confirmed by acceptable performance of dual-alcohol blends containing these alcohols and ethanol. The dual-alcohol approach has potential to increase the portion of biofuel in the current gasoline system with no or only minor changes to current SI engine architectures and fuel delivery infrastructure. The results presented here suggest that research into the identification of combustion/emissions characteristics is warranted.

References

1- Elfasakhany A, Mahrous AF. Performance and emissions assessment of n-butanol–methanol–gasoline blends as a fuel in spark-ignition engines. Alexandria Eng J 2016;55:3015–24. doi:10.1016/j.aej.2016.05.016.

2- Pumphrey JA, Brand JI, Scheller WA. Vapour pressure measurements and predictions for alcohol-gasoline blends. Fuel 2000;79:1405–11. doi:10.1016/S0016-2361(99)00284-7.

3- Regulation to mitigate the misfueling of vehicles and engines with gasoline containing greater than ten volume percent ethanol and modifications to the reformulated and conventional gasoline programs. Fed Regist 2011;76:44406–50.

4- Bergthorson JM, Thomson MJ. A review of the combustion and emissions properties of advanced transportation biofuels and their impact on existing and future engines. Renew Sustain Energy Rev 2015;42:1393–417. doi:10.1016/j.rser.2014.10.034.

5- Masum BM, Masjuki HH, Kalam MA, Rizwanul Fattah IM, M Palash S, Abedin MJ. Effect of ethanol-gasoline blend on NOx emission in SI engine. Renew Sustain Energy Rev 2013;24:209–22. doi:10.1016/j.rser.2013.03.046.

6- Surisetty VR, Dalai AK, Kozinski J. Alcohols as alternative fuels: An overview. Appl Catal A Gen 2011;404:1–11. doi:10.1016/j.apcata.2011.07.021.

7- Wallner T, Ickes A, Lawyer K. Analytical assessment of C2-C8 alcohols as spark-ignition engine fuels. Lect. Notes Electr. Eng., vol. 191 LNEE, 2013, p. 15–26. doi:10.1007/978-3-642-33777-2_2.

8- Sayin C. Engine performance and exhaust gas emissions of methanol and ethanol-diesel blends. Fuel 2010;89:3410–5. doi:10.1016/j.fuel.2010.02.017.

9- Koç M, Sekmen Y, Topgül T, Yücesu HS. The effects of ethanol-unleaded gasoline blends on engine performance and exhaust emissions in a spark-ignition engine. Renew Energy 2009;34:2101–6. doi:10.1016/j.renene.2009.01.018.

10- Balki MK, Sayin C, Canakci M. The effect of different alcohol fuels on the performance, emission and combustion characteristics of a gasoline engine. Fuel 2014;115:901–6. doi:10.1016/j.fuel.2012.09.020.

11- Karavalakis G, Short D, Vu D, Russell RL, Asa-Awuku A, Jung H, et al. The impact of ethanol and iso-butanol blends on gaseous and particulate emissions from two passenger cars equipped with spray-guided and wall-guided direct injection SI (spark ignition) engines. Energy 2015;82:168–79. doi:10.1016/j.energy.2015.01.023.

12- Masum BM, Kalam MA, Masjuki HH, Palash SM, Fattah IMR. Performance and emission analysis of a multi cylinder gasoline engine operating at different alcohol–gasoline blends. RSC Adv 2014;4:27898–904. doi:10.1039/C4RA04580G.

13- Lawyer, K., Ickes, A., Wallner, T., Ertl, D., 2013a. Blend Ratio Optimization of Fuels Containing Gasoline Blendstock, Ethanol, and Higher Alcohols (C3eC6): Part Imethodology and Scenario Definition, pp. 02e15. SAE Technical Paper 2013-01- 1144.

14- Thewes M, Müther M, Brassat A, Pischinger S, Sehr A. Analysis of the Effect of Bio-Fuels on the Combustion in a Downsized DI SI Engine. SAE Int J Fuels Lubr 2012;5:274–88. doi:10.4271/2011-01-1991.

15- Dahmen M, Marquardt W. Model-Based Design of Tailor-Made Biofuels. Energy and Fuels 2016;30:1109–34. doi:10.1021/acs.energyfuels.5b02674.

16- Fatouraie M, Wooldridge MS, Petersen BR, Wooldridge ST. Effects of Ethanol on In-Cylinder and Exhaust Gas Particulate Emissions of a Gasoline Direct Injection Spark Ignition Engine. Energy & Fuels 2015;29:3399–412. doi:10.1021/ef502758y.

17- Ratcliff MA, Burton J, Sindler P, Christensen E, Fouts L, Chupka GM, et al. Knock Resistance and Fine Particle Emissions for Several Biomass-Derived Oxygenates in a Direct-Injection Spark-Ignition Engine. SAE Int J Fuels Lubr 2016;9:2016-01–0705. doi:10.4271/2016-01-0705.

18- Christensen E, Yanowitz J, Ratcliff M, McCormick RL. Renewable oxygenate blending effects on gasoline properties. Energy and Fuels 2011;25:4723–33. doi:10.1021/ef2010089.

19- Yüksel F, Yüksel B. The use of ethanol-gasoline blend as a fuel in an SI engine. Renew Energy 2004;29:1181–91. doi:10.1016/j.renene.2003.11.012.

20- Muzikova Z, Siska J, Pospisil M, Sebor G. Phase stability of butanol-gasoline blends. Chem List 2013;107:638–42.

21- Gautam M, Martin II DW, Carder D. Emissions characteristics of higher alcohol/gasoline blends. Proc Inst Mech Eng Part A J Power Energy 2000;214:165–82. doi:Doi 10.1243/0957650001538263.

22- Andersen VF, Anderson JE, Wallington TJ, Mueller SA, Nielsen OJ. Vapor pressures of alcohol-gasoline blends. Energy and Fuels, vol. 24, 2010, p. 3647–54. doi:10.1021/ef100254w.

23- Siwale L, Kristóf L, Bereczky A, Mbarawa M, Kolesnikov A. Performance, combustion and emission characteristics of n-butanol additive in methanol-gasoline blend fired in a naturally-aspirated spark ignition engine. Fuel Process Technol 2014;118:318–26. doi:10.1016/j.fuproc.2013.10.007.

24- Ratcliff MA, Luecke J, Williams A, Christensen E, Yanowitz J, Reek A, et al. Impact of higher alcohols blended in gasoline on light-duty vehicle exhaust emissions. Environ Sci Technol 2013;47:13865–72. doi:10.1021/es402793p.

25- Shirazi SA, Foust TD, Reardon KF. 2018. Development and Application of a Fuel Property Database for Mono-Alcohols as Fuel Blend Components for Spark Ignition Engines. Submitted.

26- ASTM D5191-15 Standard Test Method for Vapor Pressure of Petroleum Products (Mini Method), West Conshohocken, PA, 2015, https://doi.org/10.1520/D5191-15

27- ASTM D5188-16 Standard Test Method for Vapor-Liquid Ratio Temperature Determination of Fuels (Evacuated Chamber and Piston Based Method), West Conshohocken, PA, 2016, https://doi.org/10.1520/D5188-16

28- ASTM D240-17 Standard Test Method for Heat of Combustion of Liquid Hydrocarbon Fuels by Bomb Calorimeter, West Conshohocken, PA, 2017, https://doi.org/10.1520/D0240-17

29- Aikawa K (Honda RCL., Sakurai T (Honda RCL., Jetter JJ (Honda RAI. Development of a Predictive Model for Gasoline Vehicle Particulate Matter Emissions. SAE Int J Fuels Lubr 2010;3:610. doi:10.4271/2010-01-2115.

30- ASTM D6729-14 Standard Test Method for Determination of Individual Components in Spark Ignition Engine Fuels by 100 Metre Capillary High Resolution Gas Chromatography, West Conshohocken, PA, 2014, https://doi.org/10.1520/D6729-14

31- Burke, S.C., Ratcliff, M., McCormick, R., Rhoads, R., Windom, B. (2017). Distillation-based Droplet Modeling of Non-Ideal Oxygenated Gasoline Blends: Investigating the Role of Droplet Evaporation on PM Emissions.SAE International. https://doi.org/10.4271/2017-01-0581

32- Burke S, Rhoads R, Ratcliff M, McCormick R. et al. Measured and Predicted Vapor Liquid Equilibrium of Ethanol-Gasoline Fuels with Insight on the Influence of Azeotrope Interactions on

Aromatic Species Enrichment and Particulate Matter Formation in Spark Ignition Engines. SAE Technical Paper.2018; 2018-01-0361.doi:10.4271/2018-01-0361.

33- Backhaus, J. (2013). Design methodology of bio-derived gasoline fuels .M.S., Mechanical Engineering, University of Wisconsin, Madison, WI.

34- G.M. Chupka, E. Christensen, L. Fouts, T.L. Alleman, M.A. Ratcliff, R.L. McCormick, Heat of Vaporization Measurements for Ethanol Blends Up To 50 Volume Percent in Several Hydrocarbon Blendstocks and Implications for Knock in SI Engines, SAE Int. J. Fuels Lubr. 8 (2015) 2015-01–0763. doi:10.4271/2015-01-0763.

35- Design Institute for Physical Property Data (U.S.), DIPPR Project 801, full version: evaluated standard thermophysical property values, Des. Inst. Phys. Prop. Res. (2005).

36- Gibbs L, Anderson B, Barnes K, Engeler G, Freel J, Horn J, Ingham M, Kohler D, Lesnini D, MacArthur R, Mortier M. Motor gasolines technical review. Chevron Products Company, San Ramon, CA. 2009.

37- ASTM International. ASTM D86-17 Standard Test Method for Distillation of Petroleum Products and Liquid Fuels at Atmospheric Pressure. West Conshohocken, PA; ASTM International, 2017. doi: https://doi.org/10.1520/D0086-17

38- Ratcliff MA, McCormick RL, Burke S, Rhoads R, Windom B. Measured and Predicted Vapor Liquid Equilibrium of Ethanol-Gasoline Fuels with Insight on the Influence of Azeotrope Interactions on Aromatic Species Enrichment and Particulate Matter Formation in Spark Ignition Engines. National Renewable Energy Lab.(NREL), Golden, CO (United States).

39- Lapuerta M, García-Contreras R, Campos-Fernández J, Dorado MP. Stability, lubricity, viscosity, and cold-flow properties of alcohol-diesel blends. Energy and Fuels 2010;24:4497–502. doi:10.1021/ef100498u.

40- Elkotb MM. Fuel atomization for spray modelling. Prog Energy Combust Sci 1982;8:61–91. doi:10.1016/0360-1285(82)90009-0.

41- dos Santos F, le Moyne L. Spray atomization models in engine applications, from correlations to direct numerical simulations. Oil Gas Sci Technol 2011;66:801–22. doi:10.2516/ogst/2011116.

42- Stach, T., Schlerfer, J., Vorbach, M., New Generation Multi-hole Fuel Injector for Direct-Injection SI Engines - Optimization of Spray Characteristics by Means of Adapted Injector Layout and Multiple Injection, SAE Paper 2007-01-1404-,2007.

43- Lapuerta M, García-Contreras R, Campos-Fernández J, Dorado MP. Stability, lubricity, viscosity, and cold-flow properties of alcohol-diesel blends. Energy and Fuels 2010;24:4497–502. doi:10.1021/ef100498u.

44- Mužíková Z, Pospíšil M, Šebor G. Volatility and phase stability of petrol blends with ethanol. Fuel 2009;88:1351–6. doi:10.1016/j.fuel.2009.02.003.

5 Physiochemical Property Characterization of Hydrous and Anhydrous Ethanol Blended Gasoline [*]

5.1. Summary

Water removal during the production of bio-ethanol is highly energy intensive. At the azeotropic point, the mixture can no longer be separated via fractional distillation expensive and energy intensive methods are required for further purification. Hence, there is an interest in using hydrous ethanol at the azeotropic point to improve the energy balance of ethanol fuel production. Currently there is a lack of available thermophysical property data for hydrous ethanol gasoline fuel blends. This data is important to understand the effect of water on critical fuel properties and to evaluate the potential of using hydrous ethanol fuels in conventional and optimized spark ignition engines. In this study, gasoline was blended with 10, 15, and 30 vol% of anhydrous and hydrous ethanol. The distillation curve, Reid vapor pressure, vapor lock index, viscosity, density, copper strip corrosion, haze and phase separation points, and lower heating value were measured for each blend and the results were compared to ASTM D4814, the standard specification for automotive spark ignition engine fuels. The properties of low and mid-level hydrous ethanol blends are not significantly different from those of anhydrous ethanol blends, suggesting that hydrous ethanol blends have the potential to be used in current internal combustion engines as a drop-in fuel with few or no modification.

[*] *Submitted as "Physiochemical Property Characterization of Hydrous and Anhydrous Ethanol Blended Gasoline" by Saeid Aghahossein Shirazi, Bahareh Abdollahipoor, Jake Martinson, Kenneth F. Reardon and Bret C. Windom. In the study presented in this chapter, I selected the tests and blends, designed the experiments, conducted the characterization tests, and wrote the manuscript.*

5.2. Introduction

In the United States, the Renewable Fuel Standard (RFS) created by the U.S. Environmental Protection Agency (EPA) calls to produce 36 billion gallons of biofuels annually by 2022 to reduce greenhouse gas emissions and improve energy security [1]. Ethanol is one of the most likely candidates to reach this goal. Based on the most recent report from U.S. Energy Information Administration, fuel ethanol production capacity reached 15.5 billion gallons per year at the beginning of 2017 in the United States [2]. Almost all gasoline engine vehicles made after 2001 can use gasoline blends with 10 and 15 vol % ethanol (E10 and E15). Flexible fuel vehicles (FFVs) can operate with significantly higher ethanol concentrations such as E85 and E100. Ethanol fuel in the United States must be anhydrous, meaning a maximum water content of 1 wt %. Since fermentation of maize to ethanol usually results in a product that contains only 8-12 wt % ethanol, a significant amount of energy is required for separation and dehydration. Based on the report by Shapouri et al. [3], dehydration accounts for 14% (~3.5 MJ/L) of the total output energy (~25 MJ/L) accounting for the higher heating value (HHV) of ethanol and co-product energy credits. During purification, once the azeotropic mixture of ethanol and water (95.6/4.4 % ethanol/water) is reached, it is no longer possible to use standard distillation techniques and thus expensive alternative methods are required [4, 5]. Therefore, there is an interest in using hydrous ethanol (at the azeotropic mass fraction) as a fuel in internal combustion engines to reduce the cost and energy of production.

Several studies have investigated the influence of hydrous ethanol on performance and emissions of gasoline-fueled vehicles. Schifter et al. [6] compared the exhaust emissions and engine performance of gasoline blended fuels containing 10 to 40 vol% of hydrous ethanol (4 vol% water + 96 vol% ethanol) to those of gasoline-anhydrous ethanol blends with the same ratios in a

single cylinder port fuel injection spark ignition (SI) engine with equivalence ratio varying from 0.9 to 1.1. Their results suggest that the presence of water is more important than the amount of water. The intake temperature decreased with the presence of water due to the high heat of vaporization (HoV) of water. However, the intake temperature did not change notably with increasing water concentration. The increase in water content was found to decrease the NO_x emissions as a result of reduced peak combustion temperature but also led to increased fuel consumption due to the lower calorific value of the hydrous blends. In terms of thermal efficiency, the hydrous ethanol blends performed almost identically to the anhydrous ethanol blends. The authors credited this observation to the higher charge cooling effects of hydrous blends, which compensates for their slower combustion process and lower heating value. In the same study, Schifter et al. [6] also reported octane ratings for both anhydrous and hydrous ethanol blends up to 30 vol% by way of measurements with a Cooperative Fuel Research (CFR) engine. The effect of water on the octane value was negligible, although CFR engines and the knock tendencies of a fuel are highly sensitive to the fuel's charge cooling [7].

Kyriakides et al. [8] compared a specific mixture of 60:30:10 gasoline:ethanol:water (E40h) to an anhydrous ethanol-gasoline blend (E40) in an Otto engine. Similar to the results of Schifter et al. [6], they reported a significant reduction in NOx and an increase in fuel consumption with E40h. In addition, no difference in engine torque was noticed between E40 and E40h. Costa and Sodré [9] used a flexible fuel engine to compare neat hydrous ethanol (6.8 vol% water + 93.2 vol% ethanol) with an anhydrous ethanol-gasoline blend (E22). In terms of emissions, the use of hydrous ethanol produced lower levels of CO and unburned hydrocarbons (UHC) emissions than E22, but higher CO_2 and NO_x. The increase in NO_x was attributed to the faster flame speed and the use of more advanced ignition timing for the hydrous ethanol fuel, which both favor the

production of higher peak temperatures. Hydrous ethanol fuels had a higher thermal efficiency compared to E22, which was explained by reduced heat loss to cylinder walls due to the higher HoV and faster flame speed of the hydrous ethanol. However, the lower heating value of hydrous ethanol led to an increase in brake-specific fuel consumption (BSFC). Hydrous ethanol produced lower torque and brake mean effective pressure (BMEP) at low engine speeds (below 3250 rpm), with the trend inversed at higher speeds (over 4000 rpm). To explain this behavior, the authors stated that since there is enough time for complete combustion at low engine speeds, the lower heating value is the dominant factor. However, faster flame velocity is favorable at higher engine speeds due to the limited time for a complete combustion. Melo et al. [10] studied combustion and emission characteristic of gasoline blends with hydrous ethanol at different ratios operating in a 1.4-L, flexible-fuel Otto engine. In this study, E25 was used as a base fuel and subsequently was blended with 30, 50, 80 and 100 vol% of hydrous ethanol (H30, H50, H80 and H100). The hydrous ethanol contained 4.3 vol% water to match the azeotrope proportions. In general, engines operating on blends with higher ethanol content had higher BSFC and CO_2 emissions, but lower CO and UHC emissions. NO_x emissions had complex trends with ethanol addition and were highly dependent on the operating conditions.

Wang et al. [11] compared combustion and emission characteristics of pure gasoline, E10, and hydrous ethanol (H10) operating in a port injection gasoline engine. In this study, hydrous ethanol contained 5 vol% water. The use of gasoline exhibited the highest peak pressure at the low and medium loads, followed by H10 and E10, respectively, while at high load, H10 produced the highest peak in-cylinder pressure. This behavior has its roots in the high HoV of ethanol which decreases combustion temperatures, leading to a lower peak in-cylinder pressure at low and medium loads; however, the negative effect of high HoV diminished at higher loads. The peak

heat release rates observed when using H10 were higher than both gasoline and E10 at all the tested operating conditions. At low and medium loads, the peak heat release rates of gasoline were higher than E10 while at high load the peak heat release rates of E10 were higher than those of gasoline. These behaviors were justified with the same rationale for peak in-cylinder pressure. Ethanol addition increased NO_x emissions, especially at high load. This increase was attributed to relative oxygen-enrichment in the reaction regions and a faster flame propagation and combustion process, resulting in a higher temperature in the cylinder. The increase in NO_x emission was slightly lower for H10 in comparison to E10 because the HoV of water is higher than ethanol, leading to a stronger cooling effect. The presence of oxygen in both hydrous and anhydrous ethanol blends caused less CO and UHC emissions compared to gasoline especially at low and medium loads. The level of CO and UHC emissions at low and medium loads for H10 was greater than E10 which can be attributed to higher charge cooling effect of water slowing the oxidation kinetics of CO and unburned hydrocarbons.

All previous studies evaluating hydrous ethanol have been limited to combustion and emission characteristics. In general, negligible differences in fuel economy, engine performance, and emissions were observed when comparing hydrous and anhydrous ethanol blended fuels. Notably, the stock engines used in these investigations were not tuned to operate on higher ethanol concentrations with water. Tuning engine parameters related to the compression ratio, injector design, boost pressure, along with spark and valve timing could lead to the realization of better performance with the hydrous ethanol fuels. This is consistent with the goals of an ongoing DOE research program related to the co-development of advanced SI engines and biofuels [12].

The goal of this study was to provide a comprehensive assessment of the thermophysical properties of hydrous ethanol-gasoline blends to examine their potential as a fuel blend for

conventional SI engines. The fuel properties of hydrous ethanol-gasoline blends (H10, H15 and H30), anhydrous-ethanol gasoline blends (E10, E15 and E30), and pure gasoline (E0) were compared to ASTM D4814 [13], the standard specification for automotive spark ignition engine fuel to determine the feasibility of replacing gasoline with hydrous alternative fuels without requiring significant changes to current engine design and fuel delivery infrastructure.

5.3. Materials and Methods

5.3.1. Test fuels

In this study, the E0 fuel was unleaded test gasoline (UTG-96) from Phillips 66. This gasoline was blended by volume with 10, 15, and 30% of anhydrous and hydrous ethanol to produce E10, E15, E30, H10, H15, and H30. Hydrous ethanol was prepared by blending 96 vol% of anhydrous ethanol with 4 vol% of deionized water. All test fuels were stored in a freezer at -18 °C to avoid errors as a consequence of unintentional evaporation. Blends containing 10 and 15 vol% ethanol were selected because they are the common ethanol concentration and maximum allowable ethanol concentration in the US market, respectively. Blends consisting of 30 vol% ethanol were considered to study the effects of higher concentration of ethanol and water content on fuel specifications.

5.3.2. Fuel Characterization

The test fuel blends were characterized by measuring the distillation curve, Reid vapor pressure (RVP), vapor lock index, viscosity, density, copper strip corrosion, phase separation point, and lower heating value (LHV). The Advanced Distillation Curve approach developed at the National Institute of Standards and Technology (NIST) was used to obtain distillation curves [14]. RVP and vapor lock index were measured using a Grabner Instruments Minivap VPXpert vapor pressure analyzer according to ASTM 5191 [15] and ASTM D5188 [16], respectively. An

Anton Paar SVM 3000 viscometer-densitometer was used to measure viscosity and density. The copper strip corrosion test was conducted using a copper strip tester (Protest) based on ASTM D130-12 [17]. The phase separation temperature was determined with a Lawler cloud point DR4-14 instrument according to ASTM D6422–99 [18]. LHV was measured with an IKA C200 calorimeter according to ASTM D240-14 [19]. Each test was repeated a minimum of three times. The complete set of characterization data for all tests fuels and corresponding standard deviations is given in Table 5.1.

Table 5.1. Properties of tested gasoline blends with hydrous (H10, H15, H30) and anhydrous (E10, E15, E30) ethanol. Values are shown as the mean +/- one standard deviation of triplicate measurements.

Property	Gasoline (E0)	E10	E15	E30	H10	H15	H30
Ethanol content (vol %)	0	10	15	30	9.6	14.4	28.8
Water content (vol %)	0	0	0	0	0.4	0.6	1.2
Reid vapor pressure (kPa)	53.13 ± 0.16	59.54 ± 0.28	59.26 ± 0.17	55.03 ± 0.18	61.36 ± 0.86	61.49 ± 0.57	57.88 ± 1.16
$T_{V/l=20}$ (°C)	66.33 ± 0.34	57.2 3± 0.41	56.85 ± 0.35	58.63 ± 0.28	55.40 ± 0.08	55.5 ± 0.3	57.67 ± 0.05
Initial boiling point (°C) at 1 atm	53.4 ± 0.5	53.45 ± 0.93	53.61 ± 0.59	54.32 ± 0.88	53.63 ± 0.32	53.67 ± 0.41	53.86 ± 1.00
T10 (°C) at 1 atm	76.06 ± 0.49	64.78 ± 0.83	64.85 ± 0.79	66.46 ± 0.74	64.45 ± 0.94	63.75 ± 0.93	65.07 ± 0.86
T50 (°C) at 1 atm	108.94 ± 0.7	107.97 ± 0.7	87.03 ± 3.9	78.54 ± 0.0	108.57± 1.4	91.16 ± 1.2	77.3 ± 0.6
T90 (°C) at 1 atm	161.97 ± 1.3	167.24 ± 3.9	165.22 ± 11.9	151.46 ± 5.9	166.33 ± 8.5	179.34 ± 6.0	164.38 ± 3.8
Driveability index (°C) at 1atm	602.87	601.64	602.50	n/a	602.02	627.35	n/a
Lower heating value (kJ/g)	45.32 ± 0.28	43.87 ± 0.21	42.82 ± 0.34	40.78 ± 0.14	42.77 ± 1.00	42.76 ± 0.42	39.03±0.28
Density @ 20 °C (g/cm^3)	0.74 ± 0.00	0.75 ± 0.00	0.75 ± 0.00	0.75 ± 0.00	0.75 ± 0.00	0.76 ± 0.00	0.78 ± 0.00
Dynamic viscosity@ 20 °C (cP)	0.36 ± 0.03	0.42 ±0.00	0.43 ± 0.01	0.56 ± 0.01	0.42 ± 0.01	0.49 ± 0.02	0.79 ± 0.01
Kinematic viscosity @ 20 °C (mm^2/s)	0.49 ± 0.04	0.57 ± 0.00	0.57 ± 0.01	0.74 ± 0.01	0.57 ± 0.01	0.65 ± 0.03	1.01 ± 0.02
Copper strip corrosion test, 3 h at 50 °C	1a	1a	1a	1a	1a	1a	1a
Haze point (°C)	n/a	n/a	n/a	n/a	−5.00 ± 0.47	−11.00 ± 0.47	−26.00 ± 1.25
Phase separation (°C)	n/a	n/a	n/a	n/a	−7.00 ± 0.82	−15.00 ± 0.82	−28.00 ± 1.41

5.4. Results and Discussion

5.4.1. Volatility

The vaporization of a fuel precedes all combustion and can limit the ability and/or rate of the fuel to mix with the air to create the desired homogeneous or stratified charge important for combustion phasing and emissions [20]. As such, the volatility and properties associated with the phase change of the fuel, including vapor pressure, distillation curve, HoV, and the derived vapor

lock indices and drivability indices are important properties that must match specification for effective engine operation. There is no single best volatility defined for a smooth driveability because volatility is highly dependent on altitude and seasonal temperature of the location. Three indices are used in the United States to characterize the volatility of a fuel: vapor pressure, distillation curve, and vapor lock index. ASTM D4814 sets limits for vapor pressure, distillation temperatures (at 10, 50, and 90% evaporated points), and vapor lock index. The experimental results for these properties are presented and compared to the gasoline specification ASTM D4814 in Table 5.2.

5.4.1.1. Vapor pressure

With regard to cold-start and warm-up driveability, vapor pressure is one of the most important fuel properties. Low vapor pressure results in cold start problems while high vapor pressure can lead to vapor lock and evaporative emissions 21. RVP is the metric commonly used to characterize a fuel's vaporization potential. The RVP is the vapor pressure (two-phase) at a temperature of 100 °F (37.8 °C) while maintaining the volume ratio of the vapor to liquid phase of the sample at 4:1, according to ASTM D5191 [22]. Generally, mixtures of non-polar hydrocarbons with polar compounds deviate from ideal solution behavior due to formed positive azeotropes. Ethanol can form positive azeotropes with C5-C8 hydrocarbons (alkanes, olefins, aromatics) with normal boiling points in the range from ~30 °C - 120 °C [23]. This behavior, stemming from the polarity of ethanol, increases the RVP of the fuel when ethanol is blended with gasoline up to about 45 vol% [24] despite the much lower RVP of ethanol in its pure state.

The RVP results are presented in Figure 5.1. The addition of anhydrous and hydrous ethanol to the base gasoline increased the RVP, and the maximum RVP was observed at 10 vol% and 15 vol% for anhydrous and hydrous ethanol, respectively. The results for anhydrous ethanol

are in agreement with previous studies [24-27]. For each blend ratio, the RVP of the hydrous ethanol blend was higher than that of the anhydrous ethanol blend, which can be attributed to the higher polarity of water compared to ethanol and the increased potential to form positive azeotropes. For anhydrous blends, the highest RVP was observed for E10 while for hydrous ethanol blends, the highest was H15.

The optimum volatility for fuels highly depends on temperature and altitude of the location. Fuels with moderate volatility are desired for hot seasons and locations with high altitudes while relatively high volatile fuels are required for cold seasons and low altitude regions. To address the dependency of the volatility on elevation and seasonal climatic changes, ASTM D4814 provides six vapor pressure/distillation classes (AA, A, B, C, D, E) and six vapor lock protection classes (1-6) for fuels (Table 5.2). The seasonal and geographic distribution of the combined vapor pressure/distillation-vapor lock classes is specified by an alphanumeric designation that uses a letter from vapor pressure/distillation classes and a number from vapor lock protection classes. Class AA in vapor pressure/distillation classes accounts for hottest regions while Class E accounts for coldest regions. The maximum allowable RVP for each class is available in the ASTM D4814. Here, E0 was found to qualify for ASTM D4814 Class AA, while all of the blends qualify for Class A.

Table 5.2. ASTM D4814 requirements for vapor pressure/distillation and vapor lock protection classes [13].

	Vapor Pressure/Distillation Class					
	AA	**A**	**B**	**C**	**D**	**E**
Reid vapor pressure (kPa), max	54	62	69	79	93	103
Distillation temperatures(°C)						
T10, max	70	70	65	60	55	50
T50, min	77	77	77	77	77	77
T50, max	121	121	118	116	113	110
T90, max	190	190	190	185	185	185
End point, max	225	225	225	225	225	225
Driveability index (°C), max	597	597	591	586	580	569
	Vapor Lock Protection Class					
	1	**2**	**3**	**4**	**5**	**6**
$T_{V/l=20}$ (°C), min	54	50	47	42	39	35

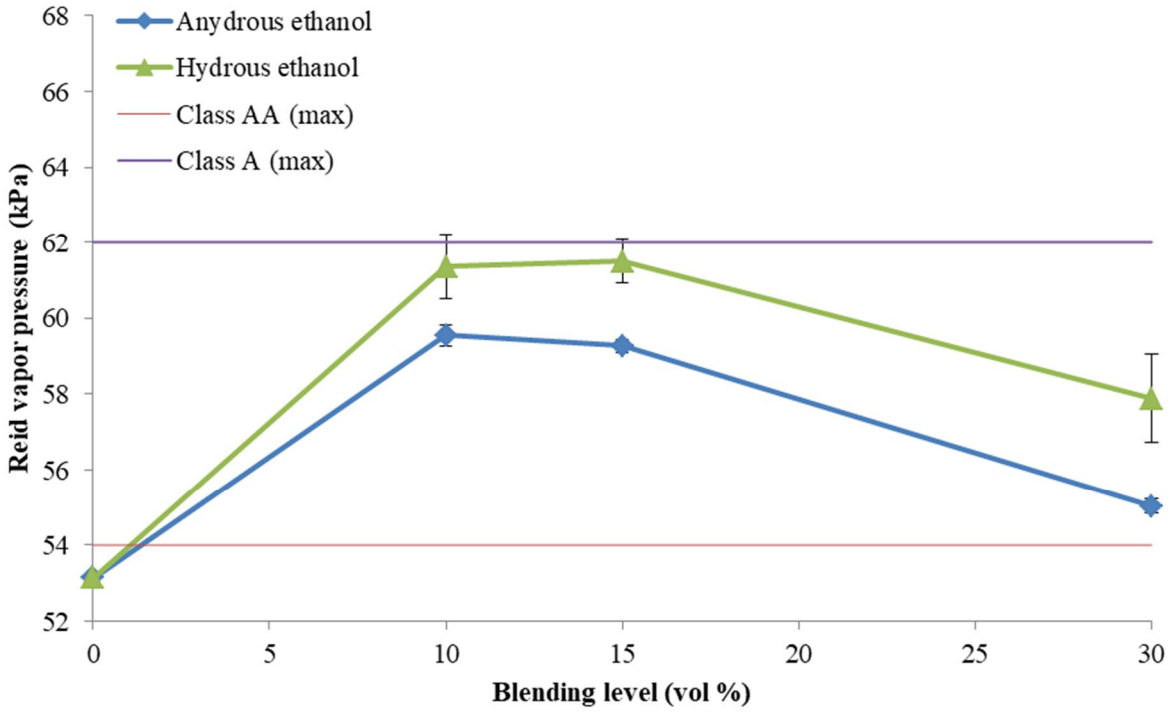

Figure 5.1. Effects of ethanol (anhydrous and hydrous) blending on the RVP of gasoline. Error bars represent +/- one standard deviation of triplicate measurements.

5.4.1.2. Vapor lock index

The vapor-locking tendency of a fuel can be attributed to its vapor pressure and the front end of the distillation curve, but the property that best relates to hot fuel handling problems is the vapor lock index, defined as the temperature at which a fuel forms a volumetric vapor-liquid ratio of 20 ($T_{V/L=20}$). ASTM D4814 identifies six vapor lock protection classes (1 to 6) for minimum $T_{V/L=20}$ in order to eliminate the vapor lock problem. In this classification, Class 1 accounts for hottest regions while Class 6 accounts for coldest regions. A fuel with a higher $T_{V/L=20}$ exhibits greater protection against vapor lock. The measured $T_{V/L=20}$ values for the anhydrous and hydrous ethanol-gasoline blends are presented in Figure 5.2. Blending gasoline with both hydrous and anhydrous ethanol decreased the $T_{V/L=20}$ compared to E0 due to the formation of positive azeotropes. Christensen et al. [28] reported similar trends with anhydrous ethanol blended gasoline. This reduction is more pronounced in the case of hydrous ethanol because of higher polarity of the water. Thus, at each blend ratio, the $T_{V/L=20}$ of the hydrous ethanol blend was less than that of the anhydrous ethanol blend, which is consistent with results obtained for RVP. All of these blends can be best categorized under ASTM D4814 Class 1 (minimum of 54 °C).

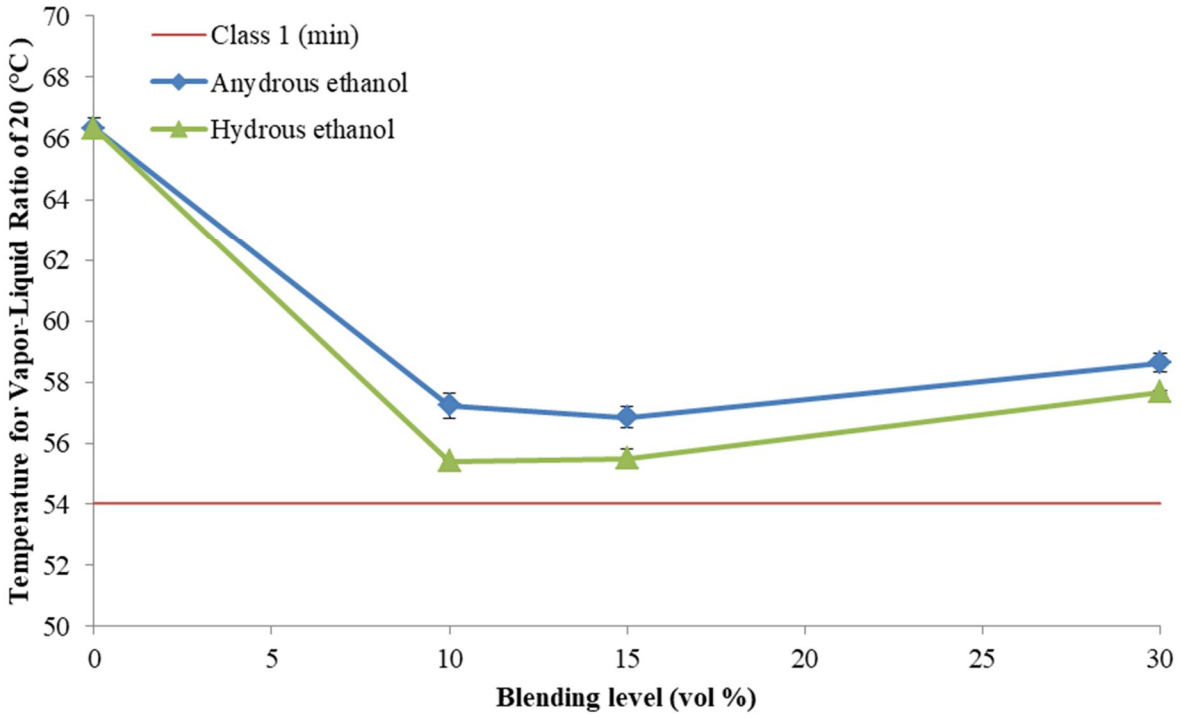

Figure 5.2. Effect of ethanol (anhydrous and hydrous) blending on vapor lock index of gasoline. Error bars represent +/- one standard deviation of triplicate measurements.

5.4.1.3. Distillation Curve

A distillation curve is a plot of the boiling temperature of a fluid mixture versus the volume fraction distilled and can be related to parameters such as engine startability, icing and vapor lock in the fuel system, fuel autoignition, fuel injection schedule, and even exhaust emissions in both gasoline and diesel engines [29-31]. Conventionally, gasolines are composed of compounds with boiling points ranging from about 20 to 225 °C [31]. Front-end volatility (T0 to T20) has a vital role in cold start, engine warm-up, evaporative emissions, and vapor lock. Midrange volatility (T20 to T90) is relevant to fuel economy 10, warming up, acceleration, and cold weather performance [28]. The tail-end volatility (T90 to end-point) which represents the fraction of hydrocarbons with high boiling points is important to avoid the formation of deposits inside the

engine and particulate matter formation [32]. Usually SI engines are relatively flexible and are not highly affected by small changes in the distillation curve. The ASTM D4814 sets maximum boundaries for T10, T90, and end-point distillation temperatures and a boundary range for T50. T10 should be lower than maximum allowable limits to provide a fast start of the engine at cold temperatures and low engine RPM. T50 is adjusted to ensure the balance between low and high boiling point compounds. End-point is set to a maximum of 225 °C as components with higher boiling temperatures can cause combustion failure due to reduced fuel/air mixing as well as oil dilution [28].

Since the ASTM D8418 specifies limits at atmospheric pressure while distillation temperatures were obtained at 84 kPa in this study, temperature readings were corrected to 101.3 kPa by applying the Sydney-Young equation (Eq. 5.1) as stated in ASTM D86 33:

$$C_c = 0.0009\ (101.3 - P_k)(273 + t_c) \qquad \text{Eq 5.1}$$

where C_c is the correction factor added algebraically to the observed temperature readings, P_k is barometric pressure at the time and location of the test (84 kPa), and t_c is the observed temperature reading in °C. Based on ASTM criteria, only the unblended gasoline exceeded the T10 test requirements; all the other fuel blends were within the temperature limits for at least one of the volatility classes.

The distillation curves for each blend are depicted in Figure 5.3 and distillation temperatures (initial boiling point, T10, T50, T90) for each of the blends are listed in Table 5.1. No significant difference was observed among the initial boiling points of the blends and gasoline; however, it was observed that ethanol (anhydrous and hydrous) addition significantly changed the shape of the distillation curve. These changes can be attributed to the near-azeotropic behavior of ethanol-gasoline blends. The near-azeotropic behavior is apparent from a localized near-flat region

in the distillation curve and is more accentuated when large amounts of oxygenate were used [34] as observed for E30 and H30 (Figure 5.3). All ethanol blends (hydrous and anhydrous) reduced the front-end and midrange distillation temperatures due to the formation of azeotropes. Compared to the unblended gasoline, lower boiling temperatures were observed for the first 50% evaporated for E10 and E15 and nearly 75% of the distillation curve for E30, which are consistent with previous observations by Anderson et al. [35]. Since the tail-end volatilities for all blends approached that of gasoline and most of the ethanol and water are evaporated by this point, changes in T90 compared to E0 are negligible. Small differences between blends at the tail-end can be attributed to the reduced concentration of heavy hydrocarbons due to dilution and also through the formation of azeotropes with the ethanol and water resulting in their accelerated removal from the liquid phase. For ethanol blends, the sudden rise in boiling temperatures after the nearly isothermal boiling behavior occurs at volume fractions corresponding to the point at which all of the ethanol is evaporated, resulting in the convergence of the distillation curves to that of the E0 fuel.

At each blend ratio, hydrous and anhydrous ethanol blends presented similar patterns and their differences are statistically negligible. All hydrous ethanol blends demonstrated a slightly faster temperature rise at the inflection point where the distillation curve approaches that of the E0. This may be due to the increased positive azeotropic behavior of blends containing water.

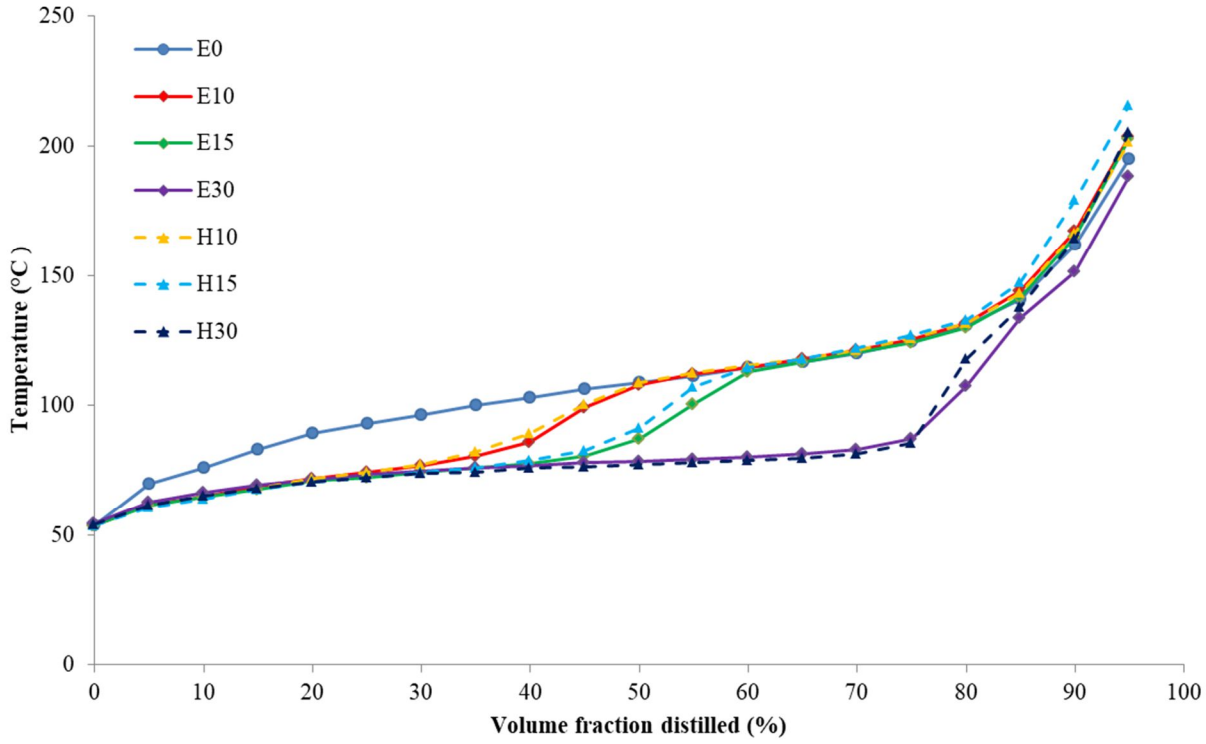

Figure 5.3. Distillation curves for gasoline and blends of hydrous and anhydrous ethanol measured at 1 atm. The average standard deviation for all data points is 2.2°C.

5.4.2. Driveability index

Driveability index (DI_c), a function of T10, T50, T90 and ethanol concentration, is a parameter listed in ASTM D4814 and used to ensure smooth driveability during the cold start and warm-up phases of an engine. The values for driveability indices are available in Table 5.1. For E10 and H10, the equation provided in the standard for gasoline and gasoline-ethanol blends containing up to 10 vol% was used:

$$DI_c = 1.5\,T_{10} + 3\,T_{50} + T_{90} + 1.33 \times (Ethanol\ \%\ by\ volume) \quad \text{Eq.5.2}$$

For E15 and H15, the equation for gasoline-ethanol blends containing 10–15 vol% was used:

$$DI_c = 1.5\,T_{10} + 3\,T_{50} + T_{90} + 5.26 \times (Ethanol\ \%\ by\ volume) \quad \text{Eq.5.3}$$

It is not clear how Equation 5.3 should be modified for the application of blends containing more than 15 vol% ethanol and therefore this parameter was not evaluated for E30 and H30. Gasoline and all of the 10 and 15 vol% blends exceeded the maximum drivability index. This is most likely due to the high T10 value for the base gasoline being out of the acceptable range. The use of a gasoline with better front-end volatility characteristics may produce blends with acceptable DI_c values.

5.4.3. Corrosion and water phase stability

ASTM D130-12 17 describes a copper strip corrosion test and standards to ensure that there would be no corrosion to fuel system metal surfaces due to reactive sulfur compounds in the fuel. However, corrosion is not limited to sulfur corrosion. Generally, ethanol can cause corrosion in three ways: (1) Ethanol is a relatively strong solvent due to the high polarity and can be corrosive to some metallic and non-metallic parts of the engine which is known as dry corrosion [36], (2) Low quality commercial oxygenates may contain ionic impurities such as chloride ions and acetic acid which can be corrosive [36], (3) ethanol is highly hygroscopic and is able to absorb water which can trigger phase separation especially at low temperatures when the amount of water adjacent to the fuel is massive. Therefore, a corrosive mixture of water and ethanol can form at the bottom of fuel tanks which can also adversely affect the combustion by reducing the octane value of the fuel [37]. The stability of water in ethanol-gasoline blends is a function of ethanol concentration, temperature, gasoline composition and presence of co-solvents [23]. As shown in Table 5.1, all fuel samples tested as Category 1a (slight tarnish), which means no corrosion. In addition, no notable difference was observed in the appearance of the copper strips when submerged in the fuels containing different amounts of ethanol and water. While these measurements were taken with completely miscible samples, it is essential to identify the phase

separation temperatures for hydrous ethanol-gasoline blends in order to evaluate whether a phase containing a higher fraction of ethanol could form and cause corrosion.

To find the phase separation point, fuel is cooled at a controlled rate and is checked for phase separation at each temperature. The haze point was also measured as the temperature prior to the phase separation point at which cloudiness in the liquid is observed visually and is followed by an ice crystal formation (or phase separation). Phase separation for hydrous ethanol blends with higher ethanol content (and accordingly higher water content) was found to occur at lower temperatures than other blends. The lowest phase separation temperature was observed at -28 °C for H30 followed by H15 (-15 °C) and H10 (-7 °C). This behavior can be attributed to the high hygroscopicity of ethanol so that hydrous ethanol blends with higher blending ratios are able to hold more water in a single phase at low temperatures. The separated phase was not in a crystalline form; instead, water absorbed a portion of the ethanol due to ethanol's hygroscopic nature. Therefore, the mixture is not frozen at such a low temperature (below 0 °C). Formation of ethanol-water phase can be considered damaging because not only it is highly corrosive, but also this phenomenon can alter the ethanol concentration in the combusted fuel as the separated ethanol/water mixture may settle and remain in the fuel tank. A fuel with lower content of ethanol relative to the original state has a lower octane value and oxygen content, which can adversely impact the combustion and emission characteristics. Relatively high phase separation temperatures, especially for the blends containing low and medium hydrous ethanol concentrations, indicate that it may be necessary to use additives such as higher alcohols to avoid phase separation.

5.4.4. Lower heating value

Since the heating value of ethanol is lower than that of gasoline, blending ethanol with gasoline decreases the heating value of the blend. Thus, to produce the same power from a given gasoline-fueled engine (at a given compression ratio), a larger mass of an ethanol-gasoline blend must be injected in each cycle compared to a non-oxygenated fuel. This is needed since the air-fuel ratio must be kept as close as possible to the stoichiometric ratio in SI engines to fully take advantage of the three-way catalyst. However, since ethanol is more resistant to autoignition, a higher compression ratio can be used to compensate for the lower heating value and lower stoichiometric air-fuel ratio.

The measured LHV values are presented in Figure 5.4. The addition of water reduced the heating value of the hydrous ethanol fuel blends as expected given that water exhibits zero chemical potential. However, due to the small amounts of water present in each hydrous ethanol mixture, differences compared to the anhydrous (with same ethanol blending ratios) blends were small (less than 5%) even at 30 vol%.

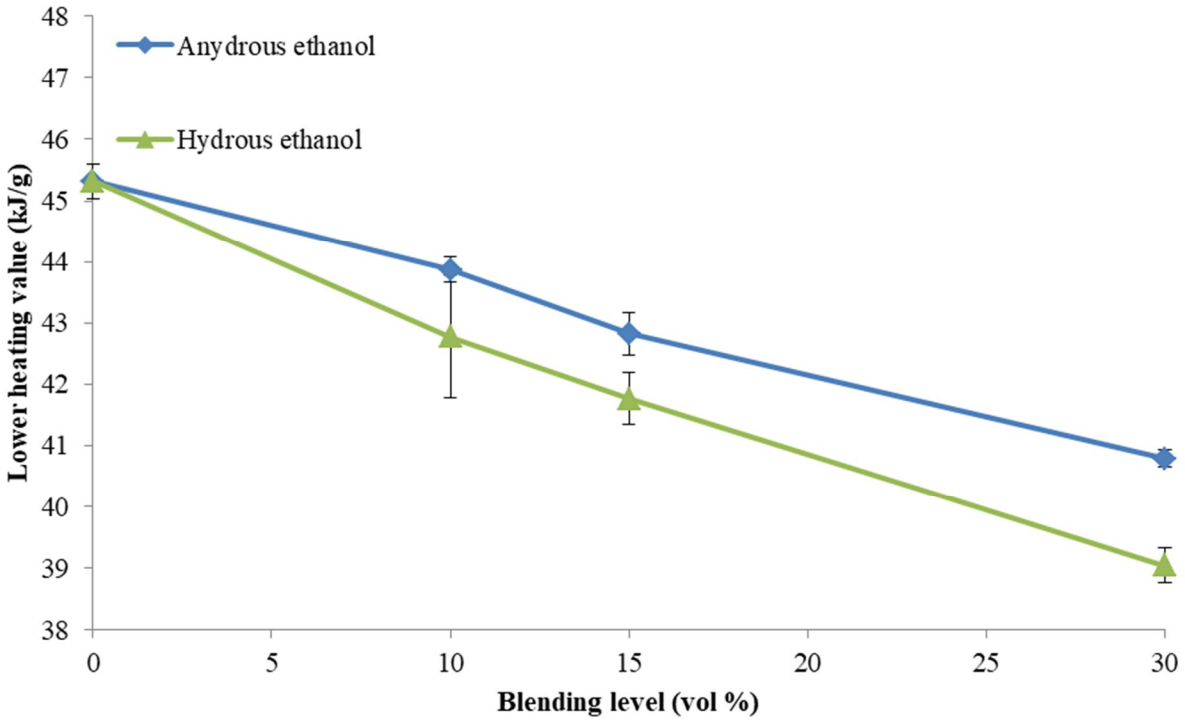

Figure 5.4. Effects of ethanol (anhydrous and hydrous) blending on the lower heating value of gasoline. Error bars represent +/- one standard deviation of triplicate measurements.

5.4.5. Viscosity and density

No limit is specified for density and viscosity in ASTM D4814; however, appropriate values for density and viscosity are vital to enhance the atomization, spray pattern, and mixture formation, and consequently reduce the emissions especially in direct injection systems [38]. Results showed that the higher density and viscosity of water compared to both ethanol and gasoline non-linearly increased the viscosity and density of hydrous ethanol blends compared to anhydrous ethanol blends, especially at higher blend levels (15 and 30 vol%) (Figure 5.5). This may be problematic due to the formation of larger droplet sizes, especially in direct injection systems, as droplet diameters have been shown to increase proportionally with the kinematic

viscosity [38]. At the same time, however, increased viscosity may provide better lubrication and less wear in engine parts [36].

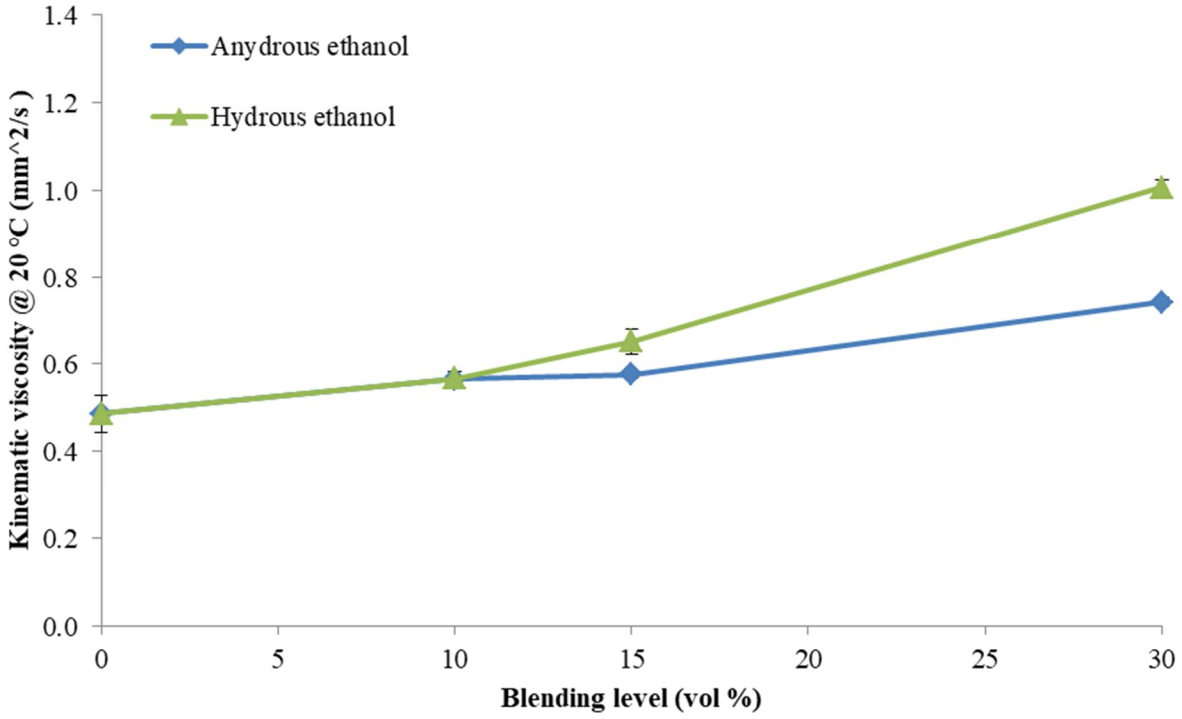

Figure 5.5. Effects of ethanol (anhydrous and hydrous) blending on kinematic viscosity of gasoline. Error bars represent +/- one standard deviation of triplicate measurements.

5.5. Conclusions

Available thermophysical property data for hydrous ethanol-gasoline blends is sparse. These data are important to evaluate the fuel's potential for use in state of the art vehicle technologies and to optimize engine strategies to maximize engine efficiency. In this study, the distillation curve, Reid vapor pressure, vapor lock index, viscosity, density, copper strip corrosion, haze and phase separation points, and lower heating value of gasoline, hydrous ethanol-gasoline, and anhydrous ethanol-gasoline blends at different volumetric ratios were compared to assess the substitution potential of hydrous ethanol comprised of the azeotropic proportions of water and

ethanol (4: 96 vol % water: ethanol) with blends containing anhydrous ethanol. Results suggested that hydrous ethanol-gasoline blends have the potential to be used in current SI engines as a drop-in fuel with no or only minor changes. It is recommended that future work be conducted on the characterization of fuels with higher water/ethanol ratios, compatibility of fuel delivery/storage systems and economical/energy life cycle aspects of replacing hydrous ethanol with anhydrous ethanol to examine potential of hydrous ethanol- gasoline mixtures as fuel blends.

References

1- Environmental Protection Agency. Renewable Fuel Standard Program (RFS2) Regulatory Impact Analysis. 2010. doi:EPA-420-R-10-006., February 2010.

2- Independent Statistics & Analysis (EIA). Electric Power Monthly: with data for January 2016. US Energy Inf Adm 2016:237. doi:10.2172/123200.

3- Shapouri H, Duffield JA, Wang M. The energy balance of corn ethanol revisited. Trans ASAE 2003;46:959–68. doi:10.1016/j.enpol.2006.02.007.

4- Lawson KW, Lloyd DR. Membrane distillation. J Memb Sci 1997;124:1–25. doi:10.1016/S0376-7388(96)00236-0.

5- Pacheco-Basulto J ángel, Hernández-McConville D, Barroso-Muñoz FO, Hernández S, Segovia-Hernández JG, Castro-Montoya AJ, et al. Purification of bioethanol using extractive batch distillation: Simulation and experimental studies. Chem Eng Process Process Intensif 2012;61:30–5. doi:10.1016/j.cep.2012.06.015.

6- Schifter I, Diaz L, Gómez JP, Gonzalez U. Combustion characterization in a single cylinder engine with mid-level hydrated ethanol-gasoline blended fuels. Fuel, vol. 103, 2013, p. 292–8. doi:10.1016/j.fuel.2012.06.002.

7- Sluder CS, Szybist JP, McCormick RL, Ratcliff MA, Zigler BT. Exploring the Relationship Between Octane Sensitivity and Heat-of-Vaporization. SAE Int J Fuels Lubr 2016;9:2016-01–0836. doi:10.4271/2016-01-0836.

8- Kyriakides A, Dimas V, Lymperopoulou E, Karonis D, Lois E. Evaluation of gasoline-ethanol-water ternary mixtures used as a fuel for an Otto engine. Fuel 2013;108:208–15. doi:10.1016/j.fuel.2013.02.035.

9- Costa RC, Sodré JR. Hydrous ethanol vs. gasoline-ethanol blend: Engine performance and emissions. Fuel 2010;89:287–93. doi:10.1016/j.fuel.2009.06.017.

10- Cordeiro de Melo T, Bastos Machado G, Jesus de Oliveira E, Pereira Belchior C, Colaço M, Mautone Barros J, et al. Combustion and emission analysis of different hydrous ethanol-gasoline blends on a Flex-Fuel Engine. 10. Int. Symp. für Verbrennungsdiagnostik, 2012, p. 310–9. doi:10.4271/2010-36-0469.

11- Wang X, Chen Z, Ni J, Liu S, Zhou H. The effects of hydrous ethanol gasoline on combustion and emission characteristics of a port injection gasoline engine. Case Stud Therm Eng 2015;6:147–54. doi:10.1016/j.csite.2015.09.007.

12- Farrell JT. Co-Optimization of Fuels & Engines (Co-Optima) Initiative. National Renewable Energy Lab. (NREL), Golden, CO (United States); 2017 Oct 4.

13- ASTM D4814-17 Standard Specification for Automotive Spark-Ignition Engine Fuel, West Conshohocken, PA, 2017, https://doi.org/10.1520/D4814-17

14- Smith BL, Bruno TJ. Advanced distillation curve measurement with a model predictive temperature controller. Int J Thermophys 2006;27:1419–34. doi:10.1007/s10765-006-0113-7.

15- ASTM D5191-15 Standard Test Method for Vapor Pressure of Petroleum Products (Mini Method), West Conshohocken, PA, 2015, https://doi.org/10.1520/D5191-15

16- ASTM D5188-16 Standard Test Method for Vapor-Liquid Ratio Temperature Determination of Fuels (Evacuated Chamber and Piston Based Method), West Conshohocken, PA, 2016, https://doi.org/10.1520/D5188-16

17- ASTM D130-12 Standard Test Method for Corrosiveness to Copper from Petroleum Products by Copper Strip Test, West Conshohocken, PA, 2012, https://doi.org/10.1520/D0130-12

18- ASTM D6422-99 Standard Test Method for Water Tolerance (Phase Separation) of Gasoline-Alcohol Blends Test, West Conshohocken, PA, (Withdrawn 2007)

19- ASTM D240-17 Standard Test Method for Heat of Combustion of Liquid Hydrocarbon Fuels by Bomb Calorimeter, West Conshohocken, PA, 2017, https://doi.org/10.1520/D0240-17

20- Bergthorson JM, Thomson MJ. A review of the combustion and emissions properties of advanced transportation biofuels and their impact on existing and future engines. Renew Sustain Energy Rev 2015;42:1393–417. doi:10.1016/j.rser.2014.10.034.

21- Chevron. "Motor Gasoline Technical Review", Chevron Product Company, USA, Downloaded November 2016, http://www.chevron.com/

22- ASTM D5191-15 Standard Test Method for Vapor Pressure of Petroleum Products (Mini Method), West Conshohocken, PA, 2015, https://doi.org/10.1520/D5191-15

23- Mužíková Z, Pospíšil M, Šebor G. Volatility and phase stability of petrol blends with ethanol. Fuel 2009;88:1351–6. doi:10.1016/j.fuel.2009.02.003.

24- Andersen VF, Anderson JE, Wallington TJ, Mueller SA, Nielsen OJ. Vapor pressures of alcohol-gasoline blends. Energy and Fuels, vol. 24, 2010, p. 3647–54. doi:10.1021/ef100254w.

25- Da Silva R, Cataluña R, Menezes EW De, Samios D, Piatnicki CMS. Effect of additives on the antiknock properties and Reid vapor pressure of gasoline. Fuel 2005;84:951–9. doi:10.1016/j.fuel.2005.01.008.

26- Pumphrey JA, Brand JI, Scheller WA. Vapour pressure measurements and predictions for alcohol-gasoline blends. Fuel 2000;79:1405–11. doi:10.1016/S0016-2361(99)00284-7.

27- Kar K, Last T, Haywood C, Raine R. Measurement of Vapor Pressures and Enthalpies of Vaporization of Gasoline and Ethanol Blends and Their Effects on Mixture Preparation in an SI Engine. SAE Int J Fuels Lubr 2008;1:2008-01–0317. doi:10.4271/2008-01-0317.

28- Christensen E, Yanowitz J, Ratcliff M, McCormick RL. Renewable oxygenate blending effects on gasoline properties. Energy and Fuels 2011;25:4723–33. doi:10.1021/ef2010089.

29- Smith BL, Ott LS, Bruno TJ. Composition-explicit distillation curves of diesel fuel with glycol ether and glycol ester oxygenates: Fuel analysis metrology to enable decreased particulate emissions. Environ Sci Technol 2008;42:7682–9. doi:10.1021/es800067c.

30- Karonis D, Lois E, Zannikos F, Alexandridis A, Sarimveis H. A Neural Network Approach for the Correlation of Exhaust Emissions from a Diesel Engine with Diesel Fuel Properties. Energy & Fuels 2003;17:1259–65. doi:10.1021/ef020296p.

31- Hadler AB, Ott LS, Bruno TJ. Study of azeotropic mixtures with the advanced distillation curve approach. Fluid Phase Equilib 2009;281:49–59. doi:10.1016/j.fluid.2009.04.001.

32- Delgado RCOB, Araujo AS, Fernandes VJ. Properties of Brazilian gasoline mixed with hydrated ethanol for flex-fuel technology. Fuel Process Technol 2007;88:365–8. doi:10.1016/j.fuproc.2006.10.010.

33- Surisetty VR, Dalai AK, Kozinski J. Alcohols as alternative fuels: An overview. Appl Catal A Gen 2011;404:1–11. doi:10.1016/j.apcata.2011.07.021.

34- ASTM International. ASTM D86-17 Standard Test Method for Distillation of Petroleum Products and Liquid Fuels at Atmospheric Pressure. West Conshohocken, PA; ASTM International, 2017. doi: https://doi.org/10.1520/D0086-17

35- Andersen VF, Anderson JE, Wallington TJ, Mueller SA, Nielsen OJ. Distillation curves for alcohol-gasoline blends. Energy and Fuels, vol. 24, 2010, p. 2683–91. doi:10.1021/ef9014795.

36- Hansen AC, Zhang Q, Lyne PWL. Ethanol-diesel fuel blends - A review. Bioresour Technol 2005;96:277–85. doi:10.1016/j.biortech.2004.04.007.

37- Heuser B, Jakob M, Kremer F, Pischinger S, Kerschgens B, Pitsch H. Tailor-made fuels from biomass: Influence of molecular structures on the exhaust gas emissions of compression ignition engines. 22nd SAE Bras Int Congr Display, Bras 2013 2013;13. doi:10.4271/2013-36-0571.

38- dos Santos F, le Moyne L. Spray atomization models in engine applications, from correlations to direct numerical simulations. Oil Gas Sci Technol 2011;66:801–22. doi:10.2516/ogst/2011116.

6 Azeotropic Volatility Behavior of Hydrous and Anhydrous Ethanol Gasoline Mixtures *

6.1. Summary

After fermentation, the concentration of bioethanol is only 8-12 wt%. To produce anhydrous ethanol fuel, a significant amount of energy is required for separation and dehydration. Once the azeotrope composition is reached, distillation can no longer be exploited for purification and more expensive methods must be used. Replacing anhydrous ethanol fuel with hydrous ethanol (at the azeotrope composition) can result in significant energy and cost savings during production. The goal of this study was to characterize the volatility behavior and the droplet evaporation dynamics of hydrous and anhydrous ethanol gasoline blends. Three hydrous ethanol-gasoline blends (10, 15, and 30 vol%) in which the hydrous ethanol was composed of the azeotropic proportions of ethanol and water, and three anhydrous ethanol gasoline blends (10, 15, and 30 vol%) were prepared and analyzed with the advanced distillation curve method. Distillation curves were obtained for all test fuels and distillate samples were taken during the distillation process. A droplet evaporation model validated with the distillation data was exploited to understand how the non-ideal volatility behavior of these blends, the high heat of vaporization of water, and altered fluid properties can affect the transient droplet evaporation phenomena and thus the fuel's potential to effectively mix with air in direct injection internal combustion engines. Minor differences in the

---

Submitted as "Azeotropic Volatility Behavior of Hydrous and Anhydrous Ethanol Gasoline Mixtures" by Bahareh Abdollahipoor, Saeid Aghahossein Shirazi, Kenneth F. Reardon and Bret C. Windom. In the study presented in this chapter, I proposed the idea of examining different droplet sizes based on physiochemical properties. In addition, I contributed to the distillation curve testing and composition analysis, interpretation of the results, and the writing.

distillation curves and vapor-liquid equilibrium between the hydrous and anhydrous fuels were measured. Droplet modeling results showed that the higher heat of vaporization and viscosity of water relative to ethanol can lead to significant differences in the net droplet evaporation time between the two types of blends, especially at the higher blending ratios evaluated. These results suggest that the presence of water in ethanol-gasoline blends may extend droplet lifetimes and increase the susceptibility of the fuel to form particulate matter emissions. This is the first study to use distillation methods to gain a better understanding of evaporation behavior and the role of water and its stronger azeotropic effect on droplet evaporation dynamics.

6.2. Introduction

In recent years, biofuels have been used to offset the consumption of gasoline and diesel because they can be derived from renewable resources while being less harmful to the environment and humans, especially regarding greenhouse gas production [1]. Among biofuels, bioethanol has been produced in the largest quantities and is blended with gasoline at 10 vol% in nearly all the United States. The primary motivation to use ethanol is that it can be produced with low cost from renewable feedstocks. Despite having lower specific energy content than the gasoline it is replacing, the use of ethanol can lead to some improvements in combustion and emission characteristics stemming from its oxygen content. Ethanol has a high octane number, allowing engines to operate at higher compression ratios, thereby promoting fuel efficiency. In addition, its high heat of vaporization (HoV) can lead to a charge cooling effect that can enhance volumetric efficiency through increased brake mean effective pressure [2-4]. In 2012, the U.S. Environmental Protection Agency approved ethanol-blended gasoline at volumetric concentrations up to 15 vol% for use in Model Year 2001 and newer cars, light-duty trucks, medium-duty passenger vehicles, and all flex-fuel vehicles. In the United States, the ethanol blended in gasoline is anhydrous, with

a maximum water content of 1 wt%, as specified by ASTM D5798-99 [5] for fuel ethanol for automotive spark-ignition engines. However, ethanol produced by fermentation results in a mixture with a concentration of only 8-12 wt% ethanol; the rest is composed primarily of water along with organic acids, carbon dioxide, and other trace species [6]. Thus, to produce the anhydrous ethanol fuel, a significant amount of energy is required for separation and dehydration. Shapouri et al. [7] conducted a study to identify the net energy value of corn ethanol. In their study, the total output energy based on the higher heating value of ethanol and the energy credits of the co-products was estimated to be around 25 MJ/L. These authors determined that the energy required for water removal to obtain anhydrous ethanol accounts for 37% (~ 9.5 MJ/L) of the total output energy, including distillation (23%) and dehydration (14%) processes.

Separating water and ethanol by way of distillation is an energy-intensive process, especially when distillation-based separation techniques are applied to mixtures containing more than 90% ethanol. This is a result of azeotrope interactions; at the ethanol-water azeotrope point (95.6/4.4 wt% ethanol/water at 1 atm) no further separation can be achieved at constant pressure. Instead, additional energy must be provided to overcome this limitation [8, 9]. Once an azeotropic mixture forms, distillation can no longer be exploited for further purification [10]. Instead, methods such as membrane-distillation hybrids, pressure-swing distillation, entrainer-addition distillation methods, and molecular sieve separation techniques are required [11, 12]. These alternate methods add expense, complexity, and energy requirements. The expense of anhydrous ethanol production suggests opportunities for improvements from economic, energy, and greenhouse gas points of view. One option to address these shortcomings is to use hydrous ethanol (at the water/ethanol azeotropic composition) blended with gasoline. This could save up to 14% of the fuel energy during its production (~3.5 MJ/L) [6]. However, questions related to the water

addition and its impact on engine operation, fuel economy, and fuel supply systems must be answered.

Although hydrous ethanol may cause negative long-term impacts such as lubricant deterioration and fuel system corrosion [10], its overall impact on combustion and emission characteristics has been shown to be positive. Several studies have been conducted to investigate the impact of hydrous ethanol on engine performance and emissions [10, 13-19]. Generally, in comparison to anhydrous ethanol blends, hydrous ethanol blends show higher brake thermal efficiency and brake-specific fuel consumption (BSFC) with lower unburned hydrocarbon (UHC), CO, and NO_x emissions. BSFC is increased due to the lower heating value of hydrous ethanol [10]. Although the lower heating value and lower flame speed of hydrous ethanol compared to anhydrous ethanol result in a lower peak heat release rate and pressure, efficiency improvements are observed because of charge cooling effects stemming from the HoV of hydrous ethanol which decreases heat losses to the cylinder walls and allows for increased mass loading into the cylinder [13]. The HoV-influenced cooling and subsequent lower flame temperatures also leads to reduction in NO_x emissions. At low loads, the presence of water decreases the exhaust gas temperature and limits the oxidation of CO and UHC. However, at high loads, breakdown of water into hydroxyl and hydrogen radicals promotes the oxidation of CO and UHC at high temperature conditions [18]. It should be noted that these previous studies were carried out with current engine platforms designed for anhydrous fuels and did not examine the effect of tuning/optimizing engine design to leverage gains in octane numbers and charge cooling corresponding to water addition on fuel economy. Such modifications could potentially offset the reduction in overall fuel heating value when water is present.

In direct injection spark ignition (DISI) engines, the spray atomization and fuel evaporation processes play an essential role in the combustion efficiency and emission formation [20]. In several studies conducted on DISI engines, it has been observed that use of a gasoline containing moderate ethanol concentrations (10 – 20 vol%) increases particulate matter (PM) emissions relative to base-gasoline stemming from slowed spray/droplet evaporation dynamics resulting from the high HoV of ethanol [21-25]. The goal of this study was to characterize the volatility behavior and mixing/sooting potential of hydrous and anhydrous ethanol blends. An advanced distillation apparatus was used to obtain distillation curves for gasoline, gasoline-hydrous ethanol and gasoline-anhydrous ethanol mixtures. Distillate samples were withdrawn at various points during distillation and their corresponding compositions were quantified, including the transient distillate water concentration. A distillation-based droplet evaporation model containing more than 50 species was validated with the experimental data and used to provide insight into the spray and evaporation processes, which have been shown to play an important role in PM formation, of the hydrous and anhydrous fuel blends by tracking the changes in droplet composition and physical properties during evaporation.

6.3. Material and methods

6.3.1. Test fuels

Unleaded test gasoline (UTG-96) from Phillips 66 was used as the base fuel (E0). The base gasoline was blended with 10, 15 and 30 vol% of anhydrous and hydrous ethanol. The blends were designated as E10, E15, E30, H10, H15, and H30 corresponding to either anhydrous (E) or hydrous (H) ethanol and the blended volume percentage. Hydrous ethanol was obtained by mixing 96 vol% of anhydrous ethanol with 4 vol% of deionized water to match the reported composition for the

azeotrope mixture. Ethanol (200 proof, ≥ 99.5%) was purchased from Pharmco-AAPER. The proof of ethanol was verified via Karl Fischer.

6.3.2. Methods

A vapor pressure analyzer (Grabner Instruments Minivap VPXpert) was used to measure Reid vapor pressure (RVP) according to ASTM 5191 [26]. Each test was repeated three times. A custom-built Advanced Distillation Curve (ADC) apparatus was used to obtain the distillation curves [27-29]. Details of the ADC method have been reported elsewhere [30]. In brief, a temperature-controlled heating mantle is placed around the boiling kettle containing 200 ml of the fuel blend, which is stirred to ensure a uniform composition and temperature within the boiling mixture. Temperatures of the liquid in the kettle and vapor in the distillation head are monitored with two K-type thermocouples. These thermocouples continuously record temperatures using a data acquisition system. The temperature of the heating mantle is continuously adjusted to lead the boiling fluid temperature by ~20 °C ensuring even heating throughout the distillation process. The condenser tube is chilled with water maintained at 5 °C. The apparatus is equipped with a custom sampling adapter located between the condenser tube and the volumetric receiver, which provides the ability to withdraw samples of the distillate during the distillation process. The volumetric receiver collects the condensed liquid and is calibrated to measure the distilled liquid volume. The receiver is cooled by chilled air from a vortex tube at 2 °C to prevent any vapor loss. At every 5% volume distilled, the liquid temperature in the kettle is recorded and used to create an accurate distillation curve. Distillation curves for each mixture were measured twice. Generally, the initial boiling temperature is difficult to observe and measure. In this study, the initial boiling temperature corresponds to the temperature of the boiling liquid (in the kettle) at the point when a sudden rise

in the head temperature was observed (or the point of maximum gradient during post-processing) similar to the methods suggested by Ferris and Rothamer [19].

Distillate samples were taken at the first drop, and then at 10, 20, 30, 40, 50, 60, 70, 80, and 90% volume distilled. An HP 5890 Series II GC-FID was used to analyze the composition of the samples according to ASTM D6729 [31]. The GC was equipped with 100-m long Petrocol DH fused silica capillary column coated with polydimethyl siloxane. Species were identified by comparing peak retention times to those measured with reference standards. It was noticed that the heavy fraction of UTG-96 gasoline contained many species with small peak areas (or mass fraction). Though the individual species were a minor fraction of total composition, the combined area of these peaks was found to be a significant portion of the fuel. To ensure a proper distribution of species needed for accurate prediction of distillation curves (described in the following section), a grouping approach was exploited to determine a simplified composition for the gasoline. To identify unknown hydrocarbons with excessively small chromatogram peak areas, this approach assumed the small peaks to be of the same composition to the nearest known identified hydrocarbon peak. By lumping together species with similar molecular weight and physiochemical properties, this approach could simplify the complex composition of the gasoline to 54 compounds while maintaining a strong agreement between predicted and measured distillation curves (demonstrated in Results and Discussion). Chromatogram peak areas were then converted to the mass concentrations following calibration. The chromatogram of the UTG-96 and a list of the simplified composition are provided in the supplementary materials (Figure S6.1 and Table S6.1). After obtaining the simplified composition of each sample, mass fraction of each component was multiplied by its molecular weight and then inversed to calculate the average molecular weight. The water content of the distillate samples was measured twice for each sample by Karl Fischer

titration using a Metrohm 831 KF coulometer. The proof of ethanol was also verified via this method.

6.3.3 Distillation and droplet models

In this study, a distillation curve model similar to that developed by Backhaus [32] was used to predict the distillation curve and changes in composition and HoV of the test fuels during distillation. Blends composed of the simplified UTG-96 composition (described earlier) blended with the appropriate concentration of ethanol/water were used as inputs for this model.

The droplet evaporation model of Burke et al. [33] was used to infer the potential of water addition on PM formation due to depressed droplet evaporation rates stemming from charge cooling effects and aromatic enrichment as described in [34]. This model simulates the distillation process in a droplet while incorporating the D^2 law and appropriate energy and mass transfer dynamics. Mixture properties including the HoV were determined using a mass fraction weighted average approach as described in [35].

Both models used the UNIFAC group contribution theory to predict the non-ideal interactions between oxygenates and hydrocarbons. The distillation curve model was validated with the experimental distillation curve and distillate composition data and the droplet evaporation model was used to predict evaporation time for the test blends under different temperatures and droplet size conditions.

6.4. Results and Discussion

6.4.1. Distillation curves and composition evolution during distillation

Volatility is an important fuel property for SI engines and is often characterized with the vapor pressure and the distillation curve. Key volatility measurements (taken at 83.3 kPa, the

average local ambient pressure of Fort Collins, CO) important in qualifying a fuel for use for the hydrous and anhydrous ethanol/gasoline fuels are provided in Table 6.1.

The addition of both anhydrous and hydrous ethanol caused an increase in RVP compared to the gasoline because of positive azeotropic behaviors. The RVP of the hydrous ethanol blend at each blending ratio was observed to be 2.9-4.9% greater than corresponding anhydrous ethanol blends, most likely due to added azeotropic effects from the inclusion of water, however, the differences were found to be statistically insignificant with a P-value= 0.28 stemming from the lack of replicate data. For anhydrous blends, the highest RVP was observed for E10, while for the hydrous ethanol blends, H15 exhibited the highest.

Distillation curves for all the test fuels are depicted in Figure 6.1 and selected data points are provided in Table 6.1. The addition of anhydrous and hydrous ethanol caused a significant reduction in the first 50% to 80% of the distillation curve depending on the ethanol (or ethanol/water) concentration, but with no notable impact on initial boiling points. This is a well-known behavior resulting from the polarity of ethanol and water and the formation of positive azeotropes between these molecules and the hydrocarbons in gasoline causing lower mixture boiling temperatures when compared to those of the individual molecules. The near-azeotropic behavior is apparent from localized near-flat regions in the distillation curves, which are longer for higher oxygenate concentrations [36]. At the end of each plateau region, there is a relatively sharp rise in the boiling temperatures and convergence to the distillation curve of the unblended gasoline. The point of rise in boiling temperature for the blended fuels corresponds to the moment that ethanol is completely vaporized from the boiling mixture. For each blending ratio, the hydrous and anhydrous ethanol blends presented similar patterns with the only noticeable difference of the hydrous ethanol blends demonstrating a slightly faster temperature rise at the inflection point

where the distillation curve approaches the gasoline boiling temperatures possibly due to the presence of water diluting the ethanol and/or promoting additional azeotropic behaviors.

Table 6.1 Volatility characteristics of test fuels at 83.3 kPa. E: anhydrous ethanol blends. H: hydrous ethanol blends. Error ranges correspond to +/- one standard deviation.

Property	Gasoline (E0)	E10	E15	E30	H10	H15	H30
Reid vapor pressure (kPa)	53 ± 0	60 ± 0	59 ± 0	55 ± 0	61 ± 1	61 ± 1	58 ± 1
Initial boiling point (°C)	48 ± 1	48 ± 1	49 ± 1	49 ± 1	49 ± 0	49 ± 0	49 ± 1
T10 (°C)	71 ± 1	60 ± 1	60 ± 1	61 ± 1	59 ± 1	59 ± 1	60 ± 1
T50 (°C)	103 ± 1	102 ± 1	81 ± 4	73 ± 0	103 ± 1	86 ± 1	72 ± 1
T90 (°C)	155 ± 1	160 ± 4	158 ± 12	145 ± 6	160 ± 8	172 ± 6	158 ± 4

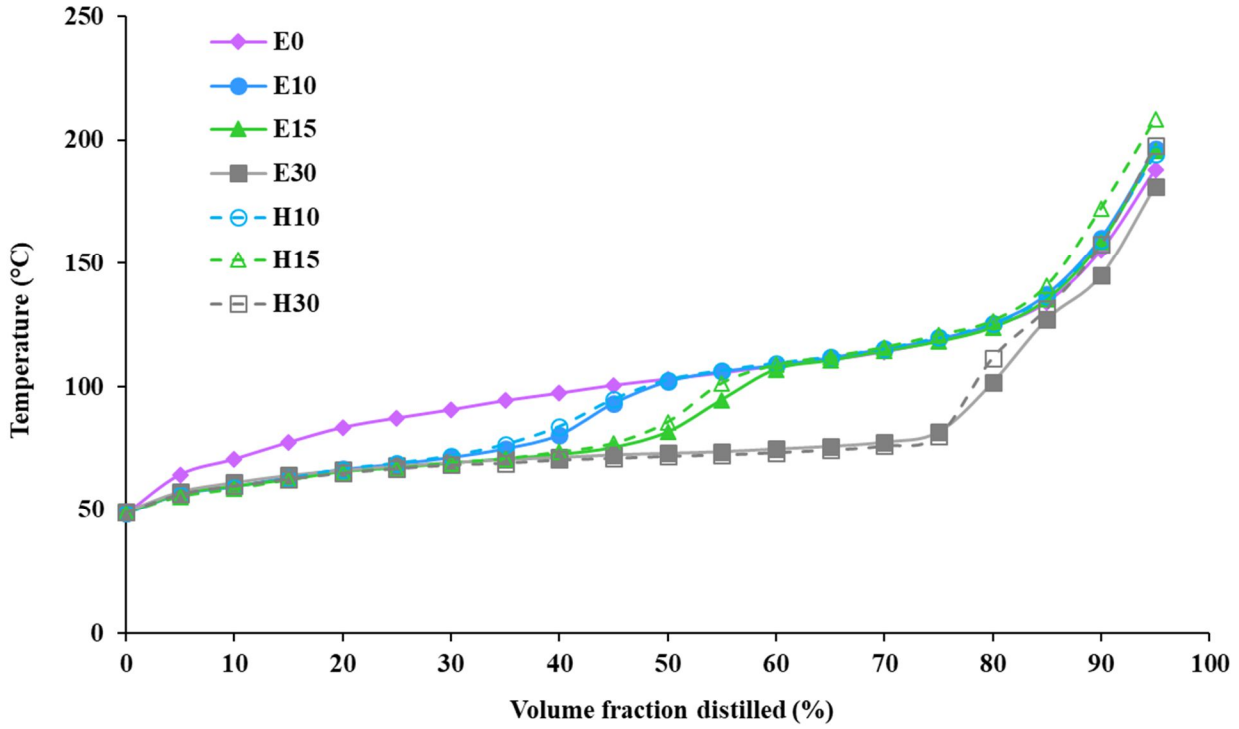

Figure 6.1. Distillation curves at 83.3 kPa for gasoline and blends of hydrous (dotted lines) and anhydrous (solid lines) ethanol. Data represent the average of two distillation tests with average coefficient of variation of 1.69%.

The evolution of the composition of unblended gasoline and the oxygenated blends during the distillation was measured by sampling and analyzing the condensate (distillate) samples during

the distillation process. The distillate ethanol, water, and aromatic concentrations are shown in Figure 6.2. It is shown that presence of oxygenates retards the evaporation of aromatics compared to the gasoline. From the sharp rise in the concentration of aromatics once the ethanol and water (if present) were nearly completely evaporated, it can be inferred that the presence of ethanol and water suppressed the distillation of aromatic species. The larger initial concentration of oxygenates results in a longer delay prior to the evaporation of the aromatics, causing an enrichment in the liquid fuel in the aromatics at late stages of the distillation. Interestingly, the mass percentages of aromatics are relatively close for all blends at the end of the distillation (in the range of 71–79% at 90% distilled) despite having very different initial amounts depending on the initial oxygenate concentration. These observations, coupled with the fact that aromatics have shorter kinetic pathways to produce soot [37], may partially explain recent observations of increased PM emission when using blends containing moderate ethanol concentrations (20-40 vol%) in DISI engines [21, 25]. Figure 6.2 also shows that the differences between hydrous and anhydrous blends in the suppression of aromatic compounds are negligible. Interestingly, however, at the beginning of each distillation, while water is being evaporated, the concentration of ethanol in the anhydrous ethanol blends is 14.8% higher on average than in the corresponding hydrous ethanol blends possibly due to the formation of ternary azeotropes (ethanol/water/non-polar hydrocarbons) in which the presence of water is altering the ethanol/hydrocarbon interactions exhibited in the anhydrous fuels.

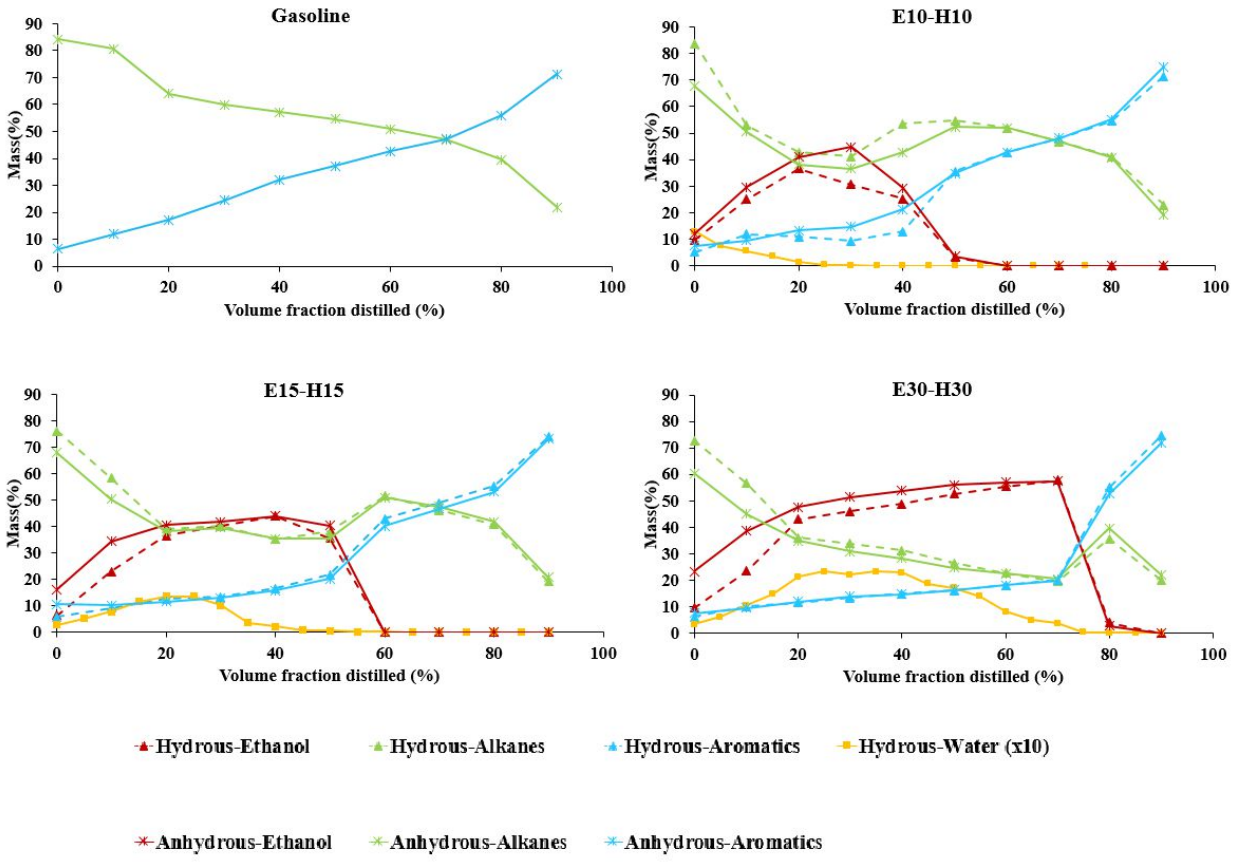

Figure 6.2. Distillate composition analysis for gasoline and blends of hydrous (dashed lines) and anhydrous (solid lines) ethanol in gasoline. E: anhydrous ethanol blends. H: hydrous ethanol blends. The average coefficient of variation of the data is ± 4.06% from duplicate tests.

6.4.2. Distillation model validation

To model the distillation curve of a fuel, prediction of the vapor-liquid equilibrium (VLE) or the changing thermodynamic state points defining the fluid temperature and composition is required. VLE predictions can be obtained from Raoult's Law for mixtures with ideal behavior. However, to quantify VLE for a non-ideal mixture such as gasoline-water-ethanol, methods such as the UNIFAC group contribution approach need to be applied to accurately predict the molecular interactions. In the UNIFAC model, an activity coefficient (γ) is applied to Raoult's law to correct

for these interactions. The activity coefficient is a dimensionless correction factor between 0 and 1 that is equal to unity for ideal mixtures but non-unity for mixtures consisting of compounds that are chemically dissimilar. The UNIFAC approach brings geometric and polarity-driven interactions into account to calculate the non-ideal activity coefficient. The distillation model used in this study, developed by Backhaus [32], uses UNIFAC theory to predict non-ideal VLE of the oxygenate-hydrocarbon mixtures, distillation curves, and compositions. The initial compositions of the blends (see Table S6.1 for the gasoline composition used) were used as inputs for the simulations.

There was a strong agreement between the predicted and measured distillation curves for gasoline, anhydrous, and hydrous blends (Figures 6.3, S6.2, and S6.3) as well as agreement between the measured and predicted distillate molecular weight for the same fuels (Figures 6.4, S6.4, and S6.5). These results demonstrate that the model is accurate and capable of predicting the physics required to characterize the vaporization behavior of the anhydrous and hydrous blends. Thus, the results of the droplet model [33], which is derived from the distillation curve model can be used with confidence.

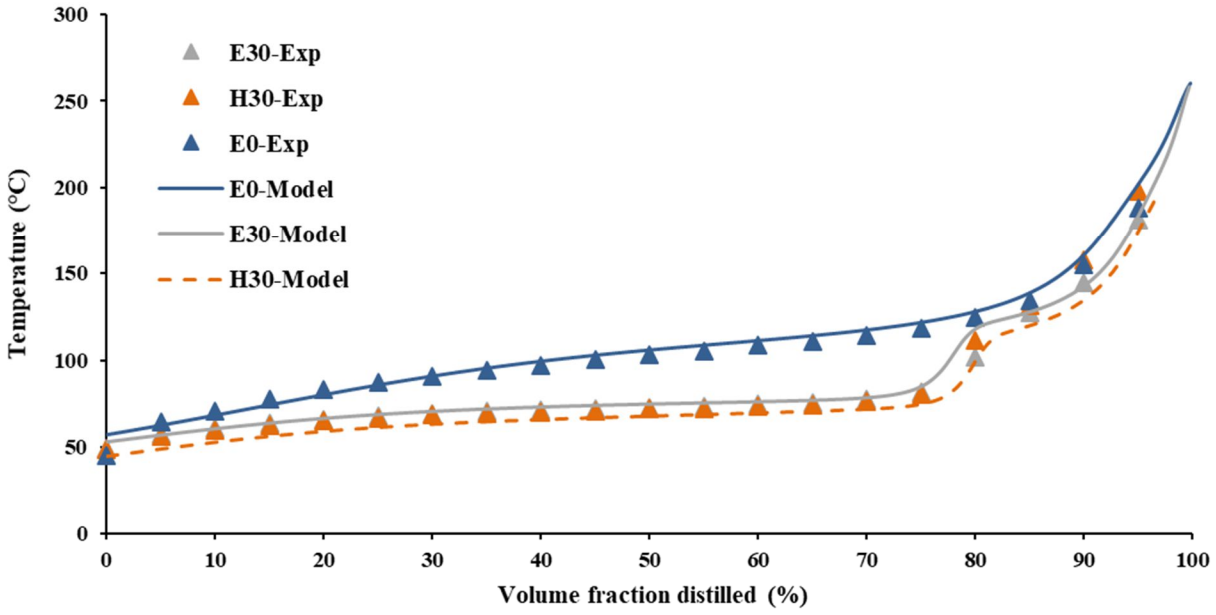

Figure 6.3. Comparison of experimental distillation curves to those modeled. Gasoline, E30, and H30 were selected as representative fuels for presentation. Exp: Average of duplicate experimental distillation curves. Model: predicted distillation curves. E: anhydrous ethanol blends. H: hydrous ethanol blends.

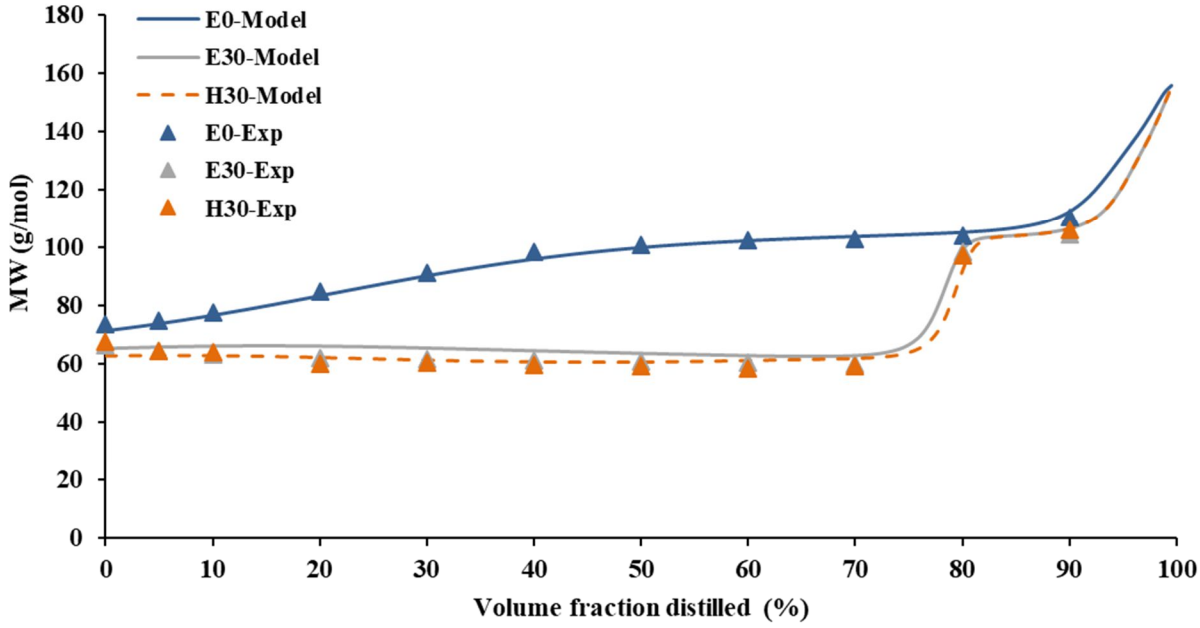

Figure 6.4. Comparison of experimentally measured and predicted average molecular weight. Gasoline, E30, and H30 were selected as representative fuels for presentation. Exp: Average of duplicate experimentally calculated average molecular weights. Model: predicted average molecular weight. E: anhydrous ethanol blends. H: hydrous ethanol blends.

6.4.3. Droplet evaporation dynamics

The droplet evaporation model predicts evaporation rate, composition, and HoV of a single droplet as the temperature changes due to heat conduction and evaporative cooling. In this study, this model was used to monitor how the vapor-liquid equilibrium can change owing to the higher HoV and heat capacity of water relative to ethanol and iso-octane, as a representative hydrocarbon in gasoline (Table S6.2). Results of the droplet model were used to link oxygenate content to PM emission potential stemming from incomplete evaporation. Although there are sooting indices such as the Particulate Matter Index (PMI) [37], they do not incorporate charge cooling effects

(from higher HoVs found in oxygenated fuels) and the non-ideal interactions between oxygenates and hydrocarbons in determining the tendency of a mixture to soot in a DISI engine. The droplet model does not incorporate convective transport phenomenon that are experienced in a turbulent engine environment and thus is not able to quantify absolute PM emissions, nevertheless, the model can be used as an indicator of a particular fuel's tendency to soot by comparing two fuels and their differences in volatility and VLE that ultimately drive droplet evaporation and species mixing. Furthermore, Burke et al. [38] showed that the measured PM correlated better with the predicted (from a droplet evaporation model similar to that used herein) liquid mass of aromatic remaining in an oxygenate blend at gasoline's net evaporation time than with the PMI.

As a reference state, all blends were modeled with initial 25-μm droplet diameters at a constant ambient temperature (323 K) and 1 atm. An injector's nozzle design, operational conditions, and the physical properties of the fuel can influence the droplet size and other spray characteristics. An initial droplet diameter of 25 μm was chosen for blends because this is in the usual range for mean droplet diameters produced when gasoline is used in traditional DISI injector technology [39]. Surprisingly, the model predicts that complete evaporation of the base gasoline droplet (E0) takes longer than all the other blends, as seen in Figure 6.5 (red columns). These results are opposite to those presented by Burke et al. [33], in which they showed longer evaporation times for blends containing ethanol (regardless of concentration) relative to the base gasoline at temperatures of 315 K when a droplet diameter of 50 μm was used. The gasoline used in this previous study was FACE B, which is more volatile than the gasoline used here (T90 for FACE B was 109 °C while it was 158 °C for the UTG96). As such, when ethanol is added to the gasoline in this study, the increase in volatility (which speeds up evaporation) is more dominant than the increase in HoV (which slows evaporation), as compared to this previous work, thus

explaining why droplet evaporation times are shortened when ethanol is present. Despite having significantly higher HoV (Table S6.2), which can slow evaporation, the mixtures containing water only showed slightly longer evaporation times than the corresponding anhydrous blend with similar oxygenate concentrations. As seen in Figure 6.6, the presence of oxygenates (ethanol and water) increased the HoV of the mixture, as expected, resulting in an initial temperature drop (Figure 6.7). The HoV and temperature remain high and low, respectively, until ethanol and water are depleted from the droplet (Figure 6.8); after this point, the HoV and temperature are the same for all the fuels. The temperature drop remains longer into the droplet's lifetime as the oxygenate blending ratio is increased. The hydrous ethanol mixtures exhibited a noticeable difference in the transient HoV when compared to their anhydrous counterparts (Figure 6.6), caused by the high HoV of water. However, this does not translate into a noticeable difference in the droplet temperature between the hydrous and anhydrous mixtures (Figure 6.7), explaining the similarity in their predicted droplet lifetimes as seen in Figure 6.5 (red columns). The similarities in droplet temperature, despite differences in HoV, may be due to the relatively high specific heat capacity of water, which suppresses the temperature change. Furthermore, as the temperature difference between the ambient environment (323 K) and the droplet increases, conductive heat transfer becomes more dominant in heating the droplet than the evaporative cooling.

The above analysis assumed a constant initial droplet diameter for all fuels, however, the physical properties of the blends must be incorporated to obtain more realistic results and a more comprehensive understanding related to the addition of ethanol and water on droplet evaporation dynamics. The physical properties (viscosity, density, and surface tension) of a fuel are important factors in atomization, spray pattern, and mixture formation. To take these physical properties into account, a model developed by Elkotb [41, 42] was exploited to estimate the initial droplet size of

all the fuel blends (or the relative proportion to that of gasoline) based on bulk fluid physical properties:

$$\text{Sauter Mean Diameter} = 3.085 \nu_l^{0.385} \sigma_l^{0.737} \rho_l^{0.737} \rho_g^{0.06} \Delta P_l^{-0.54} \quad \text{Eq. 6.1}$$

In Eq. 6.1, ν_l is the kinematic viscosity of liquid, ρ_g and ρ_l are the gas and liquid density, σ_l is the surface tension of liquid and ΔP_l *is* the difference between injection pressure and ambient pressure. As seen in Table 6.2, the addition of water non-linearly increases the kinematic viscosity and surface tension of hydrous ethanol blends compared to anhydrous blends, especially at medium and high blending ratios [43, 44]. Since ΔP_l is identical for all blends, the initial droplet diameter of gasoline (E0) was assumed to be 25 µm and the droplet sizes of the other blends were determined relative to the this diameter by using Eq. 1 with the physical properties listed in Table 6.2. Calculations show that the addition of water leads to larger droplets (Table 6.2, 5th column), which can be problematic because larger droplets in the cylinder can increase spray tip penetration resulting in a reduced spray angle, slower evaporation, and increased likelihood of incomplete mixing and pool generation/burning. These phenomena increase chances of PM/soot exhaust emissions [40].

To determine the influence of droplet size on droplet evaporation lifetime, the droplet evaporation model was used with the calculated droplet sizes (Table 6.2) for each blend at constant ambient temperature (323 K) and pressure (1 atm). In contrast to the first simulations with identical initial diameter for all blends, the results of using the refined estimate of initial droplet size reveal that oxygenated blends retarded the droplet evaporation from 3.8% (E10) to 32.3%(H30) longer than that of the base gasoline (Figure 6.5). This result shows that the higher HoV and viscosity of water relative to ethanol are effective factors that contribute to notable differences in the net evaporation time such that hydrous blends had 1.73 -27.4% higher droplet lifetime compared to

corresponding anhydrous blends. As such, once accounting for changes in properties responsible for droplet atomization, fuels containing hydrous ethanol may possess slower in-cylinder evaporation behaviors and as a result could be potentially more prone to produce PM emissions.

Table 6.2. Physical properties of the test fuels and corresponding droplet sizes obtained from the Elkotb model [41] relative to an assumed diameter of 25 µm for E0. [a] *Obtained from [43].* [b] Predicted by the DIPPR databases *[44]*.

Fuel	Kinematic viscosity (mm^2/s) [a]	Surface tension (N/m) [b]	Density (g/cm^3) [a]	Initial droplet size (µm)
E0	0.49	0.02158	0.74	25.00
E10	0.57	0.02158	0.75	26.49
E15	0.58	0.02159	0.75	26.85
E30	0.74	0.02156	0.75	29.40
H10	0.57	0.02178	0.75	26.64
H15	0.65	0.02189	0.76	28.46
H30	1.01	0.02216	0.78	34.42

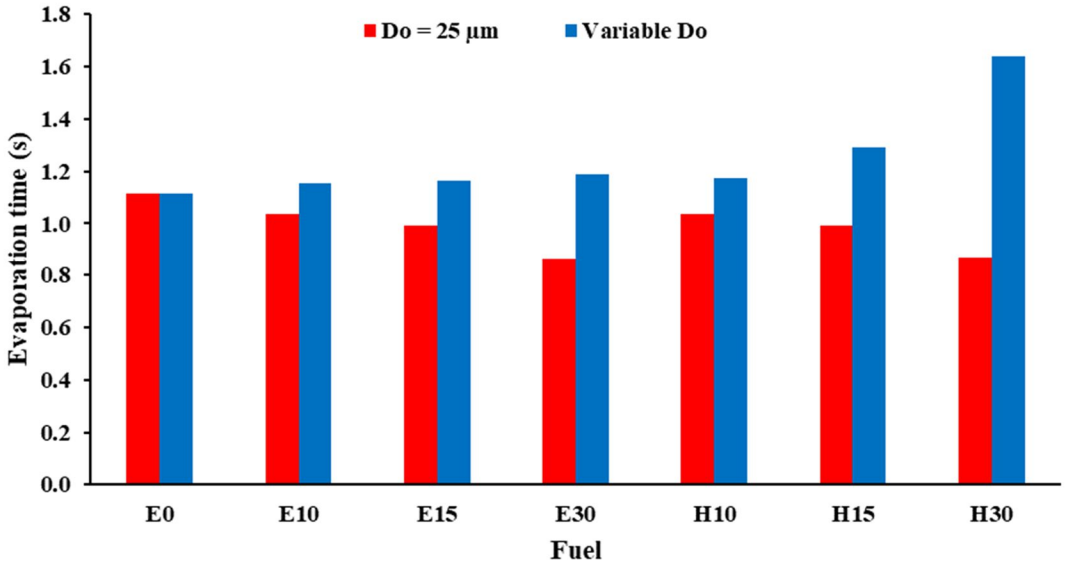

Figure 6.5. Droplet evaporation time for all blends obtained from the droplet evaporation model at 1 atm and 323 K. D_0: initial diameter. Red: with initial droplet diameter of 25 µm for all blends. Blue: with initial droplet sizes listed in Table 6.2.

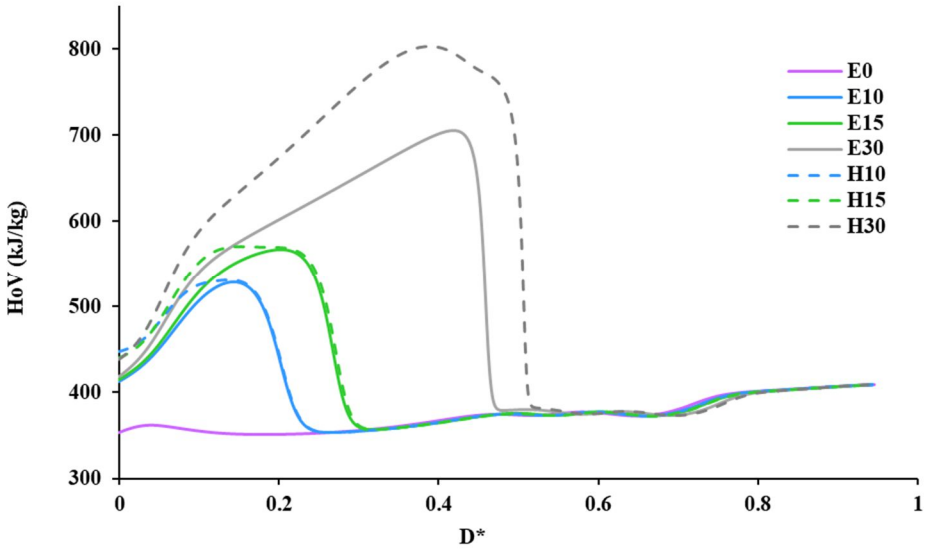

Figure 6.6. HoV profiles of each blend obtained from the droplet evaporation model as a function of dimensionless D^* at 1 atm and 323 K. E: anhydrous ethanol blends. H: hydrous ethanol blends. D: Diameter. D_0: Initial diameter (Table 6.2). $D^*=1-D/D_0$.

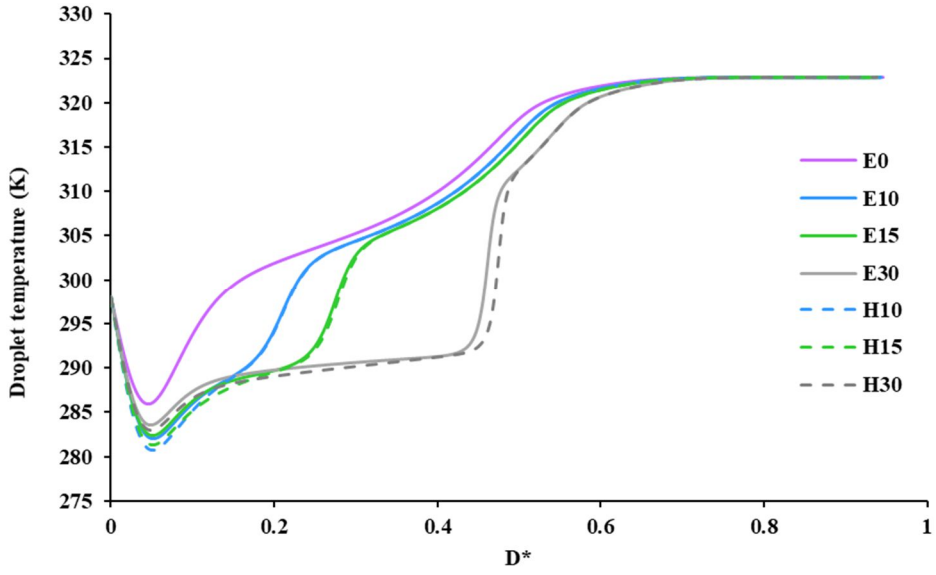

Figure 6.7. Temperature profiles of gasoline and blend obtained from the droplet evaporation model as a function of dimensionless D* at 1 atm and 323 K. E: anhydrous ethanol blends. H: hydrous ethanol blends. D: Diameter. D_0: Initial diameter (Table 6.2). $D^*=1-D/D_0$.

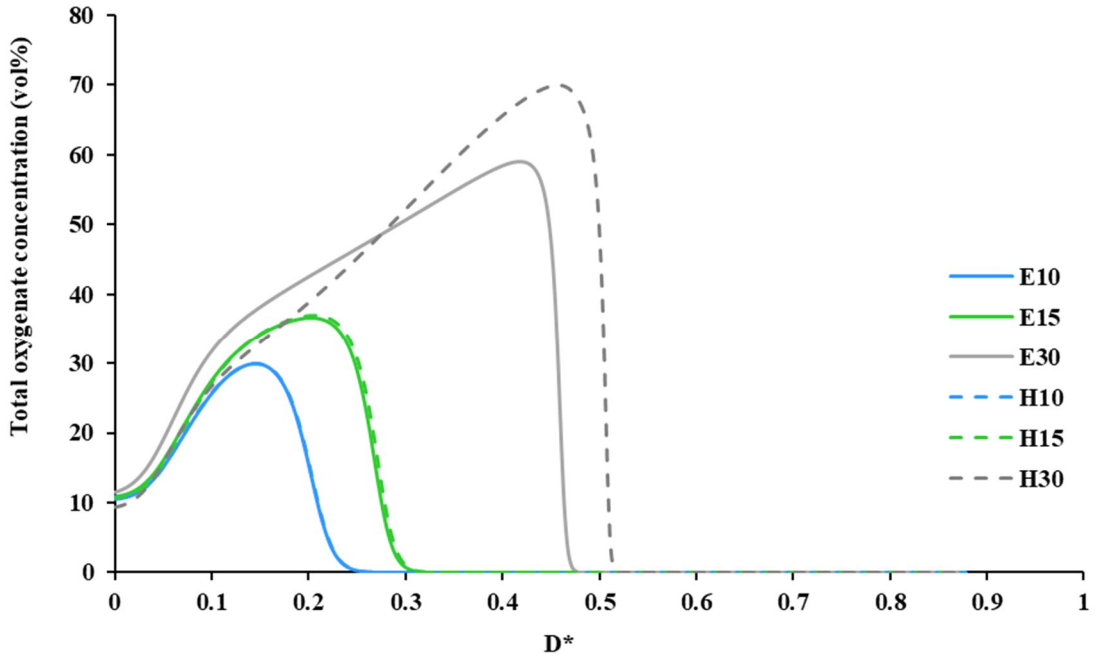

Figure 6.8. Total oxygenate concentration profiles of gasoline and blend obtained from the droplet evaporation model as a function of dimensionless D^* at 1 atm and 323 K. E: anhydrous ethanol blends. H: hydrous ethanol blends. D: Diameter. D_0: Initial diameter (Table 6.2). $D^*=1-D/D_0$.

6.5. Conclusions

Experimental data shows that the addition of both anhydrous and hydrous ethanol into gasoline can cause a significant reduction in boiling temperatures at the front end of the distillation curve depending on the initial concentration. However, at each blending ratio, hydrous and anhydrous ethanol blends presented similar trends with negligible observed differences in boiling temperatures. Analysis of the distillate samples revealed that ethanol and water suppress the evaporation of the aromatic species, which are well-known soot precursors, to later in the distillation curve, however, again, no significant difference was observed between hydrous and anhydrous blends in the distillate aromatic composition. Results from droplet evaporation simulations showed that with modified droplet sizes based on the measured and predicted physical

properties of the fuel blends, the presence of oxygenates led to longer droplet evaporation times than gasoline because of larger initial droplet sizes. Comparing hydrous blends with anhydrous blends, while accounting for variation in droplet sizes, the higher HoV and viscosity of water relative to ethanol can play a significant role leading to notable differences in the net evaporation time between the hydrous and anhydrous blends especially at moderate to high blending ratios.

The results of this study suggest that without updates to the fuel injection system, the presence of water in hydrous ethanol gasoline blends may extend droplet lifetimes. Taking these results into account, it can be concluded that at low engine speeds in which there is enough time for evaporation, there may be no notable difference between gasoline and the other blends in terms of PM emissions. However, at some engine conditions (e.g., high loads and speeds), there may not be enough time for complete droplet evaporation, which would increase the probability of fuel spray impingement on the cylinder walls in a DISI platform. This slowed evaporation, coupled with the suppression by ethanol and water of the evaporation of aromatic hydrocarbons, may cause higher PM emissions relative to gasoline. Therefore, to investigate the potential of spray impingement/pool burning responsible for increased PM, further research, including spray characterization experiments and engine testing/PM measurements, is suggested.

References

1- H.K. Reddy, T. Muppaneni, J. Rastegary, S.A. Shirazi, A. Ghassemi, S. Deng, ASI: Hydrothermal extraction and characterization of bio-crude oils from wet *Chlorella sorokiniana* and *Dunaliella tertiolecta*, Environ. Prog. Sustain. Energy. 32 (2013) 910–915. doi:10.1002/ep.11862.

2- B.M. Masum, H.H. Masjuki, M.A. Kalam, I.M. Rizwanul Fattah, S. M Palash, M.J. Abedin, Effect of ethanol-gasoline blend on NOx emission in SI engine, Renew. Sustain. Energy Rev. 24 (2013) 209–222. doi:10.1016/j.rser.2013.03.046.

3- P. Bielaczyc, J. Woodburn, D. Klimkiewicz, P. Pajdowski, A. Szczotka, An examination of the effect of ethanol-gasoline blends' physicochemical properties on emissions from a light-duty spark ignition engine, Fuel Process. Technol. 107 (2013) 50–63. doi:10.1016/j.fuproc.2012.07.030.

4- K.R. Szulczyk, B.A. McCarl, G. Cornforth, Market penetration of ethanol, Renew. Sustain. Energy Rev. 14 (2010) 394–403. doi:10.1016/j.rser.2009.07.007.

5- ASTM D5798-99 Standard Specification for Fuel Ethanol (Ed75-Ed85) for Automotive Spark-Ignition Engines, ASTM International, West Conshohocken, PA, 1999, https://doi.org/10.1520/D5798-99

6- C.A. Cardona, Ó.J. Sánchez, Fuel ethanol production: Process design trends and integration opportunities, Bioresour. Technol. 98 (2007) 2415–2457. doi:10.1016/j.biortech.2007.01.002.

7- H. Shapouri, J.A. Duffield, M. Wang, The energy balance of corn ethanol revisited, Trans. ASAE. 46 (2003) 959–968. doi:10.1016/j.enpol.2006.02.007.

8- D.R. Lide, CRC Handbook of Chemistry and Physics, 84th Edition, 2003-2004, Handb. Chem. Phys. 53 (2003) 2616. doi:10.1136/oem.53.7.504.

9- J.A. Dean, Lange's handbook of chemistry, Mater. Manuf. Process. 5 (1990) 687–688. doi:10.1080/10426919008953291.

10- R. Munsin, Y. Laoonual, S. Jugjai, Y. Imai, An experimental study on performance and emissions of a small SI engine generator set fuelled by hydrous ethanol with high water contents up to 40%, Fuel. 106 (2013) 586–592. doi:10.1016/j.fuel.2012.12.079.

11- K.W. Lawson, D.R. Lloyd, Membrane distillation, J. Memb. Sci. 124 (1997) 1–25. doi:10.1016/S0376-7388(96)00236-0.

12- J. ángel Pacheco-Basulto, D. Hernández-McConville, F.O. Barroso-Muñoz, S. Hernández, J.G. Segovia-Hernández, A.J. Castro-Montoya, A. Bonilla-Petriciolet, Purification of bioethanol using extractive batch distillation: Simulation and experimental studies, Chem. Eng. Process. Process Intensif. 61 (2012) 30–35. doi:10.1016/j.cep.2012.06.015.

13- I. Schifter, L. Diaz, J.P. Gómez, U. Gonzalez, Combustion characterization in a single cylinder engine with mid-level hydrated ethanol-gasoline blended fuels, in: Fuel, 2013: pp. 292–298. doi:10.1016/j.fuel.2012.06.002.

14- A. Kyriakides, V. Dimas, E. Lymperopoulou, D. Karonis, E. Lois, Evaluation of gasoline-ethanol-water ternary mixtures used as a fuel for an Otto engine, Fuel. 108 (2013) 208–215. doi:10.1016/j.fuel.2013.02.035.

15- T. Venugopal, A. Sharma, S. Satapathy, A. Ramesh, M.K. Gajendra Babu, Experimental study of hydrous ethanol gasoline blend (E10) in a four stroke port fuel-injected spark ignition engine, Int. J. Energy Res. 37 (2013) 638–644. doi:10.1002/er.1957.

16- R.C. Costa, J.R. Sodré, Hydrous ethanol vs. gasoline-ethanol blend: Engine performance and emissions, Fuel. 89 (2010) 287–293. doi:10.1016/j.fuel.2009.06.017.

17- T. Cordeiro de Melo, G. Bastos Machado, E. Jesus de Oliveira, C. Pereira Belchior, M. Colaço, J. Mautone Barros, D. Gatto de Oliveira, Combustion and emission analysis of different hydrous ethanol-gasoline blends on a Flex-Fuel Engine, in: 10. Int. Symp. Für Verbrennungsdiagnostik, 2012: pp. 310–319. doi:10.4271/2010-36-0469.

18- X. Wang, Z. Chen, J. Ni, S. Liu, H. Zhou, The effects of hydrous ethanol gasoline on combustion and emission characteristics of a port injection gasoline engine, Case Stud. Therm. Eng. 6 (2015) 147–154. doi:10.1016/j.csite.2015.09.007.

19- A.M. Ferris, D.A. Rothamer, Methodology for the experimental measurement of vapor-liquid equilibrium distillation curves using a modified ASTM D86 setup, Fuel. 182 (2016) 467–479. doi:10.1016/j.fuel.2016.05.099.

20- F. Wang, J. Wu, Z. Liu, Surface tensions of mixtures of diesel oil or gasoline and dimethoxymethane, dimethyl carbonate, or ethanol, Energy and Fuels. 20 (2006) 2471–2474. doi:10.1021/ef060231c.

21- M.A. Ratcliff, J. Burton, P. Sindler, E. Christensen, L. Fouts, G.M. Chupka, R.L. McCormick, Knock Resistance and Fine Particle Emissions for Several Biomass-Derived Oxygenates in a Direct-Injection Spark-Ignition Engine, SAE Int. J. Fuels Lubr. 9 (2016) 2016-01–0705. doi:10.4271/2016-01-0705.

22- A.D. Butler, R.A. Sobotowski, G.J. Hoffman, P. Machiele, Influence of fuel PM Index and ethanol content on particulate emissions from light-duty gasoline vehicles. , SAE Int. J.. No. 2015-01-1072.

23- M. Fatouraie, M.S. Wooldridge, B.R. Petersen, S.T. Wooldridge, Effects of Ethanol on In-Cylinder and Exhaust Gas Particulate Emissions of a Gasoline Direct Injection Spark Ignition Engine, Energy & Fuels. 29 (2015) 3399–3412. doi:10.1021/ef502758y.

24- M. Fatouraie, M. Wooldridge, S. Wooldridge, In-Cylinder Particulate Matter and Spray Imaging of Ethanol/Gasoline Blends in a Direct Injection Spark Ignition Engine, SAE Int. J. Fuels Lubr. 6 (2013) 2013-01–0259. doi:10.4271/2013-01-0259.

25- M. Storch, M. Koegl, M. Altenhoff, S. Will, L. Zigan, Investigation of soot formation of spark-ignited ethanol-blended gasoline sprays with single- and multi-component base fuels, Appl. Energy. 181 (2016) 278–287. doi:10.1016/j.apenergy.2016.08.059.

26- ASTM D5191-15 Standard Test Method for Vapor Pressure of Petroleum Products (Mini Method), West Conshohocken, PA, 2015, https://doi.org/10.1520/D5191-15

27- B.C. Windom, T.J. Bruno, Improvements in the measurement of distillation curves. 5. Reduced pressure advanced distillation curve method, in: Ind. Eng. Chem. Res., 2011: pp. 1115–1126. doi:10.1021/ie101784g.

28- T.J. Bruno, M.L. Huber, Evaluation of the physicochemical authenticity of aviation kerosene surrogate mixtures. Part 2: Analysis and prediction of thermophysical properties, Energy and Fuels. 24 (2010) 4277–4284. doi:10.1021/ef1004978.

29- B.L. Smith, T.J. Bruno, Improvements in the measurement of distillation curves. 3. Application to gasoline and gasoline + methanol mixtures, Ind. Eng. Chem. Res. 46 (2007) 297–309. doi:10.1021/ie060937u.

30- T.J. Bruno, L.S. Ott, T.M. Lovestead, M.L. Huber, The composition-explicit distillation curve technique: Relating chemical analysis and physical properties of complex fluids, J. Chromatogr. A. 1217 (2010) 2703–2715. doi:10.1016/j.chroma.2009.11.030.

31- ASTM D6729-14 Standard Test Method for Determination of Individual Components in Spark Ignition Engine Fuels by 100 Metre Capillary High Resolution Gas Chromatography, West Conshohocken, PA, 2014, https://doi.org/10.1520/D6729-14

32- J. Backhaus, Design methodology of bio-derived gasoline fuels .M.S., Mechanical Engineering, University of Wisconsin, Madison, WI (2013).

33- S.C. Burke, M. Ratcliff, R. McCormick, R. Rhoads, B. Windom, Distillation-based Droplet Modeling of Non-Ideal Oxygenated Gasoline Blends: Investigating the Role of Droplet Evaporation on PM Emissions, SAE Int. J. Fuels Lubr. 10 (2017) 2017-01–0581. doi:10.4271/2017-01-0581.

34- S.C. Burke, M. Ratcliff, R. McCormick, R. Rhoads, B. Windom, Measured and predicted vapor liquid equilibrium of ethanol-gasoline fuels: The influence of azeoptrope interactions on aromatic species enrichment and particulate matter formation in spark ignition engines. SAE Technical Paper Series, (2018), In Press.

35- G.M. Chupka, E. Christensen, L. Fouts, T.L. Alleman, M.A. Ratcliff, R.L. McCormick, Heat of Vaporization Measurements for Ethanol Blends Up To 50 Volume Percent in Several Hydrocarbon Blendstocks and Implications for Knock in SI Engines, SAE Int. J. Fuels Lubr. 8 (2015) 2015-01–0763. doi:10.4271/2015-01-0763.

36- A.B. Hadler, L.S. Ott, T.J. Bruno, Study of azeotropic mixtures with the advanced distillation curve approach, Fluid Phase Equilib. 281 (2009) 49–59. doi:10.1016/j.fluid.2009.04.001.

37- K. Aikawa, T. Sakurai, J.J. Jetter, Development of a Predictive Model for Gasoline Vehicle Particulate Matter Emissions, SAE Int. J. Fuels Lubr. 3 (2010) 610–622. doi:10.4271/2010-01-2115.

38- S.C. Burke, M. Ratcliff, R. McCormick, R. Rhoads, B. Windom, UNIFAC-based approach to gasoline droplet evaporation and the role of oxygenates on PM precursor vaporization, In *10th US National Meeting on Combustion, College Park, MD*. 2017.

39- T. Stach, J. Schlerfer, M. Vorbach, New generation multi-hole fuel injector for direct-injection SI engines-optimization of spray characteristics by means of adapted injector layout and multiple injection (No. 2007-01-1404). SAE Technical Paper (2007).

40- M. Lapuerta, R. García-Contreras, J. Campos-Fernández, M.P. Dorado, Stability, lubricity, viscosity, and cold-flow properties of alcohol-diesel blends, Energy and Fuels. 24 (2010) 4497–4502. doi:10.1021/ef100498u.

41- M.M. Elkotb, Fuel atomization for spray modelling, Prog. Energy Combust. Sci. 8 (1982) 61–91. doi:10.1016/0360-1285(82)90009-0.

42- F. dos Santos, L. le Moyne, Spray atomization models in engine applications, from correlations to direct numerical simulations, Oil Gas Sci. Technol. 66 (2011) 801–822. doi:10.2516/ogst/2011116.

43- Shirazi SA, B Abdollahipoor, J Martinson, KF Reardon, BC Windom. 2018. Physiochemical Property Characterization of Hydrous and Anhydrous Ethanol Blended Gasoline. Submitted.

44- Design Institute for Physical Property Data (U.S.), DIPPR Project 801, full version: evaluated standard thermophysical property values, Des. Inst. Phys. Prop. Res. (2005).

7 Conclusions and Recommendations

7.1. Project I: Development and Application of a Fuel Property Database for Mono-Alcohols as Fuel Blend Components for Spark Ignition Engines

7.1.1. Significant findings

There are many alcohols that could be considered for use as fuels or in fuel blends, but it is not feasible to experimentally investigate the fuel potential of all of these molecules. In the Project I, a systematic product design methodology was developed for the first time for all C1 to C10 alcohols to identify alcohols that might be suitable for blending with gasoline for use in SI engines.

Forty-eight and 46 alcohols were identified as good candidates for blending with gasoline at levels up to 15 vol%, depending on whether a stringent requirement was imposed on the increased volatility of the blend over the base gasoline.

The more challenging requirements for blending at more than 40 vol% resulted in a much shorter list of six alcohols: 1-propanol, 1-butanol, 2-methyl-1-propanol (iso-butanol), 2-methyl-2-pentanol, 3-methyl-3-pentanol, and (1-methylcyclopropyl)methanol were identified as most promising alcohol molecules for blending with gasoline at high concentrations.

7.1.2. Future works

New research could focus on how and from what feedstocks the promising molecules can be produced, and on fuel characterization tests, combustion and emission characteristics, and technoeconomical and environmental assessments. All of those are necessary to fully understand

whether these alcohols have the necessarily characteristics to be blended with gasoline at a commercial scale.

The approach used in this study for identification of alcohols for SI engines could be modified for the evaluation of other classes of fuel molecules (e.g., esters, ketones, ethers) and other engines. If target values for the critical fuel properties that maximize the efficiency is identified for a given engine with its specified combustion strategy, then fuels that have properties close to those values can provide acceptable performance. Therefore, based on the molecular structure of other classes of fuel molecules, their possible blending effect with the base fuel should be predicted and appropriate criteria can be set.

7.2. Part II: Dual-Alcohol Blending Effects on Gasoline Properties

7.2.1. Significant findings

The dual-alcohol approach can be an option to circumvent the issues with neat alcohols and blends containing a single alcohol. In project II of this study, for the first time the fuel potentials of ten dual-alcohol blends over a wide range of blending ratios (10 to 80 vol %) and corresponding single alcohol-gasoline blends were evaluated based on their vapor-liquid equilibrium and physiochemical properties as compared to the neat gasoline. Furthermore, this was the first investigation of the fuel potential of 3-methyl-3-pentanol in single- and dual-alcohol blends and iso-butanol in dual-alcohol blends.

Regardless of total alcohol concentration, dual-alcohol blends successfully kept the RVP very close to that of gasoline. This addresses limitation associated with high volatility of single lower alcohol blends at low to medium blending ratios as well as low volatility of single higher alcohol blends at medium to high blending ratios.

Distillation curves of dual-alcohol blends lie between the curves of the corresponding single alcohol blends. At early stages of the distillation, curves are relatively close to the corresponding single lower alcohol blend. However, after evaporation of the lower alcohols at a temperature close to the lower alcohol's boiling point, the distillation curve converging the corresponding single higher alcohol blend at a temperature close to the boiling point of the higher alcohol.

Addition of 3-methyl-3-pentanol reduces the volatility of the gasoline more than iso-butanol due to the higher boiling point, lower RVP, less polarity, and longer hydrocarbon chain. Composition evolution during the distillation revealed that dual alcohol blends suppress the evaporation of the aromatic species even more than a corresponding ethanol blend.

Results from droplet evaporation simulations showed that the dual-alcohol blends had longer droplet evaporation times compared to gasoline (up to 17.1% increase) which may cause a poorer mixing. Given the approximately identical vapor pressures of dual-alcohol blends with that of gasoline, these results can be explained by higher HoVs and physical properties (viscosity, density, and surface tension) of higher alcohols relative to the gasoline.

Increase in alcohol content increases the water tolerance of the blend.

Among single alcohol blends, ethanol blends exhibited the highest water tolerance followed by i-butanol, methanol and 3-methyl-3-pentanol. Blends of iso-butanol showed relatively acceptable water tolerance especially at moderate to high blending ratios, while 3-methyl-3-pentanol showed the lowest even at high blending ratios possibly due to the lower polarity and longer hydrocarbon chain. Dual-alcohol blends showed higher water tolerance relative to their corresponding single alcohol blends at blending ratios of 40 vol% and higher.

Kinematic viscosity values increased with a non-linear manner with increased alcohol content, especially in case of higher alcohols.

Results showed that it may be advantageous to use dual-alcohol blends containing up to 40 vol% as they minimize the limitations of single-alcohol blends, in particular volatility, while exhibiting satisfactory properties for an acceptable performance in existing spark ignition engines particularly in terms of volatility, kinematic viscosity, and water tolerance.

Both iso-butanol and 3-methyl-3-pentanol exhibit promising properties as blendstocks for being used as a single alcohol or along with ethanol.

The dual-alcohol approach has potential to increase the portion of biofuel in the current gasoline system with no or only minor changes to current SI engine architectures and fuel delivery infrastructure.

7.2.2. Future works

Build on promising characterization results for dual-alcohol blends, this project can be taken to the next level by including engine and ignition quality tests, flame studies, and spray soot characteristics tests for light- and medium-duty SI engines. Conduction of these tests can give insights into the influences of alternate and dual-alcohol gasoline blends on engine performance with focus on blends that have both high RON and low soot emissions.

New research could focus on metabolic engineering of microorganisms to find out how to produce 3-methyl-3-pentanol and other promising alcohols.

7.3. Part III: Characterization of physiochemical properties and volatility behavior of hydrous and anhydrous ethanol gasoline blends

7.3.1. Significant findings

Replacing anhydrous ethanol fuel with hydrous ethanol (at the azeotropic composition) can result in significant energy and cost savings during production. Currently there are a lack of available thermophysical property data for hydrous ethanol gasoline fuel blends. These data are important to understand the effect of water on critical fuel properties and to evaluate the potential of using hydrous ethanol fuels in conventional and optimized spark ignition engines. All previous studies evaluating hydrous ethanol have been limited to combustion and emission characteristics. The goal of this study was to provide a fundamental and comprehensive assessment of the thermophysical properties of hydrous ethanol-gasoline blends to examine their potential as a fuel blend for conventional SI engines.

Phase separation occurred at relatively high temperatures for hydrous ethanol blends, especially low and medium blending levels (i.e. 10% and 15%) indicating that the use of additive for preventing phase separation may be necessary.

Use of hydrous ethanol blends decreases the LHV of the blends relative to the anhydrous ethanol blends.

Addition of both anhydrous and hydrous ethanol into gasoline caused a reduction in boiling temperatures of the distillation curve and an increase in RVP depending on the initial concentration. However, at each blending ratio, differences between hydrous and anhydrous ethanol blends was negligible.

Ethanol and water delays the evaporation of the aromatic species with no significant difference between hydrous and anhydrous ethanol blends.

Results from droplet evaporation simulations showed that the higher HoV and viscosity of water relative to ethanol may cause significant differences in the net evaporation time between the hydrous and anhydrous blends especially at moderate to high blending ratios.

Based on the results, it is concluded that without updates to the fuel injection system, the utilization of water (i.e. hydrous ethanol) may extend droplet lifetimes.

Results suggest that at low engine speeds in which there is enough time for evaporation, there may be no notable difference between gasoline and the other blends in terms of PM emissions, however, at some engine conditions (e.g. very high loads and speeds) there may not be enough time for complete droplet evaporation, which would increase the probability of fuel spray impingement on the cylinder walls in a DISI platform. This slowed evaporation coupled with the suppression of the aromatics' evaporation by ethanol and water may cause higher PM emissions relative to gasoline.

7.3.2. Future works

To investigate the potential of spray impingement/pool burning responsible for increased PM, further research including spray characterization experiments and engine testing/PM measurements is suggested.

It is also recommended that future work be conducted on the characterization of fuels with higher water/ethanol ratios, compatibility of fuel delivery/storage systems and economical/energy life cycle aspects of replacing hydrous ethanol with anhydrous ethanol to examine potential of hydrous ethanol- gasoline mixtures as fuel blends.

8 Appendix

8.1. Supplemental materials (Chapter3)

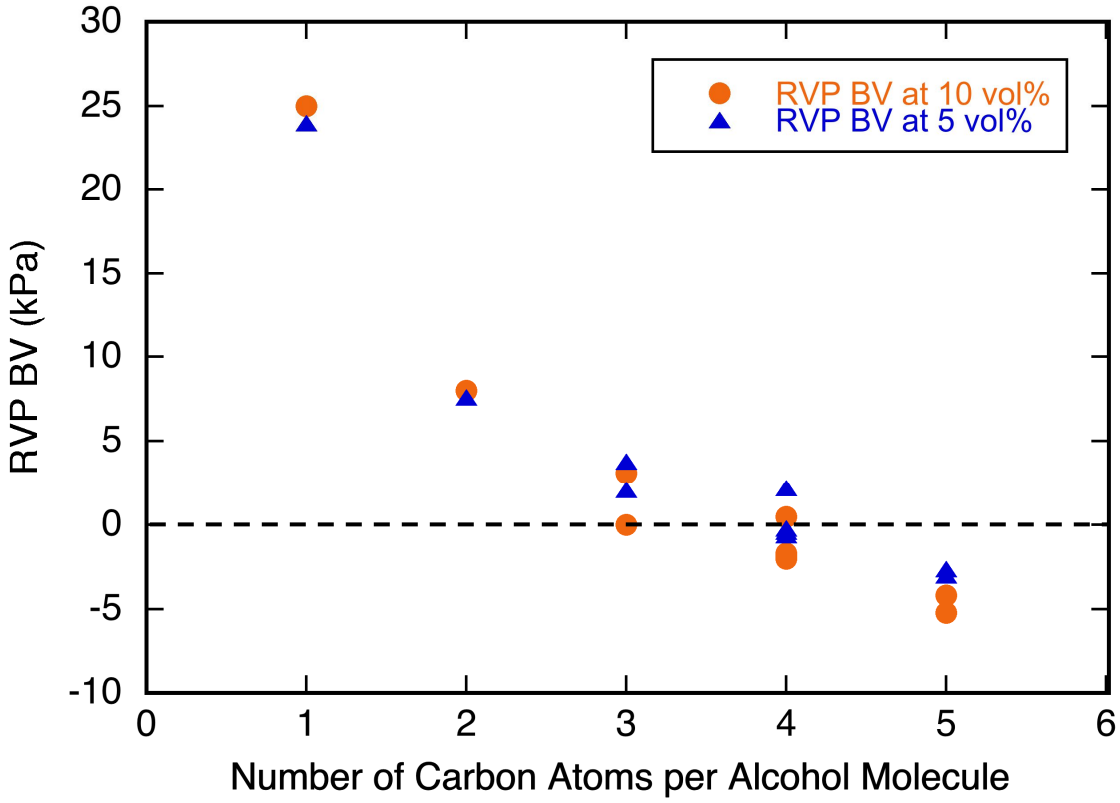

Figure S3.1. Reid Vapor Pressure blending value vs. carbon content of alcohols at 5 vol% and 10 vol% gasoline. For C1-C4 alcohols (methanol, ethanol, 1-propanol, 2-propanol, 1-butanol, 2-methyl-2-propanol, 2-butanol, 2-methyl-1-propanol), data at 5 and 10 vol% were obtained from Andersen et al. [43]. For 1-pentanol, data were obtained from Christensen et al. [45] at 5 vol% and linearly interpolated for 10 vol%. For 3-methyl-1-butanol, data were obtained from Christensen et al. [45] and linearly interpolated for 5 and 10 vol%.

Table S3.1. List of alcohols with fuel potential

Linear and branched alcohols		Cyclic alcohols
Methanol	2,4,4-Trimethyl-1-pentanol	(1-Methylcyclopropyl)methanol
Ethanol	2,2,4-Trimethyl-1-pentanol	(2,2-Dimethylcyclopropyl)methanol
1-Propanol	2,3,4-Trimethyl-3-pentanol	2-Cyclopentylethanol
1-Butanol	2,4,4-Trimethyl-2-pentanol	2-Cyclopropyl-2-butanol
2-Methyl-1-propanol	2,3,4-Trimethyl-2-pentanol	(1-Ethylcyclobutyl)methanol
2-Methyl-2-pentanol	2,3,4-Trimethyl-1-pentanol	1,3-Dimethylcyclopentanol
3-Methyl-3-pentanol	3-Ethyl-2-methyl-3-pentanol	1,2-Dimethylcyclopentanol
2,2-Dimethyl-1-butanol	3,4,4-Trimethyl-1-hexanol	2-Cyclobutyl-2-propanol
2,3-Dimethyl-1-butanol	2,5,5-Trimethyl-1-hexanol	Cyclohexylmethanol
3,3-Dimethyl-1-butanol	4,5,5-Trimethyl-1-hexanol	1-Isopropylcyclopentanol
4,4-Dimethyl-1-pentanol	3,5,5-Trimethyl-3-hexanol	2-Cyclopropyl-3-methyl-2-butanol
3,3-Dimethyl-1-pentanol	3-Ethyl-2,4-dimethyl-3-pentanol	2-Cyclopropyl-2-pentanol
2-Ethyl-2-methyl-1-butanol	2,4,6-Trimethyl-4-heptanol	(2,3,4-Trimethylcyclobutyl)methanol
2,3,3-Trimethyl-1-butanol	2,3,4,5-Tetramethyl-3-hexanol	3-Cyclopropyl-3-pentanol
2,2,3-Trimethyl-1-butanol	4-Ethyl-2,3-dimethyl-3-hexanol	1-Cyclopentyl-2-propanol
3,4-Dimethyl-3-hexanol	3-Isopropyl-2,4-dimethyl-3-pentanol	
2,2-Dimethyl-1-hexanol	3-Methyl-2-(2-methyl-2-propanyl)-1-pentanol	

Table S3.2. List of alcohols with potential to be blended at low (<15%) range in gasoline (scenario 2).

Linear and branched alcohols		Cyclic alcohols
1-Butanol	2,3,4-Trimethyl-3-pentanol	(1-Methylcyclopropyl)methanol
2-Methyl-1-propanol	2,4,4-Trimethyl-2-pentanol	(2,2-Dimethylcyclopropyl)methanol
2-Methyl-2-pentanol	2,3,4-Trimethyl-2-pentanol	2-Cyclopentylethanol
3-Methyl-3-pentanol	2,3,4-Trimethyl-1-pentanol	2-Cyclopropyl-2-butanol
2,2-Dimethyl-1-butanol	3-Ethyl-2-methyl-3-pentanol	(1-Ethylcyclobutyl)methanol
2,3-Dimethyl-1-butanol	3,4,4-Trimethyl-1-hexanol	1,3-Dimethylcyclopentanol
3,3-Dimethyl-1-butanol	2,5,5-Trimethyl-1-hexanol	1,2-Dimethylcyclopentanol
4,4-Dimethyl-1-pentanol	4,5,5-Trimethyl-1-hexanol	2-Cyclobutyl-2-propanol
3,3-Dimethyl-1-pentanol	3,5,5-Trimethyl-3-hexanol	Cyclohexylmethanol
2-Ethyl-2-methyl-1-butanol	3-Ethyl-2,4-dimethyl-3-pentanol	1-Isopropylcyclopentanol
2,3,3-Trimethyl-1-butanol	2,4,6-Trimethyl-4-heptanol	2-Cyclopropyl-3-methyl-2-butanol
2,2,3-Trimethyl-1-butanol	2,3,4,5-Tetramethyl-3-hexanol	2-Cyclopropyl-2-pentanol
3,4-Dimethyl-3-hexanol	4-Ethyl-2,3-dimethyl-3-hexanol	(2,3,4-Trimethylcyclobutyl)methanol
2,2-Dimethyl-1-hexanol	3-Isopropyl-2,4-dimethyl-3-pentanol	3-Cyclopropyl-3-pentanol
2,4,4-Trimethyl-1-pentanol	3-Methyl-2-(2-methyl-2-propanyl)-1-pentanol	1-Cyclopentyl-2-propanol
2,2,4-Trimethyl-1-pentanol		

Table S3.3. List of alcohols with potential to be blended at high (>40%) range in gasoline (scenario 3).

Linear and branched alcohols	Cyclic alcohols
1-Propanol	(1-Methylcyclo-propyl)methanol
1-Butanol	
2-Methyl-1-propanol	
2-Methyl-2-pentanol	
3-Methyl-3-pentanol	

8.2. Supplemental materials (Chapter4)

Table S4.1 The list of the simplified composition of UTG-96 gasoline

Compound	Mass fraction
i-Butane	0.0055
n-Butane	0.0329
i-Pentane	0.0833
2-Methyl-1-butene	0.0072
n-Pentane	0.0061
trans 2 pentene	0.0067
Cis-2-pentene	0.0037
2-methyl-2-butene	0.0098
2,3-Dimethylbutane	0.0107
2-Methylpentane	0.0213
3-Methylpentane	0.0157
n-Hexane	0.0066
2-Methyl-2-penten	0.0093
Methylcyclopentane	0.0142
2,4-Dimethylpentane	0.0076
3-methyl Cyclopentene	0.0044
Benzene	0.0054
2,3,dimethylPentane	0.0282
3-Methylhexane	0.0097
Cyclopentane, 1,3-dimethyl-, cis-	0.0076
2,2,4-Trimethylpentane	0.2005
n-Heptane	0.0028
Cis-3-heptene	0.0067
Methylcyclohexane	0.0100
2,3,3-Trimethylpentane	0.0103
2,4-Dimethylhexane	0.0087
2,3,4-Trimethylpentane	0.0245
Toluene	0.2166
2,3-Dimethylhexane	0.0051
2-Methylheptane	0.0074
3-Methylheptane	0.0086
1-methyl-1-ethylcyclopentane	0.0062
2,2,5-trimethylhexane	0.0091
Ethylbenzene	0.0132
p-Xylene	0.0162
2-methyl-Octane	0.0066
3-Methyloctane	0.0052
1-nonene	0.0180
1 ethyl-2 methyl benzene	0.0191
1,2,4-trimethylbenzene	0.0112
1,2,3-trimethylbenzene	0.0172
1,4-diethylbenzene	0.0049
C10 aromatic	0.0039
2-ethyl-1,4-dimethyl	0.0043
C11-paraffin	0.0062
C11-aromatic	0.0102
1,2,3,4-tetrahydronaphthalene	0.0035
Naphthalene	0.0025
n-Dodecane	0.0035
Biphenyl	0.0070
Hexylbenzene	0.0117
Hexamethylbenzene	0.0074
2,6-dimethylnaphthalene	0.0073
Acenaphthalene	0.0084

Table S4.2 Vapor pressure/distillation and vapor lock protection classes in ASTM D4814 [49]

	Vapor Pressure/Distillation Class					
	AA	**A**	**B**	**C**	**D**	**E**
Reid vapor pressure (kPa), max	54	62	69	79	93	103
Distillation temperatures(°C)						
T10, max	70	70	65	60	55	50
T50, min	77	77	77	77	77	77
T50, max	121	121	118	116	113	110
T90, max	190	190	190	185	185	185
End point, max	225	225	225	225	225	225
	Vapor Lock Protection Class					
	1	**2**	**3**	**4**	**5**	**6**
$T_{v/l=20}$ (°C), min	54	50	47	42	39	35

Table S4.3 Corrected temperatures for 1 atm based on the Sydney-Young equation

Fuel	T10 (°C)	T50 (°C)	T90 (°C)
Gasoline	77.90	110.45	159.12
E10	66.55	108.67	148.39
B10	80.32	105.20	150.59
H10	83.13	111.95	152.87
EB10	76.43	106.42	149.52
EH10	71.45	109.06	150.19
E20	65.24	79.08	150.65
B20	79.31	101.65	140.73
H20	87.08	113.46	143.86
EB20	70.63	94.78	140.42
EH20	68.24	100.04	142.98
E40	67.54	77.95	146.64
B40	84.39	102.15	115.86
H40	96.32	117.90	134.58
EB40	70.01	81.36	113.98
EH40	67.92	78.84	132.18
M60	58.50	65.09	67.13
B60	93.02	106.72	111.80
H60	107.92	122.20	130.13
MB60	65.11	77.16	111.58
MH60	63.25	74.43	129.80
M80	63.28	66.12	66.93
B80	104.43	110.32	112.95
H80	117.32	124.38	127.94
MB80	63.95	67.86	76.97
MH80	65.08	68.57	123.24

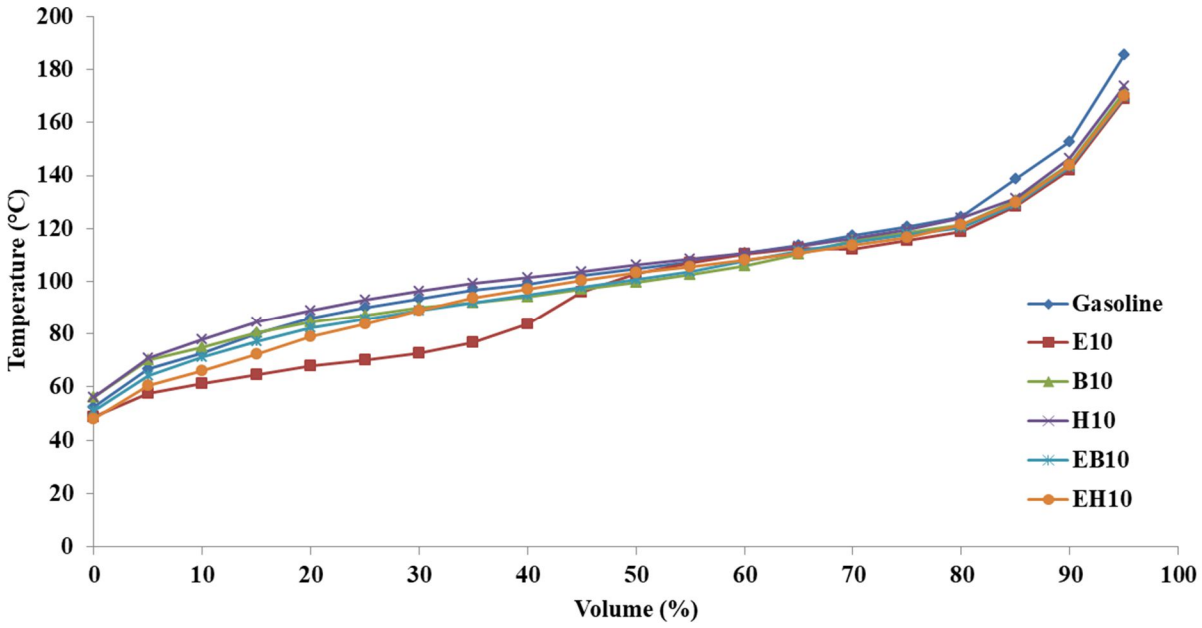

Figure S4.1 Distillation curves at 84.3 kPa for gasoline and blends containing 10 vol% alcohol. Data was taken at. M: methanol. E: ethanol. B: i-butanol. H: 3-methyl-3-pentanol. The average standard error for all data points is 1.68.

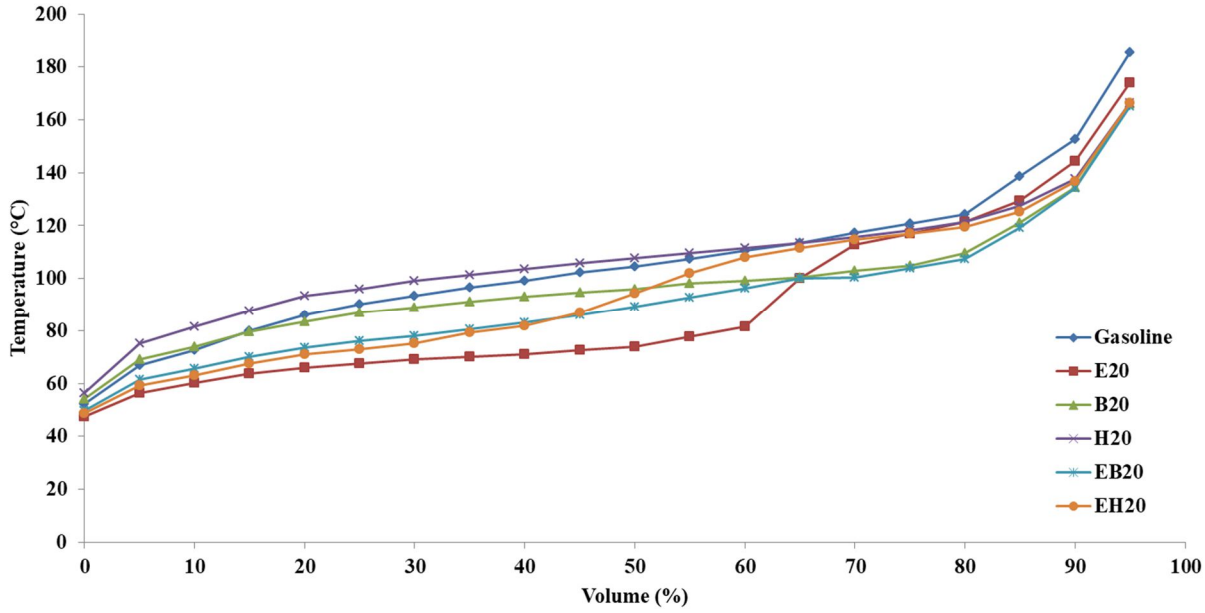

Figure S4.2 Distillation curves at 84.3 kPa for gasoline and blends containing 20 vol% alcohol. M: methanol. E: ethanol. B: i-butanol. H: 3-methyl-3-pentanol. The average standard error for all data points is 0.84.

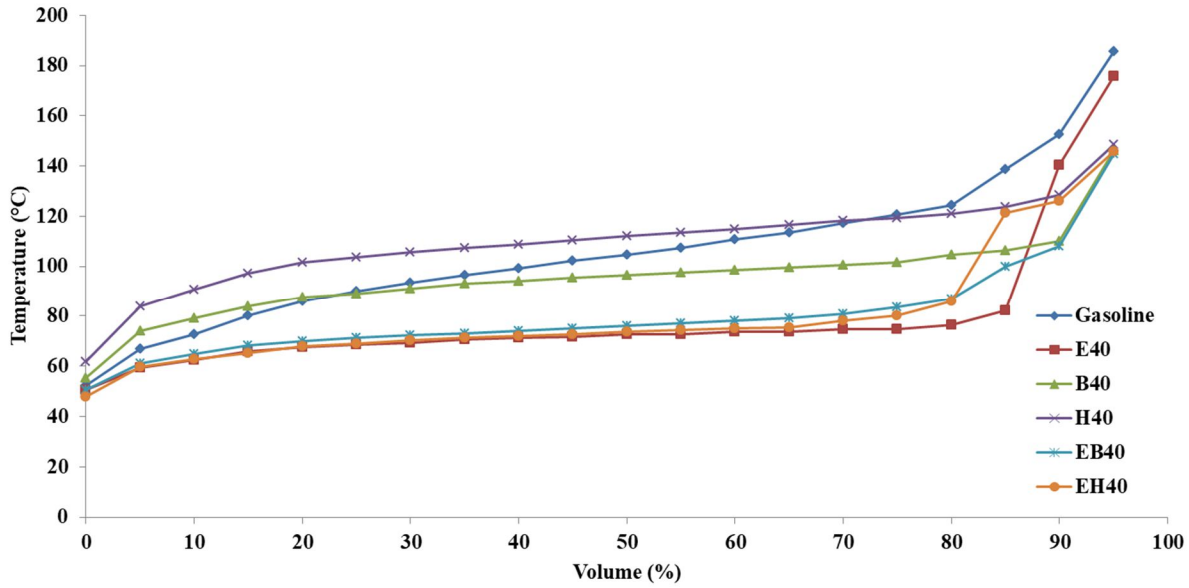

Figure S4.3 Distillation curves at 84.3 kPa for gasoline and blends containing 40 vol% alcohol. M: methanol. E: ethanol. B: i-butanol. H: 3-methyl-3-pentanol. The average standard error for all data points is 0.56.

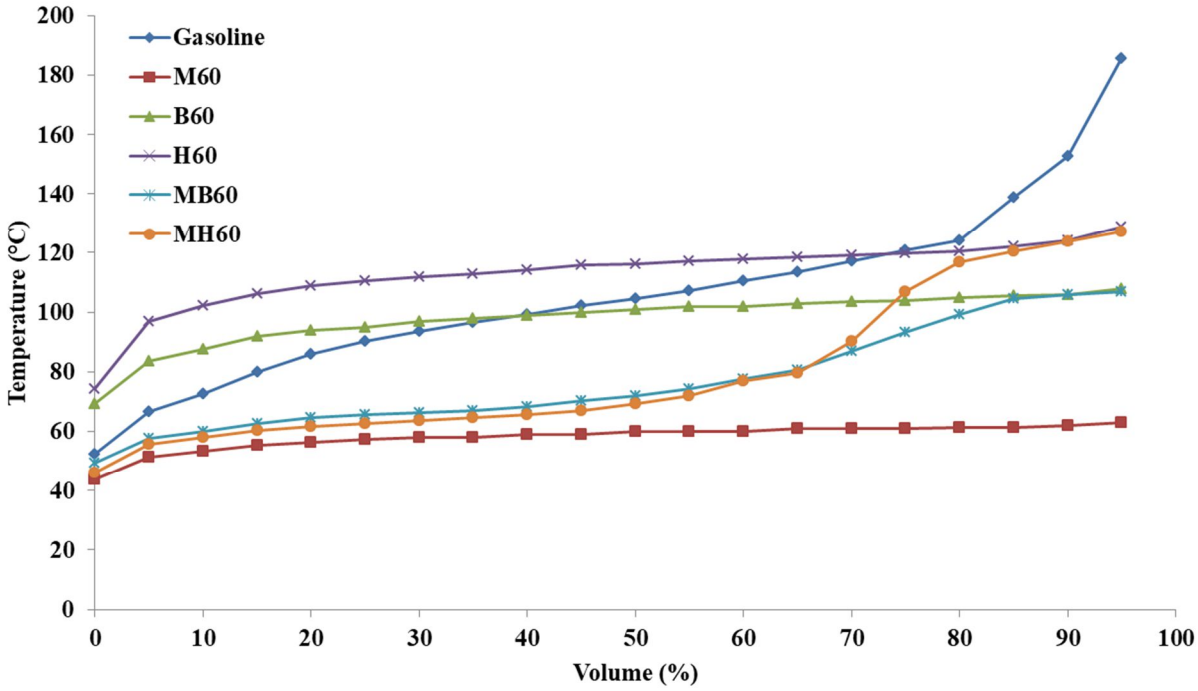

Figure S4.4 Distillation curves at 84.3 kPa for gasoline and blends containing 60 vol% alcohol. M: methanol. E: ethanol. B: i-butanol. H: 3-methyl-3-pentanol. The average standard error for all data points is 0.49.

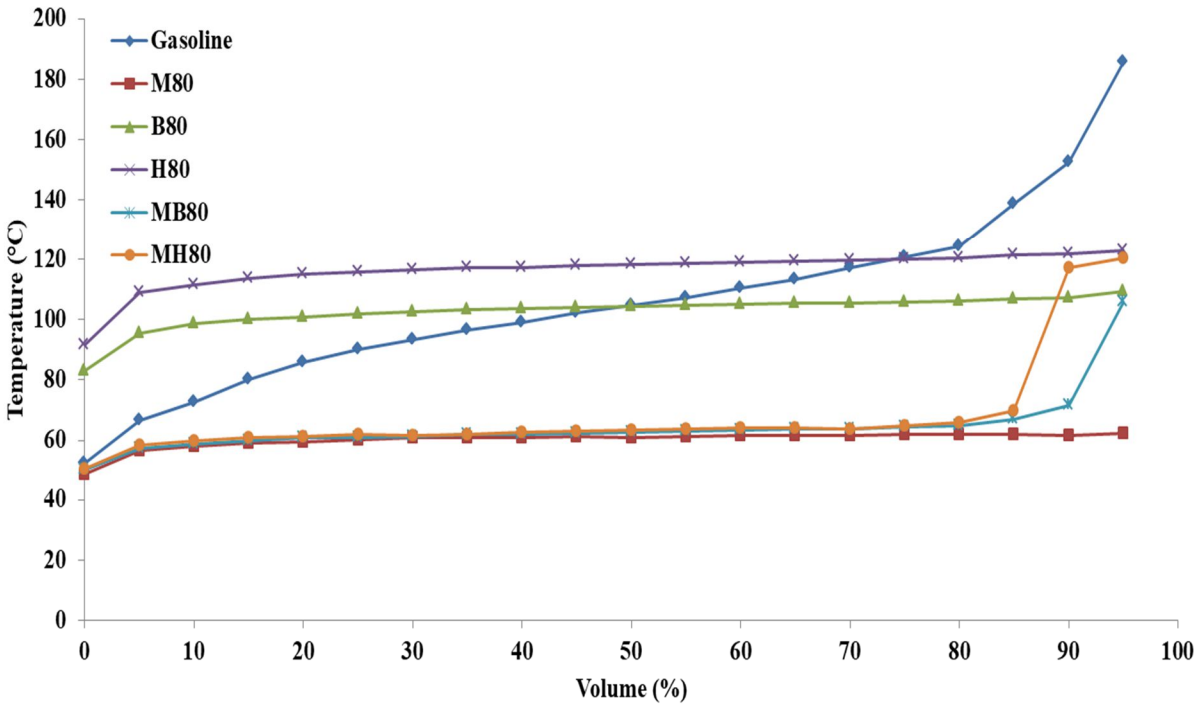

Figure S4.5 Distillation curves at 84.3 kPa for gasoline and blends containing 80 vol% alcohol. M: methanol. E: ethanol. B: i-butanol. H: 3-methyl-3-pentanol. The average standard error for all data points is 0.52.

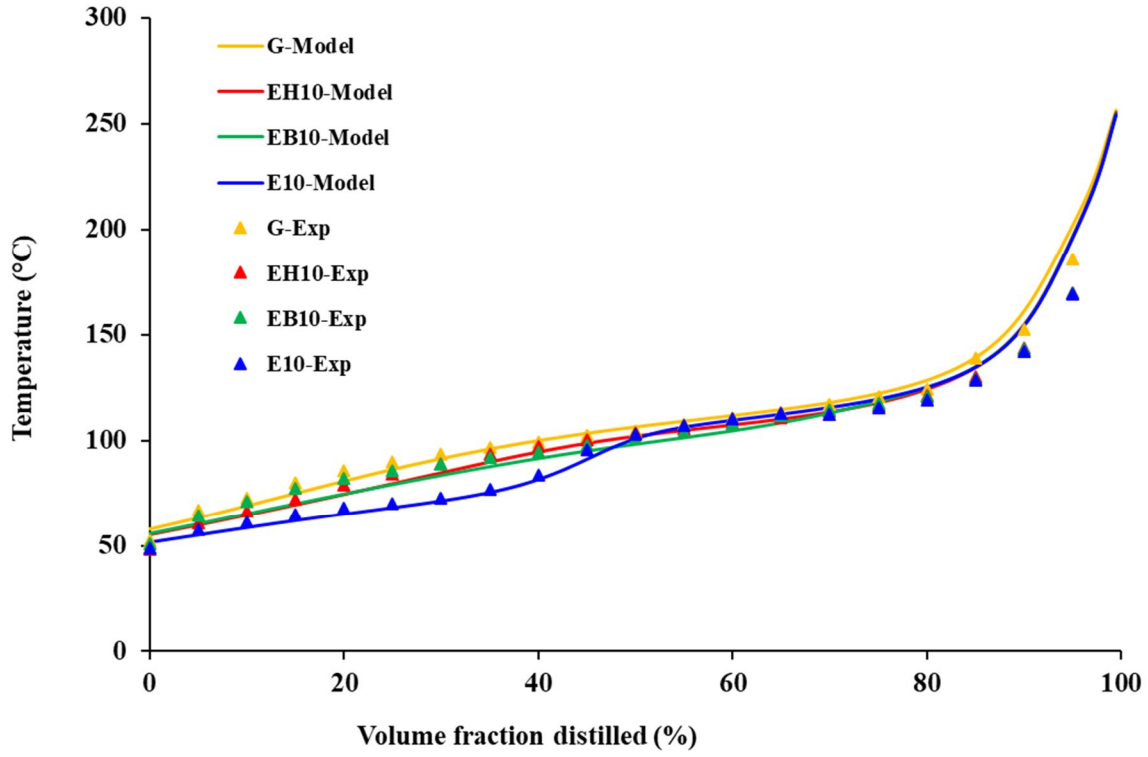

Figure S4.6 Comparison of experimentally measured and predicted distillation curves for gasoline and blends containing 10 vol% alcohol. Exp: experimentally measured average molecular weight. Model: predicted average molecular weight. G: gasoline. E: ethanol. B: i-butanol. H: 3-methyl-3-pentanol.

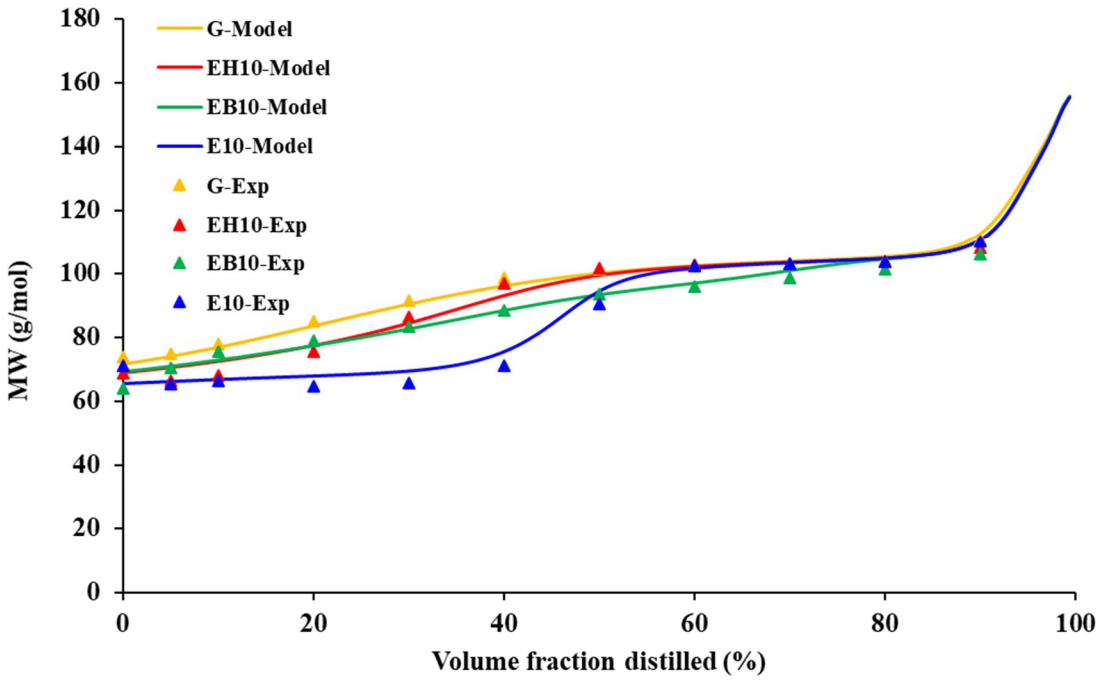

Figure S4.7 Comparison of experimentally measured and predicted average molecular weight for gasoline and blends containing 10 vol% alcohol. Exp: experimentally measured average molecular weight. Model: predicted average molecular weight. G: gasoline. E: ethanol. B: i-butanol. H: 3-methyl-3-pentanol.

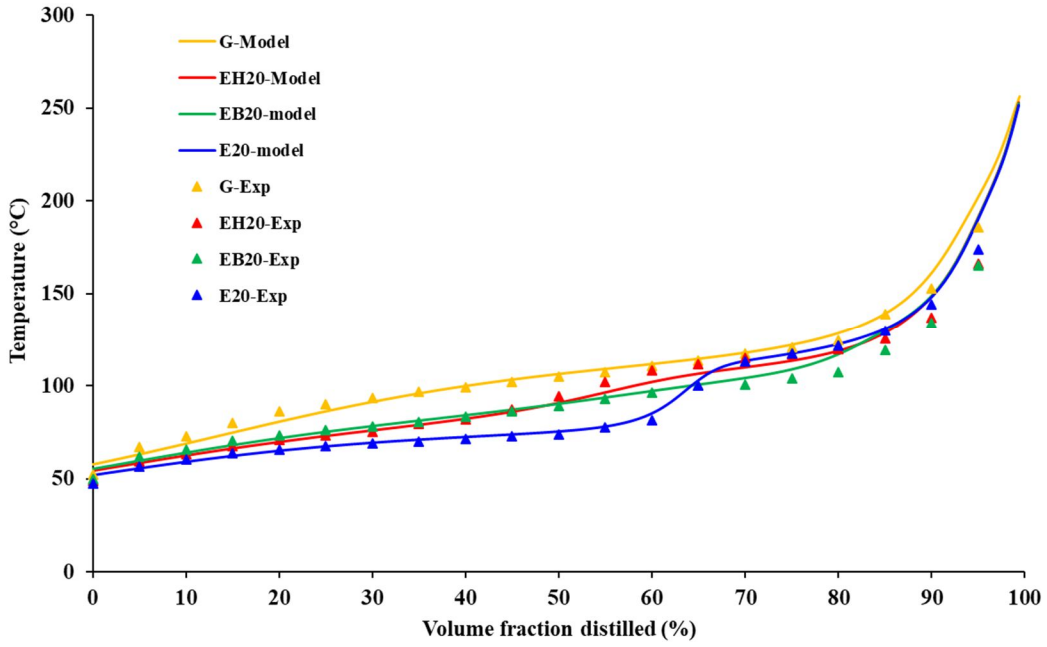

Figure S4.8 Comparison of experimental distillation curves to those modeled for gasoline and blends containing 20 vol% alcohol. Exp: experimentally measured average molecular weight. Model: predicted average molecular weight. G: gasoline. E: ethanol. B: i-butanol. H: 3-methyl-3-pentanol.

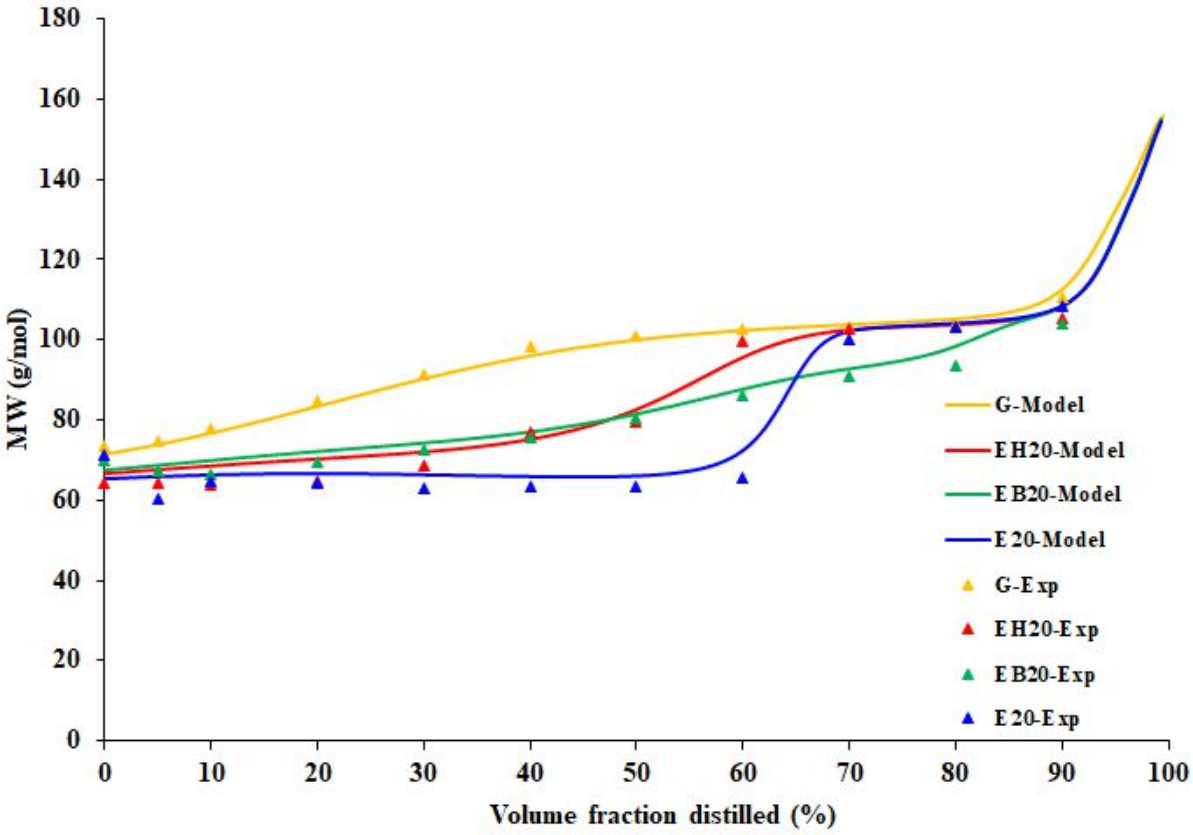

Figure S4.9 Comparison of experimentally measured and predicted average molecular weight for gasoline and blends containing 20 vol% alcohol. Exp: experimentally measured average molecular weight. Model: predicted average molecular weight. G: gasoline. E: ethanol. B: i-butanol. H: 3-methyl-3-pentanol.

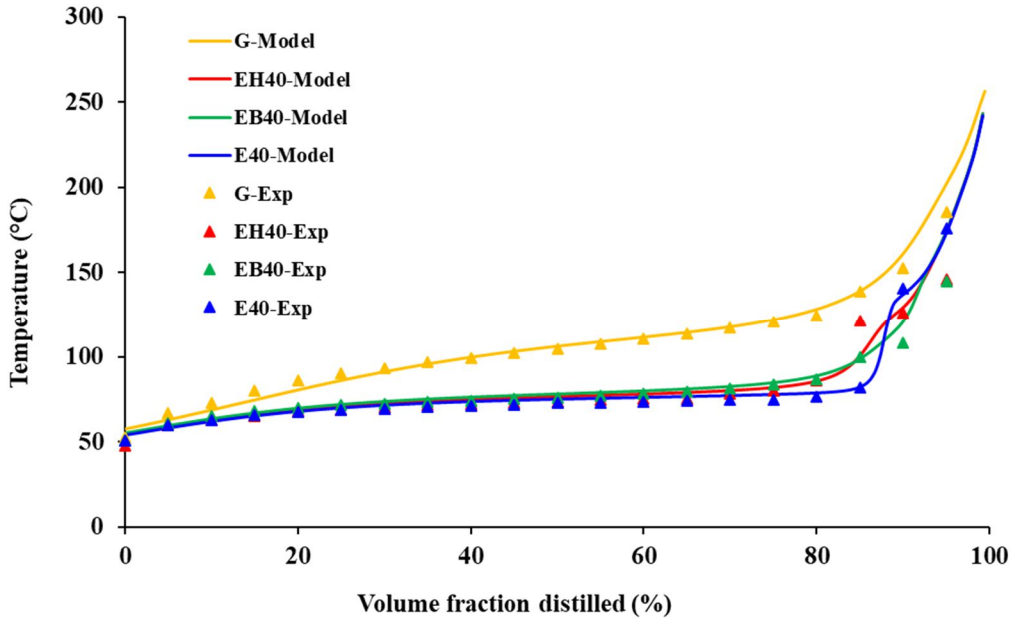

Figure S4.10 Comparison of experimentally measured and predicted distillation curves for gasoline and blends containing 40 vol% alcohol. Exp: experimentally measured average molecular weight. Model: predicted average molecular weight. G: gasoline. E: ethanol. B: i-butanol. H: 3-methyl-3-pentanol.

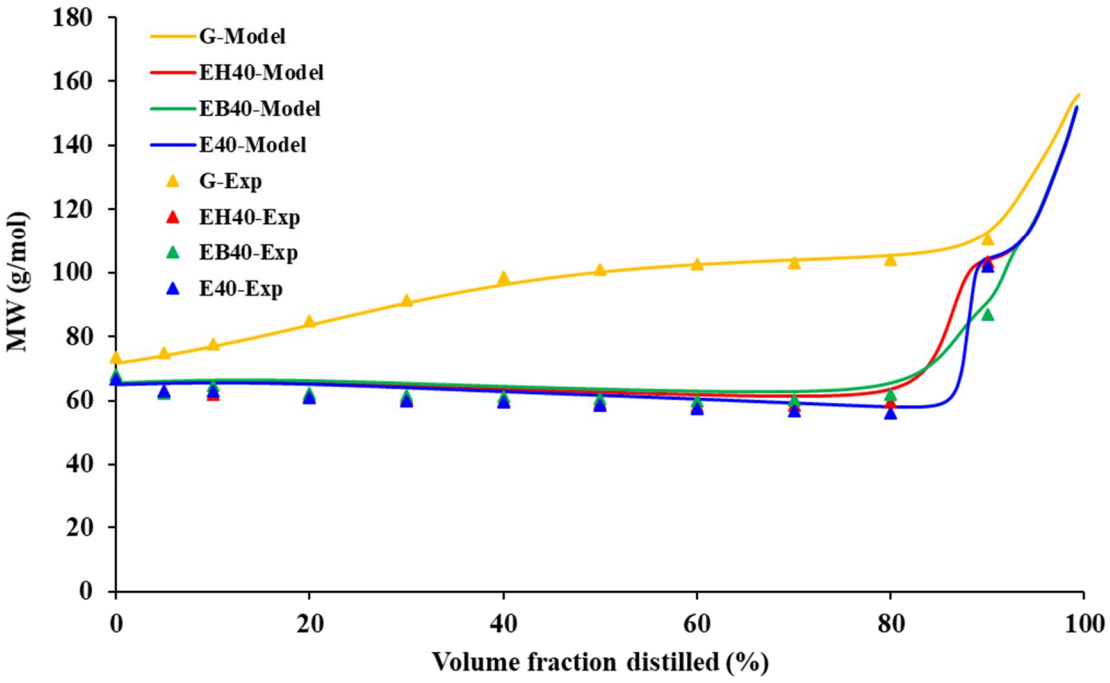

Figure S4.11 Comparison of experimentally measured and predicted average molecular weight for gasoline and blends containing 40 vol% alcohol. Exp: experimentally measured average molecular weight. Model: predicted average molecular weight. G: gasoline. E: ethanol. B: i-butanol. H: 3-methyl-3-pentanol.

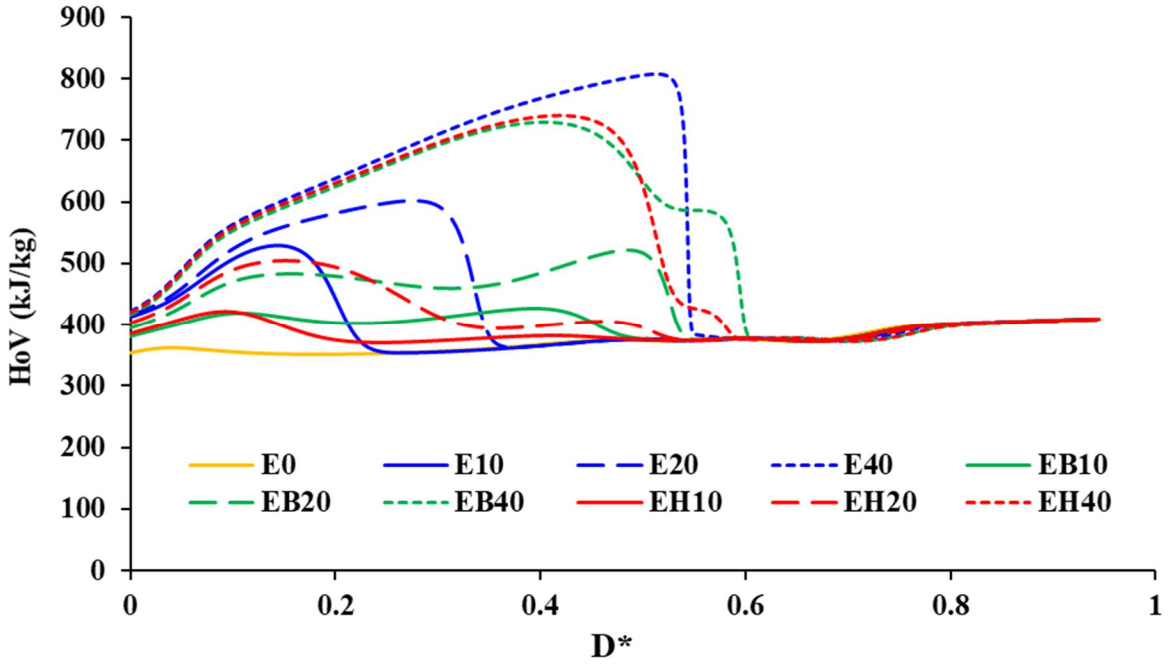

Figure S4.12 HoV profiles of gasoline and blend obtained from the droplet evaporation model as a function of dimensionless D^* at 1 atm and 323 K. (D_0= 25 µm). D^*=1-D/D_0. E: anhydrous ethanol blends. H: hydrous ethanol blends. D: Diameter. D_0: Initial diameter.

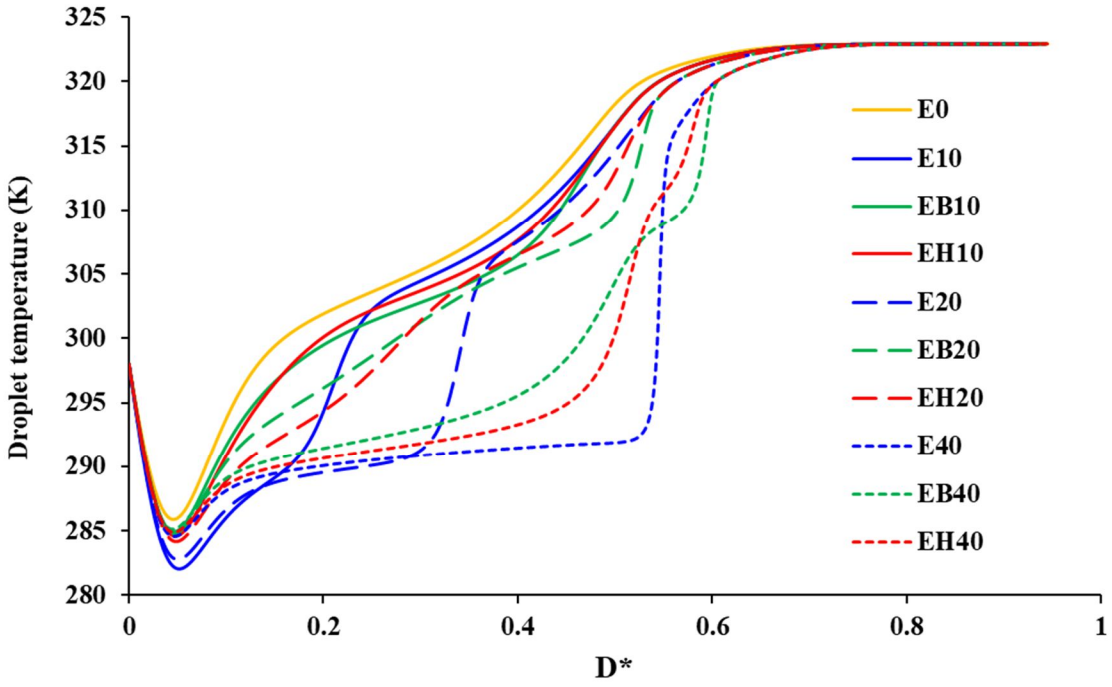

Figure S4.13 Temperature profiles of gasoline and alcohol blends obtained from droplet evaporation model as a function of dimensionless D^* at 1 atm and 323 K. $D^*=1-D/D_0$. G: gasoline. E: ethanol. B: i-butanol. H: 3-methyl-3-pentanol. D: Diameter. D_0: Initial diameter.

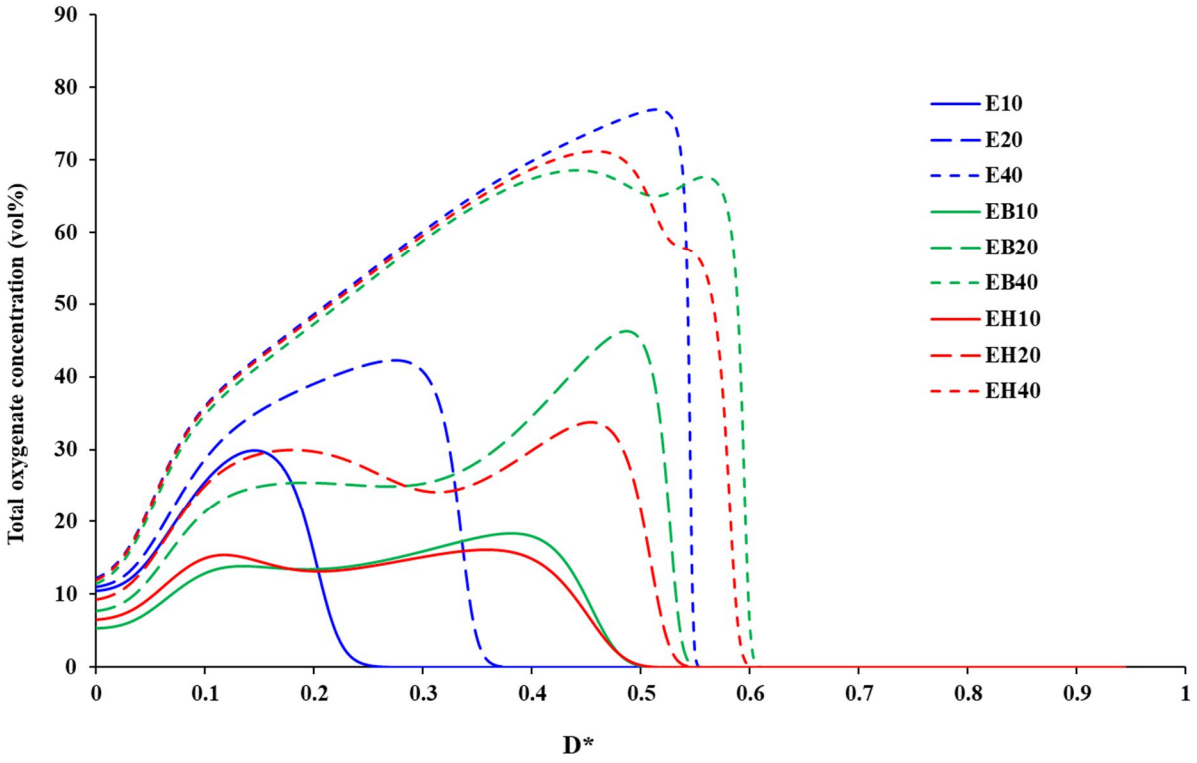

Figure S4.14 Total oxygenate concentration profiles of gasoline and blend obtained from the droplet evaporation model as a function of dimensionless D^* at 1 atm and 323 K. (D_0= 25 µm). D^*=1-D/D_0. E: ethanol. B: i-butanol. H: 3-methyl-3-pentanol

8.3. Supplemental materials (Chapter6)

Table S6.1 The list of the simplified composition and the corresponding mass fraction of UTG96 gasoline

Compound	Mass fraction
i-Butane	0.0055
n-Butane	0.0329
i-Pentane	0.0833
2-Methyl-1-butene	0.0072
n-Pentane	0.0061
trans 2 pentene	0.0067
Cis-2-pentene	0.0037
2-methyl-2-butene	0.0098
2,3-Dimethylbutane	0.0107
2-Methylpentane	0.0213
3-Methylpentane	0.0157
n-Hexane	0.0066
2-Methyl-2-penten	0.0093
Methylcyclopentane	0.0142
2,4-Dimethylpentane	0.0076
3-methyl Cyclopentene	0.0044
Benzene	0.0054
2,3,dimethylPentane	0.0282
3-Methylhexane	0.0097
Cyclopentane, 1,3-dimethyl-,	0.0076
2,2,4-Trimethylpentane	0.2005
n-Heptane	0.0028
Cis-3-heptene	0.0067
Methylcyclohexane	0.0100
2,3,3-Trimethylpentane	0.0103
2,4-Dimethylhexane	0.0087
2,3,4-Trimethylpentane	0.0245
Toluene	0.2166
2,3-Dimethylhexane	0.0051
2-Methylheptane	0.0074
3-Methylheptane	0.0086
1-methyl-1-ethylcyclopentan	0.0062
2,2,5-trimethylhexane	0.0091
Ethylbenzene	0.0132
p-Xylene	0.0162
2-methyl-Octane	0.0066
3-Methyloctane	0.0052
1-nonene	0.0180
1 ethyl-2 methyl benzene	0.0191
1,2,4-trimethylbenzene	0.0112
1,2,3-trimethylbenzene	0.0172
1,4-diethylbenzene	0.0049
C10 aromatic	0.0039
2-ethyl-1,4-dimethyl	0.0043
C11-paraffin	0.0062
C11-aromatic	0.0102
1,2,3,4-tetrahydronaphthalen	0.0035
Naphthalene	0.0025
n-Dodecane	0.0035
Biphenyl	0.0070
Hexylbenzene	0.0117
Hexamethylbenzene	0.0074
2,6-dimethylnaphthalene	0.0073
Acenaphthalene	0.0084

Table S6.2 Heat of vaporization and heat capacity of water, ethanol, and iso-octane at 298 K [42]

Property	Water	Ethanol	Iso-octane
Latent heat of vaporization (kJ/kg)	2441.38	923.90	347.01
Heat capacity (J/kg.K)	4185.50	2460	2201.08

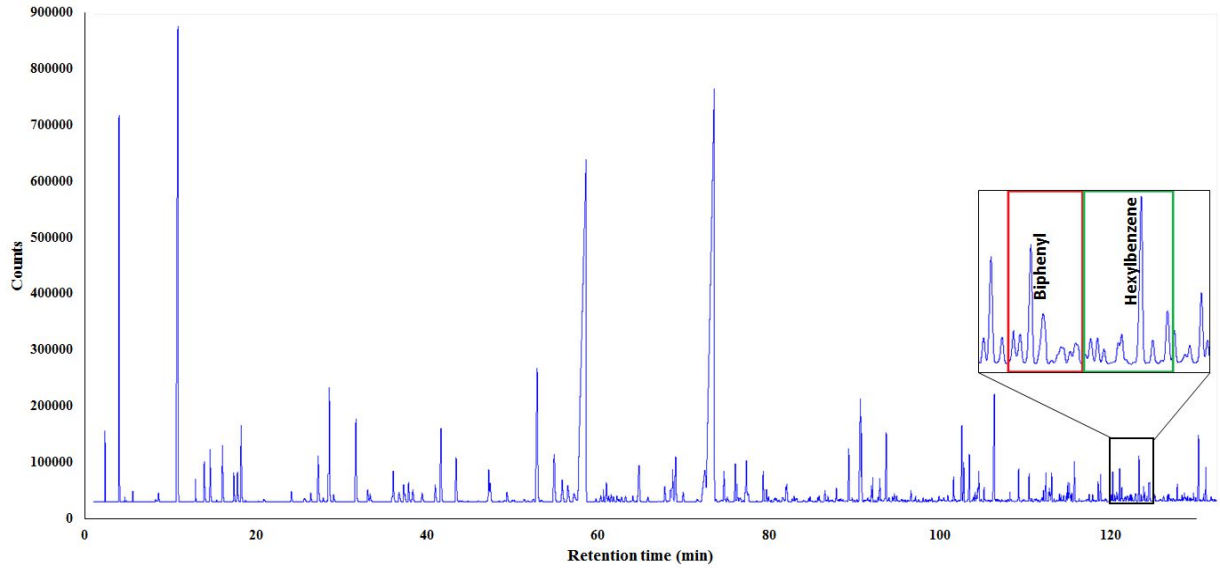

Figure S6.1. Gas chromatogram of the UTG-96 gasoline illustrating the lumping approach used to identify the simplified composition of the complex gasoline. Small chromatogram peak areas were assumed to be of the same composition to the nearest known identified hydrocarbon peak. An example is shown in the enlarged region; in this case, biphenyl and hexylbenzene represent neighboring peaks, the chromatogram area within the red box is assigned a composition of biphenyl and the chromatogram area within the green box is assigned a composition of hexylbenzene.

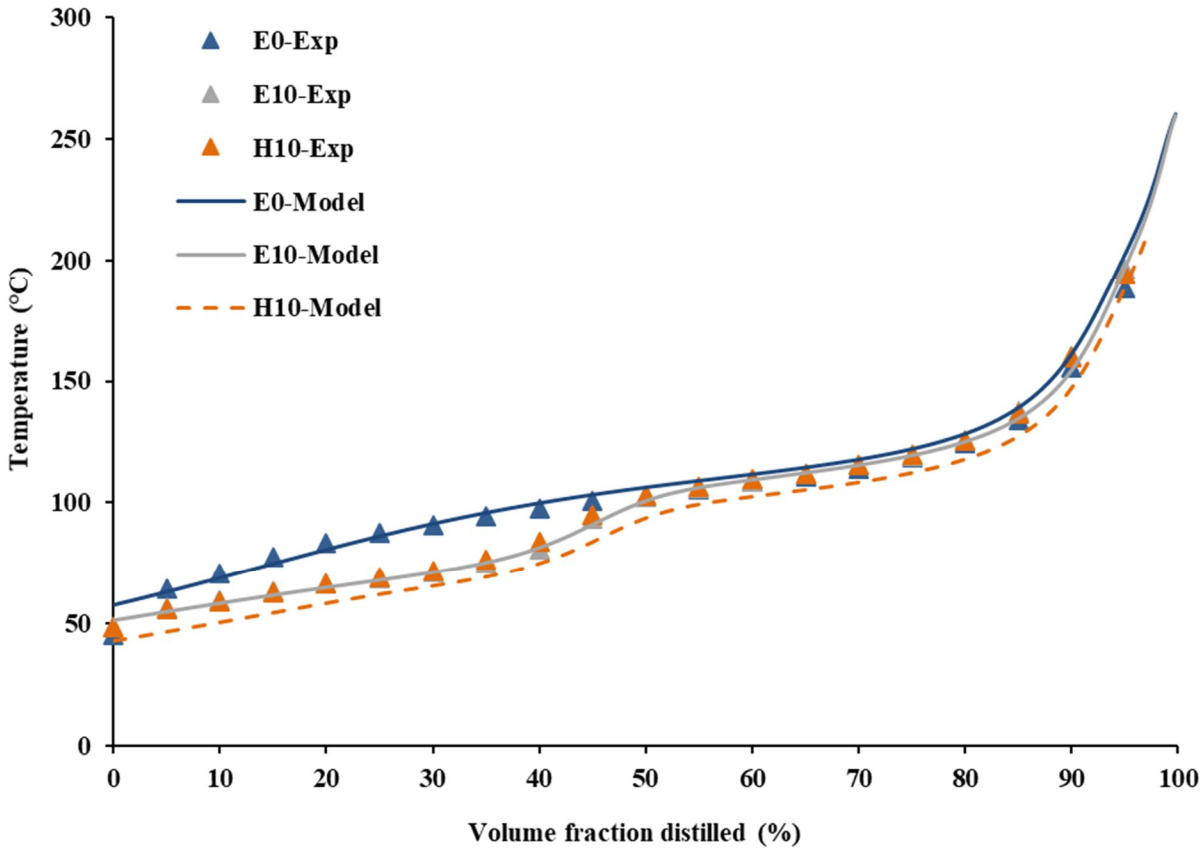

Figure S6.2. Comparison of experimentally measured and predicted distillation curves for blends with blending level of 10 vol%. Exp: Average of duplicate experimental distillation curves. Model: predicted distillation curves using the distillation model.. E: anhydrous ethanol blends. H: hydrous ethanol blends.

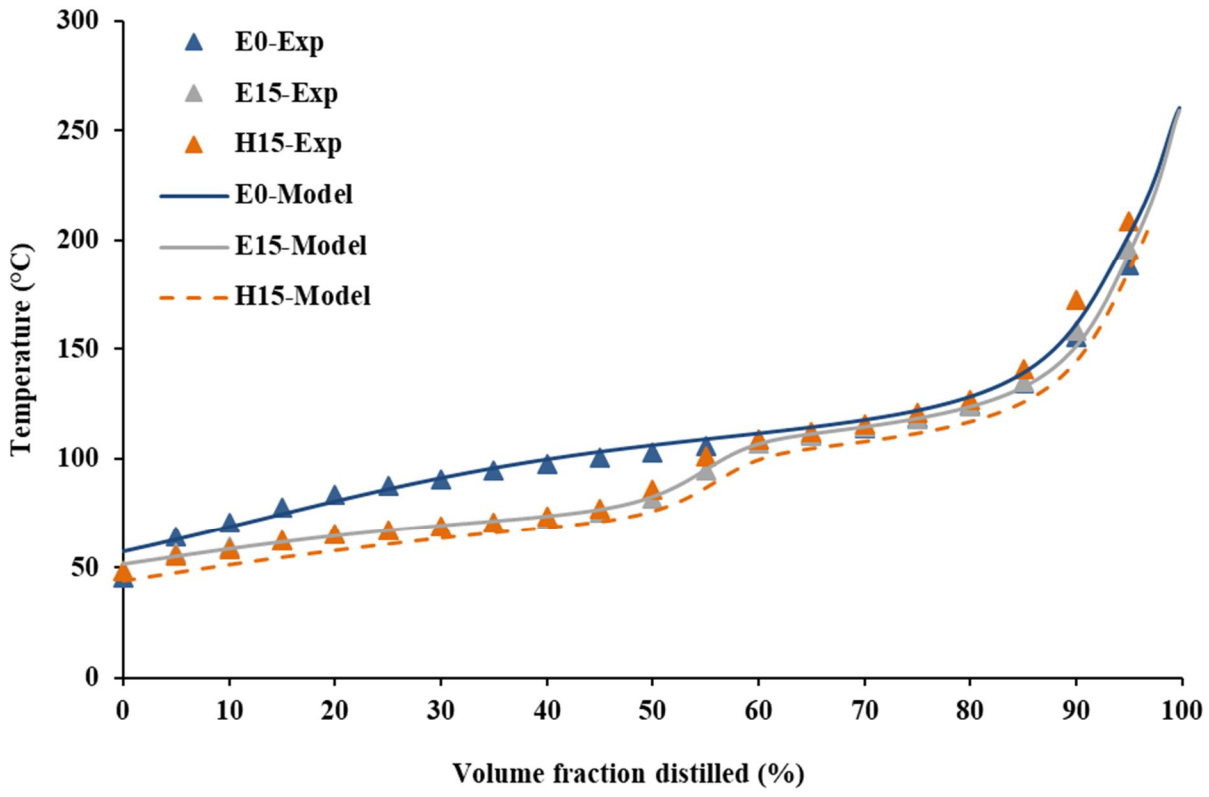

Figure S6.3 Comparison of experimentally measured and predicted distillation curves for blends with blending level of 15 vol%. Exp: Average of duplicate experimental distillation curves. Model: predicted distillation curves using the distillation model.. E: anhydrous ethanol blends. H: hydrous ethanol blends.

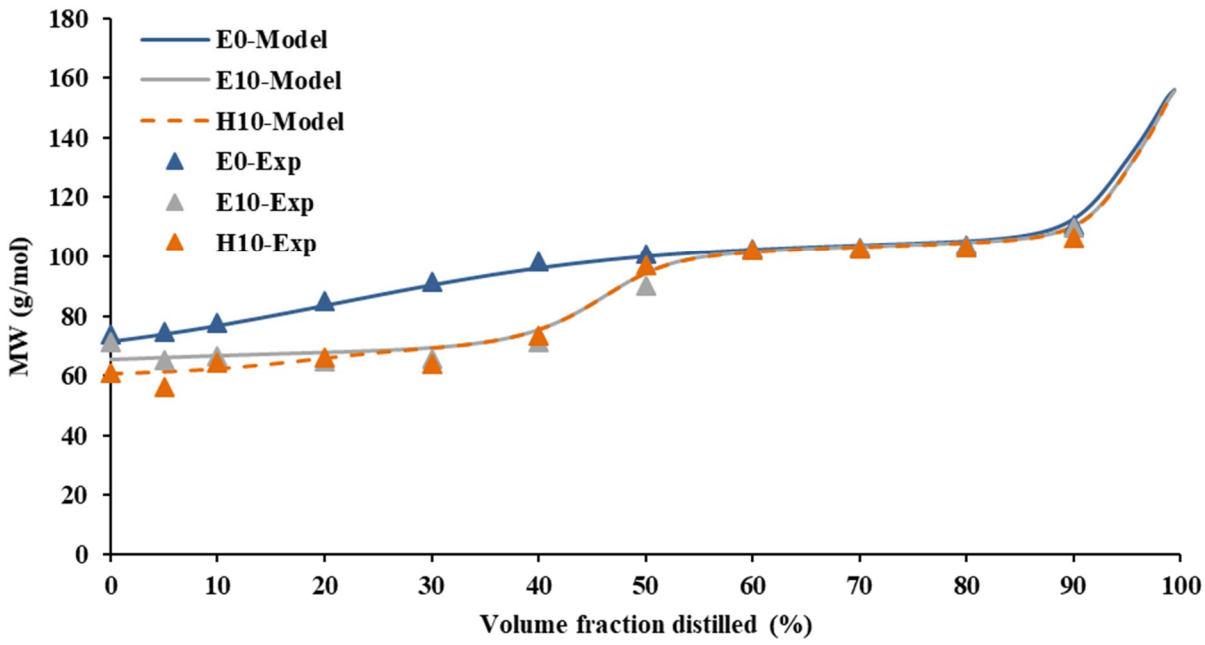

Figure S6.4 Comparison of experimentally measured and predicted average molecular weight for blends with blending level of 10 vol%. Exp: Average of duplicate measurements of the average molecular weight. Model: predicted average molecular weight using the distillation model.. E: anhydrous ethanol blends. H: hydrous ethanol blends.

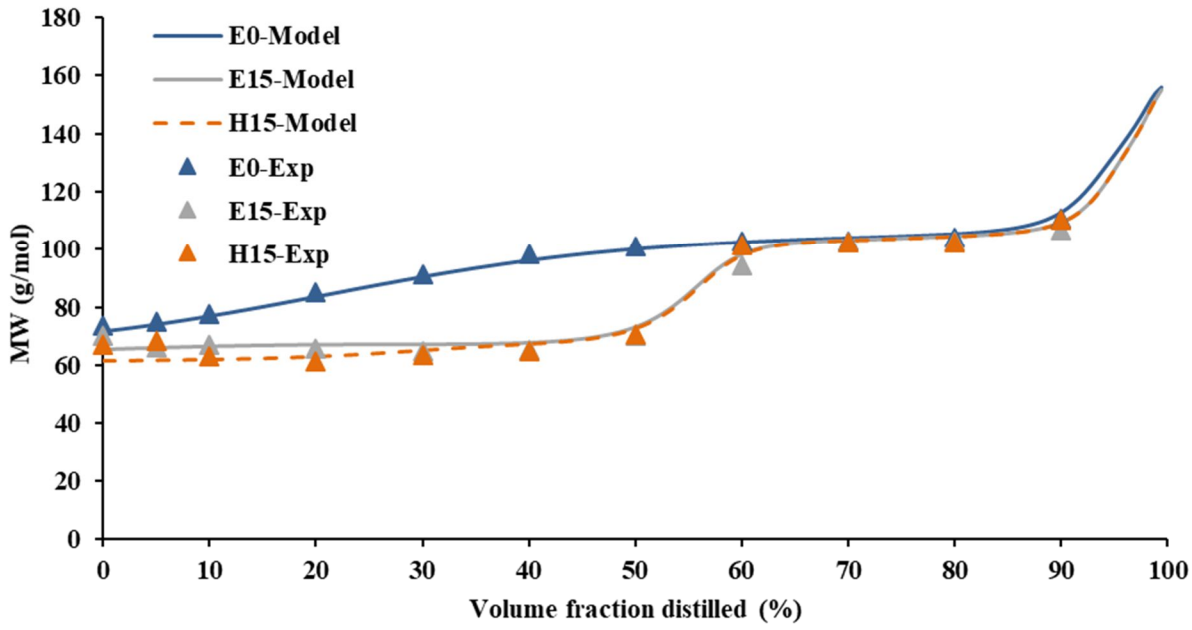

Figure S6.5 Comparison of experimentally measured and predicted average molecular weight for blends with blending level of 15 vol%. Exp: Average of duplicate measurements of the average molecular weight. Model: predicted average molecular weight using the distillation model. E: anhydrous ethanol blends. H: hydrous ethanol blends.